CHAPTER ONE

INTRODUCTION

1.1 Background of the Study

Refractory is derived from the Latin word “refractarius” meaning to break, resist, or refuse to subjugate. When applied to a material, it means “which resists high temperatures”. The material must “resist” (that is, retain its physical properties and its integrity) and must be found above a certain threshold for it to be classified as refractory material. Therefore, refractory materials are said to be materials whose temperature at which a sample of the product subjected to a gradual increase in temperature under normal conditions, softens and sags under its own weight is equivalent to at least $1{,}500^0$C (Musa et al, 2012).

Refractories are materials which can withstand high temperature (usually above $1{,}580^0$C) under the physical and chemical action of molten metal, slag and gas in the furnace (Nnuka and Agbo, 2000).

Among the oxides found in refractory mixtures, those of silicon (SiO_2) and aluminium Al_2O_3 are the most common. Silica (SiO_2) and alumina (Al_2O_3) are the principal constituents of aluminosilicate minerals, particularly the clays.

The performance of a refractory material in high temperature application depends mostly on the property of the raw material it is made of. Better property combination can be developed from the combination of two or more distinct

materials. Most single clay materials does not have all the required properties needed for a particular service and as such individual raw clays are selected and blended to provide product with consistent characteristics (www.ima-na.org). The problem of inadequate properties of single clay has placed limitations on the use of some low quality clays for refractory production and this has led to their importation. Hence, the need to use local waste materials to improve and develop high quality refractory products becomes imperative.

The use of agricultural by product as additives in brick industry is gaining increased research attention due to their effective role in decreasing the total energy needs of industrial furnaces. In addition, these additives leave pores upon burning which cause decrease in thermal conductivity and affect the mechanical properties of bricks as well (Safeer et al, 2017).

At the beginning, sawdust, wood chips and other based materials were used. Recently, polymers and renewable agricultural waste like rice peel or seed shell were also used as additives in the brick industry. (Lingling et al, 2005).

Industrial standards and specifications have made the demand for clay brick with higher insulation ability to be high. Insulation capacity of brick can be increased by increasing its porosity. Combustible organic pore forming materials are most frequently used for this purpose (Demir, 2008). Increase in the quantity of organic by products in the clay material decreases thermal conductivity of refractory

product significantly (Banhidi and Gomze, 2008)

Considering industrial demands for refractory products with adequate properties, it becomes necessary to blend different clays, so as to exploit the good properties of the different deposits. It also becomes imperative to select clays based on the physical, chemical and thermal properties from different deposits and blend them with some agro wastes to enhance their performance in service. This study seeks to use blend of two clays with different agro waste additives to develop low density clay bricks with high porosity without compromise to the mechanical properties.

1.2 Problem Statement

The under listed problem statement led to this research work:

1. Our nation has so many clay deposits which are of low quality for high temperature application. Though this problem has been identified, yet it has not been solved. These deposits are expected to have industrial potential if they are improved to meet internationally accepted standards.
2. Most of the bricks in use are found to be produced with single additive which usually results to problem of inadequate physico-mechanical and thermal properties required for high temperature performance.
3. Dumping of agro wastes like rice husk, saw dust and groundnut shells cause environmental pollution and hazard in waste disposal and management, hence there is need to use them in the industries for value addition.

4. There has not been any information regarding the use of multiple additives of three or more which are used in combined form at various formulations to enhance refractory properties of clay brick.

1.3 Aim and Objectives

The aim of this work is to investigate the performance effect of agricultural wastes (by products) as additives on the blend of two locally sourced clay deposits.

The specific objectives are:

- To characterize two Nigerian clay deposits and classify them.
- To characterize the agro wastes (rice husk, saw dust and groundnut shell) and to establish their usefulness.
- To produce insulating bricks with blend of two clays with the additives in different formulations.
- To test the physico-mechanical properties of the bricks produced and hence determine the extent of enhancement of the refractory properties.
- To identify the blends that will yield optimum property value and use them to produce insulating bricks that meet international standards.
- To develop mathematical model for predicting the properties and optimize the production conditions using central composite design.

1.4 Scope of the Study

This study is limited to results evaluated from the two clays studied. Results generated cannot be applied to other clays. The properties of the blended and composite clays which were investigated include linear shrinkage, apparent porosity, and bulk density, modulus of rupture, thermal conductivity, thermal shock resistance and refractoriness.

1.5 Justification of the Study

This study has developed light weight refractory bricks with enhanced insulating and refractory properties which are suitable for high temperature application in furnaces used for melting metal, heat treatment and for firing of ceramic products. The highly insulating porous bricks developed reduced thermal conduction which improved high temperature characteristics of the material and also reduced energy consumption of the production process. Hence, this technology gave rise to a more economic production process which is an improvement to the previous industrial process with high energy consumption and production cost.

CHAPTER TWO

LITERATURE REVIEW

2.1 The Origin and Formation of Clay Minerals

Clay formation involves the dissolution of a given mineral or group of minerals composing rock like granites. The dissolution produces a solution of different aggregate solute composition from that of each of the reacting solids/minerals. From this solution, clays can precipitate and grow since it is the least soluble portion of the mineral reaction. The clay material produced is a function of the minerals present in the rock (Mark, 2007).

Velde , (1992) identified four basic geological processes, which are water-rock interaction processes, giving rise to clay mineral formation. These are weathering (either sub-aerial or sub-aqueous); precipitation from concentrated solutions (saline lakes and closed marine basins); burial digenesis (effects of chemical and thermal change); and hydrothermal alteration (water-rock interaction at higher temperature due to thermal effect of magmatic intrusions).

The variable for all these geological environments are the same, water-rock ratio and rock composition as well as the temperature at which the reactions take place. Essentially this ranges from conditions at the earth-air or earth-water interface which gives minimum temperature of 4^0C for ocean bottom formation and around 15^0C average for land occurrence to the upper limit at which clay minerals are

found, which is near 200^0C in young rocks. Burial depths are usually not greater than 6-7km (Velde, 1992).

Some inorganic impurities present in the primary rock (unchanged rock particles) also find their way into the resulting clay, and impart various colours to pristine whiteness of the clay substance (Idenyi and Nwajagu, 2003). For instance, ferric oxide will make it reddish. Plant growth and animal life may introduce a considerable proportion of organic matter into the clays, turning them grayish or almost black (Mark, 2007).

When clays are found where they were originally formed, they are known as residual or primary clays. Often they are formed deep underground, the necessary chemical changes having been brought about by superheated acidic water that was forced up under pressure through the mass of primary granite. Clay deposits of this kind are commonly characterized by their great thickness and by their high content of large grained primary mineral such as quartz, mica, and feldspar. Far more common than residual clays are sedimentary or secondary clays that have been transported, perhaps more than once from their sites of origin by the action of seas and rivers. These vary greatly in composition according to the mode of transportation and age (Velde, 1992).

2.2 Clay Minerals

Clays have been known and used by man since ages for varied purposes. Different classes of people have given diverse definition to clay. An agriculturist has seen it as a type of soil that has high water retentive capacity. An artist (sculpture) considers it as useful earthen material utilized in traditional ceramic production such as chinaware, tiles, bricks, etc (Idenyi and Nwajagu, 2003). The word 'ceramics' comes from Greek word 'keramikos' which means 'burnt clay stuff' indicating that mechanical strength of these materials are achieved through firing – a high temperature heat treatment (Mark, 2007).

In general, clay as a material is important in different fields of work. The mineralogist, the geologist, the chemist, the soil scientist, the civil engineer and the material science engineer all study clay from different points of view taking into consideration areas of interest/application.

To mineralogists, it depicts a certain group of hydrous minerals that show similar physical and chemical properties with particle sizes of about two microns or less. To a materials engineer, clays are hydrous alumino-silicate materials which are plastic when the fine particles are wet, rigid when dried and vitreous when heated to high temperature (Nnuka and Agbo, 2000).

American Ceramic Society defined clay as that fine-grained rock which when crushed and pulverized becomes plastic when wet, leather hard when dried and on

firing is converted to a permanent rock like mass. In general, clay has been defined as a natural earthy, fine granular material which acquires plasticity on being mixed with limited quantity of water (hydro-plasticity) and which has maximum size of about two microns and showing sheet-like crystallographic habit; or it is a fine-grained rock which when suitably crushed and pulverized, becomes plastic when wet, leather hard when dried and on firing is converted to a permanent rock-like mass. (Idenyi and Nwajagu, 2003).

From chemical or mineralogical point of view, clays are complex aluminosilicate compounds containing attached water molecules, which have their origin in the chemical and mechanical disintegration of rocks, such as granites. Clay is referred to as minerals. The term ‘mineral’ connotes a naturally occurring solid inorganic substance with distinctive physical properties and a composition that can be described by a chemical formula. Similarly, Hurlbert and Klein (1977) observed that minerals are inorganic homogeneous crystalline solids with definite (but generally not fixed) chemical composition and an ordered atomic structure/arrangement. However, a mineral economist may refer to it as a commercially traded product derived from naturally occurring non-living, organic or inorganic, solid, liquid or gaseous substances (Mark, 2007). In describing resources, Mckelvery (1986) noted that the term mineral, generally refers to

naturally occurring nonliving, organic or inorganic, solid, liquid or gaseous substances that have a known or potential use.

2.3 Fire Clay: Nature and Description

Clays are product of decomposition of igneous rocks. The kind of clay depends on the kind of parent rock and presumably on the treatment it has had. Fireclay is derived from acid rocks like granite, in which feldspars of the type $K_2O.Al_2O_3.6SiO_2$ are decomposed by H_2O and CO_2 (possibly at high pressure and temperature) to give K_2CO_3, SiO_2nH_2O and $Al_2O_3SiO_2.2H_2O$. The last is the formula for kaolinite (Mark, 2007).

Clay is composed of silica (SiO_2), alumina (Al_2O_3) and water (H_2O) plus appreciable concentration of oxides of iron, alkali and alkaline earth, and contains group of crystalline substances known as clay minerals such as quartz, feldspar and mica. (Folaranmi, 2009).

A group of refractory clays which can stand temperatures above pyrometric cone equivalence (PCE) 19 are called fireclay. The clay which fuses below PCE 19 is not classified as refractory. Fireclay is essentially of kaolinite group and has a composition similar to that of china clay. In nature, it is usually found to contain 24-32 percent Al_2O_3, 50-60% SiO_2 and LOI between 9 to 12%. Impurities like oxides of calcium, iron, titanium and magnesium and alkalis are invariably present, making it white, grey or black in colour. Fireclay is generally of sedimentary origin

and is mainly found in the coal measures, as bedded deposits. All refractories are based on fireclay with alumina and silica as their major constituent.

Fireclay is classified under acid refractories which are those that are not attacked by acid slag. Clay is a very fine grained, unconsolidated rock matter, which is plastic when wet, but becomes hard and stony when heated. It has its origin in natural processes, mostly complex weathering, transported and deposited by sedimentation within geological periods.

2.4 Classification of Clay

Clays may be classified as low melting, high melting and refractory. Typical composition of each type is shown in Table 2.1

Table 2.1: Typical Chemical Composition of Clay

Composition, %						
Clay type	SiO_2	Al_2SO_3	Fe_2O_3	CaO+MgO	K_2O+Na_2O	LOI
Low melting	35-80	7-21	3-12	0.5-3	1-5	3-15
High melting	53-73	16-29	1-9	0.5-2.6	0.7-3.2	4-12
Refractory	46-62	25-39	0.4-2.7	0.2-1.0	0.3-3.0	8-18

Source: Nnuka and Agbo, (2000).

According to Velde , (1992), several basic properties of clay mineral guide all of the study devoted to them. The researcher's classification was based on the capacity of certain clays to change volume by absorbing water molecules or other

polar ions into their structure i.e. its swelling property. In the work, the scientist classified clay into swelling and non-swelling type. Swelling clays are called smectites.

The researcher also went further to classify clay on the basis of composition and structure which was used to classify the remaining clay minerals. Based on this, clay was classified into two groups namely; illite and chlorite as two mineral groups that are similar to the metamorphic minerals and are usually compared to these higher temperature phases. One type is the potassic, mica-like minerals, which are dominated by illite. Also there are chlorites which are compositionally and structurally contiguous with the high-temperature chlorite phase.

The kaoline family has no equivalence in metamorphic mineral groups. Also, the needle shaped sepiolite-palygorskites are found uniquely in low temperature environments. The mineral groups smectite, illite, chloride, kaolinite, sepiolite-palygorskite account for by far the greatest part of the clay minerals found in nature.

2.5 The Structure of Clay Mineral

Clays are of two major types, swelling and non-swelling type. Since all clays are dominated by silica, their SiO_2 content is not of great diagnostic help in their identification. Generally, the elements Al, Mg, Fe, K, and to a lesser extent Na and Ca, are useful indicators of clay type. The distance between the sheet layers of the

crystal structure is also an important criterion for structural identification of clay. This is called the basal spacing which is determined after heating to 200^0C to eliminate absorbed water. Swelled spacing is determined using ethylene glycol vapour to expand the layers to a standard distance.

Taking these elements as a basis for rapid identification, one can construct a table of clay mineralogy as shown in Table 2.2

Table 2.2 Clay Mineralogy.

Swelling types Smectites	**Dominant elements**	**Basal Spacing (Å)**	
		Dry	**Glycol**
Beidellites	Al	10	17
Montmorillonite	Al (Mg, Fe^{2+} minor)	10	17
Nontronite	Fe^{2+}	10	17
Saponite	Mg, Al	10	17
Vermiculite	Mg, Fe^{2+}, Al (Fe^{3+} minor)	10-12	15.5
Mixed layer minerals		<10	10-17
Non-swelling types			
Illite	K, Al (Fe, Mg minor)	10	
Glauconite	K, Fe^{2+}, Fe^{3+}	10	
Celadonite	K, Fe^{2+}, Mg, Fe^{3+}, Al^{3+}	10	
Chlorite	Mg, Fe, Al	14	
Berthierine	Fe^{2+}, Al^{3+}(Minor Mg)	7	
Kaolinite	Al	7	
Halloysite	Al	10.2	
Sepiolite	Mg, Al	12.4	
Palygorskite	Mg, Al	10.5	
Talc	Mg, Fe^{2+}	9.6	

Source: Velde . (1992)

The clay structure is well understood when the fundamental molecular units involved in the clay structure and the arrangements of these molecules in the overall patterns is defined. Most clay minerals have a special or at least characteristic arrangement of their constituent atoms in long, interlinked planes. This structure, called sheet silicate or phyllosilicate structure is determined by an essentially two dimensional cross-linking of SiO_2 units. Each silicon atom is surrounded by four oxygen atoms to form a tetrahedron.

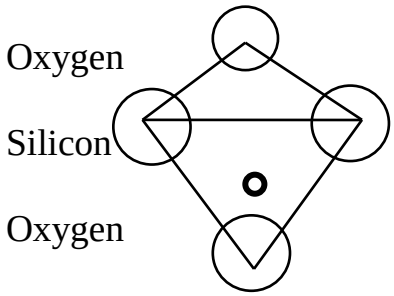

Figure 2.1 Silicon tetrahedral arrangements with one silicon atom surrounded by four oxygen anions

This is the most basic unit of the clay structures. The tetrahedral coordinated silicon cations are linked one to another by highly covalent bonding through sharing of oxygen. These shared oxygen form a plane of atoms along one base of the tetrahedral structural units. The interlinked oxygen are called basal oxygen. The linked tetrahedral structure forms a two-dimensional array of atoms which is the basis of the sheet structure. (Mark, 2007)

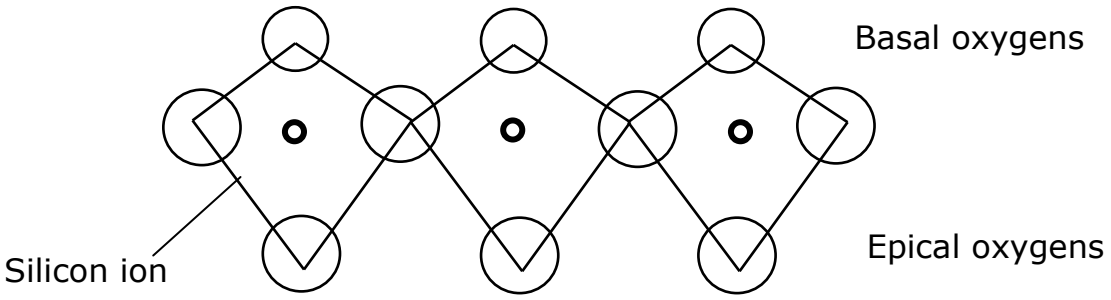

Figure 2.2 Linked silica tetrahedral showing the shared oxygen ions between two silicon ion (Mark, 2007).

The arrangement of the interlinked basal oxygen of the tetrahedral structure occurs in such a way as to leave a hexagonal shaped hole in the network of oxygen atoms. These holes or cavities are important in processes of attraction between successive basal tetrahedral planes and linking the sheets of the clay structures one to another. (Velde,1992)

According to Brindley et al, (1951), clay minerals consist of layers identified by a specific arrangement of sheets. One sheet comprises two planes of oxygen atoms arranged in tetrahedral coordination around silicon atoms by sharing the basal oxygen between adjacent tetrahedral. The other sheet consists of OH group ordered in octahedral coordination around centrally aluminium atoms as shown in Figure 2.2.1.

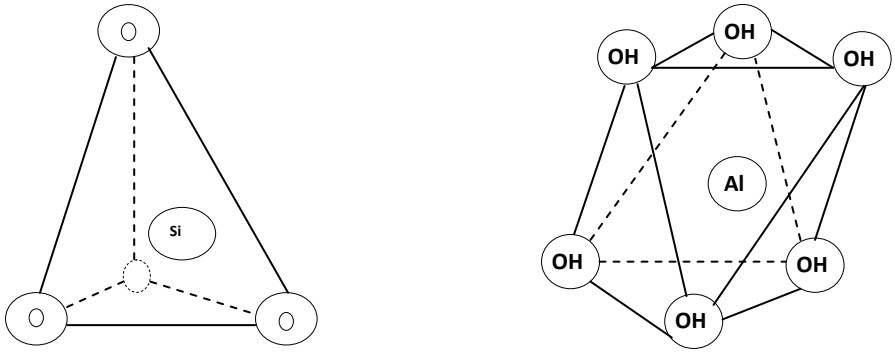

Figure 2.2.1Tetrahedra and octahedral layers as basic unit of clay mineral (Brindley et al, 1951).

The tetrahedral and octahedral layers of Si and Al are linked together in a planar arrangement of sheets. The clays can be formed by two layers, three layers, etc. Thus, the clays can be classified according to the number of layers. The corresponding classification of the most common clay minerals is listed in table 2.2.1.The classification based on layers refers to the tetrahedral: octahedral sheet ratio.

Table 2.2.1 Classification of Clay Minerals.

Layer type	Group	Mineral species
1:1	Kaolin-Serpentine	-kaolinite, dickite, nactric and hallosite
2:1	Mica-Illite	-muscovite, illite, glauconite, celadonite, paragonite.
	Smectite	-montmorillonite, beidellite, nontronite.
	Chlorite	-clinochlore, chamosite, pennantite.
	Vermiculite	-vermiculite.

Source: Edwin, (2015).

As shown in table 2.2.1, the most basic arrangement is kaolin and serpentine. Kaolin is formed by two layers that comprise of one tetrahedral and one octahedral sheet in the unit cell. Illitemica, smectite, veremiculite and chlorite consist of three layers built up by one octahedral sheet sandwiched by two tetrahedral sheets in the unit cell. Each clay mineral group can be identified by a characteristic arrangement of the sheets in layers. These layers are displaying very distinct basal spacing (d) for a specific clay mineral which can be identified by XRD.

2.6 Clay Transformation on Heating

According to Velde (1992), there are four ranges of temperature which produce characteristic transformations in clay materials which are:

- the free water dehydration range (50-120^{0}C).
- the clay stability range (120-600^{0}C).
- the anhydrous clay range (600-900^{0}C)
- the recrystallization range (above 900^{0}C)

In the manufacture of ceramics, the 600-1000^{0}C zone is of greatest importance in transforming the dried clay into a new, more rigid substance. In this range the interaction of the clay and non-clay additives occurs to form new minerals or physical states (glass or new crystalline phases). In clays, an important volume change takes place as they recrystallize into other phases, losing their crystalline water above 1000^{0}C. Significant shrinkage occurs as this water is lost. When firing

brings the material into this thermal region, the shrinkage effects must be modified by the addition of sufficient non-clay materials, called temper, or grits for which sands of various types are normally used. The role of temper agents is to diminish the overall volume change occurring when clays lose their crystalline water.

According to Mark (2007), all clay minerals, when heated to temperatures in excess of 1200^0C, are capable of being re-crystallized to form the minerals mullite $3Al_2O_3.3SiO_2$), corundum (Al_2O_3), and where Mg is present, olivine $(Mg.Fe)_2SiO_4$) while trihymite or cristobalite (SiO_2) results both from changes in the mullite composition, and from the incorporation of free quartz. Figure 2.3 shows the relationship between these high temperature ceramic phases with temperature and composition.

However, the temperatures and times used in industrial brick production are inadequate for these changes to go to completion and fusion usually eases at a stage of vitrification in which some of these minerals are beginning to form. Nevertheless, the development of the felted crystals of mullite is believed to be important in the production of strength in the fired brick (Mark, 2007).

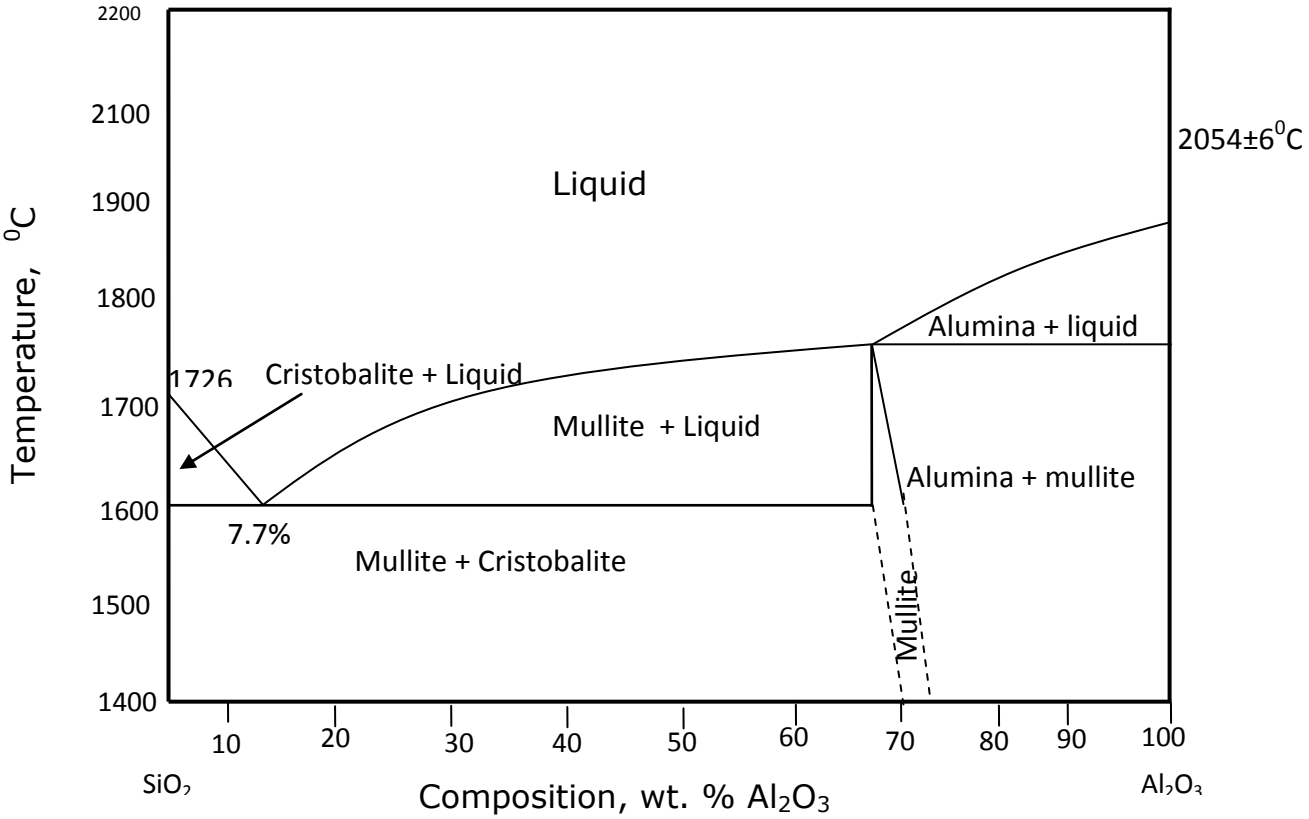

Figure 2.3. The silica- alumina phase diagram (Mark, 2007).

2.7 Metallurgical Refractories

According to Nnuka and Adekwu (1997), refractories primarily are materials which can withstand high temperatures. Their usefulness depends on their ability to maintain their mechanical strength at high temperatures, when in contact with corrosive liquid (slags) and gases. Most industrially used refractories are composed of a mixture of metal oxide. Besides, carbon, graphite, and silicon carbides are now widely used as refractories. Other carbides, nitrides, silicides and borides are used in special applications, mostly in the space and nuclear industry. This group of

refractories apart from refractoriness has an added advantage of stability in oxidizing environment.

Nnuka and Agbo (2000) described refractories as materials which can withstand very high temperature conditions (usually above 1580^0C) under the physical and chemical action of molten metal, slag and gases in the furnace without losing their chemical and mechanical integrity. Chemically, they are acidic, basic or neutral. Acidic refractories contain predominantly acidic oxides. They are generally alumino-silicate and include siliceous fireclays, sillimanite and high alumina. Basic refractories are made from oxides which are oxygen ion donors and include magnesite, chrome-magnesite, and dolomite. Neutral or amphoteric refractories manifest both acidic and basic characteristics. They are special or exotic refractories and these include SiC, SiN_3, ZrO_2, $ZrSiO_4$, etc.

Refractories may be grouped into natural or artificial depending on the process of manufacture, into roasted or unroasted depending on method of heat treatment and into common, special and diverse shaped, depending on the shape. Refractories may also be grouped into the following according to refractoriness;

(a) those of common refractoriness (1580^0C to 1770^0C)

(b) those of high refractoriness (1770^0C to 2000^0C)

(c) those of the highest refractoriness (above 2000^0C)

Refractories were studied from the point of view of the origin and natures of raw materials used in their manufacture. (Nnuka and Agbo, 2000). Hence, they were grouped into the following categories:

- Magnesia or Magnesia-Lime group
- Magnesia chrome group
- Siliceous group
- Fire clay group
- High Alumina group
- Carbon group

According to Nnuka and Agbo (2000), fire clays are mostly located in Nigeria at places like Ukpor, Ozubulu, Enugu, Kankara, Kwi. The important varieties of fire clay are as follows:

1. Siliceous fire clays**.** They are clays with a wide range of silica content usually above 75% SiO_2 and low percentage of impurities for example alkalis, alkaline earths and iron oxides.
2. Plastic fire clays are of sufficient natural plasticity to bond non-plastic materials.
3. Flint fire clay is a hard or flint-like fireclay occurring as an unstratified massive rock, practically devoid of natural plasticity.

4. Nodular fire clays are called burley flint clays, occurring in the form of rock containing aluminous or ferruginous nodules, or both bonded fireclay.
5. Kaolins are refractory of both sedimentary and residual origin. They are usually quite pure and of the general clay composition represented by the formula. $Al_2O_3.2SiO_2.2H_2O$

Among the oxides found in refractory mixtures, those of silicon SiO_2 and alumina (Al_2O_3) are the chief constituents of all aluminosilicate minerals, particularly the clays. The amount of alumina in a clay mineral determines its potential use as an aluminosilicate refractory raw material. Of all clay minerals, fireclay has been found to be among the types that possess higher content of alumina (24-32%).

Refractories are widely used in most high temperature manufacturing processes such as iron and steel making, copper and aluminum smelting, glass or ceramic manufacture, cement, ore processing, petroleum refining and petrochemicals manufacture. However, iron and steel making account for almost two thirds of all refractories used and in this industry, many refractory developments have occurred. Thus, the progress in refractory manufacture is closely connected with metallurgy which consumes up to 60 percent of all refractories produced. For example, the metallurgical industries in the USA are said to consume 72% of all refractories used, with ferrous applications accounting for 63%. The ceramic industry consumes 11.8%, the glass industry 6.2%, the minerals industry 6.2% and

the chemical and petrochemical industries 2.5%, the balance being consumed by utilities and other industries (Mark, 2007).

Table 2.3. Refractory Needs for the Chemical and Metallurgical Industries in Nigeria

Industry/Type of Refractory	DSC	Ajaokuta Steel Co.	Steel Roll Mill	Cement	Ceramic Glass	Total
Alumino Silicates	18.0	36.4	3.0	4.0	2.24	63.64
Magnesites	27.0	5.0	5.0	5.9	1.04	43.94
TOTAL	45.0	41.4	8.0	9.9	3.28	107.58

(Nnuka and Adekwu, (1997)

Considering the enormous need of refractory in our local industries, the only viable option is for the nation to develop its own refractory industry, based on available local raw materials, which the country is highly blessed with. This calls for the need to look inward and find how to harness available local mineral resources and improve their service performance by incorporating into them some useful additives containing elements and compounds that can improve their service properties. This could be done using some useful waste materials, which could be converted into wealth, thereby improving technological advancement and the national economy which is the sole vision of this research work.

Mark, (2007) noted that the development of iron and steel industry in Nigeria implies that there will be a great increase in the need for refractory materials. For

example, it is reported of the Ajaokuta Steel Complex that on completion, about 36, 000 tonnes of refractory bricks worth over ₦60 million (prices as at 1993) will be required just for furnace lining purposes only. In fact, more than 80% of the refractory bricks needed for use at Ajaokuta will be fireclay i.e., aluminosilicate refractories. Similarly, the Delta Steel Company will require 25, 000 tonnes/year of fireclay i.e. about 51.5% of its refractory need. (Mark, 2007)

It has been observed that small scale industries in Nnewi e.g. Jimex Nig Ltd, research institutes like Project Development Institute (PRODA) Enugu and Scientific Equipment Development Institute (SEDI), and other related establishments in the country are presently embarking on the fabrication of machine spare parts. These spare parts are fabricated using high temperature furnace (foundry melting furnaces and heat treatment furnaces) that require refractories as linings. Most of these refractories consumed in this country are imported, whereas the country is richly blessed with much clay deposits. These clay minerals if properly harnessed could be useful in filling the gap. New developments in refractory technology where local input content is used to enhance the quality performance of the refractory properties of the refractory material can then be exploited. By so doing, better quality refractory products than those imported could be developed in our country-Nigeria.

According to Nnuka and Okunoye (1991), the present economic reality has forced local entrepreneurs to look inwards for the sourcing of their industrial inputs. Results of these attempts have been impressive as large reserves of suitable industrial raw materials have been cited in various parts of the country. It is believed that if properly processed, our local mineral resources are capable of sustaining almost completely, our metallurgical and ceramic industries.

The Nigerian metallurgical development centre (NMDC), Jos (1999) reported that there are no organized manufacturers of refractories in Nigeria. Instead, there are isolated cases of fireclay refractories production by such organizations as Nigeria Railway Corporation, Enugu and a certain Brick plant at Okigwe (Burnt Brick Factory). The products of these organizations are generally of poor quality as quality control is not taken into consideration during production.

Therefore, there is serious need for Nigeria to develop the locally available refractory raw materials for manufacture of high quality refractory product suitable to meet the technological need in our metallurgical industries. Some useful research works from many researchers like Nnuka et al (2000) have proved that clay materials from many deposits like Ukpor and others are capable of finding extensive application for refractory purposes especially in the non-ferrous industry.

2.8. Classification of Refractories

According to Gilchrist (1977), there is no general definition of a refractory. Essentially, it is a material of "high melting point", but this is a relative term and melting point is not the only criterion of usefulness. Most refractories are ceramic materials made from high melting point oxides, particularly SiO_2, Al_2O_3 and MgO. Carbon is now an important refractory, however, and carbides, borides and nitrides are also being developed for high temperature work. Metals like Mo and W are refractory metals and find uses in research apparatus. Finally, there are materials like asbestos which have not a high melting point, but which are used as medium or low temperature insulation and as such should not be excluded from consideration.

Mark (2007) noted that refractories may be classified on the following basis:

- by their refractoriness (ability to withstand high temperature in service).
- By chemical composition
- By the chemical nature of refractory oxide
- By the method of manufacture and end use

(1). By refractoriness, they are classified into the following groups:

(a) The common refractories (up to 1580-1770^{0}C);

(b) The high refractoriness (1770-2000^{0}C)

(c) The highest refractoriness (above 2000^{0}C)

(2). By their chemical and mineral composition, refractories are classified as:

(a) Siliceous, in which the refractory base is SiO_2 (e.g. silica, quartzite);

(b) Alumina-siliceous, where the refractory components are Al_2O_3 and SiO_2 (e.g. fireclay or aluminosilicate refractory).

(c) Magnesium is based on MgO (magnesite, dolomite, etc).

(d) Chromic, with the refractory base composed of Cr_2O_3 and MgO.

(e) Carbon refractories, with the base being carbon or graphit;

(f) Carbide refractories, which contain refractory compounds of the type MeC (e.g. carborundum, SiC).

(g) Oxide refractories composed mainly of pure oxides, such as MgO, Al_2O_3, BeO, Cr_2O_3, etc.

(h) Zirconia refractories, based on Zircon and ZrO_2.

(3). By the chemical nature of refractory oxide, all refractories, are divided into:

(a) Acid refractories e.g. SiO_2, ZrO_2.

(b) Basic refractories e.g. MgO, CaO

(c) Inert or neutral e.g. Al_2O_3, Cr_2O_3.

(4). By the method of manufacture, physical form and shape, all refractories are divided into:

(a) Refractory bricks, which are preformed shapes such as straights, splits, arches, etc. Approximately 70% of all refractories used by industry are in the form of bricks.

(b) Monolithic refractory castables, which are special, mixes or blends of dry granular or stiffly plastic refractory materials with which virtually joint-free (i.e. monolithic) linings are formed. Castables are furnished in dry form and upon mixing with water they develop an unusually strong hydraulic set; i.e. they are not fired or roasted. They are usually poured or cast in much the same manner as ordinary cement concrete.

(c) Refractory plastics and ramming mixes. These are unburnt blocks and ramming mixes (mortars) in a plastic state, which are placed directly in the furnace and fired in site to develop a monolithic wall.

2.9 Aluminosilicate Refractories

Aluminosilicate refractories are those refractories which contain more than 25 percent Al_2O_3 and not more than 70 percent SiO_2 (Mark, 2007). Depending on the content of SiO_2 and Al_2O_3, aluminosilicate refractories are subdivided basically into semi-acid or semi-silica (15-25 percent Al_2O_3) fireclay (25-45 percent Al_2O_3), and high alumina type (over 45 percent Al_2O_3). The high alumina kind is subdivided into sillimanite, mullite, mullite-corundum and corundum. Typical

compositions for fireclay and high-alumina fireclay refractories are listed in the table 2.4.

Table 2.4 Typical Compositions of Aluminosilicate Refractories

Refractory type	**Compositions (wt.%)**						**Apparent porosity (%)**
	Al_2O_3	SiO_2	MgO	CaO	Fe_2O_3	TiO_2	
Fire clay	25-45	70-50	0-1	0-1	0-1	1-2	10-25
High-alumina Fire clay	90-50	10-45	0-1	0-1	0-1	0-4	18-25

Source: Mark, (2007)

According to Nnuka and Agbo (2000) , fireclay is an important input in refractory product with its composition varying within the following limits (in percentages); SiO_2 (52-60%), Al_2O_3 (30-42%), Fe_2O_3 (1.5-2.5%), Ca (0.5-1.5), MgO (0.1-1.0) and alkalis (1.0-2.0).

Hence, fireclay is an alumino-silicate and contains essentially between 50-70 percent silica and between 25-40 percent alumina. Fireclay finds application at temperatures between 1400^0C and 1600^0C depending on the composition, especially as lining of heat treatment furnaces, melting furnaces for low melting point metal (Nnuka and Agbo, 2000).

2.10 Properties of Refractories

Refractories are a family of technical ceramics (Schacht, 2004) They manage industrial process heat, defying thermal and mechanical stresses, high temperature and chemical attack. Hence the most important requirements include:

- Rigidity and maintenance of size, shape and strength at the operating temperature, which will presumably be "high".
- Ability to withstand thermal shock such as is met in heating and cooling of furnace, or in fluctuations during charging or during normal operation.
- Resistance to chemical attack by gases, slag or metals likely to be encountered.

The refractory material in the course of service bears mechanical loads and therefore must be capable of withstanding the load impact at the high temperature level, erect a solid barrier between "hot inside and tolerable outside" both at the service temperature and often through repeated temperature cycles. The function also entails heat transport. The refractory serves as a thermal insulator, but less frequently, as a conductor of heat.

Notwithstanding, the greatest challenges of refractories occur as they face hot corrosive fluids. Corrosive attack increases in severity with increasing temperature. Corrosive attack is thus further enhanced by erosion – which occurs due to abrasion effect caused by entrained particles in the fluid (Chima, 2015).

Refractory materials by definition are supposed to be resistant to heat and are exposed to different degrees of mechanical stress and strain, thermal stress and strain, and corrosion/erosion from solids, liquids and gases, gas diffusion and mechanical abrasion at various temperatures. Hence, different refractories are designed and manufactured so that the properties of the refractories will be appropriate for their applications. In most cases, refractory properties can be predicted from the results of appropriate tests; for others, knowledge and experience predict the refractory properties where direct tests correlating the properties are not available. The testing of these refractory properties can, in most cases, indicate the performance of a refractory in actual application.

The significant properties of any refractory depend on its mineral make up, the particle size distribution of the minerals and the way these minerals react to high temperatures and furnace environments. Upon firing, the fines form a ceramic bond between the larger particles. The fired refractory consists of bonded crystalline mineral particles and glass or smaller crystalline particles, depending largely on the composition of the refractories (Callister, 2003).

In fireclay and high-alumina refractories, elongated mullite crystals tend to interlace and form relatively strong bonds at temperatures approaching their melting point. When the bond in the refractor is glassy in nature, the brick has good strength at lower temperatures. If at furnace temperatures the glass has a low

viscosity, however, it will soften and the refractory will deform under load (Mark, 2007).

Chemical composition has a lot to do with the properties of a refractory. In fireclay and high-alumina refractories, the refractoriness usually increases as the alumina-silica ratio increases. Also, the presence of certain impurities or accessed oxides; such as soda (Na_2O), potash (K_2O), lime (CaO), and iron oxide (Fe_2O_3), which promote the formation of low melting glasses tends to reduce the refractoriness. Soda and potash also retard mullite formation in particular (Mark, 2007).

It is on this basis that the technology involving the use of local content input to improve the service performance of blended fireclay in order to meet international standards was established. The primary objective being to explore those useful elements and compounds present in those waste materials which can contribute to improve the properties of the refractory and come up with products that will match required standards. This forms the underlying vision that gave birth to this research work.

Refractory properties can be classified under physical, thermal and chemical properties. (Schacht, 2004), Table 2.5.1 shows the composition and some properties of standard refractories.

Table 2.5.1 International Standard values for physical properties of refractory

Clay type	Bulk density g/cm^2	Apparent porosity %	Permeability	Linear Shrinkage %	Thermal Shock Resistance (cycle)	Cold Crushing Strength Kg/cm^3	Refractoriness ^0C
Fire clay	1.71-2.1	2-30	25-50	7-10	25-30	15000	1500-1700
Siliceous fireclay	2	23.7	-	-	-	15000	1500-1600

Source: Yami, (2007) and Grimshaw, (1971)

Table 2.5.2 Composition and some properties of refractories.

Material	Al_2O_3 %	SiO_2 %	MgO %	TiO_2 %	C %	Fe_2O_3 %	SiC %	Cr_2O_3 %	CaO %	Bulk density (kg/m^3)	Apparent porosity (%)	Typical cold crushing strength (MPa)
60% alumina brick	60	32.5	—	—	—	—	—	—	—	2600 2300–2550	17–28	39
50% alumina brick	51	44	—	—	—	—	—	—	—	2300 2100–2350	18–28	55
42% alumina brick	42	51	0.5	1	—	3	—	—	0.5	2050–2350	20–22	41–90
Magnesite	0.8	2.5	92	—	—	1.8	—	—	2.3	2670–2950	17–24	34–55
Mag chrome	12	2.9	53	—	—	—	—	25	—	3080 2950–3050	16–22	38–55
Silica	0.7	96	—	—	—	0.7	—	—	2.3	1680–1870	20–25	28–34
Dolomite	2	3	37	—	—	1.5	—	—	55	2500–2800	16–22	48
1800°C convent. castable	94	0.2	—	—	—	—	—	—	3	2890	—	55
1600°C low-cement castable	50	45	—	—	—	—	—	—	1	2400	—	75
Insulation brick	99	0.6	0.01	—	—	—	—	—	0.1	1440	—	17

Source: Schacht, (2004)

2.11 Physical Properties

When considering refractory material for any service requirement, some useful physical properties including density, porosity, strength and abrasion are taken into consideration.

The density, strength and porosity of fired products are influenced by factors like quality of the material, size of the particles, moisture content at the time of moulding, pressure of moulding, temperature and duration of firing, kiln atmosphere and cooling rate (Idenyi and Nwajagu, 2003).

Refractory materials are characterized by their physical properties, which often indicate the use and performance of the refractory materials. Hence, the basic physical properties can often indicate whether a refractory material can be used for intended applications. The following basic physical properties are often used to predict, select and prescribe refractories for specific application: density, porosity, strength and abrasion resistance.

2.11.1 Density: Under this property are the bulk density and true density. The bulk density of a porous material is the ratio of mass of the material to its bulk volume ignoring the volume occupied by the pores. Density of the refractories is an indirect measure of their capacity to store heat. Bulk density and apparent porosity are generally used for quality control checks. They have an effect on other properties such as thermal conductivity and thermal shock resistance of a material. Mathematically, it is expressed as:

$$\text{Bulk density} = \frac{\text{mass in air}}{\text{Soaked mass} - \text{suspended mass}} \qquad (2.1)$$

The density is the ratio of the mass of a material to its true volume.

2.11.2 Porosity: Porosity as a property of a refractory material is of two types: apparent and true porosity. Pores occur as a result of water and gases that are given up during the burning or firing process of the material. Pores in refractories may be open, through or closed.

Apparent porosity is the ratio of the volume of open pores to the bulk (total) volume. The open pores are the ones that are open to the surface of the refractory. Refractories with low apparent porosity have greater resistance to penetration by slags and fluxes, resistance to corrosion and erosion and usually lower gas permeability than those with high porosity. Thermal conductivity is also influenced by porosity. However, on account of insulating effect, porosity is preferred.

True porosity is the ratio of the total volume of open and sealed pores to the bulk volume expressed as a percentage.

2.11.3 Strength: The refractory physical strength in both cold and hot condition is often characterized as measures of the use of refractory. Strength as a property is grouped into cold strength and hot strength.

2.11.4 Cold crushing strength: The cold crushing strength of a material is the maximum load at failure per unit of cross-sectional area when compressed at ambient temperature. It could be considered as the ability of a refractory to withstand handling impact or abrasion at low temperatures. It does not however, give an indication of the refractory's strength at service temperature.

Cold crushing strength is generally used for quality control checks and does not give any specific indication of a material's in -service behavior.

According to Schacht (2004), cold strengths indicate the handling and installation of the refractory, whereas hot strength indicates how the refractory will perform

when used at elevated temperature, initial strength develops in refractory materials during the forming process. For shaped refractories, the strength often develops during the physical processing of the products and sometimes followed by higher temperatures where the refractory goes through a firing process. For monolithic refractories, the initial strength develops during the installation or forming process. For precast shapes, the final strength develops while in application.

In recent years, much relevance has been adduced to high temperature strength of refractories rather than cold strengths since refractories are used at elevated temperatures and not at room temperatures. Strengths of refractories are measured as cold compressive strength, cold modulus of rupture, or hot modulus of rupture. Hot modulus of rupture provides the best indication of the performance of a refractory material in use.

2.11.5 Cold compressive strength

The cold compressive strength of a refractory material is an indication of its suitability for use in construction. It is a combined measure of the refractory for the strength of the grains and also of the bonding system.

It is indicative of the strength of the bonding system of the refractory product. The test is done at room temperature. It provides no indication of how the refractory will behave at elevated temperature.

2.11.6 Cold modulus of rupture

The cold modulus of rupture of a refractory material indicates the flexural strength and its suitability for use in construction. It is indicative of the strength of the bonding system of a refractory product. Since the test is done at room temperature, it can only show its suitability and its use in construction. It provides no indication of how the refractory will behave at elevated temperatures.

2.11.7 Hot modulus of rupture

The hot modulus of rupture provides the indication of refractory material, about its flexural strength at elevated temperatures. Since refractories are used at elevated temperatures, the hot modulus of rupture is the true indicator of the suitability and performance of a refractory at high temperature. Hence, in recent years, the hot modulus of rupture has been prescribed and required by users as the most important test criterion for selection and use of refractories.

2.11.8 Abrasion resistance

This is a measure of the resistance of a refractory material when high velocity particles abrade the surface of the refractory. It measures the strength of the bond and the refractory particles and its resistance to the flow of high velocity particles across its surface. The need for good abrasion resistance of refractory materials is most evident in petrochemical industries where fine particles impinge on the refractory surface at high velocities at moderately elevated temperatures. A direct

correlation between abrasion resistance and cold crushing strength has recently been established. Hence, the cold crushing strengths can provide, and have a direct indication about the predictability of a refractory material regarding its resistance to abrasion. (Schacht, 2004)

2.12 Thermal Properties

2.12.1Thermal expansion

This is a measure of the linear stability of the refractory when it is exposed to different ranges of high temperatures and then cooled at room temperature. It is defined as a permanent linear change (ASTM C-113) and is measured by the changes in the longest linear dimensions. Most refractory materials expand when heated; hence when refractories are installed at room temperatures, the whole structure tightens up when heated. But if the temperature reaches higher than the softening temperature of the bonding system, the structure may distort or collapse. Hence, refractory system should always be designed in such a way that the maximum temperature attainable in the system is lower than the softening or melting temperature of the refractory ingredients (grains and bonding system).

2.12.2Thermal shock (spalling) resistance

This is a measure of the refractory property when the refractory is exposed to alternate heating and cooling. Most high temperature processes experience heating

and cooling and both refractory grains and the bonding system expand while being heated and contract during cooling. (Schacht, 2004)

The thermal shock resistance depends on the matrix bonding and the grains. Thus, refractories having structures with built-in micro cracks of defects show better thermal shock resistance than those with rigid systems. In some refractories, the bonding system, by nature possesses micro structural defects or cracks that provide better thermal shock resistance.

2.12.3 Thermal conductivity

This is the ability of a refractory material to conduct heat from the hot to the cold face – when it is exposed to high temperatures. It depends on the nature and porosity of a material and on the temperature. It diminishes with increasing porosity. Except for rare cases when high conductivity is desirable (e.g. crucibles), refractories should have a low thermal conductivity.

2.13 Chemical Properties

2.13.1Corrosion/Erosion resistance

The chemical properties of a refractory are defined by the chemical analysis of the refractory grains, by the nature of the bonding, and also by the ability of the refractory to resist the action of liquids when exposed to high temperatures. (Schacht, 2004). When refractories are exposed to corrosive liquids at high

temperatures, the extent of corrosion/erosion depends on the refractory grains and the chemical bonding system of the refractory.

Refractory corrosion may be caused by mechanisms such as dissolution in contact with liquid, vapour-liquid or solid-phase reactions. (Schacht, 2004). It may also occur due to penetration of the vapour or liquid in the pores, resulting in an alternate zone. In most cases, corrosion is the result of some combination of these factors. The nature and rate of dissolution of a refractory in a liquid can be calculated from a phase equilibrium diagram. A concentration gradient occurs in the refractory composition at the boundary region when the refractory comes in contact with the molten slag. The refractory components diffuse through the interfacial film and dissolve in the liquid. The interfacial film influences the rate of dissolution. The larger the concentration gradient, the faster the dissolution rate and thus the refractory dissolves more readily.

Corrosion/erosion resistance is one of the most important characteristics of refractories, which are exposed to molten metal and slag, hence during the formulation of a refractory, close attention is given to a refractory composition in choosing the refractory grains and bonding system. Thus, refractories used in an iron-making process will differ from that of a steel making process since the nature of the metal and slag is different in these cases. In iron-making, the metal and liquid slag is primarily neutral or slightly acidic in nature, whereas the slag is

distinctively basic in the steel making process. Refractories chosen for iron making are based on alumina and silica, whereas magnesia-base refractories are the choice of steel making (Schacht, 2004).

2.14 Service Properties

While some authors viewed the properties of refractory material as stated above, others put into consideration some of the service properties. These are properties that are more relevant to the in-service performance of a refractory. Knowledge of these properties gives a closer indication of how a material may act in a particular application. Hence, it is established that not only must a refractory withstand the maximum service temperature of the furnace but in many cases it must also resist spalling, heavy loads, dimensional changes, abrasion and erosion or corrosion caused by liquid and gases. Among these properties are;

2.14.1 Refractoriness

According to Mark (2007), refractoriness of a material is its ability to withstand high temperature with no load applied. Its degree in aluminosilicate refractories depends on the content of alumina. Refractoriness is measured by a standard technique and practically reported in pyrometric cone equivalents, PCEs which measures the softening point of a refractory material by comparing the behaviour of its test cone with reference cones of standard composition designated by PCE values between 12 and 42 Orton series. The PCE value assigned to the test

specimen is that of the reference cone whose tip touches (since it softens and deforms under its own weight as temperature rises) the ceramic plague (on which the cones are mounted) at the same time as does the cone (ASTMC 71-81).

It is not generally practicable to measure the melting point of a refractory since melting extends over a range of temperature, however, at a higher temperature where the proportion of liquid exceeds a critical value which may depend on its viscosity, the material will either collapse and appear liquid or pasty or will exude liquid and collapse slowly later. (Chima, 2015).

Idenyi and Nwajagu (2003), noted that since refractories in service are usually expected to withstand loads due to the weight of the furnace parts and contents and other stresses induced by temperature change, what matters in practice is not necessarily refractoriness, but the refractoriness under load (RUL).

2.14.2 Linear shrinkage/Dimensional stability

This is a measure of the change in dimension of a refractory either in terms of expansion or contraction. (Schacht, 2004).The shape and size stability of refractories is very important as it indicates the maximum expected dimensional change in a stress-free condition.

Chima (2015) noted that low permanent linear and volumetric changes are generally desirable, as they indicate good material stability and minimize shrinkage to prevent loosening of a refractory lining in service.

2.15 Manufacturing Processes of Refractory Bricks

Fireclay refractories are prepared from refractory clays whose principal constituent is kaolinite, $Al_2SO_3.2SiO_2.2H_2O$, with additions of ferric oxides, alkali and alkaline earth elements as impurities. The exact chemical composition of any particular clay deposit or sample is revealed by chemical analysis. The alkali metals (Na, K) can be removed or reduced by washing the clay.

The most characteristic properties of clays important for brick making are plasticity, binding capacity (workability index) and sintering capacity. Plasticity ensures that particles can slip relatively to one another and at the same time the bonding between them is retained. Binding capacity of clays, i.e., capacity of combining non-plastic or inert materials into a uniform plastic mass, to a great extent depends on their plasticity.

It has been noted that clays lose their plasticity on drying at 110^0C but restore this property upon addition of water. The plasticity lowers with increasing temperature and disappears entirely on heating above 450^0C. Thus fireclay can be calcined to set a non-plastic material called chamotte or grog. Again, clays are sintered into a stone-like crock when heated up to 800^0C. Hence, brick can be produced from them.

The mixture for making fireclay brick is made up of refractory clay, chamotte and crater. The clay is preliminarily dried, finely ground and screened to obtain a

fraction under 0.5 mm (500μm). The calcined clay (chamotte) is also grouped-up and screened.

Refractory clay shrinks substantially on roasting, which results in cracking. The shrinkage of fireclay bricks is diminished by the addition of chamotte or grog, which is a lean substance. The smaller the particles of clay, the better they can envelop the larger particles of the leaner, which is needed to obtain a mass of a good moulding ability. The proportion of clay and chamotte in moulding mass is determined by the plasticity of the clay. (Mark, 2007).

According to Gilchrist (1977), each kind of brick is made from a different raw material and its treatment usually involves some very special features. However, for general principles, the following procedures are involved in the process of brick production.

2.15.1 Identification and collection of raw materials. The raw materials for the production of refractory bricks are mineral deposits – clays, sand, ores, and rocks – which must be mined or quarried and then crushed. The materials if imported, is usually bagged to maintain purity.

2.15.2 Crushing. Crushing is carried out by simple ore-dressing equipment and materials are graded and stored by size. The composition of the brick is adjusted by blending the materials along with any flux or bond additions that may be required. Blending is however; not only by composition but also by size and the properties

of the product depend very much on this stage. Low porosity can be attained by using a “close packing grading” such that interstices between the largest particles are filled by a smaller grade and residual interstices filled by a smaller grade again. Thus, there is some control on the ultimate porosity and on strength, for the maximum number of contacts will also be made with the closest packing.

In basic bricks the coarse and fine fractions are sometimes of different composition and the fine fraction ultimately acts as the bond. “Grog”, or prefired materials, may also be mixed in at this stage. This may consist of broken and crushed scrap brick but sometimes specially hard fired material is prepared for the purpose.

2.15.3 Blending

Blending is carried out in a paddle mill with a kneading action where addition of water and bonds (sometimes temporary) are added. Clays attain some plasticity at this stage. Fireclay bricks can be moulded by plastic or semi-dry method. With the plastic (soft mud) method, the moulding mass may have moisture content of 16 to 25 percent depending on plasticity and sintering capacity of the clay. Also, the moulding mass is made up of 50 to 60 percent chamotte and 50 to 40 percent kaolinite clay. The content of chamotte is taken at the upper limit if the refractory clay used has a good plasticity. The mixed mass is pressed in a mould at a pressure of 295-590N/cm^2 into raw bricks. The shrinkage of bricks on firing is 3-4%

Gilchrist (1977) added that hand-moulding is most successful with plastic mixes usually rather wet (14-20% water), which can be "thrown" into the wooden box-type mould and relied on to fill it. He also noted that it's cheaper than machine-moulding on a jobbing basis, but the machine is preferred for mass production.

Another forming process is slip casting, applicable mainly to clays which can be formed into a colloidal suspension with water and poured into a mould of plaster of paris which absorbs the water and causes a uniform deposit of clay to build up in the inside of the mould. This is useful for awkward shapes and for hollow wares. It is also used for special refractories which are prepared from very fine powders.

2.15.4 Drying

Bricks must be dried. This is conducted either on large drying floors (heated by waste heat from kilns) where the bricks are laid out in open array, or in tunnel kilns where they are stacked on bogeys and passed through a tunnel against a stream of hot air. This is faster and more compact process but cannot readily be adopted where sizes and shapes are not fairly constant (Gilchrist, 1977). Drying is done to eliminate the hygroscopic water and increase green strength of bricks.

2.15.5 Firing

The final temperature of firing does not exceed 1400^0C. the firing schedule should be carefully planned. It is recommended that a low heat be applied first to the green bricks in order to drive off any residual moisture – a process known as water

smoking. Heating and soaking (holding at temperature for some time) should be applied to allow complete heat diffusion and phase transformations. Once heating is discontinued, the bricks should be allowed to cool with the furnace/kiln to avoid rapid cooling rate (Mark, 2007).

2.16 Method of Testing of Refractory Properties of Materials

Selecting the most suitable refractory materials to prolong service life and make a process more cost-effective is now more critical than ever in today's society. It is important to carefully assess materials to ensure that they are suitable for the environment and conditions in which they will operate. Hence, testing refractory materials is therefore an essential step in selection and improvement process.

According to Chima (2015), refractory materials are given specific test for the following reasons:

- To characterize new material
- For quality control of processes and product
- To help rank and select materials for a particular application and predict in service behavior.
- To examine the effects of service condition.
- To establish properties required for mathematical modeling to compare current and new designs.

A wide range of test methods is available to measure all aspects of refractory behaviour. The majority of tests are characterized as national or international standards..

These tests are grouped under

- Characterization/data sheet properties test
- Service related test
- Design test.

In characterization test, the first test is the chemical analysis which gives the elemental composition in the refractory. Generally, the quickest and most commonly used method is by x-ray fluorescence. The technique is based on the phenomenon that each element fluoresces characteristically when exposed to x-ray. The result for each element present is usually reported as oxides. However, the technique is not viable for elements low in the periodic table (from fluorine downward).

The mineralogical analysis is done by the help of x-ray diffraction (XRD) analysis. This provides a means by which different crystalline phases can be characterized and identified. X-ray diffraction works by diffracting incident x-rays along crystallographic planes. The angle by which x-rays are diffracted is in accordance with Bragg's law in which

$$n\lambda = 2dsin\theta$$

Where n is an integer value

λ is the wavelength of the diffracting x-ray.

d is the spacing between successive diffracting planes in the crystal.

θ is the angle between the crystallographic plane and the diffracted beam.

The microscopic examination of refractories can range from simple hand lens examination to the use of sophisticated scanning or transmission electron microscopes with magnification in the order of many thousands.

Examination may be conducted on the surface of the refractory, internally to evaluate the normal structure, or across interfaces between materials or material and service environments to evaluate changes that occur. Procedures involved include polishing, which provides greatly improved spatial resolution. This is followed by etching to enhance features like grain boundaries and phase identification.

Evaluating the microstructure of a refractory material is necessary to examine grain structure, grain distribution, bond mechanisms and degree and distribution of porosity which all control the in-service behavior.

Other properties test including design and service properties test are as stated in the literature. (Gilchrist, 1997).

According to the scientist, empirical tests have been developed. The following tests are commonly carried out. British Standard Specifications are available for some

of them and details can be found in B.SS (1952). Similar series of tests are specified by the American Society of Testing Materials (ASTM)

2.16.1Test for expansion (or Contraction)

This is determined by heating a suitable sample of bricks for a prolonged time at the proposed working temperature. The cut sample is measured before and after treatment to determine the permanent change in dimensions which should of course be small.

If the expansion (usually a contraction) is too great, more thorough firing is required or another kind of brick. High values lead to severe cracking of furnace walls during use, or to distortion of the structure. A small expansion is preferred to give tight joints and for some special purposes like ladle linings , a fairly high value is deliberately arranged.

2.16.2 Test for refractoriness

The test for refractoriness is to compare the sagging of a “cone” of the material (either cut from the solid or made up from powder and a bond of dextrin) with that of standard Seger cones, when they are heated together, at a standard rate in an oxidizing atmosphere, until the test cone bends over. The number of the best matching seger cone is quoted as the refractoriness of the brick; or its nominal melting point (which can be checked by pyrometer) is referred to as the pyrometric cone equivalent (PCE) temperature.

2.16.3 Test for hot strength

This is very important in high quality bricks but is not measured directly. Instead it is a temperature that is determined – that at which deformation under standard load is rapid. The test is called the refractoriness under load test (R.U.L.). A constant load of 100 or 200Lb (or 25 or 50Lb/in^2) is applied to a prism of brick 2 inches square by 3½inches. The specimen is heated in a carbon granule furnace at a standard rate (10^0C/min) and a record of its height made, preferably by plotting, until the test piece collapses or sinks to 90 percent of its original length. The refractoriness under load may be quoted as the range of three temperatures:

1. Initial softening
2. Rapid collapse
3. Total collapse.

2.16.4 Test for thermal shock resistance

This is measured by a spalling test. There is no fully standardized test but materials can be compared using constant test conditions and these should be chosen to suit the brick under test and the working conditions under which it is to be used. For example, silica bricks have excellent thermal shock resisting properties above 300^0C if properly made, but shatter if cooled quickly below that hence any spalling test on silica must avoid cooling under 300^0C.

Various tests used involve heating either a brick or a prism cut from bricks, slowly up to a working temperature and then cooling it rapidly for 10 minutes in a cold air jet, or on a steel plate, then reheating for 10 minutes in the furnace held at the working temperature. This is repeated until a piece of the brick becomes detached. The number of cycles to failure is noted. A brick surviving 30 cycles is claimed to be very good and quoted as having a spalling resistance of +30 cycles. A more adequate method of heating involves heating and cooling applied to the face or end only and not along the sides as well.

The result of a spalling test must depend on at least four properties of the brick.

- Its thermal conductivity which determines the temperature gradients set up under the test conditions;
- The coefficient of thermal expansion which determines the strain induced by these thermal gradients.
- The modulus of elasticity.
- The shear strength of the brick substance, which together determine the stresses set up and whether or not they will be relieved by crack formation or propagation. The formation of crack during early cycles would probably modify the temperature distribution during the later cycles in favour of even more severe stresses so that cracks once formed are likely to get worse.

2.16.5 Test for slag resistance

There are many ways to test this property but the most common one involves drilling holes in the brick and packing these with samples of typical slag likely to be encountered. The assembly is then heated to a working temperature for about an hour, cooled and sectioned. The extent of the penetration of slag into the brick is noted and compared with others. This method takes some account of the effect of brick texture and slag surface tension as they affect reaction rates.

2.16.6 Test for apparent porosity and bulk density

These are determined in one and the same test in accordance with ASTM C 20-80a, standard test methods for apparent porosity, water absorption, apparent specific gravity, and bulk density of refractory bricks and shapes of boiling water (Mark, 2007).

Alternative method is by evacuation in a vacuum dessicator and flooding with paraffin (Gilchrist, 1977). After determining dry weight of brick (W_d), weight when soaked in water (W_s), and weight suspended in air of the previous soaked specimen (W_a), the apparent porosity (P_a) and the bulk density (D_b) are calculated from the relationships.

$$P_a, \% = \left\{\frac{W_a - W_d}{W_a - W_s}\right\} \text{ x } 100 \qquad (2.2)$$

$$D_b, g/cm^2 = \left\{\frac{W_d}{W_a - W_s}\right\} \qquad (2.3)$$

2.16.7 Test for cold crushing strength

The ASTM C-93-67 (reapproved 1977); standard test methods for cold crushing strength and modulus of rupture of insulating firebrick specify this. The testing machine is a mechanical or hydraulic compression-testing machine with a sensitivity of at least 89N in the range 0 to 67kN. The hydraulic type is preferable, though a universal strength-testing machine is the best.

A dial-type micrometer is generally used for obtaining the necessary measurement for calculating the percentage of deformation during the compression. The cold crushing strength, S, is calculated from;

$$S = \frac{W}{A} \qquad (2.4)$$

Where W = total maximum load at 3% deformation or at visible failure, whichever is small, N;

A = average of the gross areas of two faces of the specimen compressed, mm^2.

2.16.8 Test for moisture content of moulding mass

The ASTM C 72-76, standard test methods for sieve analysis and water content of refractory materials, specifies this test. About 50g of material is required. The test sample should be obtained quickly to avoid loss of water. It is weighed to the nearest 0.1g both before and after drying for 3 hours at 105 to 110^0C. The moisture content is calculated as a percentage to the nearest 0.1% on the as received basis, thus:

$$\text{Moisture content, \%} = \left\{\frac{Wet\ Mass - Dry\ mass}{Wet\ mass}\right\} \text{ x } 100 \qquad (2.5)$$

2.16.9 Test for linear shrinkage

This is usually determined by measuring the dimensions of green bricks, and comparing with the dimensions of the fired product. It is expressed in percentage and is calculated using:

$$\text{Linear shrinkage, = \%} \left\{\frac{L_g - L_f}{L_f}\right\} \text{ x } 100 = \frac{\Delta_L}{L_f} \text{ x } 100 \qquad (2.6)$$

Where L_g and L_f are the green length and fired length of brick respectively.

2.17 Previous Research Works on Refractory Clays

Nnuka and Enejor (2001) reported that the characteristics properties of clay determine the areas of application and that it is influenced by the chemical structure of the dominant minerals while Nnuka and Agbo (2000) showed specified values of different oxide composition for clay and used it to classify clay into low melting, high melting and refractory clay. Yami (2007) and Omowumi (2001) showed specified internationally accepted values of refractory properties and used them to compare local clays. Most of these properties especially linear shrinkage, porosity, density and thermal conductivity are inter related (Nnuka et al, 1992).

Hence high alumina content suggest high value of refractoriness while high alumina to silica ratio is a strong indication of high refractoriness under load and low silica suggest high melting point. Nnuka and Agbo (2000) stated that fire clay must have 25 -40% alumina and 50 - 70% silica. However, Nnuka and Apeh(1997) put it that 20 -40% of alumina in clay qualifies it for siliceous fire clay. High Fe_2O_3 suggest reddish color of clay, CaO gives relatively high plasticity while sodium form flux which contribute to degrade alumino silicate refractory.(Nnuka et al, 1992). Phosphorus oxide has advantages in clay material by forming phosphate bond when reacted with alumina to produce non wetting effect against molten metal, resistance to CO attack and excellent thermal shock resistance.(Decker in Siljan, 2003 and Chung, 2003)

2.18. Summary of Reviewed Literatures

Previous research works in industrial applications of refractories have proved that there is no single material with the capacity of providing all the required properties demanded by the requirements for a particular service. In one way or the other, a material may be deficient in an area while at the same time, it may be found efficient in another area depending on the factors which are put into consideration.

The stated industrial challenge has prompted technological researches to look inward and consider the idea of blending more clay samples with varied chemical compositions and properties to achieve a combination of desirable properties required for different applications. It has also led to the use of some industrial waste materials (which may even constitute environmental hazards), as additives to clay material with intention of performance enhancement of the desired properties of refractory material.

This idea has not only added to the improvement of refractory properties, but it has yielded a process that converts waste to wealth – an idea that will move both the economic and technological status of the nation forward. This forms the basis for this dissertation..

The recycling of industrial wastes as alternative raw material is not a new process and has been done successfully in many countries. So many of these wastes have been converted into useful additives which were incorporated into the matrix of

clay products to form useful refractory materials that met international industrial standards.

Previously, foreign researchers like Rahman (1988) produced bricks using uncontrolled burning of rice husk and reported that the ash has potential to increase the compressive strength of bricks.

Gutierrez and Delvasto (1995) worked on the use of rice husk in ceramic bricks to produce fireclay brick using roasted rick husk (RH) and controlled burnt rice husk ash (RHA). They concluded that the brick containing controlled burnt rice husk ash gave better results than the brick incorporated with ground roasted rice husk.

Recently, Danupon (2008) investigated the potential use of uncontrolled burnt rice husk ash to produce lightweight fireclay brick. From the results obtained, it was found that lightweight brick could be produced by increasing the rice husk ash replacement though the compressive strength of the brick was reduced.

Izwan et al, (2011) investigated the influence of different types of rice husk ash on the chemical and physical properties of fire clay. The work was restricted to only rice husk though of different types. Controlled burnt rice husk ash (CBRHA), uncontrolled burnt rice husk ash (UCBRHA) and ground rice husk (GRH) were used. The research came to the following conclusions:

- The silica (SiO_2) content for UCBRHA was found to be the highest compared to CBRHA and GRH. However, the setback for this material was that the carbon content detected in UCBRHA led to a porous structure.
- The thermal analysis showing the changes in the clay when heated proved that the clay started losing water when heated up to 250^0C and that dehydroxylation of clay occurred between 500 - 570^0C.
- Among the materials used for the work were clay, GRH, CBRHA and UCBRHA, the percentage of loss of ignition (LOI) value was 8.75%, 3.53%, 2.02% and 0.79% respectively. It was concluded that the high LOI value in clay was because the clay by nature contained more water in the grains.
- The water adsorption of clay, GRH, CBRHA and UCBRHA were 0.991g, 0.9337g, 0.2644g and 0.1475g respectively.

In all the works, investigation was restricted to limited number of properties of refractories. Considering the fact that other useful properties of refractories like strength, abrasion resistance, corrosion/erosion resistance, linear shrinkage, volume stability, etc count when considering the service behaviour of refractory materials, it can be concluded that the works were incomplete. Also, other wastes thatcould be used to enhance performance of materials were not considered. Besides, the researchers studied the influence of chemical properties on the said material but did not investigate the chemical composition of the composite materials when the

additives were incorporated. This would have enabled them to consider the changes in the chemical/elemental analysis of the new material and compare with that of original clay. This would have led to more credible inference, hence more logical scientific conclusions. This therefore raised the need for this research.

Ajay et al; (2012), investigated the properties and industrial applications of rice husk and concluded that bricks made using rice husk developed many pores during heat treatment due to burning out of organic material. The study also showed that the more the percentage of rice husks in a brick, the more porous would be the brick and therefore better the thermal insulation. Hence, it was concluded that the presence of entrapped air in pores have thermal insulating characteristics and so make the porous fire brick structure suitable only for back up insulation.

Viewing the above work from experimental point of view, it will be observed that information relating to the mixing ratio between rice husk and clay was not taken into consideration neither was there any range for lower and upper limit for the husk below which or beyond which the properties could be impaired or stabilized. Beside these, detail explanation was not given regarding the most relevant refractory properties of clay that may be affected by the addition of rice husk. Therefore, there is much need to explain the work further with clearer experimental details.

Furthermore, Odo et al; (2013) produced fireclay insulating bricks from a blend of clays and rice husks. A blend of two Nigerian clays (Nafuta and Nsu clays) were formulated at the ratio of 7:3 and further decreased Nafuta clay sample in proportion to the quantity of rice husk addition. Though many properties of the clay were investigated but the emphasis was on porosity as a property which is considered most important for distinguishing insulating bricks from conventional dense bricks. The researcher did not consider the chemical composition of the rice husk which is believed to have influenced the clay properties. Hence the chemistry of the reaction process was not accounted for.

Similar work on the insulating effect of rice husks addition on the mechanical properties of clay samples from Kaduna state in Nigeria was carried out by Manukaji, (2013). The scientist varied the proportion of rice husk from (0-40)% at 5% intervals and observed that increasing the percentage addition of rice husk gave refractory properties that were close to the range of international accepted standard thereby concluding that the addition of the rice husk has the capacity of improving their insulating properties. Though the work was considered elaborate, but it still lacked explanations on the chemical compositions of the rick husk addition used.

Furthermore, all these works done by these researchers were centered on the use of one additive (rice husk). There is need to combine two or three additives and observe if there will be better improvement of the properties in question.

Alternatively, other researchers including John and Olayinka (2014) considered the use of sawdust additive as a better option. They explored the effect of sawdust on the insulating property of Ikere clay as refractory lining. It was observed that the presence of air in these pores reduced the conductive capacity of the refractories, thereby increasing their insulating characteristics. The investigation covered properties like porosity, thermal conductivity, linear shrinkage and bulk density. It was observed and recommended that better results could be obtained if other agricultural wastes were used in the same way.

In this research, the use of those other agricultural wastes like saw dust, groundnut shell and rice husk will be used in three and two combinations at different mixing ratio to determine the level of improvement or deterioration of the desired properties of fireclays.

Fatai (2012) characterized porous insulating fire bricks from Ifon clay with varied sawdust admixture from mahogany tree. He varied the proportion of the admixture and fired in the furnace at 1000^0C. The results concluded the following:

- Porosity of the samples varied inversely with the thermal conductivity, cold crushing strength and bulk density of the samples.
- The porosity of the samples could be controlled by varying the percentage sawdust admixture.

- For structural insulating fire brick where the compressive strength is also important, the percentage saw dust admixture should not exceed 10 to 15 percentage.

Folaranmi (2009) reported on the effect of sawdust additive on the properties of clay from Minna, Nigeria when properties of clay like, bulk density, porosity, permeability, shrinkage on firing, cold compressive strength, refractoriness, thermal shock resistance and thermal conductivity were examined. By varying the percentage addition of sawdust from mahogany wood in the clay sample, it was observed that while some properties were improved with addition of sawdust, others were not.

Also Manukaji, (2013)A used the same sawdust on the clay sample from the Federal Capital Territory of Nigeria Abuja to investigate the effect of the sawdust on the insulating properties of the clay. The author characterized the clay considering properties like linear shrinkage, solid density, apparent porosity and thermal conductivity. Results obtained proved that both, linear shrinkage, solid density, porosity and thermal conductivity all improved to international standard on addition of sawdust from (0-40) %. The results of the study also showed that the 40% sawdust addition was the maximum, under which mechanical strength and other refractory properties of clay will remain stable. The scientist then established

from the study that by varying the proportion of the additive, particular insulating property desired could be achieved.

Considering the research work and corresponding results obtained from the three different researchers (Fatai, 2012; Folaranmi, 2009; Manukaji, 2013,) who investigated the same properties of refractory clay, it is observed that there is inconsistency of findings. For example, Manukaji, (2013) reported that between (0-40)% addition of sawdust, all the properties were influenced positively while Folaranmi, (2009) reported that while some properties were improved, others were either impaired or not affected at all. Fatai, (2012) had it that porosity varied inversely with other properties and added that the range of percentage addition of sawdust should not exceed (10-15) % contrary to Manukaji's (0-40)%.

The present study would like to lend credence to or differ from these positions based on experimental results.

Hassan et al (2014), considered sawdust and rice husk as additives that could affect the properties of refractory clay but the study used the additives separately on the clay. The physical and chemical properties of the original clay before blending it with either sawdust or rice husk were investigated for properties such as refractoriness, fired shrinkage, apparent porosity and thermal shock resistance. The results obtained proved that refractoriness reduced from 1300^0C to 1200^0C on addition of both sawdust and rice husk; shrinkage reduced from 3.89% to 3% on

introduction of additives while thermal shock resistance of samples with additives were ten times better, porosity of the sample with rice husk additive was 36.74% while that of the sample with sawdust was 45.34% as compared with that of the pure clay sample which was 27.15%. Density reduced from 1.98g/cm^3 to 1.59g/cm^3 and 1.52g/cm^3 on addition of sawdust and rice husk respectively. The chemical composition tests showed a decrease in silica content from 62% to 54% on addition of additives; alumina content reduced from 20% to 12% while iron oxide content increased from 7.58% to 8.38% and 7.99% on the addition of sawdust and rice husk to the clay respectively.

With these results, it was observed that there is need to blend the two additives (sawdust and rice husk) with the clay and invesigate the change in the properties. It will be also interesting to incorporate another additive like groundnut shell which is expected to raise alumina content to take care of the fall in the refractoriness. If the additives are uniformly blended to the clay which serves as control experiment, it is expected that better result can be obtained. That is also the pursuit in the present research work.

Manukaji (2013)B on a second attempt after using sawdust studied the suitability of groundnut shell as additives to improve the insulating properties of clay samples in Kogi state while investigating four mechanical properties – linear shrinkage,

thermal conductivity, apparent porosity and solid density. The results showed significant improvement in these properties.

Hassan, (1985) investigated the effect of additives like saw dust, graphite and asbestors on Kankara clay and reported that a good thermal insulating fire clay brick could be produced from this clay by the addition of graphite and saw dust at 15% composition.

Nuhu and Abdulahi, (2008) explained that selected clay could be properly blended with other additives to improve their physical, thermal and chemical properties of the final product.

In all the works reviewed most of the authors did not analyze the chemical composition of the additives used. This could have helped them to predict the direction of expected result. For instance, materials that have high alumina content may likely improve the refractoriness of the clay. Those that have low melting point elements/compounds will have the tendency of melting at earlier stage of firing thereby closing the pores, densifying the clay, reducing porosity and affecting linear shrinkage.

Some compositional parameters like the silica and alumina ratios were not put into consideration. Good knowledge of these parameters are useful in knowing the proportion of aluminate phase, silica phase and ferrite phase with the intention of predicting the direction of possible result in service performance.

CHAPTER THREE

MATERIALS AND METHODS

3.1 Materials

The material used in the research work were two clay samples from Nguzu Edda deposit and Amaiyi Edda deposit both from Ebonyi State, rice husk, groundnut shell, gmalina sawdust and water.

3.2 Equipment and Tools

The equipment and machines used in the work include computerized Empyrean X-ray diffraction equipment in National Steel Raw Material Exploration Agency Kaduna, X-ray fluorescence, scanning electron microscope (SEM) Zeiss model EV010, electric furnace, (Thermodyne 46200) and ceramic kiln model 88FC2468, electrical transversal strength machine model 235, digial weighing machine, spiral balance, sieves, mortar, pestle, moulds, pair of tongs, strong thread, heat conduction testing machine model H9406/02877PA Hilton, pyrometric cone, meter rule and venier caliper.

3.3 Raw Material Sourcing

The clay materials used in this research work were obtained from Amaiyi and Nguzu Edda deposit both in Afikpo South LGA, Ebonyi State, Nigeria. Other raw materials that constitute the local content input were rice husk sourced from rice mill in Abakaliki, Ebonyi State, gmalina sawdust collected from Abakaliki timber

market Nkwagu Abakaliki and groundnut shell collected from Kpirikpiri market in Abakaliki. Figure 3.1 shows the map of Ebonyi State with locations of the various areas where the raw materials were sourced.

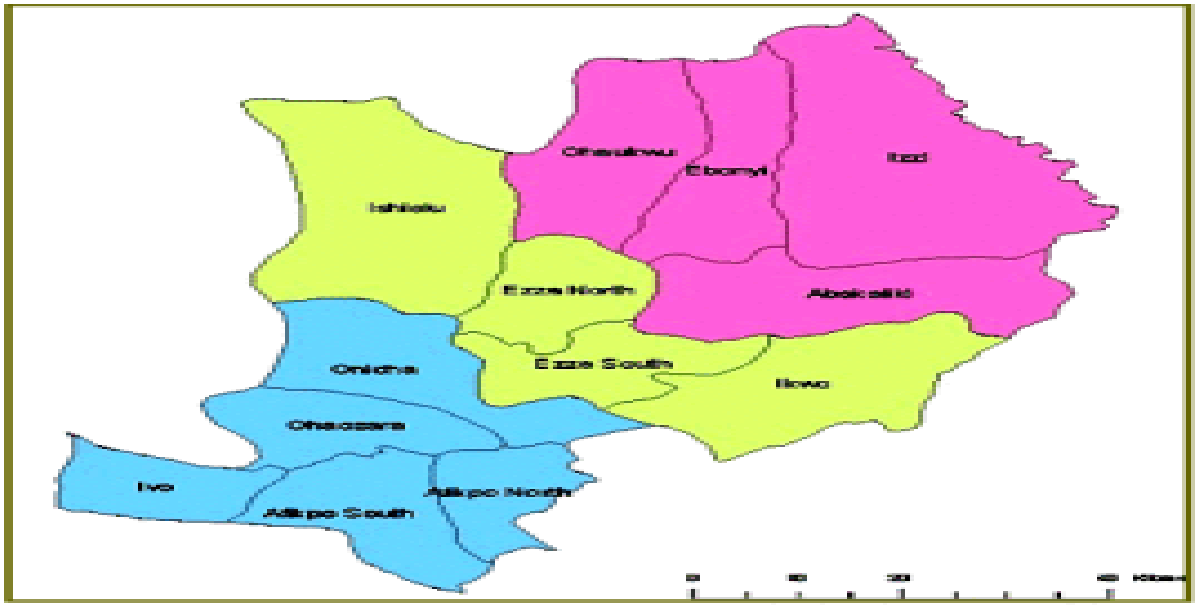

Figure 3.1 Map of Ebonyi State showing Afikpo South and Abakaliki Local Government Areas

Source: http://www.ebonyionline.com

Ebonyi State is one of the 36 states in the federal republic of Nigeria. It was created out of Enugu State in October 1996.

The state is one of the five states that make up the south east zone of the present six geopolitical zones in the country. It is administratively divided into 13 local governments under three senatorial zones namely:

Ebonyi North comprising of Abakaliki, Ebonyi, Ishielu, Ohaukwu and Izzi LGAs. Ebonyi Central comprising of Ikwo, Ezza North and Ezza South LGAs. Ebonyi South comprising Afikpo North, Afikpo South, Ivo, Ohaozara and Onicha LGAs.

The state shares border with Benue state to the north, Enugu state to the west, Imo and Abia to the south and Cross river state to the east. Ebonyi State lies between $7^0$3N and $5^0$4E longitudes, with a land mass approximated at 5,932 square kilometers.

The area is naturally endowed with enormous mineral resources among which are: lead, limestone zinc, marble, gypsum, lignite, clay , false gold, etc. http://www.ebonyionline.com

3.4 Chemical Analysis of Raw Materials

Samples of the two clay materials and the local additives (groundnut shell, gmalina sawdust and rice husk) were analyzed to determine their chemical constituents and mineralogical composition. The chemical analysis was carried out at Defense Industries Cooperation of Nigeria (DICON), Kaduna, Nigeria using X-ray Fluorescence (XRF) analysis technique while the mineralogical composition analysis was done in National Steel Raw Material Exploration Agency, Kaduna using computerized X-ray difractometer that uses Cu Kα radiation at a scan speed of 4^0/min 2Θ.

3.5 Raw Material Preparation and Processing.

The raw clay samples were air dried and crushed in a mortar to grain size of 0.425mm. The samples were soaked in a plastic container that contained 15 liters of water. The mixture of clay and water was stirred vigorously to ensure proper dissolution and allowed to settle for three days.

The dissolved clay was then filtered through a 0.425 mm mesh sieve to get rid of unwanted particles and plant materials. The filtrate was further sieved using a mesh sieve of size 0.18 mm in order to obtain finer particles. The filtrate was allowed to settle for three days after which excess water was decanted off. The clay slip obtained was sun dried for 2 days and then dried in an oven at 100^0C.

The processed dry clay was pulverized and then passed again through a 0.18mm mesh sieve. Each of the clay samples was mixed with 35% weight of water and moulded using different mould sizes that suited the respective tests they were to be subjected to. Nguzu and Amaiyi clays were later blended at ratios 10:90, 30:70, 40:60 and 50:50 to produce twelve different blends (three from each of the four compositions BL1, BL2, BL3 and BL4 respectively.

The second phase of the experiment was carried out with the incorporation of sawdust, groundnut shell and rice husk into sample BL3 i.e. 40:60 ratio. The choice of the blending ratio of the two clays was based on alumina content which

was more in Amaiyi clay while the additives were blended at 5%, 10%, 15% and 20% formulations. Based on these, the following test samples were developed:

- Blended clay with groundnut shell BGS1, BGS2, BGS3, BGS4 for the four different formulations.
- Blended clay with gmalina sawdust BMS1, BMS2, BMS3, BMS4 for the four different formulations.
- Blended clay with rice husk BRH1, BRH2, BRH3, BHR4 for the four different formulations.

Furthermore, a combination of the three local additives (saw dust, groundnut shell and rice husk mixed at equal proportion) were blended to the experimental control sample (BL3) in the same four different formulations of (5, 10, 15 and 25) % ratios respectively to have four sets of test samples coded E_1, E_2, E_3 and E_4 respectively. Combinations of two additives of sawdust and groundnut shell were blended to the sample at the same formulations to have another four sets of samples D1, D2, D3 and D4. The same procedure was repeated with blended rice husk and groundnut shell to have another four sets of samples coded F1, F2, F3 and F4.

3.6 Moulding of the Test Samples

Each of the samples was mixed with 35% weight of water to make it plastic for moulding. The clay was then moulded into three different shapes using metallic moulds with the application of used engine oil lubricants to the surface of the

moulds to ease extraction of the test pieces. The first shape was circular with 40mm diameter and 4mm thickness for thermal conductivity test. The second shape was a rectangular prism with length 8cm, width 4cm and height 1.5cm for linear shrinkage, bulk density, apparent porosity, refractoriness and thermal shock resistance tests while the third was also a rectangular prism with length 9.5cm, width 2cm and height 1.5cm used for modulus of rupture test.

The moulds were used for forming the bricks. An improvised wooden material was prepared which was used for transmitting the necessary moulding pressure to the mould when the required quantity of plastic moulding mass was fed in. After pressing, a suitable wooden plunger was used to extrude the green brick from the mould. The extruded green bricks were given a 50 mm mark using venier caliper and thereafter weighed to take the individual green weight. The test samples were sundried for two days, oven dried to 110^0C and finally fired to 1200^0C before cooling and testing for the properties.

3.7 Determination of the Refractory Properties of the Materials

The refractory properties tested in this research study were grouped into three categories:

- Physical and service properties
- Mechanical properties
- Thermal properties

The physical and service properties included linear shrinkage, apparent porosity, and bulk density.

The mechanical property that was investigated is the modulus of rupture (MOR) while the thermal properties included thermal shock (spalling) resistance, refractoriness and thermal conductivity.

3.7.1 Linear shrinkage

This test was done to determine dimensional stability of the sample after a given period of time and temperature change and the testing method was according to ASTM C-326 for testing linear shrinkage of refractory material. In all the stages of shrinkage taken, 50 mm points were marked on the surface of the test green sample. The test was carried out in three stages as follows:

The first one is the dry shrinkage. The green test sample which was given a 50 mm mark (L_o) on the surface was dried in the kiln to a temperature of 100^0C and thereafter the sample was brought out. The same previous 50 mm mark was measured to get the new length of the points after drying (L_d). Where L_d is the new dry length of the two marked points. The same specified length on the test sample was used when the sample was fired and the new dimension of the length was taken as fired length L_f. The dry-fired shrinkage was calculated as:

$$\left(\frac{L_d - L_f}{L_d}\right) \text{ x } 100 \qquad (3.1)$$

3.7.2 Determination of bulk density and apparent porosity

Bulk density and apparent porosity were determined according to ASTM C 20-80a test method. The long rectangular prism shape test sample measuring 9.5cm length, 2cm width and 5cm height was used for these two experiments. Two specimens were fired to the stated temperature in preparation for the test. The dry weight (W_a) in air was taken using digital weighing balance. They were transferred into an aluminum pot containing 3 liters of boiling water and held for 30 minutes after which the boiling was discontinued. The specimens were allowed to cool to room temperature in the vessel of water for four hours. The specimens were then tied to a string into a spiral balance suspended in a beaker of water to get the suspended weight (W_{sp}). The specimens were removed from the water and gently cleaned before weighing again to get the soaked weight (W_{so}).

The bulk density and apparent porosity were determined as follows:

$$\text{Bulk density} = \left(\frac{\text{Weight in Air } (W_a)}{\text{Soaked Weight } (W_{so}) - \text{Suspended Weight } (W_{sp})}\right) \quad (3.2)$$

$$\text{Apparent porosity} = \left(\frac{\text{Soaked Weight } (W_{so}) - \text{Weight in Air } (W_a)}{\text{Soaked Weight } (W_{so}) - \text{Suspended Weight } (W_{sp})}\right) \text{x } 100 \quad (3.3)$$

3.7.3 Determination of mechanical property

The mechanical property tested in this work was the modulus of rupture (MOR) using 3 point bend tester in line with ASTM C-648 standard for testing modulus of rupture. The long rectangular prism test pieces were dried at 105^0C until a constant

weight was obtained. They were fired to their firing temperature of 1200^0C in the kiln.

The electrical transversal strength machine was used to determine the breaking load, P (kg). A venier caliper was used to determine the distance between supports L (cm) of the transversal machine. The height H (cm) and the width B (cm) of the broken pieces were determined. The modulus of rupture was then calculated as:

$$\text{Modulus of rupture (MPa)} = \frac{3PL}{2BH^2} \quad (3.4)$$

Where P = Load applied when the specimen failed

L = Distance between the centre line of the lower bearing edges of the equipment.

B = the width of the broken specimen

H = Height of specimen (cm).

3.7.4 Thermal shock resistance

The method used for this test is the prism spalling test method according to ASTM C-484 in which the spalling resistance was measured by the number of thermal cycles (heating, cooling and testing for failure). This investigation was carried out with the help of electrical furnace (Thermodyne 46200) heated at the rate of 5^0C/min. The test pieces of refractory bricks were thoroughly dried and placed in cold furnace and heated at the rate of 5^0C/min until the furnace temperature rose to 1200^0C. The samples were then removed one after the other using a pair of tongs

and cooled in air (outside the furnace) for 10 minutes, and observed for cracks. In the absence of cracks (or fracture), the bricks were put back into the furnace and reheated for a further period of 10 minutes and then cooled for another 10 minutes. This process or cycle of heating, cooling and observing for cracks was repeated until cracks were observed. The number of complete cycles that produced visible cracks in each specimen was noted. This constituted the thermal shock (spalling) resistance.

3.7.5 Determination of refractoriness

The refractoriness or softening point was determined using the method of pyrometric cone equivalence (PCE) in accordance with ASTM C24-79 (Standard test method of pyrometric cone equivalence of refractory materials) at the Federal Institute of Industrial Research, Oshodi Lagos.

The test pieces were mounted on the refractory plaque along with some standard cone whose softening points are slightly above or below that expected of the test cones. The plaque was then inserted into the electric furnace. The temperature was raised at the rate of 5^0C per minute during which softening of Orton cone occurred along with the specimen test cone. The temperature was further raised until the tips of the test cones had bent over the level with the base. Then the plaque bearing the specimen was removed from the furnace and the test cones examined when cold. The test cones were then compared with the standard cones and the test materials

were assigned the pyrometric cone equivalent (PCE) of the standard cone that it resembled most in bending behaviour.

The refractoriness of each test cone is the number of the standard pyrometric cone that had bent over to a similar extent as the test cone. The temperature corresponding to the cone number was read off from the ASTM Orton series.

3.7.6 Thermal conductivity

The thermal conductivity was determined under steady state condition (i.e. state where heat flow does not depend on time) at room temperature. The test was conducted using heat conduction equipment in Mechanical Engineering Laboratory at Federal University of Technology, Owerri. Circular test specimens measuring 40 mm diameter and 4mm thickness were used for this test. The specimens were inserted and clamped in-between the heater and the cooler faces of the equipment. 5 Watts input power was used to investigate the thermal conductivity of the material.

The stated power inputs was selected and maintained for 30 minutes until steady state conditions were achieved. The temperature T at all six sensor points (three on the heater section and three on the cooler section) were recorded. The thermal conductivity was calculated using Fourier's law as:

$$K = \frac{Q\ dx}{A.dT} \tag{3.5}$$

Where Q is quantity of heat supplied, dx is the specimen thickness, A is the cross sectional area and dT is the temperature difference between the two circular faces.

3.8 Micro Structural Examination

The micro structure of the clay brick was observed using scanning electron microscope (SEM), Zeiss, model EV010. The specimen was sawn and the sawn section of the brick material was dried at a low temperature of 60^0C to remove water. The specimen was then placed in a container and surrounded by epoxy leaving the top surface exposed to air, allowing the low viscosity epoxy to be drawn into the microstructure by capillary suction. The epoxy impregnation of the pore system serves to fill the voids and upon curing, supports the microstructure, helping to restrain it against shrinkage cracking.

The surface was smoothened by grinding using abrasive papers of 220, 320, 400 and 600 grit (silicon carbide paper). Finer grades of abrasive paper were successively used to remove damages produced by the earlier step.

After grinding, the surface of the specimen was polished to remove the damage imparted by sawing and grinding operation. The polishing involved use of sequence of successfully finer particle size diamond polishing pastes ranging from 6 to 0.25µm and a lap wheel covered with a polishing cloth performed manually.

The scanning electron microscope was used to scan a focused beam of electrons across the specimen and the signal from the electron beam interaction with the specimen was measured.

The images reflected the electron resulting from the beam specimen interaction. Computer based image processing and analysis was used to make the imaging possible.

3.9 Design of Experiment for the Effect of Sawdust, Rice Husk and Groundnut shell Additives on the Refractory Properties of Blended Nguzu – Amaiyi Edda Clay

The effect of two independent factors- composition of clay and additives on the refractory properties (responses) of three composite clay bricks each produced with sawdust, rice husk and groundnut shell was investigated using response surface methodology with central composite design type. This involved the development of experimental design, fitting selection and optimization of the best response surface functions for the responses. Thirteen experimental runs were generated with the interaction of the two variables as shown in Table 3.2. The response variables investigated were linear shrinkage, apparent porosity, bulk density, and modulus of rupture.

⌧♋♌③♎ 🗑🗐🗍 ☛♎⑩⓪♏⑤ ⑥♋ ☛❹⑦♎⑨⓪④♎⑤⓿ ♋⑥⑨ ☞③♋❺ ☜③♎⑤♒♎♒ ❸⓪⓿♌ ⌧♋❸♒❶⑩⓿ ☚♒♒⓪⓿⓪❷♎

S/N	1	2	3	4	5	6	7	8	9	10	11	12	13
Factor 1 (Sawdust)	5	20	5	17	4	20	15	6	6	6	6	6	6
Factor 2 (Clay)	95	80	95	83	96	80	85	94	94	94	94	94	94

⌧♋♌③♎ 🗑🗐📋 ☛♎⑩⓪♏⑤ ⑥♋ ☛❹⑦♎⑨⓪④♎⑤⓿ ♋⑥⑨ ☞③♋❺ ☜③♎⑤♒♎♒ ❸⓪⓿♌ ☑⓪♊♎ ✍❶⑩② ☚♒♒⓪⓿⓪❷ ♎

S/N	1	2	3	4	5	6	7	8	9	10	11	12	13
Factor 1 (R/Husk)	5	18	6	17	4	20	10	15	15	15	15	15	15
Factor 2 (Clay)	95	82	94	83	96	80	90	85	85	85	85	85	85

⌧♋♌③♎ 🗑🗐🗑 ☛♎⑩⓪♏⑤ ⑥♋ ☛❹⑦♎⑨⓪④♎⑤⓿ ♋⑥⑨ ☞③♋❺ ☜③♎⑤♒♎♒ ❸⓪⓿♌ ✎🗋⑤❶⓿ ⌧♌♎③③ ☚♒♒⓪⓿⓪ ❷♎

S/N	1	2	3	4	5	6	7	8	9	10	11	12	13
Factor 1 (G/nut shell)	6	20	5	15	4	20	13	10	10	10	10	10	10
Factor 2	94	80	95	85	96	80	87	90	90	90	90	90	90

(Clay)													

Table 3.4 Summary of Five Level Factorial Design

	-α (-2)	Low limit (-1)	Base limit (0)	High limit (+1)	+α (+2)
Additive	4	5	6	15	20
Clay	96	95	94	85	80

CHAPTER FOUR

RESULTS AND DISCUSSION

The results obtained for the various tests are presented in Tables 4.1 - 4.10, Plates 4.1- 4.8 and Figures 4.1 – 4.12

4.1 Chemical Composition Analysis

Tables 4.1 and 4.2 show the chemical compositions of Amaiyi and Nguzu Edda clay deposits respectively while Tables 4.3, 4.4 and 4.5 show the chemical compositions of groundnut shell, rice husk and saw dust respectively.

Table 4.1 Chemical Composition of Amaiyi Clay

Oxide	Al_2O_3	SiO_2	K_2O	CaO	TiO_2	V_2O_5	Cr_2O_3	Fe_2O_3
Composition	22.9	48.9	5.15	2.79	1.63	0.098	0.037	10.51
Oxide/Element	CuO	ZnO	Ga_2O_3	MoO_3	Ag_2O	Eu_2O_3	Au	HgO
Composition	0.019	0.02	0.018	3.9	1.98	0.14	0.072	0.12

Table 4.2 Chemical Composition of Nguzu Clay

Oxide	Al_2O_3	SiO_2	K_2O	CaO	TiO_2	V_2O_5	Cr_2O_3	Fe_2O_3	Re_2O_7	Bi_2O_3
Composition	21.8	54.4	1.77	0.49	1.89	0.10	0.033	14.62	0.08	1.0

Oxide	CuO	ZnO	Ga_2O_3	MoO_3	Ag_2O	Eu_2O_3	SO3	MnO	IrO_2
Composition	0.022	0.01	0.001	0.57	0.845	0.17	2.0	0.005	0.12

From Tables 4.1 and 4.2, it is seen that Amaiyi clay contained 22.9% alumina (Al_2O_3) while Nguzu clay contained 21.8% alumina (Al_2O_3). It follows that both have low alumina content and so can be classified as high melting clays according to Nnuka and Agbo (2000). The silica contents were 48.9% and 54.4% for Amaiyi and Nguzu clay respectively. This classifies the clays as siliceous fire clay. (Nnuka and Apeh, 1997).The quantity of silica is moderate since it is within the recommended range of (50 -60) % for good clay brick. Silica is considered as filler in clay. It enabled the brick to retain its shape and imparted durability quality, prevented shrinkage and warping. These were confirmed from shrinkage tests and physical examination of the fired samples. Excess of silica is not good as it could make brick brittle and weak on burning.(Altayework, 2013).

The alumina to silica ratios of Nguzu and Amaiyi clays were 2:3 and approximately 1:2% respectively. These suggest low alumina to silica ratio which implies presence of more free quartz. (Nnuka and Agbo, 2000). However, it was observed that the percentage of uncombined silica is not much. Large percentage of uncombined silica in clay is undesirable as it can cause the problem stated previously.

Both clay samples have high Fe_2O_3 content which strongly supports the reddish colour of the fired samples. The colour of Nguzu was brown while Amaiyi clay was dark on drying to 110^0C but became reddish when fired to 1200^0C. High iron

oxide content is reported to affect high temperature characteristics. (Nnuka and Agbo, 2000). This suggests the need for reduction of the iron content by any separation method like magnetic separation.

Amaiyi clay has calcium oxide CaO content of 2.79% while that of Nguzu clay is 0.49%. Lime (CaO) is reported to normally constitute less than 10 per cent of clay. It reduces the shrinkage on drying. (Altayework, 2013). This is the reason why Amaiyi clay had lower shrinkage value of 4.0% compared to Nguzu clay which was 4.44%.The values of potassium oxide K_2O is almost of the same quantity. These low temperatures fusing agents melt at low firing temperature to fuse into the structure of the clay, hence helped to bind and densify the material and also reduced the sintering temperature.

Table 4.3A Chemical Composition of Groundnut Shell

Oxide	SiO_2	P_2O_5	SO_3	K_2O	CaO	TiO_2	MnO	Al_2O_3
Composition	16.0	8.0	5.1	10.6	30.4	1.5	0.95	7.6
Oxide	Fe_2O_3	NiO	CuO	ZnO	BaO	Eu_2O_3	CeO_2	Yb_20_3
Composition	13.0	0.2	1.2	0.3	1.5	2.2	0.6	0.9

Table 4.3B Chemical Composition of Rice Husk

Oxide	SiO_2	P_2O_5	SO_3	K_2O	CaO	TiO_2	MnO
Composition	60.8	21.3	2.76	7.77	3.07	0.35	0.771
Oxide	Fe_2O_3	NiO	CuO	ZnO	BaO	Eu_2O_3	Re_2O_7
Composition	2.41	0.024	0.059	0.24	0.13	0.09	0.19

Table 4.3C Chemical Composition of Sawdust

Oxide	SiO_2	P_2O_5	SO_3	K_2O	CaO	TiO_2	MnO
Composition	17.2	4.7	3.0	19.2	47.4	1.0	0.65
Oxide	Fe_2O_3	NiO	CuO	ZnO	BaO	Eu_2O_3	Re_2O_7
Composition	5.73	0.024	0.44	0.2	0.13	0.09	0.4

From Table 4.3(A), it was shown that groundnut shell has its most dominant oxides as 16% SiO, 10.6% K_2O, 30.4% CaO, 8% P_2O_5 and 7.6% Alumina. The percentage alumina content of groundnut shell increased the composition of alumina of the composite clay material. This increase in alumina content enhanced the refractoriness of the refractory material. This led credence to the enhanced refractoriness of the material with groundnut shell additives obtained in the results. The presence of silicon oxide in all the additives was found to be useful by reducing the drying shrinkage of material. It functioned as a filler which aided the

inter particle binding when fused together. The increase in silica content reduced excessive shrinkage in the composite material that would have occurred after firing. The presence of calcium oxide and other alkalis were noted to have also reduced shrinkage and lowered fusion point. Also, beyond 0.3% composition Calcium oxide, is reported to enhance mullite formation in fire clay thereby improving the high temperature characteristics like sintering temperature. (Nnuka, Ogo and Elechukwu, 1992).

The analysis of the rice husk in Table 4.3(B) revealed that silica (SiO_2) was the most dominant mineral of about 60.8% in the additive. However, it contains phosphorus oxide (P_2O_5) at the composition of 21.3%. Other oxides like CaO, TiO_2, K_2O, SO_3, MnO, Fe_2O_3, NiO, CuO, ZnO, BaO, Eu_2O_3 and ReO_7 are present in rice husk but in trace quantity of 1-17.9%.

Hence, the waste agro material (rice husk) can be considered as alternative natural source of silica as its silicon content conform to international standard for refractory clay.

Phosphorus oxide was found in all the additives. However, rice husk has the highest composition of 21.3%. Groundnut shell has 8.0% while saw dust has the least value of the oxide-4.7%. Phosphorus oxide is a useful oxide in refractory brick. Alumina reacts with phosphorus to form aluminum phosphate with considerable strength above 350^0C. (Decker, 2003). The aluminum phosphate bond

acts as a binder which enhances the brick's refractory properties like thermal shock resistance, refractoriness and strength. The bond improves non wetting effect of molten metal on the material and also increases the resistance of the material to carbon II oxide attack. The carbon II oxide is a byproduct of the furnace which causes cracking and destruction of the refractory lining. (Decker, 2003). Hence, the presence of the phosphorus oxide in the additives promoted excellent properties of the composite clay brick.

Rice husk contains calcium oxide and potassium oxide at a small quantity. These low temperature fluxing agents have capacity of melting at low temperature to fuse in the matrix of the material structure to reduce the porosity. (Opoku, 2015).

The gmalina sawdust additive contains little of silica but dominated by calcium oxide and other minerals at low values which effect has been discussed above.

4.2 Results for Mineralogical Analysis

The mineralogical phase analyses were done with the aid of XRD equipment and the results were interpreted using International Centre for Diffraction Data (ICDD) software. This revealed the main mineralogical phases in Amaiyi clay to be kaolinte ($Al_2Si_2O_5(OH)_4$), xonotlite ($Ca_6Si_6O_{17}(OH)_2$), chrysotile ($Mg_3[Si_2$-$xO_5](OH)_{4-4x}$, quartz (SiO_2), anhydrite ($CaSO_4$), os($KMg_2Al_3(Si_{10}Al_2)O_{30}$) and clinochryso ($Mg_3Si_2O_5(OH)_4$). The mineralogical phases found in Nguzu clay were periclase (MgO), Sep($Mg_4Si_6O_{15}(OH)_2.6H_2O$), antigorite ($Mg_3Si_2O_5(OH)_4$),

sanid $(NaK)(Si_3Al)O_8)$, os$(KMg_2Al_3\ (Si_{10}Al_2)O_{30})$, mu$(KAl_2(Si_3Al)O_{10}(OH)_2)$, riebeckit $(Na,Ca)_2\ (Fe,Mn)_3\ Fe_2(Si,Al)_8O_{22}(OH))$ and chrysotile $(Mg_3[Si_2\text{-}xO_5](OH)_{4\text{-}4x})$.

These minerals exhibit various forms when combined with other elements which influence reduction in shrinkage, thermal expansion and for higher strength development due to vitrification at low firing temperature.

Quartz is a phase derived from silica which is stable at room temperature but transforms to tridymite between temperatures of 890^0C – 1470^0C. Above temperature of 1470^0C, it transforms to crisobalite. (Singer and Singer, 1963). Quartz is considered as the major component mineral of sedimentary clay. It functions as filler in the clay. It reduces both plasticity and drying contraction in clay. Moderate quantities of quartz are beneficial in the clay. However, too much quantity would be undesirable. (Singer and Singer, 1996).

Clay material transforms at higher temperature and this enables different other phases to develop, with each phase having its own structure, composition and properties as the sintering temperature varies both in time duration and degree. (Opoku, 2015).

4.3 Results of the Micro Structural Examination

The micro structural images for Amaiyi and Nguzu clays were shown in Plates 4.1(A) and (B) respectively. The micrograph for the control sample was shown in

Plate 4.2 while those of composite clay blended with groundnut shell, saw dust and rice husk were shown in Plates 4.3, 4.4 and 4.5 respectively. The composite with combined additives of groundnut shell and saw dust is presented in Plate 4.6, while those composites made of combinations of the three additives and combinations of groundnut shell with rice husk are shown in Plates 4.7 and 4.8 respectively.

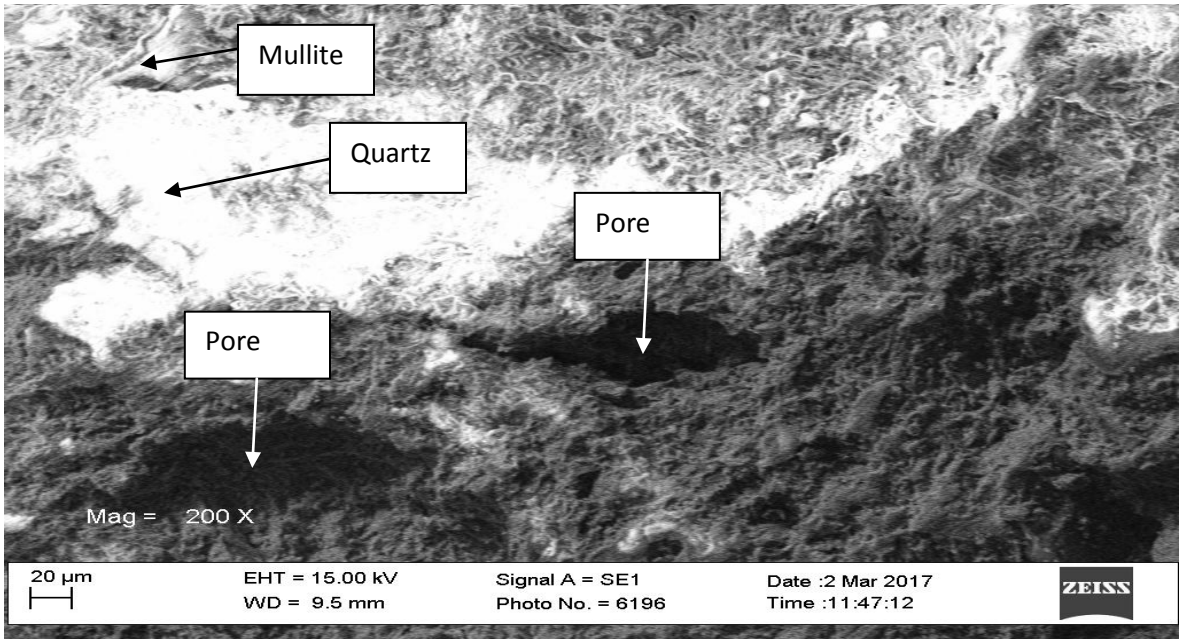

(A)

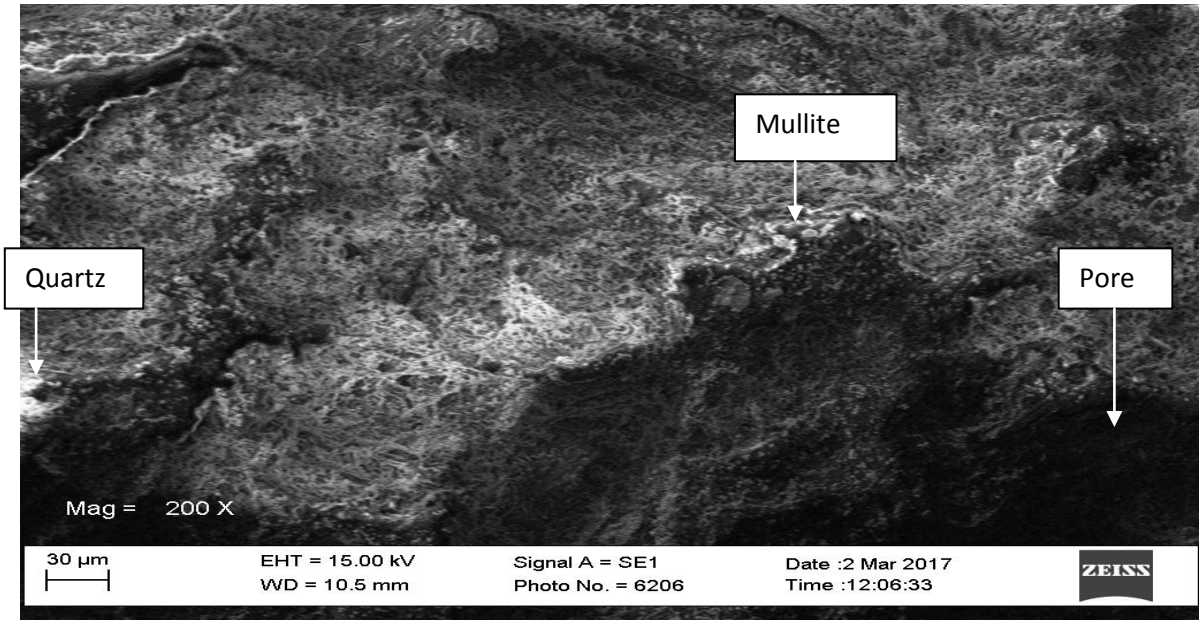

(B)

Plate 4.1: Scanning electron micrograph (SEM) for (A) Amaiyi, (B) Nguzu clays (X200)

The micro structural images shown by scanning electron microscopy on the fractured surface of the two clay samples indicate pores of limited sizes. These pores were shown as dark spots in the structure of the brick. The sizes and the distribution of the pores obtained in Amaiyi sample correlate with low apparent porosity and high thermal conductivity values obtained in the respective tests when compared to Nguzu sample. The smaller pore sizes yielded lower porosity which affected the insulating behavior of the brick sample. In Nguzu sample, the pore sizes were larger compared to the former. The same trends of behavior were observed in the other related properties.

Therefore, it was noted that the sizes and distribution of the pores in the structure of the brick material have direct effect on properties like apparent porosity, bulk density and thermal conductivity.

The micrograph of the image also revealed quartz as a mineralogical phase. The phase is shown as lump of whitish object in the structure. (Obidiegwu et al, 2015). Quartz acts as filler and as well as a modifier of fired body properties. It also helps to control warping of brick's body during firing by forming a relatively non fusible network of grain. The presence of this phase affects the linear shrinkage which indicates good dimentional stability in the brick at high temperature.

The presence of mullite was also noted in the structures. They are shown as whitish finger like shapes according to Obidiegwu et al, (2015). The presence of this phase is due to high firing temperature. The phase is formed at temperature of 1200^0C and above when alumina reacts with silica as follows:

$Al_2O_3 + 2SiO_2 = Al_2O_32SiO_2$

Mullite is considered as a binding phase in most refractory brick and it has high resistance to melting and minimum thermal expansion as well as low thermal conductivity. (Enass and Mahasin, 2015).

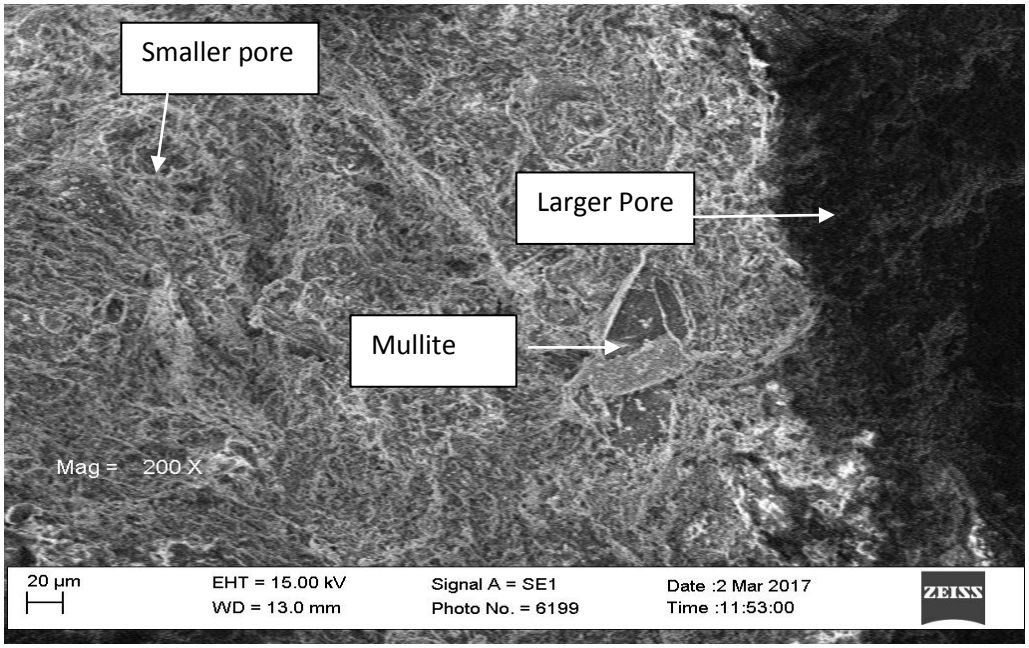

Plate 4.2: Scanning electron micrograph (SEM) for the control sample (X200)

The structure of Nguzu-Amaiyi blend showed a more homogeneous structure with the larger pores settled in one part of the material. The pores were observed to be uniformly distributed in the structure of the material. The sizes were relatively smaller compared to Nguzu sample and relatively more distributed when compared to Amaiyi sample. This was also indicated in the apparent porosity values which gave 11.56%, 15.38% and 20% for Amaiyi sample, control sample and Nguzu sample respectively.

It was noted that these results correlate with the insulating property of the material. These observations were made based on the results obtained in the above stated tests.

The presence of other phases like mullite was observed in the structure as whitish needle like shape. This phase has been reported to be responsible for the development of strength and refractoriness. (Obidiegwu et al, 2015). It is also characterized by its thermal stability. (Enass and Mahasin, 2015).

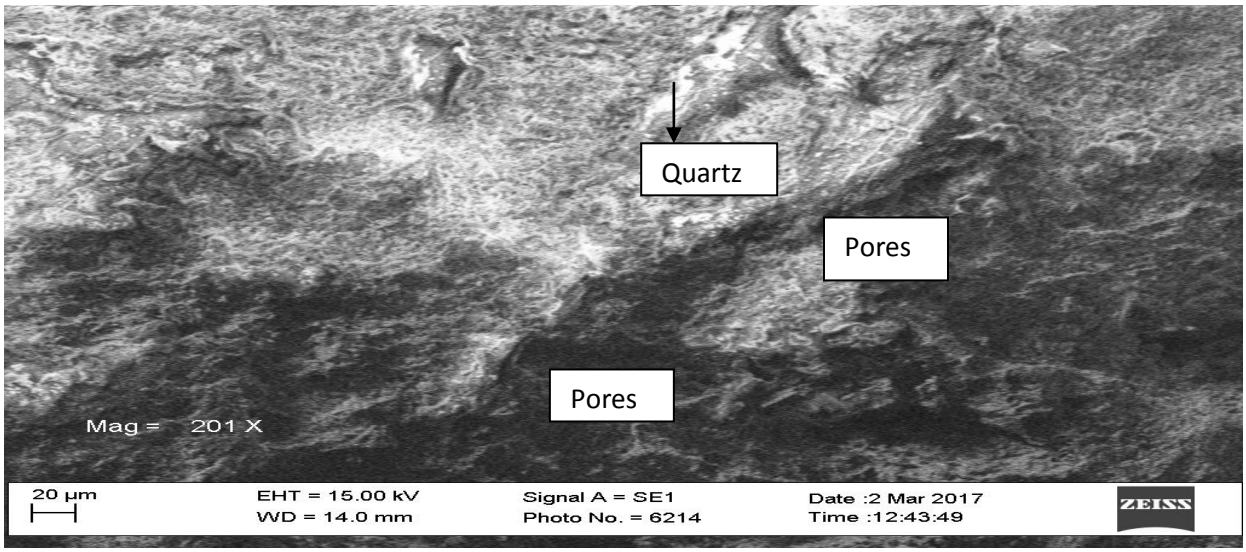

Plate 4.3: Scanning electron micrograph (SEM) for Nguzu-Amaiyi clay blended with groundnut shell (200X)

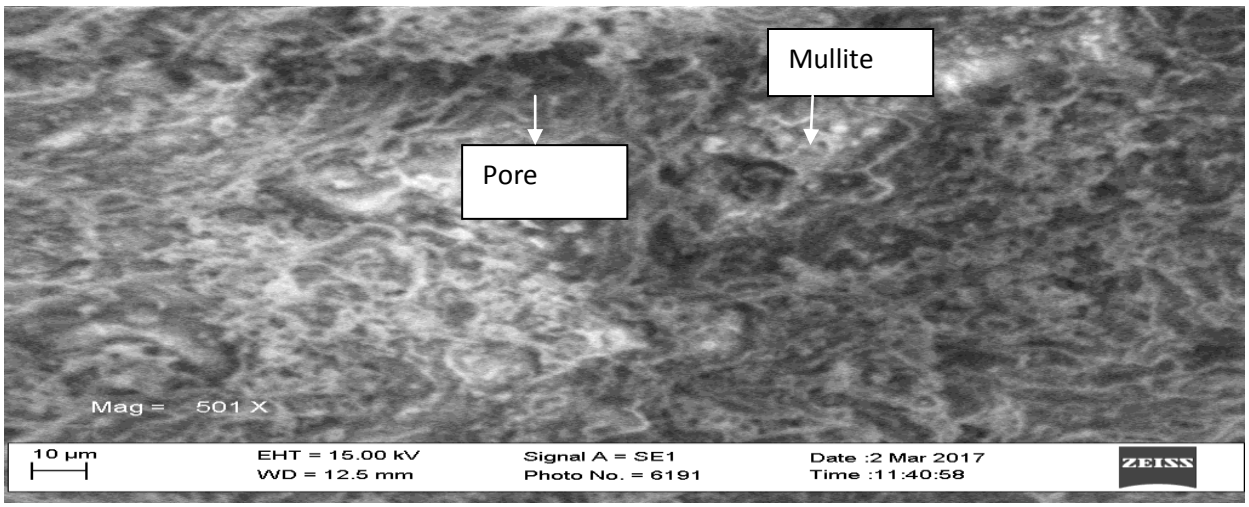

Plate 4.4: Scanning electron micrograph (SEM) for Nguzu-Amaiyi clay blended with saw dust (X501)

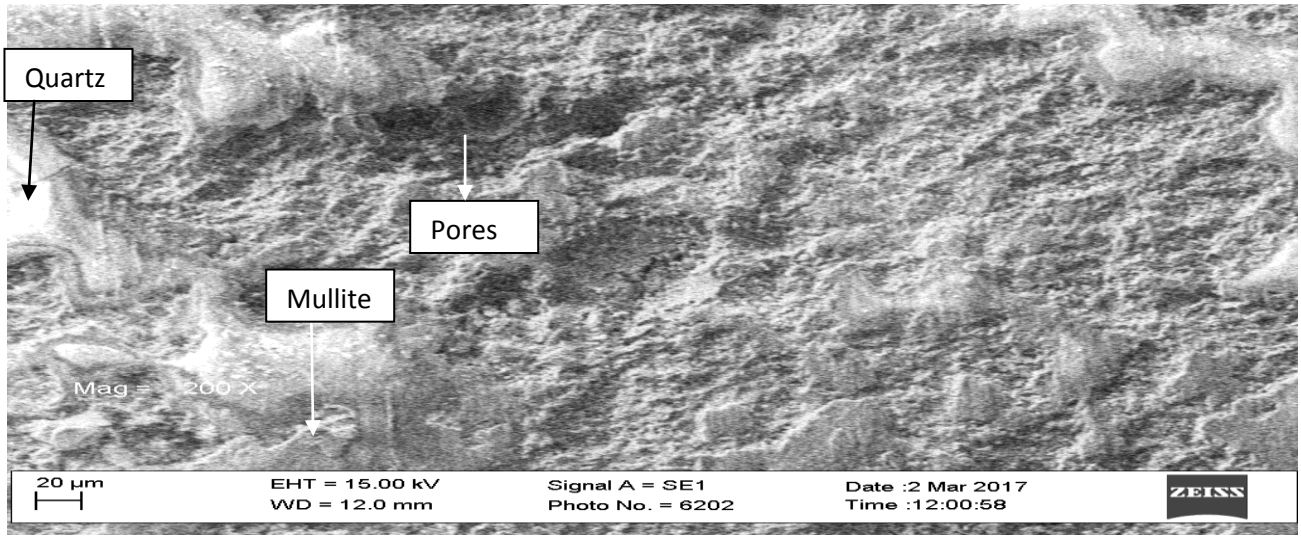

Plate 4.5: Scanning electron micrograph (SEM) for Nguzu-Amaiyi clay blended with rice husk at (X200)

The micrograph for the composite clay materials blended with groundnut shell, saw dust and rice husk additives are shown in Plates 4.3, 4.4 and 4.5 respectively.

The images revealed more heterogeneous structure compared to the single clays and the control sample. The structures have large pore sizes which were widely distributed.

The presence of the combustible additive materials strongly influenced the development of the pores, the bricks texture and the physic mechanical properties of the composite brick. The contents of the additives got burnt off at elevated temperature leaving opening which created the pores in the structure of the material.

The additives in the raw clay caused the formation of fissures. The small micro cracks at the surfaces observed in the brick can be traced to abrupt temperature changes and thermal expansion mismatch among the heterogeneously distributed phases. (Ahmed,Yaseen and Fazal, 2008).

Examination of the microstructure of the composite clay materials confirmed the presence of other phases like mullite and quartz.

Plates 4.6 – 4.8 show the structural images of composite bricks with combination of two and three additives.

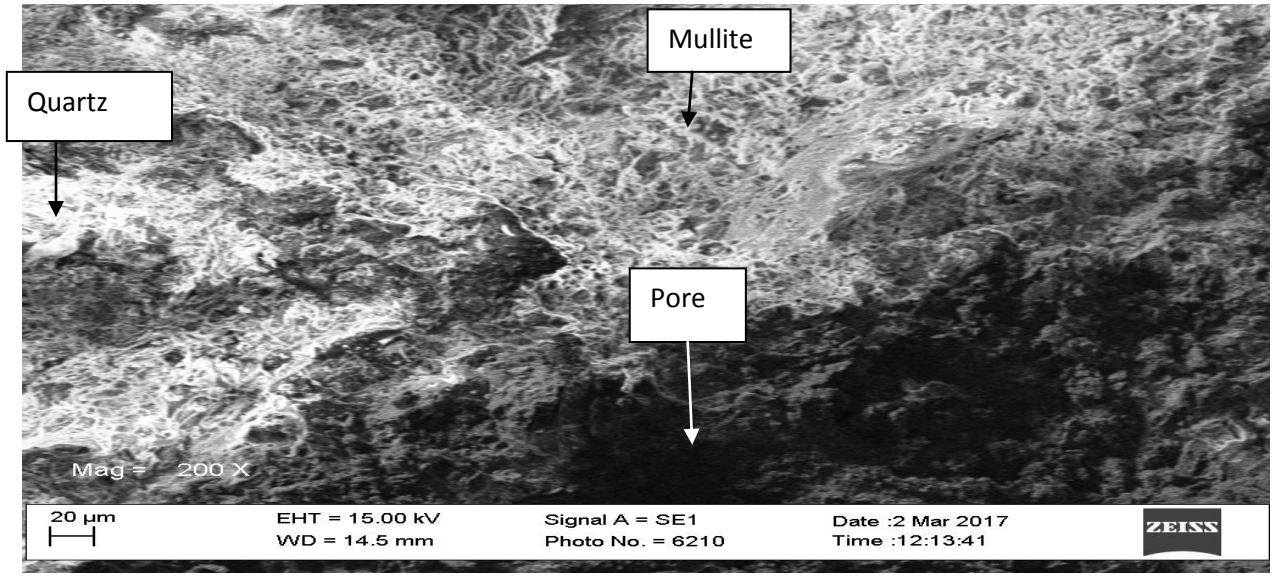

Plate 4.6: Scanning electron micrograph (SEM) for Nguzu-Amaiyi clay blended with groundnut shell with saw dust at (X200)

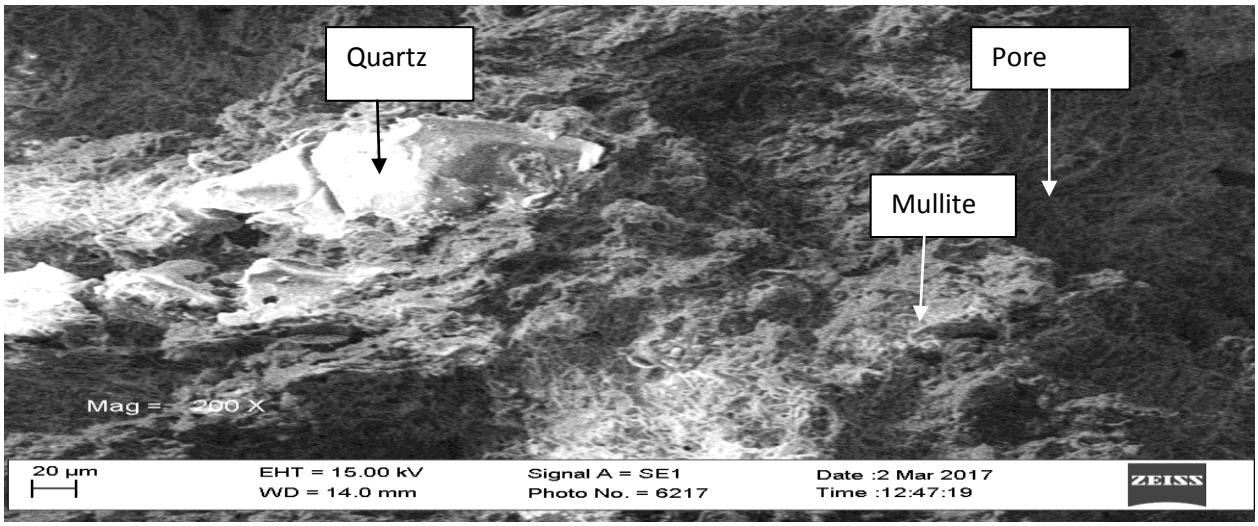

Plate 4.7: Scanning electron micrograph (SEM) for Nguzu-Amaiyi clay blended with groundnut shell, saw dust and rice husk (X200)

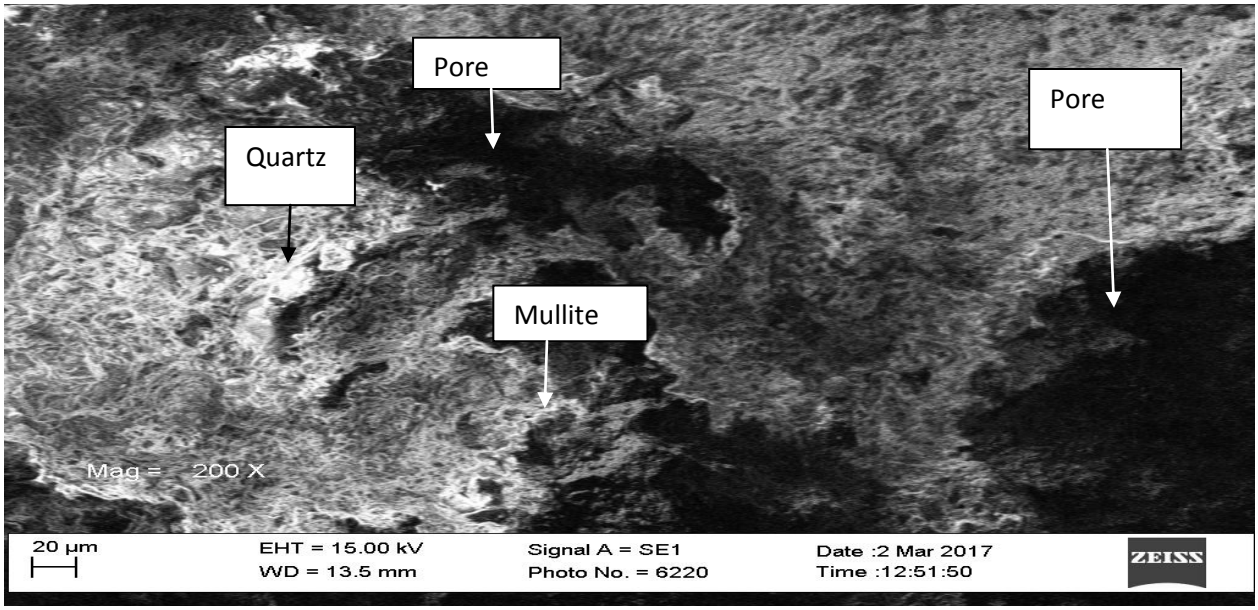

Plate 4.8: Scanning electron micrograph (SEM) for Nguzu-Amaiyi clay blended with groundnut shell with rice husk (X200)

These structures indicated higher feature of pores with wider distribution of the pores. It was observed that these larger pores tend to impede the movement of propagated cracks. This improved the thermal shock resistance of the material. The fact was proved by the excellent spalling resistance of the material regardless of the size of pores which could have impaired this property. Beside this, the large pores promoted good insulating property by providing air in the void. Air is poor conductor of heat. Hence, thermal conductivity was reduced.

4.4 Results of Refractory Properties of Nguzu Clay, Amaiyi Clay and Nguzu – Amaiyi Blended Samples.

The refractory properties of the two clays and the blended samples were shown in Table 4.4 while those for the blend of composite clay made of single and combined additives were shown in Tables 4.5 and 4.6 respectively. Figures 1 -12 show the effects of percentage composition of various additives on different refractory properties tested for.

Table 4.4 Refractory Properties of Nguzu, Amaiyi and Nguzu-Amaiyi Blended Clays.

Refractory property	**Nguzu-Amaiyi blended samples**				**Nguzu clay sample**	**Amaiyi clay sample**
	BL 1 (10:90)	**BL2 (30:70)**	**BL3 (40:60)**	**BL4 (50:50)**		
Linear shrinkage (%)	7.61	7.69	6.59	6.67	4.4	4.0
Apparent porosity (%)	12.9	13.11	15.38	15.63	20.00	11.56
Bulk density (g/cm^3)	1.8	1.87	1.77	1.81	2.13	2.15
Thermal shock resistance (cycle)	28	28	30	27	28	29
Modulus of rupture (MPa)	34.3	33.16	32.7	31.9	38.8	33.5
Thermal conductivity (W/mm^0C)	0.00318				0.00265	0.00397
Refractoriness (^0C) and Cone number in PCE	1550 (24)				1490 (21)	1520 (22)

Table 4.5 Refractory Properties of the Clay blended with Single additives.

Refractory property	**Control sample**	**Clay blended with saw dust**				**Clay blended with rice husk**				**Clay blended with groundnut shell**			
		5%	**10%**	**15%**	**20%**	**5%**	**10%**	**15%**	**20%**	**5%**	**10%**	**15%**	**20%**
Linear shrinkage (%)	**6.59**	7.53	8.7	8.7	10.64	6.5	8.7	8.7	10.64	6.52	6.52	7.6	8.5
Apparent porosity (%)	**15.38**	30.23	39.5	45.45	46.15	31.58	35	43.18	46.15	21.95	30	37.4	46.15
Bulk density (g/cm^3)	**1.77**	1.95	1.72	1.5	1.46	2.26	1.95	1.57	1.53	2.05	1.9	1.42	1.38
Thermal shock resistance (cycle)	**30**	28	31	31	30	28	30	30	27	31	32	29	32
Modulus of rupture (MPa)	**32.7**	31.2	29.9	29.8	28.8	33.2	31.2	30.4	30.2	39.6	34.5	33.1	30.9
Thermal conductivity (W/mm^0C)	**0.00318**	0.00227				0.00241				0.00284			
Refractoriness (^0C) and Cone number in PCE	**1550**	1610 (27)				1430 (19)				1640 (29)			

Table 4. 6 Refractory Properties of Clay blended with Combined Additives.

Refractory property	**Control sample**	**Clay + G/nutshell + Rice husk + saw dust (E)**				**Clay + G/nutshell + Rice husk (F)**				**Clay + G/nutshell +Sawdust (D)**			
		5%	**10%**	**15%**	**20%**	**5%**	**10%**	**15%**	**20%**	**5%**	**10%**	**15%**	**20%**
Linear shrinkage (%)	**6.59**	5.59	10.42	10.64	10.64	8.4	8.51	9.68	9.68	8.5	8.51	8.51	8.7
Apparent porosity (%)	**15.38**	36.36	43.18	54.09	54.17	23.91	34.09	42.85	44.89	28.57	42.55	48.8	54
Bulk density (g/cm^3)	**1.77**	1.73	1.48	1.32	1.25	2.00	1.87	1.43	1.39	1.73	1.62	1.3	1.3
Thermal shock resistance (cycle)	**30**	31	31	32	31	29	28	29	28	29	28	27	28
Modulus of rupture (MPa)	**32.7**	34.3	32.8	31.6	26.1	30.3	28.1	27.0	26.5	32.7	31.9	29.5	24.05
Thermal conductivity (W/mm^0C)	**0.00318**	0.00294				0.00086				0.00265			
Refractoriness (^0C) and Cone number in PCE	**1550**	1670 (29)				1580 (27)				1460 (19)			

Table 4.7 Comparison of the Refractory Properties of Brick's Samples with Internationally Accepted Standard Values

Property	Standard Value	Control sample	Nguzu Clay	Amaiyi Clay	Blend of Saw dust	Blend of Rice Husk	Blend of G/nut shell	Blend of Three additives	G/nut shell & Sawdust	G/nut shell & Rice husk
Linear shrinkage (%)	4 - 10	6.59	4.4	4	7.53 – 10.64	6.5 - 10.6	6.52 – 6.64	5.59 – 10.64	8.5 – 8.7	8.4 – 9.68
Apparent porosity (%)	20-30	15.38	20	11.56	30.2 – 46.15	31.5 – 46.1	21.95 – 46.1	36.36 – 54.17	28.57-54	23.91-44.89
Bulk density (g/cm^3)	2.3	1.77	2.13	2.15	1.9 – 1.6	2.2 – 1.57	2.05 – 1.42	1.73 – 1.25	1.73 – 1.3	2.00 – 1.39
Modulus of rupture (MPa)		32.7	38.8	33.5	29.9 – 28.5	31 – 30.2	39.6 – 30.9	34.3 – 26.1	32.7 – 24.05	30.3 – 26.5
Spalling resistance (cycle)	25-30	30	28	29	28 - 31	27 - 30	29 -32	31 - 32	29 - 27	28- 29
Thermal		.00318	0.0026	.00397	.00227	.00241	0284	.00294	.00265	.00086

conductivity (W/mm^0C			5							
Refractoriness (^0C)	1500 - 1700	1550	1490	1520	1610	1430	1640	1670	1460	1580

4.4.1 Result of Linear Shrinkage Test

The results for linear shrinkage tests for the two clays and the control sample are found in Table 4.4. Table 4.5 shows the linear shrinkage values for blends of composite brick made of different single additives (sawdust, rice husk and groundnut shell). Table 4.6 shows the linear shrinkage values for blends of composite brick made of combined additives. Figures 4.1 and 4.2 show the effect of the percentage composition of the individual single additives and their combinations on linear shrinkage respectively.

From the results in Table 4.4, it was seen that Nguzu and Amaiyi clays have linear shrinkage values of 4.44% and 4.0% respectively while that of the control sample was 6.59%.

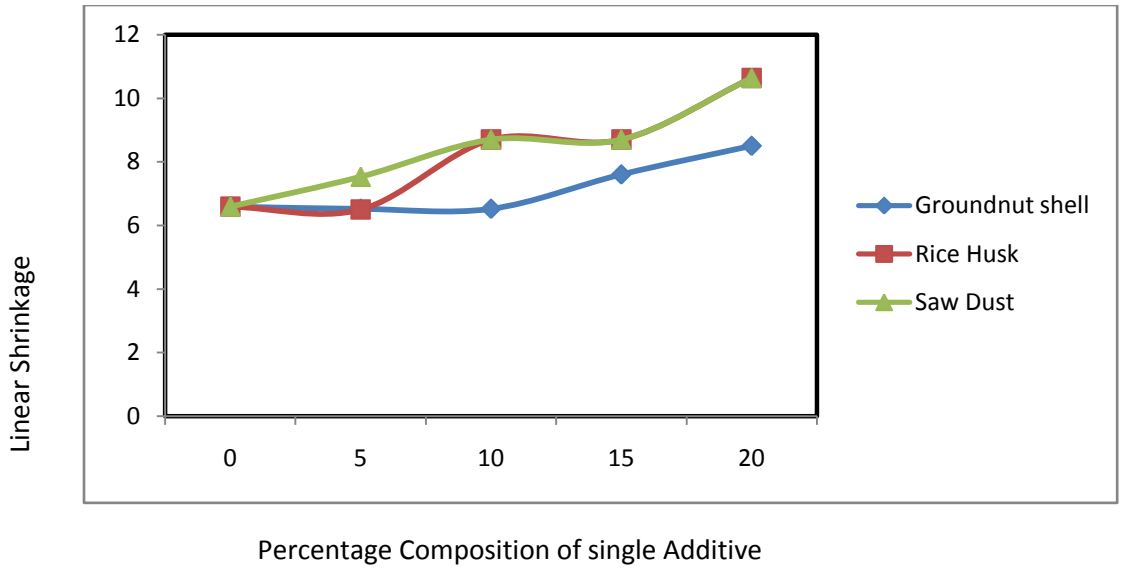

Figure.4.1A: Effect of composition of the single additives on linear shrinkage of blended clay

From Table 4.5 and Figure 4.1A, it is observed that in sawdust blended brick, the values of linear shrinkage were from 7.53 – 10.64% between 5% and 20% of percentage composition of the additive. When these values of linear shrinkage were compared to that of the control sample (BL3), it was observed that the additives had significant increase on this property. It was also noted that the value of linear shrinkage increased with increase in the composition of the additives. This is in agreement with Safeer, Yaseen and Raz, (2017) which stated that the percentage of firing shrinkage increases with increase in the quantity of additive.

Comparison of the shrinkage values of the control sample with those blended with sawdust at various compositions also shows that the level of deterioration of this

property due to the increase was between 14.2 - 60% for the range of composition investigated. However, despite the observed increase and deterioration in shrinkage values, the values obtained for the range of composition investigated were within the acceptable standard values of (4 -10) % according to Grimshaw, (1971).

The increase in linear shrinkage value is traceable to rearrangement of the particles of the composite material when the additives were burnt off. This gave rise to more compact structure of the composite clay brick with higher shrinkage value. The higher value of linear shrinkage observed is also due to migration of gases as a result of decomposition of sulphate(SO_3) in sawdust. (Safeer et al, 2017,).

From Table 4.5 and Figure 4.1A, it is also seen that rice husk blended sample gave shrinkage values of 6.5, 8.7, 8.7 and 10.64% when the composition of rice husk in the clay brick were 5, 10, 15 and 20% respectively. These results showed improvement of 1.4% of linear shrinkage property at 5% composition of the additive. However beyond this composition, the property deteriorated to 32% and 60% in 10, 15, and 20% composition respectively. Hence, it was noted that enhancement of this property with rice husk additive could be achieved with the composition of the additive not exceeding 5%.

Though the linear shrinkage values increased between 10 – 20% compositions, they were within the acceptable value. Therefore, the additive did not impair the property within the composition range tested for.

Refer to the Table 4.5 and Figure 4.1A, it is observed that among the three additives used for this study, groundnut shell had the best influence on linear shrinkage. Between 5 and 10% composition, the shrinkage value was 6.52%. This showed improvement of 1%. When the composition of groundnut shell additive increased to 15% and 20%, linear shrinkage increased to 7.6 and 8.5% respectively. It is seen that at these two values of composition, the property deteriorated by 15% and 29% respectively. However, the degree of deterioration was minimal compared to the previous additives. The improvement of linear shrinkage in this combination was due to the oxide composition and the type of phase formed during firing which improved dimensional stability of clay material at high temperature.

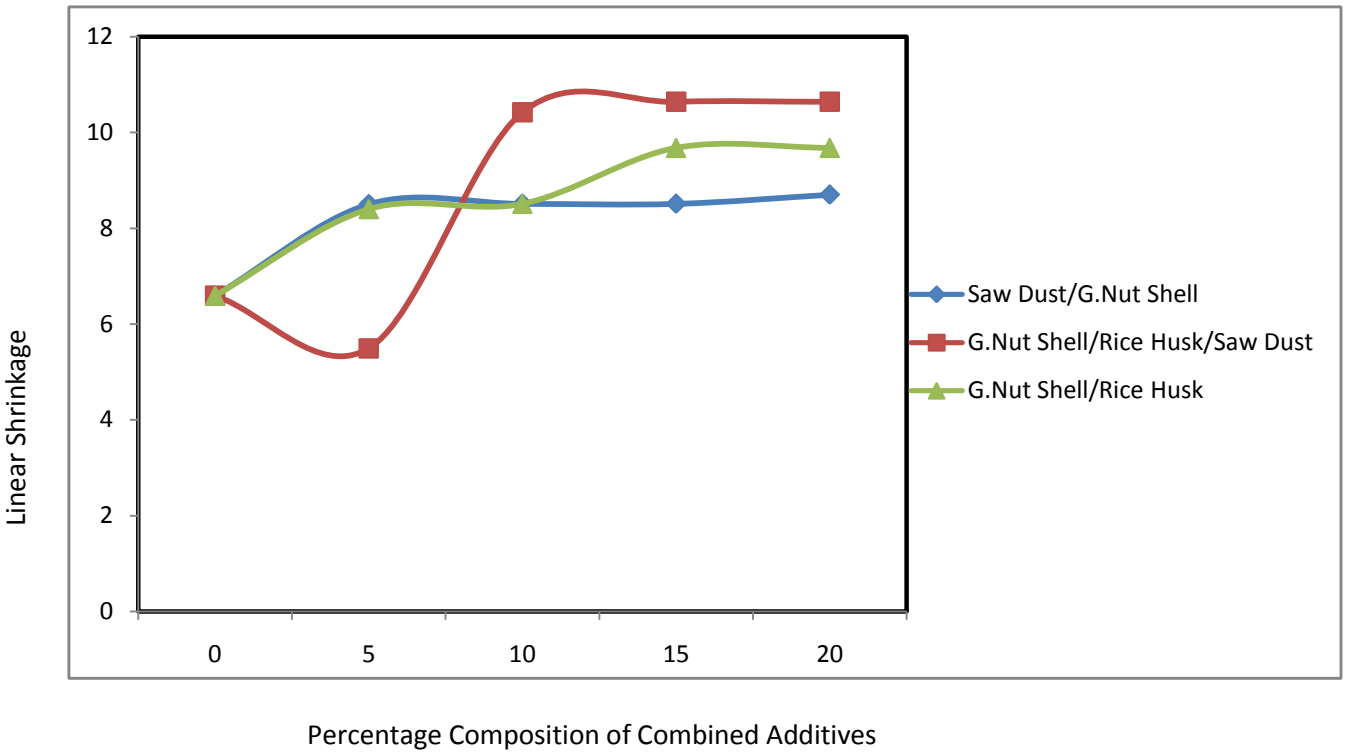

Figure.4.1B: Effect of composition of combined additives on linear shrinkage of blended clay

Table 4.6 and Figure 4.1B show the effect of combination of two and three additives on properties of the control sample. It was observed that enhancement on linear shrinkage was achieved with combination of the three additives (sawdust, rice husk and groundnut shell) at 5% composition.

From Figure 4.1B, it is seen that the composition of the three additives yielded linear shrinkage value of 5.59%, a 16.7% improvement when compared with control sample. It was also observed that between 10 – 20% compositions, the values increased to 10.42 and 10.64% respectively. Hence these compositions yielded percentage deterioration of 58 and 61.5% in the property investigated.

In the blend of two additives made of groundnut shell with rice husk, the shrinkage values were 8.4, 8.51, 9.68 and 9.68% for 5, 10, 15 and 20% compositions respectively. This indicated percentage deterioration from 27.5% to 46.8% of the property within the range of composition of the additive used.

The blend of groundnut shell with sawdust showed similar behavior with respect to the composition of the additives. The shrinkage values were 8.5, 8.51, 8.51 and 8.7% for 5, 10, 15 and 20% composition of the additive. It was seen in this blend that variation in the composition of the additives did not have much change in shrinkage value. Notwithstanding, it was noted that the property did not improve rather it deteriorated between 29 to 32%. Comparison of the values of shrinkage in this blend with the accepted standard of (4 – 10) % showed that the linear shrinkage of the material is good since the values were found within the stated range.

4.4.2 Results of Apparent Porosity Test

The results for apparent porosity tests for the two clays and the control sample are found in Table 4.4. Table 4.5 shows the apparent porosity values for blends of composite brick made of different single additives (sawdust, rice husk and groundnut shell). Table 4.6 shows the apparent porosity values for blends of composite brick made of combined additives. Figure 4.2A shows the effect of the

percentage composition of the individual single additives and their combinations on apparent porosity.

In Table 4.4, the results of apparent porosity test for both Nguzu clay, Amaiyi clay and the control sample were shown. Table 4.5 showed the apparent porosity of composite brick made with single additives (sawdust, rice husk and groundnut shell) while Table 4.6 showed the apparent porosity of values of composite brick made with combination of two and three additives.

From Table 4.4, it was seen that Nguzu clay had apparent porosity value of 20% while that of Amaiyi clay was 11.56%. This showed that Nguzu clay is more porous than Amaiyi clay. This results correlate with result of other related properties like bulk density and thermal conductivity shown in the same table. The blend of the two clays formed the control sample had apparent porosity value of 15.38%. This showed that moderate porosity level was achieved in the two clays by blending the two clays together. Apparent porosity refers to the proportion of voids or pores per unit volume of the material. It depends on clay mineralogy and internal brick structure.

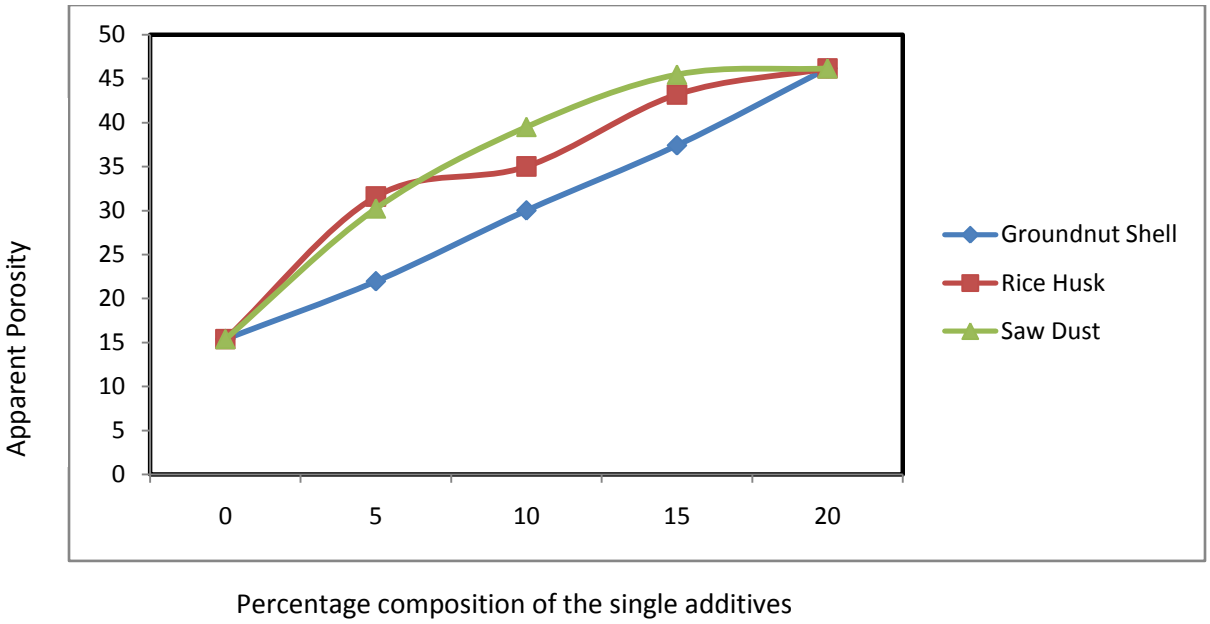

Figure.4.2A: Effect of composition of different single additives on apparent porosity

From Table 4.5 and Figure 2A., it was seen that Nguzu – Amaiyi clay blended with saw dust additive yielded apparent porosity values of 30.23, 39.5, 45.45 and 46.15% respectively. When these values were compared with that of the control sample, it was seen that apparent porosity value improved from 96% to 200% between 5 to 20% composition of the sawdust additive.

It was also noted the porosity value increased with increase in the composition of the additive. The results proved that fired bricks exhibit different apparent porosity values based on the amount of additives according to Safeer, Yaseen and Raz, (2017). This is due to the fact that more quantity of the additive gave rise to larger

pore sizes and wider distribution of the pores. These yielded higher porosity values.

From Table 4.5 and Figure 4.2A, it is also seen that rice husk additive gave apparent porosity values of 31.58, 35, 43.18 and 46.15% for 5, 10, 15 and 20% compositions respectively. The same trend was observed as previously noted in sawdust additive. However, the percentage improvement in porosity was observed from 104% - 199% between (5 – 20%) composition of rice husk.

The increase in porosity in traced to the fact that the additive is combustible. They burn off at elevated temperature. This leaves pores in the structure of the composite brick that gives rise to high porosity value.

From the same Table, it is seen that groundnut shell additive gave apparent porosity values of 21.95, 30, 37.4 and 46.15 for 5, 10, 15, and 20% composition of the additive respectively. Comparison of these values with the value of the control sample showed there is percentage improvement of 42.7 – 199% in the property. This shows that in all the compositions used, apparent porosity was found to show increase with the incorporation of the agro additives in the clay and the increase depends on the percentage composition of the additive in the clay.

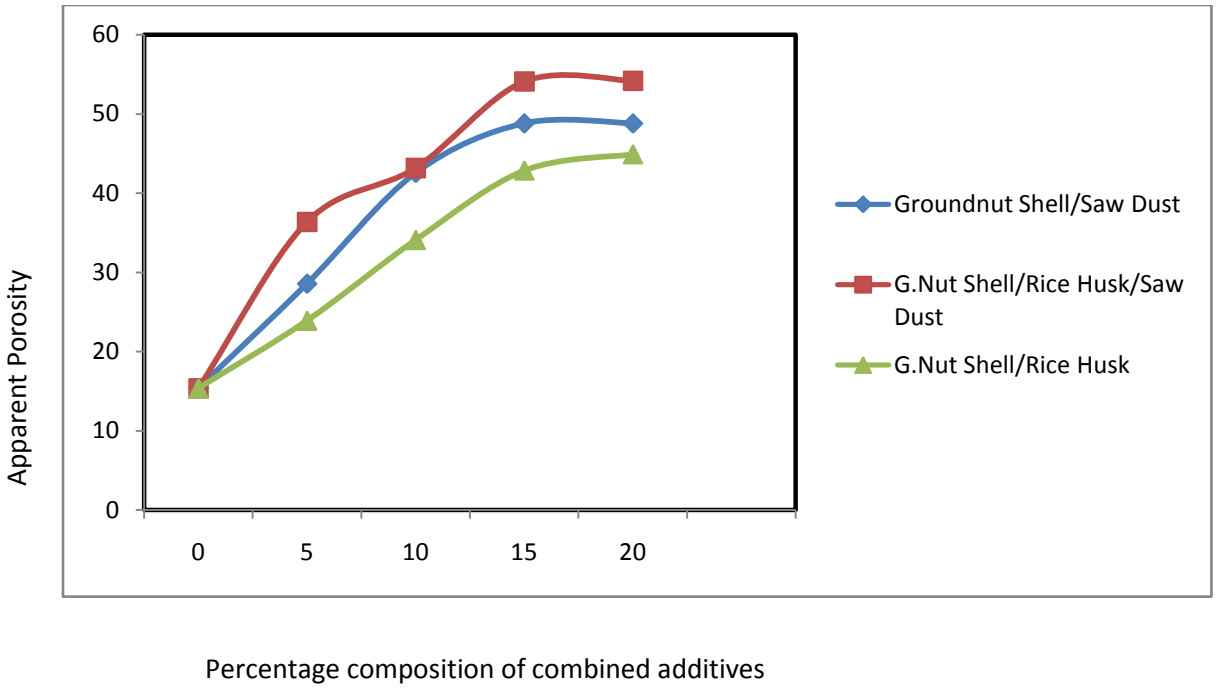

Figure.4.2B: Effect of composition of different combined additives on apparent porosity

Table 4.6 and Figure 4.2B showed the apparent porosity values of the clay bricks blended with combinations of two and three additives. It was noted that higher porosity values were obtained when compared with those of single additives.

Combination of groundnut shell, rice husk and sawdust gave apparent porosity values of 36.36, 43.18, 54.09 and 54.17% for 5, 10, 15 and 20% compositions of the additive respectively. It was seen that the apparent porosity value increased with composition of the additive as in previous cases. It was also noted that percentage improvement of 136% to 252% was achieved between 5 and 20% composition of the additive.

Combination of groundnut shell with rice husk gave values of 23.9, 34.09, 42.85 and 44.89 for 5, 10, 15 and 20% composition of the additives respectively. These results showed improvement of apparent porosity from 55.5% – 191% for the range of composition tested.

Combination of groundnut shell with sawdust gave apparent porosity values of 28.57, 42.55, 48.8 and 54% for 5, 10, 15 and 20% composition respectively. These had improvement of apparent porosity from 82% - 250% for the range of additive composition stated above.

Comparison of the extent of improvement achieved for this property with these additives and their combinations show that the performance of combined additives was better than single additive. This is shown in 5% additive composition of combination of the three which gave 136% improvement compared to 96%, 104% and 42.7% improvement obtained in sawdust, rice husk and groundnut shell single additives respectively. At the highest percentage composition of the additive like (20%), combination of the additives also performed better than the single additives. Combination of the three additives and two of groundnut shell with sawdust gave improvement of 252 and 250% respectively while the single additives gave improvement value ranging from 199 – 200%.

This shows that combination of many additives has better influence on the apparent porosity. This is traceable to both pore sizes and wider distribution of the pores. This also has direct effect on the insulating property since porosity affects of the thermal flow which decreases thermal conductivity.

4.4.3 Results for Bulk Density Test

The results of the bulk density tests for both clays and control sample were shown in Table 4.4 while those of clay blended with single and combined additives were shown in Tables 4.5 and 4.6 respectively.

It was seen from Table 4.4 that the bulk density values for Nguzu and Amaiyi clays were 2.13 g/cm^3 and 2.15g/cm^3 respectively while that of the control sample was 1.77 g/cm^3. Bulk density of clay brick is affected by the presence of some oxides like CaO and MgO. They contribute in the formation of chemical components of low fusion temperature which flow into the pores and result in an increase in the density of the brick. (Enass and Mahasin, 2015). Hence, from Tables 4.1 and 4.2, it was seen that Amaiyi clay with the higher composition of CaO than Nguzu clay indicated higher value of bulk density.

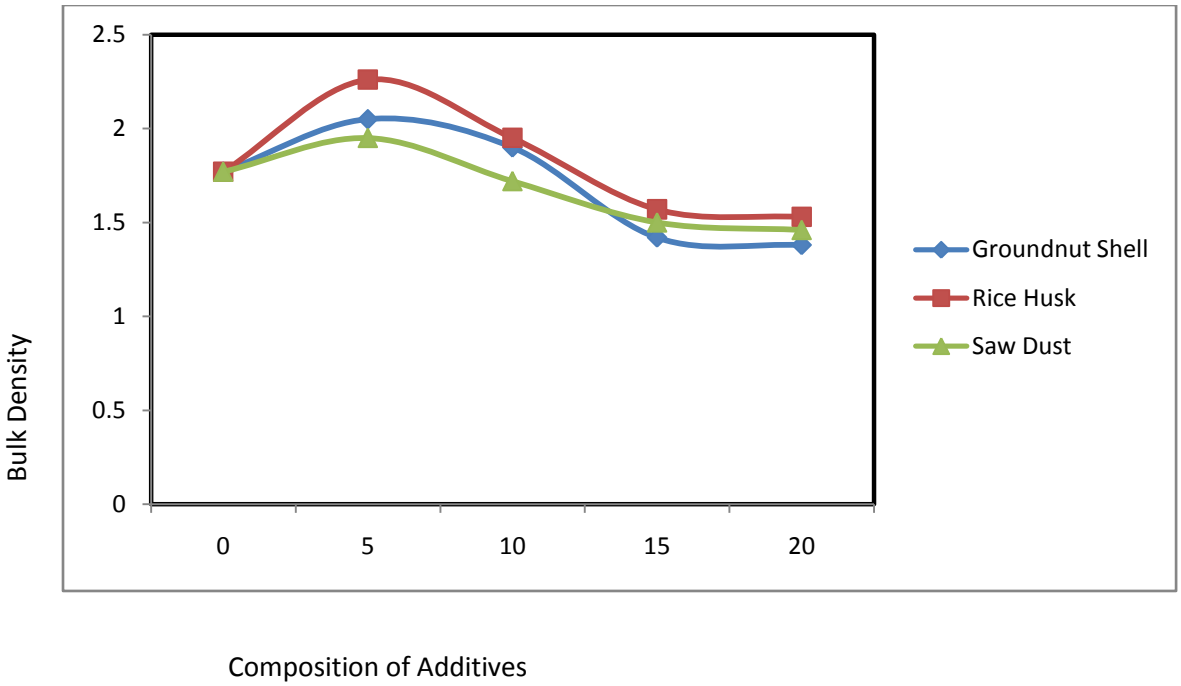

Figure.4.3A: Effect of composition of various single additives on bulk density

From Table 4.5 and Figure 4.3A, it was observed that clay blended with sawdust additives had bulk density values of 1.95, 1.72, 1.5 and 1.46g/cm^3 for 5, 10, 15 and 20% composition of the additives. When compared with the bulk density value of the control sample which was 1.77g/cm^3, it was noted that improvement of 7.3% for this property was obtained with 5% composition of the additive only. Beyond this composition, up to 20% composition of the sawdust additive, the values of the property deteriorated to 9.6%. It was also noted that bulk density values was decreasing with increase in the composition of the additive which is in contrast to apparent porosity. The decrease in density is due to the larger pores created when

more quantity of the additive was burnt off. This decreased the bulk density of the material.

Rice husk blended brick had bulk density values of 2.26, 1.95, 1.57 and 1.53g/cm^3 for 5, 10, 15 and 20% of additive composition respectively. These were shown in table 4.5. In this blend, it was observed that enhancement of 24.3% and 10% were achieved with additive composition of 5 and 10% respectively. However, composition of 15 and 20% of the additive decreased the property by 11%.

In the blend of groundnut shell with the two clays, the trend was similar to rice husk additive. Bulk density values of 2.05, 1.9, 1.42 and 1.38g/cm^3 were obtained with 5, 10, 15 and 20% additive composition. This showed percentage improvement of 15.8% and 7.3% for the property at 5 and 10% additive composition. However, percentage deterioration of 19% was observed at 15 and 20% composition of the additive.

Comparison of this property in the three blends shows that improvement on this property with these additives could be achieved between 5 -10% composition of the additive. However, beyond this composition, the property could be affected negatively.

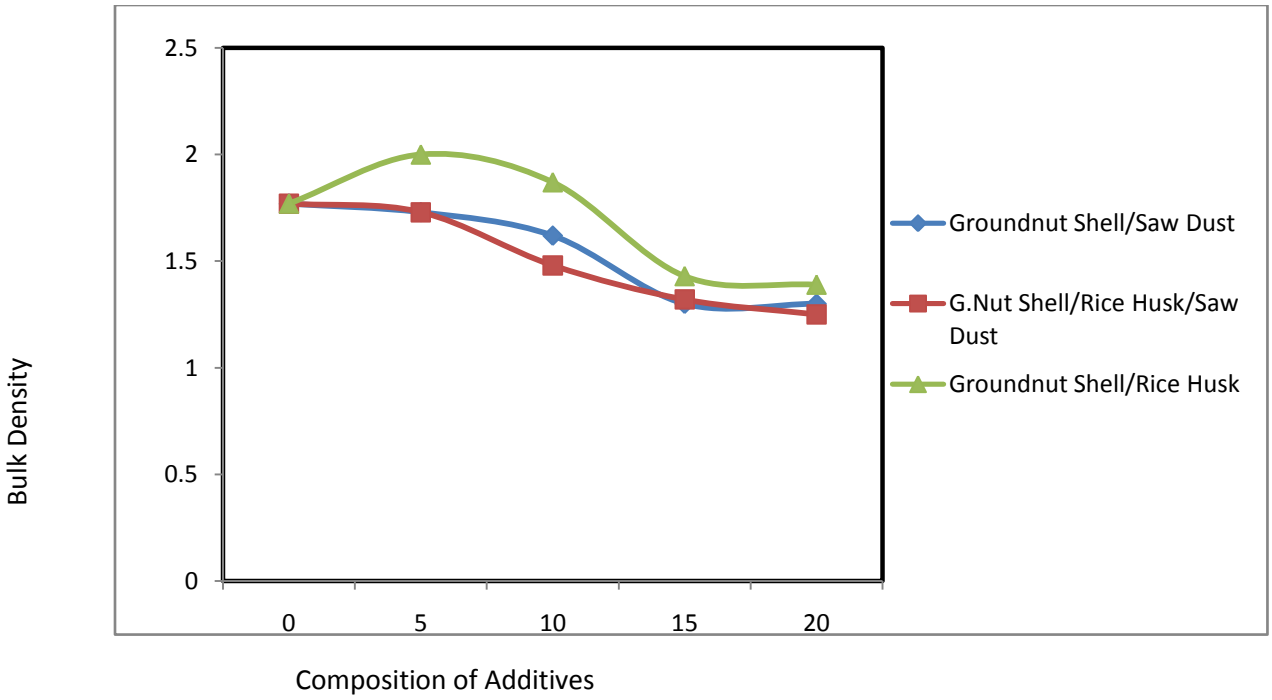

Figure.4.3B: Effect of composition of various combined additives on bulk density

From Table 4.6 and Figure 4.3B, it is seen that combination of two or three additives did not yield enhancement in bulk density except in the combination of ground nut shell with rice husk. This table shows that combination of groundnut shell with saw dust gave bulk density values of 1.73, 1.62, 1.3 and 1.3g/cm^3 for additive composition of 5, 10, 15 and 20% while combination of the three additives gave 1.73, 1.48, 1.32 and 1.25 g/cm^3 for the same respective compositions. In contrast to the above two blends, combination of groundnut shell with rice husk gave bulk density values of 2.0, 1.87, 1.43 and 1.39g/cm^3 for 5, 10, 15 and 20% composition of additive respectively.

Therefore, it was seen that in the blend of groundnut shell with saw dust additive, there was a percentage decrease of bulk density from 2.3% to 26.5% within the composition range of 5 – 20%. In the blend the three additives, the percentage decrease was between 2.3% and 29% within the same range of additive composition. In contrast, the combination of groundnut shell with rice husk, showed percentage improvement of bulk density of 13% and 5% in the additive composition of 5 and 10% respectively. However, with increase in the additive composition up to 20% of this same blend, the bulk density had percentage decreased of 21.5%.

This therefore suggests that use of single additives should be preferred to combine ones when high bulk density is of essence.

4.4.4 Results for Modulus of Rupture Test

Table 4.4 showed the values of modulus of rupture for the two clays and the control sample. Table 4.5 with Figure 4.4A and Table 4.6 with Figure 4.4B show the values of modulus of rupture and the effect of percentage composition of the additive on the same property for the clay blended with single additives and combined additives respectively.

This property indicates the maximum transverse breaking stress which the material can withstand before fracture. It shows the capability of brick to support load that is imposed on it.

From table 4.4, it is seen that the values of modulus of rupture for Nguzu clay, Amaiyi clay and the control sample were 38.8, 33.5 and 32.7 MPa.

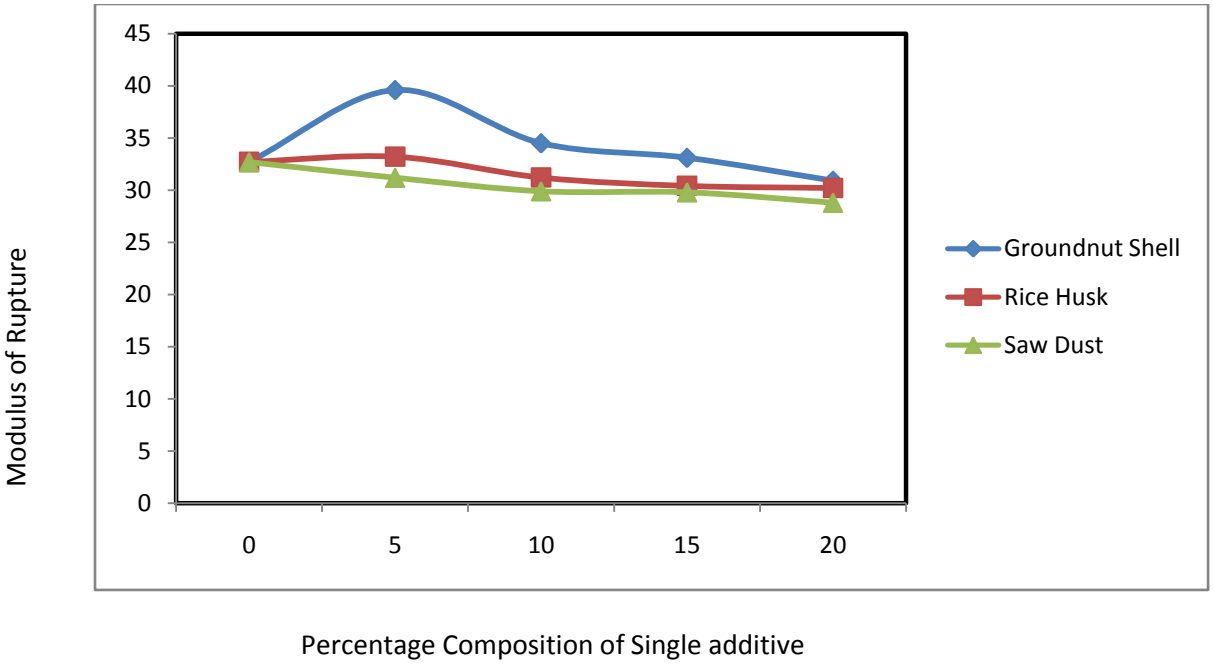

Figure. 4.4A: Effect of composition of different single additives on modulus of rupture

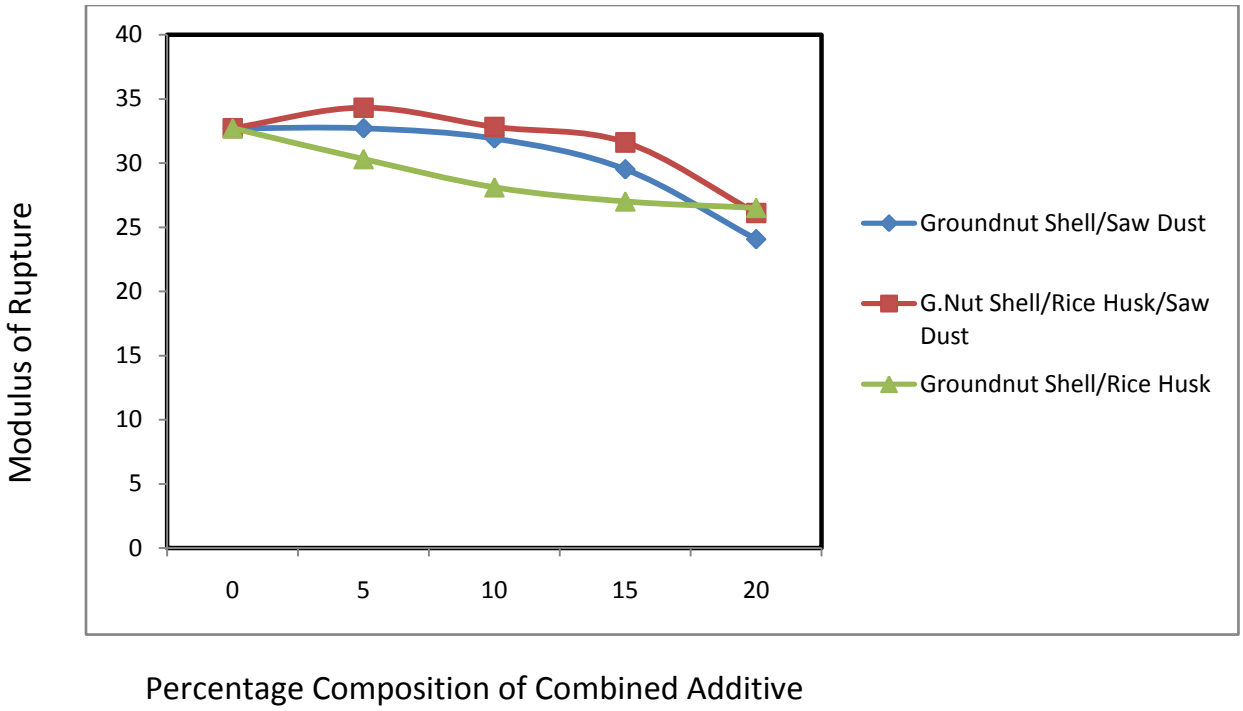

Figure. 4.4B Effect of composition of different combined additives on modulus of rupture

Table 4.5 and Figure 4.4A show that values of modulus of rupture for sawdust blends were 31.2, 29.9, 29.8 and 28.8MPa for 5, 10, 15 and 20% composition of the additive respectively. In rice husk blend, the values were 33.2, 31.2, 30.4, 30.2MPa in the same trend. Those of groundnut shell blends were 39.6, 34.5, 33.1 and 30.9MPa for 5, 10, 15 and 20% composition of the additive respectively.

From Table 4.5 and Figure 4.4A, it is seen that in sawdust blend, modulus of rupture was observed to decrease from 31.2MPa to 29.8MPa when the composition of sawdust in the clay increased from 5 to 20%. In rice husk blend, modulus of rupture improve to 33.2MPa at 5% composition but showed decrease from 31.2 to

30.2MPa when the composition of rice husk increased from 10 to 20%. In groundnut shell blend, the property improved within the range of composition of 5 to 15% with values of modulus of rupture ranging from 39.6 to 33.1MPa. This suggests that groundnut shell additive should be preferred as clay additive when strength is needful.

It was observed that the values of modulus of rupture were decreasing with increase in the composition of the additives. Generally, in clay based system, strength decreases with increase in porosity. (Safeer et al, 2017). The observed decrease in the values of modulus of rupture is due to the increase in porosity obtained with increase in composition of the additives. The increase in the quantity of the additive affected the strength adversely due to the deficiency of the main clay content. Also, the migration of gases through the matrix produced due to burning of additives created a highly porous clay body which reflected negatively on the transverse strength. Therefore, this means that the amount of the additives must be controlled to avoid adverse effects.

Table 4.6 and Figure 4.4B show that the value of modulus of rupture for the blend made of groundnut shell with sawdust was the same as the control sample when the additive composition was 5%. However, above this composition up to 20%, the property decreased from 31.9 to 24.05MPa.

In the sample made from combination of groundnut shell with rice, there was more decrease in the value of modulus of rupture in all the additive compositions from 30.3 to 26.5MPa. This shows that the combination does not improve the property at all in any composition.

In contrast to the previous two combinations, the sample produced from combination of three additives of groundnut shell, rice husk and saw dust showed percentage enhancement of 4.7% for this property precisely with additive composition of 5% i.e. from 32.7MPa of the control sample to 34.3MPa of the 5% sample.

When all the various six combinations of the additives were compared, it was noted that blends of groundnut shell and the blends made with combination of the three additives yielded the best performance for the modulus of rupture. It was also observed that the values of modulus of rupture decreased with increase in composition of the additives. This proves that strength depends on the quantity of additives according to Safeer et al, (2017).

4.4.5 Results for Thermal Shock (Spalling) Resistance Test

Table 4.4 shows the thermal shock resistance of the two clays and the control sample. Tables 4.5 and 4.6 show the thermal shock resistance for the clay blended with single additives and combined additives respectively.

It was shown in Table 4.4 that the thermal shock resistance values of Nguzu and Amaiyi clays were 28 and 29 cycles while that of the control sample was 30 cycles. This shows that the resistance to thermal shock of the clay can be slightly improved by blending the two clays at the ratio 40:60.

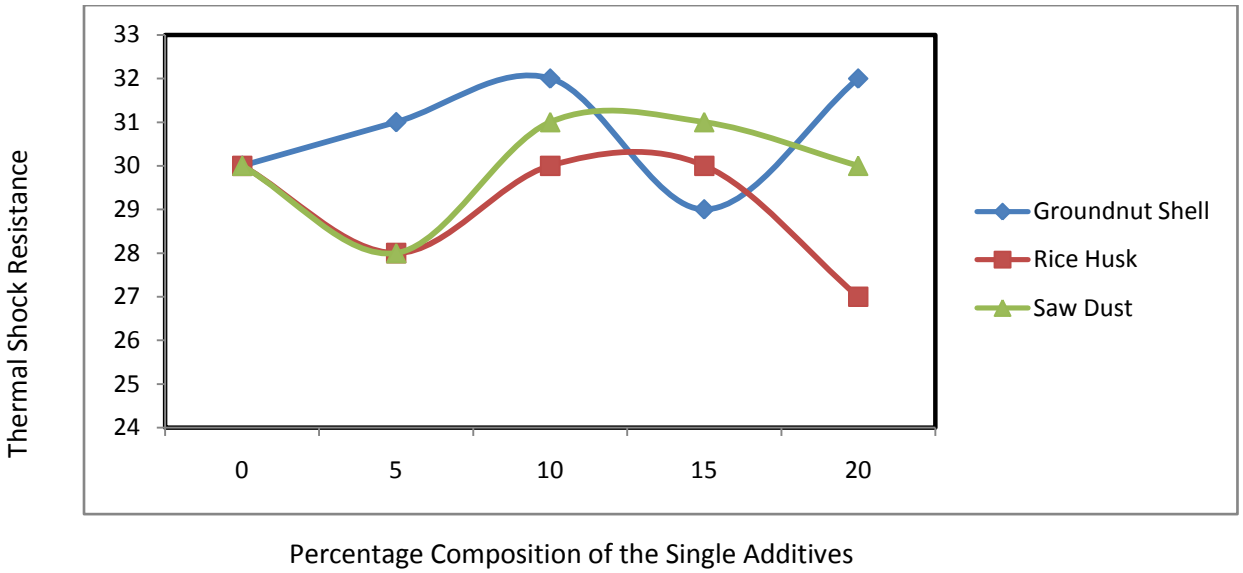

Figure. 4.5: Effect of composition of different single additives on thermal shock resistance of blended Nguzu-Amaiyi clay

From Table 4.5 and Figure 4.5, it is seen that the thermal shock resistance values of the blended clays with the different single additives ranges from 27 – 32 cycles.

It was noted that the values obtained in different combinations did not depend directly on the composition of the additive as other previous properties did. They increased and decreased at various percentage compositions. This is traced to the fact that so many other factors like oxide composition, size of pores and processing method determine this property.

It has been reported that the presence of oxides like phosphorus oxide enhances spalling resistance of brick material. (Chung, 2003). This oxide reacts with aluminia to form alumino phosphate bond which improves bonding in clay structure. The improved brick structure offer more resistance to the effect of thermal fluctuations. Beside this, it has been reported that larger pores impede the movement of crack propagation, hence improve the property. All these factors must have influenced the results for this test.

Blend of clay and saw dust had thermal shock resistance values of 28, 31, 31 and 30 cycles for percentage composition of additive of 5, 10, 15 and 20% respectively. Blend of clay and rice husk had values of 30, 28, 30, 30, 27 cycles while that of groundnut shell were 31, 32, 29, 32 cycles for the respective compositions.

Generally, it was seen from these results that higher composition of the additive in the clay gave higher value of the spalling resistance. This is traced to large pore sizes which impeded the movement of crack propagation.

It was also noted that in the blend of saw dust and rice husk additives, 5% composition deteriorated the property by 6.6%. However, 10 – 20% composition of rice husk additive achieved percentage enhancement of 3.3% in the composite

brick. This shows that better performance of this property is obtainable at higher percentage composition of the additive.

In contrast, blend of groundnut shell showed percentage improvement of 3.3 to 6.6% between 5 – 20% compositions except in 15% composition.

From this result, it is seen that groundnut shell additive yielded the best result in this property, followed by blend of sawdust while that of rice husk did not yield any improvement in this property.

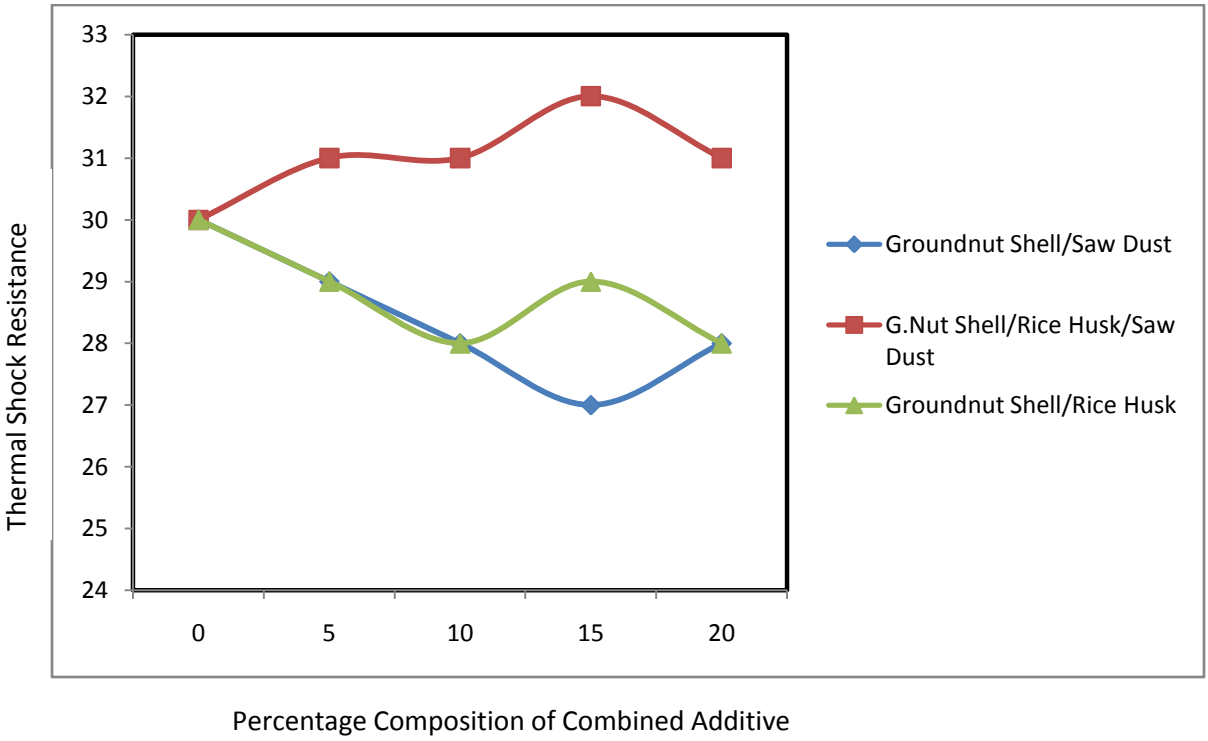

Figure. 4.6: Effect of composition of different combined additives on Thermal shock resistance

Table 4.6 and Figure 4.6 show the thermal shock resistance values for clay blended with two and three additives. From the Table, it is seen that combination of the

three additives gave values of 31, 31, 32 and 31 cycles. Combination of groundnut shell with rice husk additive gave 29, 28, 29, 28 cycles while combination of groundnut shell with sawdust additive gave 29, 28, 27, 28 cycles. These results showed that the combination of the two additives examined did not improve the property rather, a percentage deterioration of 3.3 – 10% and 3.3 – 6.7% were noted in groundnut shell with sawdust and groundnut shell with rice husk blends respectively within the range of additive composition used. In contrast, the combination of the three additives had percentage improvement of 3.3 – 6.7% between 5 to 20% composition. Therefore, it can be concluded that when higher resistance to thermal fluctuation is required, the use of combination of the three additives should be preferred to others.

4.4.6 Results for Refractoriness Test

The softening points of the clay bricks are shown in Tables 4.4 - 4.6 and also in Figure 4.7 in pyrometric cone equivalence (PCEs) and also in their corresponding temperatures.

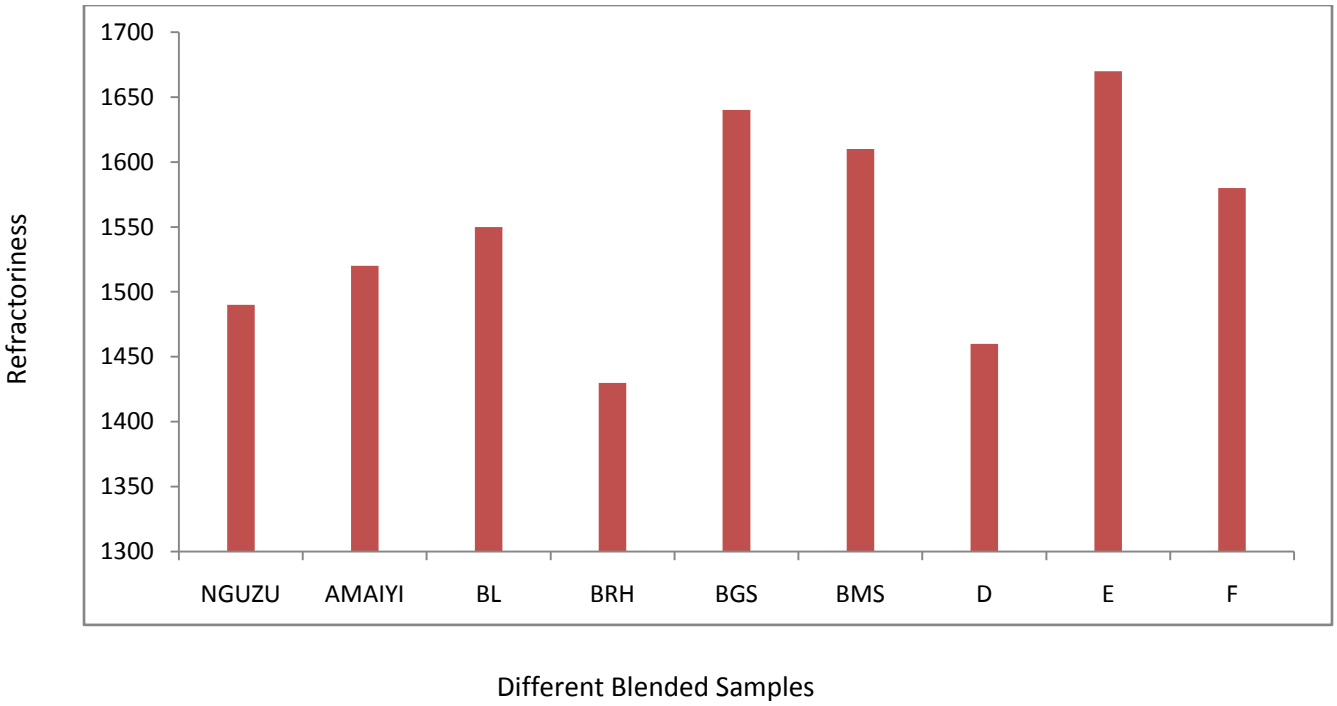

Figure.4.7: Effect of different additives on the refractoriness for Nguzu/Amaiyi clay and blended samples

D stands for blend of groundnut shell with sawdust, **E** stands for blend of the three additives, **F** stands for blends of groundnut shell with rice husk while **BL** stands for the control sample.

From Table 4.4, it can be seen that the refractoriness of Nguzu and Amaiyi clays were 1490^0C and 1520^0C respectively while that of the control sample was 1550^0C.

The refractoriness of clay brick is affected by the oxide composition. For example Al_2O_3 enhances refractoriness. The results of the oxide composition of the clays shown in Tables 4.1 and 4.2 indicate that Amaiyi clay has alumina composition of 22.9% while Nguzu clay has 21.8%. The higher value of alumina content of

Amaiyi clay is responsible for its higher value of refractoriness compared to Nguzu clay.

Table 4.5 shows that the refractoriness of the samples blended with sawdust, rice husk and groundnut shell were 1610^0C, 1430^0C and 1640^0C respectively. Table 4.6 shows that the refractoriness of the samples blended with combination of the three additives, combination of two additives made of groundnut shell with rice husk and combination of two additives made of groundnut shell with sawdust were 1670^0C, 1580^0C and 1460^0C respectively.

Results obtained show that blended clay samples of the same family of additives produced the same value of refractoriness. This is in agreement with the result of Ndaliman, (2007) which stated that values of refractoriness remain uniform for a particular type of additive.

It was found from these results that refractoriness was improved in sawdust and in groundnut shell additives by 3.9% and 5.8% respectively. However, in rice husk blend, it deteriorated by 7.7%. Improvement of 7.7% in this property was observed in the combination of the three additives while combination of groundnut shell with rice husk showed slight percentage improvement of 1.9%. In combination of groundnut shell with sawdust, refractoriness deteriorated by 5.8%.

Enhancement of refractoriness of these brick samples was traceable to the oxide composition of the additives and phase transformation in the composite clay

material during firing. Certain oxides like alumina and phosphorus oxide found in the additives must have contributed to the enhancement. More also, examination of the clay microstructure revealed the presence of mullite phase. This phase developed at high temperature and is responsible for high temperature characteristic of the clay brick.

4.4.6 Results for Thermal conductivity Test

Results for Nguzu, Amaiyi and control samples are shown in Table 4.4 while those for single additive blends and combined additives blends were shown in Tables 4.5 and 4.6 respectively. Figure 4.8 shows the values of thermal conductivity and effect of various additives and their combinations on the same property of the clays.

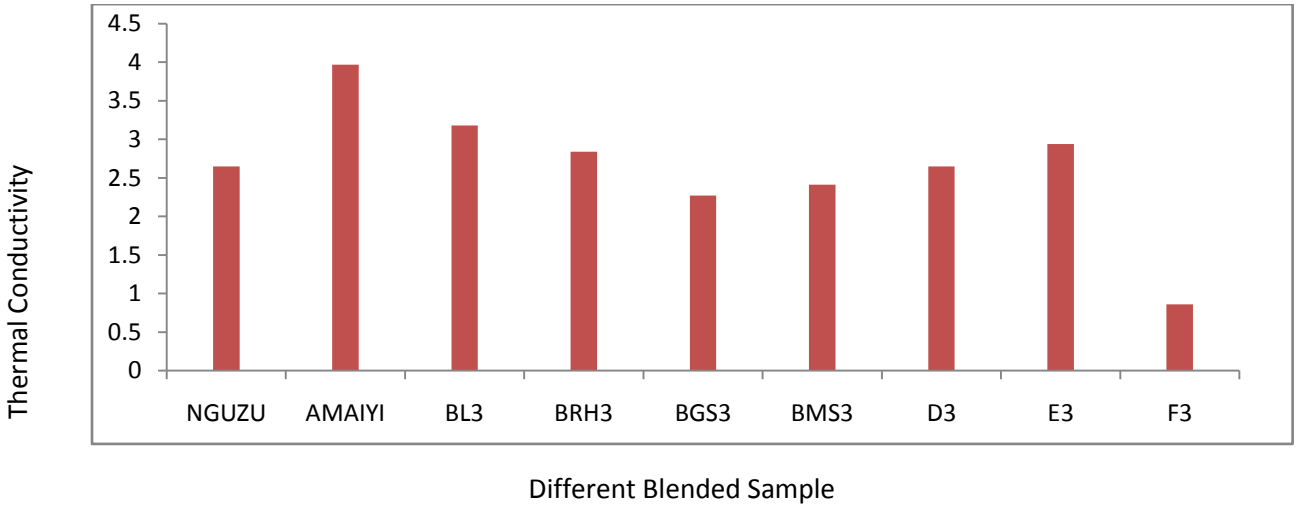

Figure. 4.8. Effect of different additives on the thermal conductivity of Nguzu/Amaiyi clay and blended samples at 5W input power.

From Table 4.4 and Figure 4.8, it is seen that the thermal conductivity values for Nguzu, Amaiyi and control samples were 0.00265W/mm^{0}C, 0.00397 W/mm^{0}C and 0.00318 W/mm^{0}C respectively. Nguzu clay had less thermal conductivity value than Amaiyi clay. These results correlate with the apparent porosity results. They show that materials which are more porous have less thermal conduction capacity and as such possess better insulating property. The thermal conductivity of the control sample shows that it is possible to improve the insulating property of Amaiyi clay by blending it with Nguzu clay which is more insulating.

The thermal conduction of a brick material is a function of pore sizes and their distribution in the brick structure. The voids in the pores contain air which is a poor conductor of heat and therefore, offers resistance to thermal flow.

Table 4.5 shows that the thermal conductivity for bricks blended with sawdust, rice husk and groundnut shell were 0.00227, 0.00241 and 0.00284W/mm^{0}C respectively. This shows that the thermal conductivity of the control sample which was 0.00318W/mm^{0}C improved by 28.6%, 24.2% and 10.7% with addition of sawdust, rice husk and groundnut shell additives respectively.

These results show that the additives were very effective in improving the insulating behavior of clay brick which led to a decrease in thermal conductivity.

Table 4.6 shows that composite bricks made with the three additives, two additives of groundnut shell with rice husk and two additives of groundnut shell with sawdust have thermal conductivity values of 0.00294, 0.00086 and 0.00265W/mm^{0}C respectively. This shows that combination of groundnut shell with rice husk yielded the best insulating property among the three combinations.

Generally, it was observed that both single and combined additives enhanced the insulating capacity of the clay brick by decreasing the thermal conductivity. The reason for the observed decrease is that the additives left voids and pores in the clay structure upon burning during firing. The pores decreased the concentration of thermal conduction pathways. When the proportion of air inside the brick body is higher, the thermal insulating capacity of the material becomes better. This is because air is a good insulator in comparison to the solid material.

Therefore, it is confirmed that the pore size, and its distribution and the amount of air space or voids created during firing of clay determines the thermal conductivity of the material.

4.5 Evaluation of the Performance of Refractory Properties for Various Blends of the Additives

In sawdust additive, the results revealed that linear shrinkage was within the range of (7.53 – 10.64)%. In rice husk blend, it was within the range of (6.5 – 10.6)% while in groundnut shell blends, it was between 6.5 and 8.5%.

These results show that groundnut shell blend has the least shrinkage which is more desirable. Higher shrinkage may result to warping and cracking of clay product and may cause loss of heat in the furnace. (Aliyu et al, 2014). Moreover, the range of linear shrinkage in groundnut shell blend was perfectly within the recommended range of 4 -10% as reported by Omowumi, (2001).

The apparent porosity for sawdust additive was between 30.2 and 46.15%, for rice husk additive apparent porosity from 31.5 to 46.1% while for groundnut shell additive from 21.95 to 46.1%.

Therefore for this property the blends are in the same range.

Bulk density for blends of sawdust is within the range of 1.9 – 1.6g/cm^3 while those for rice husk and groundnut shell blends it was between 2.2 and 1.57 g/cm^3 and 2.05 and 1.42 g/cm^{3}respectively. Therefore the accepted standard value for bulk density of 1.71 -2.1 g/cm^3 was obtained in all the blends, especially within lower percentage composition of the additives. However, higher percentage of the

additive gave bulk density values outside the acceptable range and should be discouraged.

The modulus of rupture for sawdust blends was within the range 29.9 -28.5MPa. In rice husk blend and groundnut shell blends the ranges were 31 – 30.2MPa and 39.6 – 30.9MPa respectively. This shows that the best performance of transverse strength was obtained in groundnut shell blend which showed outstanding values among the three additives used. It therefore suggests that groundnut shell blended brick is most suitable for application where high load bearing capacity is required as in refractory bricks for furnaces.

Thermal shock resistance for sawdust blends ranged from 28 to 31cycles while those for rice husk blends and groundnut shell blends ranged from 27 to 30 cycles and 29 and 32 cycles respectively. It was found that the thermal shock resistance of groundnut shell blends was the best followed by that of sawdust while rice husk was the least.

It could therefore be seen that from the above results that the negative effect of thermal fluctuation could be reduced with the use of groundnut shell additive in brick production. It was also found that each blend met the acceptable standard of 25 -30cycles for good refractory brick.

The thermal conductivity of sawdust, rice husk and groundnut shell blends were 0.00227, 0.00241, 0.00284W/mm^{0}C respectively. Comparison of these values with the control sample 0.00318 W/mm^{0}C shows that the percentage improvement of the insulating property of the clay material by these additives were 28.6%, 24.2% and 10.7% respectively.

It is therefore noted that sawdust blend has better insulating property than the other two.

The refractoriness of sawdust, rice husk and groundnut shell blends were 1610^{0}C, 1430^{0}C and 1640^{0}C respectively. Comparison of these values with that of the control sample (1550^{0}C) shows that this property was enhanced in sawdust and groundnut shell blends but not in rice husk. It was also noted that the acceptable standard value of (1500 -1700) ^{0}C was obtained in both sawdust and groundnut shell blends.

4.6 General Trends in the Properties

The results obtained in this research investigation are presented in Tables, Plates and Figures in this work. The chemical compositions of the two clays used were found to compare very well with values recommended for high melting clay according Nnuka and Agbo, (2000). When the chemical compositions of the two clays were compared with those of refractory clay, it was found that both clays were deficient in alumina content but not in silica content. The percentage composition of the alkali oxide like K_2O and CaO compares well with that of refractory clay material while the Fe_2O_3 content was excessively high.

Results obtained for the physicomechanical properties of both clays shown in Table 4. 40 and also compared with standard values in Table 4.7 indicate that some of these properties were below the acceptable standards. Blend of the two clays (control sample) was also found not to have improved these properties to the desired standard. Hence, the need to introduce the additives became paramount. The introduction of the additives into the clays was to improve the properties and widen the applications of the clay raw material. The improvements achieved on the refractory properties of the clay were reflected in the comparison shown in Table 4.7.

Considering these properties of the clays stated above, it was found that apparent porosity of Nguzu clay was 20% and is within the acceptable standard value of (20

- 30)% according to Omowumi, (2001). However, Amaiyi clay had apparent porosity value of 11.56% which is below the specified standard. Bulk density value for both Nguzu and Amaiyi clays were 2.13 and 2.15g/cm^3 respectively. These values are below the acceptable standard value of 2.3 g/cm^3.

The control sample gave apparent porosity and bulk density values of 15.38% and 1.77 g/cm^3 respectively.

When the additives were introduced into the clay, apparent porosity improved from 21.95 to 54.17% while bulk density improved from 1.9 to 2.2 g/cm^3.

Linear shrinkage of 4.4% and 4% were found in Nguzu and Amaiyi clays respectively. The control sample showed increase in shrinkage up to 6.59%. The reason for the increase was explained in section 4.4.1. The presence of the additives was observed to increase the linear shrinkage further from 6.59 to 10.64%. This was attributed to the rearrangement of the particles and grains which led to formation of more compact structure of the brick.

The thermal conductivity for Nguzu and Amaiyi clay was 0.00265 and 0.00397W/mm^{0}C respectively while that of the control sample was 0.00318 W/mm^{0}C. When these results were compared with those of porosity and bulk density previously discussed, it was noted that these results correlate. This confirms that the three properties are interrelated. Clay material with high porosity value yields low density and low thermal conductivity. Hence, it could be

confirmed that apparent porosity is inversely proportional to thermal conductivity and bulk density.

The clay blended with the additives gave thermal conductivity ranging from 0.00086 to 0.00294 W/mm^{0}C. The additives at various combinations were found to decrease the thermal conductivity, thereby improving the insulating property of the clay brick. Generally, it was noted that the additives increased porosity and decreased bulk density and thermal conductivity.

Results for thermal shock resistance test showed that Nguzu and Amaiyi clays had spalling resistance values of 28 and 29cycles respectively while the control sample gave 30cycles. These values were found within the acceptable values of (25 -30) cycles according to Omowumi, (2001). The blend incorporated with the additives gave values ranging from (27 – 32) cycles. This showed that the additives increased the thermal shock resistance of the clay material. The increase observed in this property was caused by the enlargement of pore sizes produced in the clay structure. The large pore sizes impeded the propagation of thermally induced crack. Consequently, the spalling resistance increased. (Callister, 2010).

The trend in modulus of rupture was different from other properties. The values obtained for both Nguzu clay, Amaiyi clay and the control sample were 38.8, 33.5 and 32.7 MPa respectively. It therefore shows that the transverse strength decreased in the blend of the two clays. However, this property was found to show

improvement when the clay was blended with groundnut shell additive, rice husk additive and when blended with combination of the three additives used in this work. These different combinations of the additives in the clay gave values of 39.6, 33.2 and 34.3MPa respectively. It therefore shows that the additives are capable of improving the property at the specified composition and combination.

This improvement is traceable to presence of some oxides like alumina and phosphorus oxide which form strong bond in refractory product. (Decker in Siljan, 2003, and Chung, 2003).

From results shown in Table 4.6, it is seen that the refractoriness was higher in Amaiyi clay when compared to Nguzu clay. The difference is attributed to variation in alumina content in the two clays. This oxide is responsible for high refractoriness. Observation made from the results in the same Table shows that the refractoriness of the control sample of 1550^0C was improved in the blend made with sawdust, groundnut shell, and combination of the three additives and also in combination of two additives from groundnut shell and rice husk. These combinations gave respective values of 1610^0C, 1640^0C, 1670^0C and 1580^0C. However, it was noted that in rice husk single additive and in the combination of groundnut shell and sawdust, the value of refractoriness reduced. The variation in the values of refractoriness obtained in various combinations is attributed to the presence of phases formed during firing. Phases like mullites are formed at high

temperature (above 1000^0C); they are responsible for high temperature characteristics in the clay brick.

4.7 Comparison of Result Findings with Previous Related Research Works

Considering previous related research works with the results obtained in this study, it was observed that every refractory material is unique in its properties based on the fact that factors that affect those properties like chemical and mineralogical compositions, method of processing like compacting pressure, heating and cooling rate vary for each product. Therefore, the following facts were established based on the results of previously related research studies:

- Manukaji, (2013) stated that increase in the percentage of rice husk additive gave internationally accepted values in all the properties but it was shown in this study that the values of linear shrinkage, apparent porosity and bulk density in all the various composition did not fall within the standard values, rather, certain percentage composition gave acceptable values while others did not. Thermal shock resistance values were found to be in the acceptable range in all the four compositions used while refractoriness was not enhanced in any way by the addition of rice husk single additive. Therefore, this finding is not in full agreement to all the conclusions of Manukaji (2013).

Based on the results generated from the thermal conductivity test, it was observed that the findings conformed to the conclusion of Olayinka and John (2014) on the use of sawdust to reduce thermal conductivity capacity of refractory materials.

This is in line with the conclusion made by Folaranmi, (2009), which stated that with additives, some properties improved while others did not. However, it is noted from this work that the best combination of additives that could meet the internationally accepted standard is the combination of the three (groundnut shell, saw dust and rice husk).

4.8 "Comparison with Previous Works".

Tables 4.8 and 4.9 show results of various research works done with the use of single agro additive to improve refractory properties of local clay material by previous researchers while Table 4.10 shows the improvement made with the use of multiple additives applied in this present research study.

Table 4.8A. Enhancement of Refractory Properties with Different Single Additives by Other Researchers.

Property	**Manujika, 2013 with groundnut shell**			**Fatai, 2012 with sawdust**			**Hassan et al,2014 With rice husk**		
	Control sample	Blended sample	% enhancement	Control sample	Blended sample	% enhancement	Control sample	Blended sample	% enhancement
Linear shrinkage (%)	9.1	8.9	-22%				3.89	3.0	-23%
Apparent porosity (%)	12.5	15	+16.7%	20	57	+65%	27.15	36.74	+26%
Bulk density (g/cm^3)	2.85	2.82	-1.05%	2.5	1.3	-48%	1.98	1.52	-23%
Thermal shock resistance (cycle)				27	15	-44%	1	10	+90%
Thermal conductivity (W/mm^0C)	0.5	0.32	+36%	0.25	0.08	+68%			
Refractoriness (^0C)							1300	1200	-76%

Table 4.8B Enhancement of Refractory Properties with Sawdust Single Additives by Other Authors

Property	**John 2014 with sawdust**			**Joshua, 2009 with sawdust**			**Hassan et al, 2014 With saw dust**		
	Control sample	Blended sample	% enhance ment	Control sample	Blended sample	% enhance ment	Control sample	Blended sample	% enhance ment
Linear shrinkage(%)	7.33	6.24	+15%	2.47	2.36	+1.6%	3.89	3.0	-23%
Apparent porosity (%)	47	54	+13%	37	57	+35%	27.15	44.33	+40%
Bulk density (g/cm^3)	0.98	1.18	+17%	1.51	1.51	0%	1.98	1.59	-20%
Spalling resistance (cycle)	28	26	-7%	10	10	0%	1	10	+90%
Thermal conductivity (W/m^0C)	0.1	0.11	-9%	0.25	0.19	+24%			
Refractorines s.(^0C)							1300	1200	-76%

Table 4.8C Enhancement of Refractory Properties of Blended Clay with Combined Additives

Property	**Control sample**	**Groundnut shell & sawdust blended clay**		**Groundnut shell & rice husk blended clay**		**Groundnut shell, sawdust & rice husk blended clay**	
		Blended sample	% enhancement	Blended sample	% enhancement	Blended sample	% enhancement
Linear shrinkage (%)	6.59	8.5 – 8.7	-22%	8.4 – 9.68	-21%	5.49 – 10.64	+16.7%
Apparent porosity (%)	15.38	28.57 – 54	+71.5%	23.91 – 44.89	+66%	36.36 – 54.17	+72%
Bulk density (g/cm^3)	1.77	1.73 – 1.3	-2.2%	2.0 -1.39	+11.5%	1.73 – 1.25	-2.2%
Modulus of rupture (MPa)	32.7	32.7 – 24.1	0%	30.3 – 26.5	-7.3%	34.3 – 26.1	+4.7%
Spalling resistance (cycle)	30	27 - 29	-3%	29 - 28	-3%	31 - 32	+6.2%
Thermal conductivity (W/m^0C)	3.18	2.64	+17%	0.86	+73%	2.94	+7.5%

Refractoriness (^{0}C)	1550	1460	-5.8%	1580	+1.9%	1670	+7.2%

From Tables 4.8 and 4.9, it is seen that Fatai, (2012), Joshua, (2009) and John, (2014) used sawdust additive on various clay materials. The first two achieved enhancement on porosity and thermal conductivity only while the last improved porosity and density only with other properties deteriorated.

Manujika, (2013) used groundnut shell to achieve enhancement in apparent porosity and thermal conductivity while other properties deteriorated in value. Hassan, Yami et al, (2014) used sawdust and rice husk separately and improved porosity and thermal shock resistance in the respective works. In contrast to the previous results obtained with single additives, from Table 4.10, it was found from this work that combination of the three additives yielded enhancement in six different properties with exception to bulk density. Also, combination of blend of two additives made of groundnut shell with rice husk yielded good results in apparent porosity, bulk density, thermal conductivity and refractoriness. It was noted that the few properties that did not improve when compared to the control sample were still found within the acceptable standards. This confirms that the properties were not impaired.

Therefore, the use of multiple combined additives has proved to be more suitable than single ones which were previously used by other researchers.

4.9 Results of the Experimental Design and Optimization for Refractory Properties of Blended Nguzu – Amaiyi Edda Clay Using Sawdust, Rice Husk and Groundnut shell Additives.

The relationship between the refractory properties parameters (responses) of various composite brick made from sawdust, rice husk and groundnut shell additives and the composition of additives and clay (factors) was investigated using response surface methodology with central composite design type. This involved the development of experimental design, fitting selection and optimization of the best response surface functions for the responses. The response variables investigated were linear shrinkage, apparent porosity, bulk density, and modulus of rupture. The independent variables (factors) are the composition of the additive and that of the combining clay.

	Factor 1	Factor 2	Response 1	Response 2	Response 3	Response 4
Std	A:Saw dust	B:Clay	Linear Shrinkage	Apparent porosity	Bulk Density	Modulus of rupture
	%	%	%	%	(g/cm^3)	(N/mm^2)
1	5	95	6.98	34.89	1.94	30.49
2	20	80	10.45	54.89	1.48	28.21
3	5	95	7.24	35.94	1.91	30.54
4	17	83	9.27	49.12	1.72	28.99
5	4	96	6.01	28.03	1.99	31.2
6	20	80	10.64	54.02	1.49	28.13
7	15	85	8.93	47.19	1.71	29.22
8	6	94	7.45	40.83	1.84	30.33
9	6	94	7.9	41.02	1.84	30.09
10	6	94	8.28	43.19	1.8	29.89
11	6	94	8.44	43.89	1.78	29.65
12	6	94	8.73	45.17	1.75	29.11
13	6	94	8.98	47.11	1.75	29.01

The responses obtained from different experimental runs carried out by combinations of the two factors in various runs are shown in Table 4.9. The

responses obtained from the various runs are different from each other. This shows that the factors have significant effect on the responses. The model suitability was tested using the ANOVA test.

4.10.10 ANOVA Analysis for the Effect of the Factors on Linear Shrinkage in the Blend of Sawdust

The lack of fit test and the comparison of the R-squared values were used to test for suitability of the models. The results for the test are shown in Tables 4.10.1A and 4.10.1B respectively

Table 4.10.1A: Lack of Fit Test

Lack of Fit Tests						
	Sum of		**Mean**	**F**	**p-value**	
Source	**Squares**	**df**	**Square**	**Value**	**Prob > F**	
Linear	2.38	6	0.4	2.3	0.2197	
2FI	2.26	5	0.45	2.62	0.1856	
Quadratic	0.046	3	0.015	0.088	0.9628	Suggested
Cubic	0	0				Aliased
Pure Error	0.69	4	0.17			

The test for the model fitting was done to determine the adequacy of the models and also to indicate which of the proposed model fits well or not. It was also done to know the capability of the model to interpret the level of significance or predict the function response for all the independent variables.

From Table 4.10.1A, it is seen that the linear model and 2F1 model have significant lack of fit F values of 2.3 and 2.63 respectively while the quadratic model showed a non significant lack of fit F-value of 0.088. Hence, it was observed that the quadratic model has the lowest value of F-value of lack of fit compared to other models. This showed that the model was the most fitted and desirable.

Table 4.10.1B Model Summary Statistics

Model Summary Statistics						
	Std.		**Adjusted**	**Predicted**		
Source	**Dev.**	**R-Squared**	**R-Squared**	**R-Squared**	**PRESS**	
Linear	0.55	0.8535	0.8241	0.5959	8.46	
2FI	0.57	0.8591	0.8122	0.4481	11.56	
Quadratic	0.32	0.9649	0.9398	0.8996	2.1	Suggested
Cubic	0.42	0.9671	0.9012		+	Aliased

The comparison of the R-square, R-square predicted and adjusted R-square values are shown in Table 4.10.1B. The measure of how efficient the variability in the actual response values can be explained by the experimental variables and their interactions are given by the R-squared value. If the R- square predicted and adjusted are too far from each other, there is indication of problem with the model or the data.(Taran and Agbaie, 2015).

Hence, comparison of the R-squared, R-squared adjusted and predicted R-squared values were done. Model which showed a better correlation in these values was considered best.

It can be seen from Table 4.10.1B that the quadratic model has values for R-square, R-square adjusted and R-square predicted as 0.9649, 0.9398 and 0.8996 respectively. The linear model has them as 0.8535, 0.8241 and 0.5959 respectively while the 2F1 model had them as 0.8591, 0.8122 and 0.4481 respectively. These results showed that the quadratic model showed a better correlation of these values when compared with other models.

From the results obtained in these tests stated above, it was concluded that quadratic model justified its selection as the most appropriate model as suggested by the soft ware. Therefore, the effect of each parameter was evaluated using quadratic model in Table 4.10.1C.

Table 4.10.1C Anova for Response Surface Quadratic Model

Source	Sum of Squares	df	Mean Square	F Value	p-value Prob>F	
Model	20.21	5	4.04	38.49	<0.0001	significant
A-Sawdust	10.47	1	10.47	99.66	<0.0001	
B-Clay	0.97	1	0.97	9.28	0.0187	
AB	0.6	1	0.6	5.74	0.0187	
A^2	1.65	1	1.65	15.73	0.0054	
B^2	0.77	1	0.77	7.33	0.0303	
Residual	0.74	7	0.11			
Lack of Fit	0.046	3	0.015	0.088	0.9628	Not significant
Pure Error	0.69	4	0.17			
Cor Total	20.95	12				

Std	0.32	R-Squared	0.9649
Mean	8.41	Adj R-Squared	0.9398
C.V.%	3.84	Pred R-Squared	0.8996
PRESS	2.1	Adeq Precision	21.167
-2Log likelihood	-0.45	BIC	14.94
		AICc	25.55

DF = degree of freedom

CV = Coefficient of variance

PRESS = Predicted residual sum of squares

From the Table 4.10.1C, it was seen that the model's F value of 38.49 implies the model is significant. There is only a 0.01% chance that an F-value, this large could occur due to noise. Values of prob>F" less than 0.0500 indicate model terms are significant. In this case A, B, AB, A^2, B^2 are significant terms. Values greater than 0.1000 indicate the model terms are not significant.

The independent variables in the specified model and the effect of each variable were evaluated. Hence in order to evaluate the adequacy of the selected model, several appraisal techniques were used. The coefficient of determination (R^2), the

adjusted determination coefficient (adjusted R^2) and coefficient of variation (CV) were used to weigh the adequacy of the model as used by other researchers. (Chen et al, 2010). The "lack of fit F-value" of 0.09 implies the lack of fit is not significant relative to pure error. There is a 96.28% chance that a "lack of fit F-value" this large could occur due to noise. Non significant lack of fit is good because it means the model will be well fitted. Therefore the improved model can be used to predict effectively the responses- linear shrinkage of sawdust blended clay brick.

The predicted R^2 of 0.8996 is in reasonable agreement with adjusted R^2 of 0.9398. The difference between the two is 0.0402. The difference is less than 0.2. The coefficient of variation (CV) which is defined as the ratio of standard deviation of estimate to the mean value of the observed response is calculated as 3.85% which illustrated that the model can be considered reasonably reproducible. This is because its coefficient of variation was not greater than 10%. (Chen et al, 2011). The signal to noise ratio which is given as the value of the adequacy precision is 21.167. This indicates that an adequate relationship of signal to noise ratio exist.

In terms of the coded and actual values, the selected models are given in the equations 4.1 and 4.2 respectively.

$$\text{Linear Shrinkage} = 9.23 + 1.24 *A - 0.91*B - 0.5*AB - 0.28*A^2 - 1.06*B^2 \quad (4.1)$$

A stands for sawdust and B stands for clay

$$\text{Linear Shrinkage} = -142.69456 + 7.54393*X_1 + 2.16255*X_2 - 0.033346X_1*X_2 - 0.12268*(X_1)^2 - 0.010646*(X_2)^2. \quad (4.2)$$

X_1 stands for sawdust while X_2 stands for clay

The equation in terms of coded factors can be used to make predictions about the response for given levels of each factor. By default, the high levels of the factors are coded +1 and the low levels of the factors are coded as -1. The coded equation is useful for identifying the relative impact of the factors by comparing the factor coefficient.

The equation in terms of actual factors can be used to make predictions about the response for given level of each factor. Here, the levels should be specified in the original units for each factor. The response values obtained by inserting the independent values are the predicted values of the model. These values are compared to the actual and experimental values. The result of the comparison was shown in Figure 4.10.1

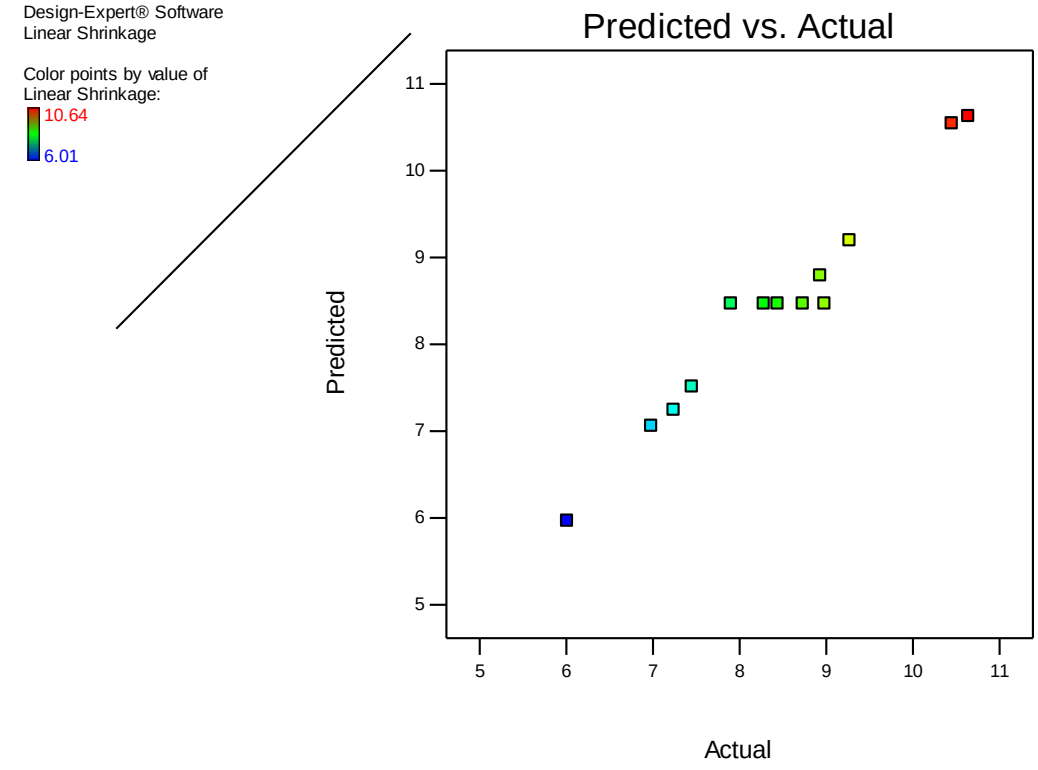

Figure 4.10.1 linear correlation between predicted Vs actual values for linear shrinkage of blended Nguzu- Amaiyi clay with sawdust additive.

From Figure 4.10.1, it can be seen that actual values were distributed relatively near to the predicted value line. This shows that there is a good correlation between the actual and the predicted values. This observation shows that the central composite design (CCD) is well fitted into the model and thus can be used to perform the optimization operation for the process.

4.10.11 Effects of Model Parameters and their Interactions

The relationship between the experimental variables and the response were studied with the plot of the individual and interactive effects of the two factors- clay and sawdust on the response - linear shrinkage.

The central composite design was used to produce three dimensional (3D) response surface and two dimensional (2D) contour plots. The 3D surfaces and 2D contour plots are graphical representations of the equation for the optimization of the experimental responses and are the most useful approach in revealing the conditions of the optimum performance of the responses.

In the plots, the response functions of the two factors are presented. The results of the interactions between two independent variables and dependent variable are shown in Figures 4.10.2 and 4.10.3.

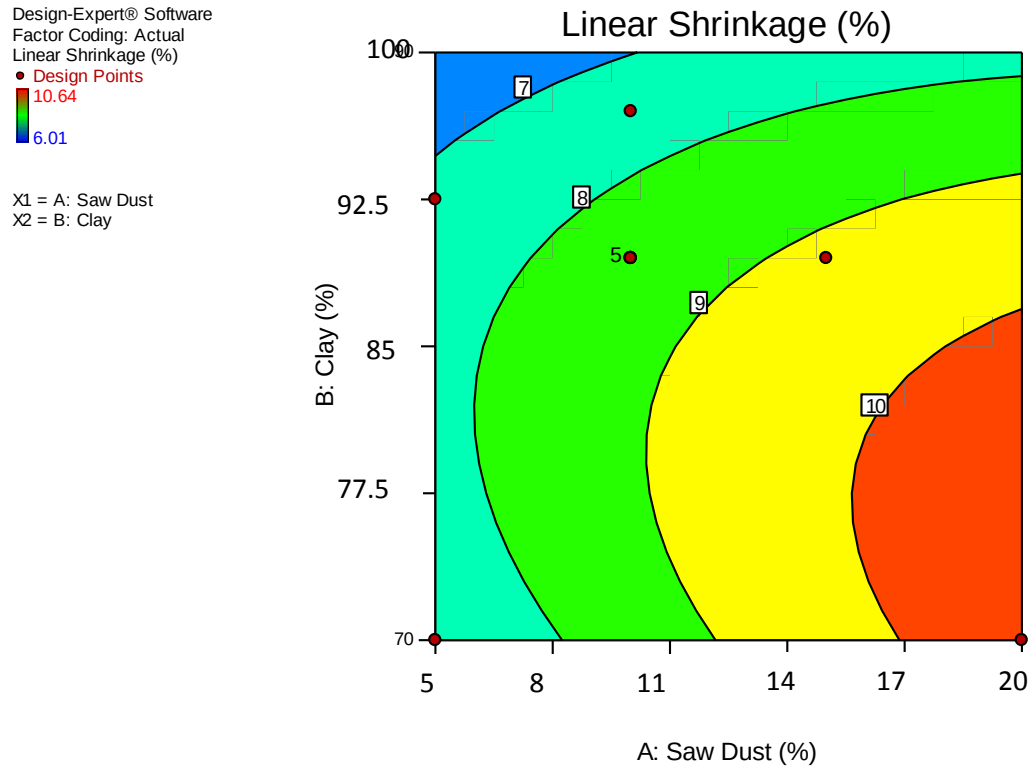

Figure 4.10.2 Two dimension contour plot for the combined effect of the composition of clay and sawdust on the linear shrinkage property

Figures 4.10.2 and 4.10.3 show the interaction effect of clay and sawdust composition on linear shrinkage. It was observed from the plot that there is increase in linear shrinkage with increase in the composition of sawdust (A). The maximum shrinkage was obtained in sawdust composition at the range of 17 -20% while minimum (optimum) shrinkage was obtained at the range of 5 - 6.3% composition of the additive. Previous studies have reported that linear shrinkage increases with increase in the quantity of additive.

On the other hand, the effect of the composition of clay shows that linear shrinkage decreases with increase in the composition of clay. Maximum shrinkage was found between 80 and 77.5% composition of clay while minimum (optimum) value of shrinkage was found at 95 – 93.7% composition of the clay.

The fact that there is increase in shrinkage value with decrease in the composition of clay and increase in the composition of sawdust is in agreement with the conclusion of Safeer et al, (2017). The conclusion stated that the percentage of firing shrinkage increases with increase in the amount of additive. The increased shrinkage was caused by rearrangement of grains and particle and orientation ordering in the crystal lattice form. This formed a compact solid texture compared to the initial state.

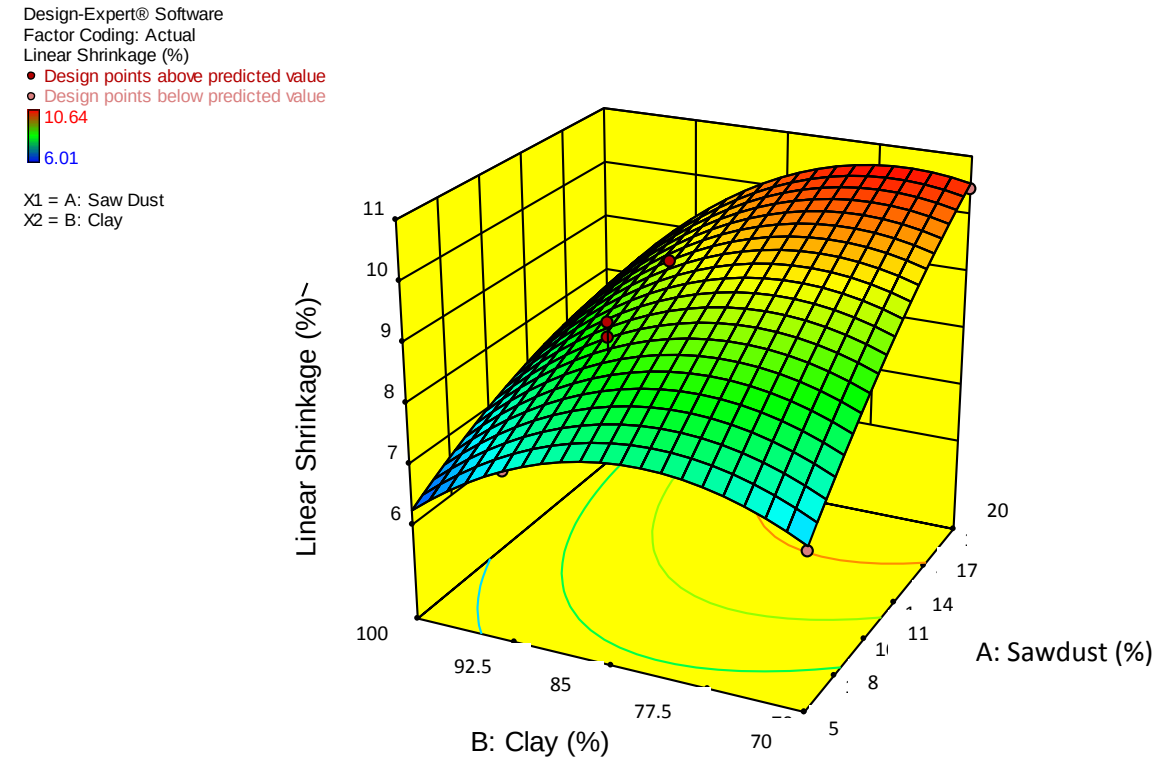

Figure 4.10.3 Three dimension surface plot for the combined effect of the composition of clay and sawdust on the linear shrinkage property

4.10.2 Results for Apparent Porosity in the Blend of Sawdust

The lack of fit test and the comparison of the R-squared values were used to test for suitability of the models. The results for the test are shown in Tables 4.10.2A and 4.10.2B respectively.

Table 4.10.2A Lack of Fit Tests

Lack of Fit Tests						
	Sum of		**Mean**	**F**	**p-value**	
Source	**Squares**	**df**	**Square**	**Value**	**Prob > F**	
Linear	115.75	6	19.29	3.75	0.1106	
2FI	114.47	5	22.89	4.45	0.0864	
Quadratic	1.18	3	0.39	0.076	0.9696	Suggested
Cubic	0	0				Aliased
Pure Error	20.56	4	5.14			

Table 4.10.2A shows the adequacy test. The adequacy of the models was evaluated with the lack of fit test. The test indicates whether a proposed model fit well or not. The test for lack of fit compares the variation around the model with pure variation within replicated observations.

From table 4.10.2A, it is seen that there was a significant difference (F-value) of 3.75 and 4.45 lack of fit for linear and 2F1 models while the quadratic model showed a non significant F-value of 0.076. The significant results of lack of fit for linear and 2F1 models showed that these models are not adequate for use.

Hence the results obtained in the lack of fit test in Table 4.10.2A showed that the quadratic model can describe the response- apparent porosity of sawdust blended clay.

Table 4.10.2B Model Summary Statistics

Model Summary Statistics						
	Std.		**Adjusted**	**Predicted**		
Source	**Dev.**	**R-Squared**	**R-Squared**	**R-Squared**	**PRESS**	
Linear	3.69	0.8012	0.7614	0.335	455.92	
2FI	3.87	0.803	0.7374	-0.01	692.41	
Quadratic	1.76	0.9683	0.9456	0.9313	47.09	Suggested
Cubic	2.27	0.97	0.91		+	Aliased

Beside the F-value and lack of fit, the R-squared, adjusted R-squared and the predicted R-squared values shown in Table 4.10.2B for the quadratic were 0.9683,

0.9456 and 0.9313 respectively. This shows that the best correlation in these values was obtained only in this model when compared to other models.

The measure of how efficient the variability in the actual response values can be explained by the experimental variables and their interaction is given by the R-squared value is to unity, the better the model predicts the response.

Table 4.10.2C ANOVA for Response Surface Quadratic Model of Apparent Porosity in the Blend of Sawdust

Source	Sum of Squares	df	Mean Square	F Value	p-value Prob > F	
Model	663.82	5	132.76	42.76	< 0.0001	significant
A-Saw Dust	421.02	1	421.02	135.59	< 0.0001	
B-Clay	110.56	1	110.56	3.4	< 0.0001	
AB	11.17	1	11.17	3.6	0.0997	
A^2	110.32	1	110.32	35.53	0.0006	
B^2	117.75	1	117.75	2.5	< 0.0001	
Residual	21.74	7	3.11			
Lack of Fit	1.18	3	0.39	0.076	0.9696	not significant
Pure Error	20.56	4	5.14			
Cor Total	685.55	12				

Based on these assessments, the effect of each parameter was evaluated with quadratic model as shown in Table 4.10.2C. From the table, it can be seen that the model F-value of 42.76 implies that the model is significant. Hence, in this case, A, B, AB, A^2 and B^2 are significant model terms. There is only 0.01% chance that an

F-value this large could occur due to noise. Values of prob > F less than 0.0500 indicated that the model terms are significant. Values greater than 0.1000 indicate the model terms are not significant. Hence the independent variable in the specified model and the effect of each variable was evaluated.

The adequacy of the selected model was evaluated on different ways. The coefficient of determination (R^2), the adjusted determination coefficient (Adj R^2) and coefficient of variation (CV) were used to determine the adequacy of the model used. Lack of fit F-value of 0.076 implies the lack of fit is not significant relative to pure error. There is 96.96% chance that a lack of fit value this large could occur due to noise. Non significant lack of fit is good for the model to fit. Hence, the improved model was used to predict effective response of apparent porosity of sawdust blended clay brick.

The F-value of the independent variable for sawdust and blended clay were 135.59 and 3.4 respectively. This shows that the effect of the most independent variable on the dependent variable was significantly high.

The coefficient of determination (R^2) and adjusted coefficient of determination (Adj R^2) were 0.9683 and 0.9456 respectively. This shows that there are excellent correlations between the independent variables and the fitting model can describe

the independent variables well. The predicted R^2 of 0.9313 is in agreement with adjusted R^2 of 0.9456 since the difference is less than 0.2.

Hence, the selected model in terms of the coded and actual values are given in the equations 4.4.3 and 4.4.4 respectively

$$\text{Apparent porosity} = 47.89 + 7.88*A - 3*B - 2.15*AB - 2.26*A^2 - 3.38*B^2 \quad (4.3)$$

(A stands for sawdust and B stands for clay)

$$\text{Apparent porosity} = -693.32859 + 49.81234* X_1 - 7.47354* X_2 - 0.14348* X_1* X_2 - 1.00254*(X_1)^2 - 0.033787(X_2)^2 \quad (4.4)$$

(X_1 stands for sawdust and X_2 stands for clay)

The response values obtained by inserting the independent values are the predicted values of the model. These values are compared to the actual and experimental values. The result of the comparison was shown in Figure 4.10.4

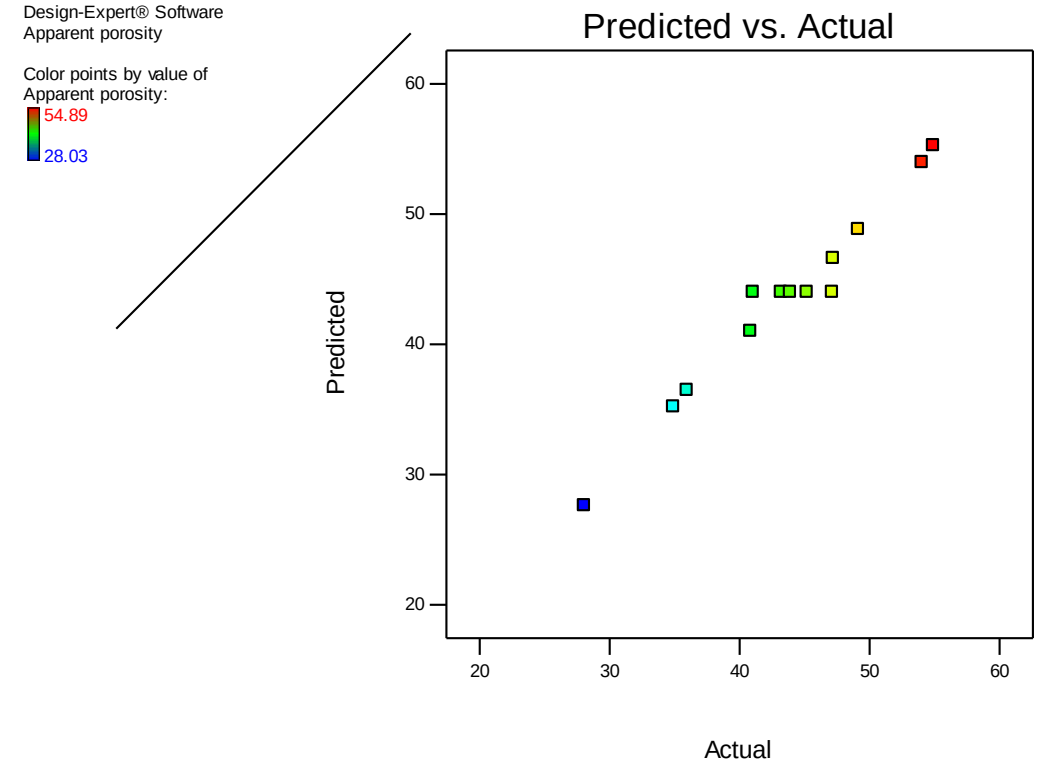

Figure 4.10.4 linear correlation between predicted Vs actual values for apparent porosity of blended Nguzu- Amaiyi clay with sawdust additive.

4.10.21 Effects of Model Parameters and their Interactions for apparent porosity

The relationship between the experimental variables and the response (apparent porosity) were studied with the plot of the individual and interactive effects of the two factors- clay and sawdust on the response – apparent porosity.

The central composite design was used to produce three dimensional (3D) response surface plots. The 3D surfaces plot is graphical representations of the equation for

the optimization of the experimental responses and is the most useful approach in revealing the conditions of the optimum performance of the responses.

In the plots, the response functions of the two factors are presented. The results of the interactions between two independent variables and dependent variable are shown in Figures 4.10.5

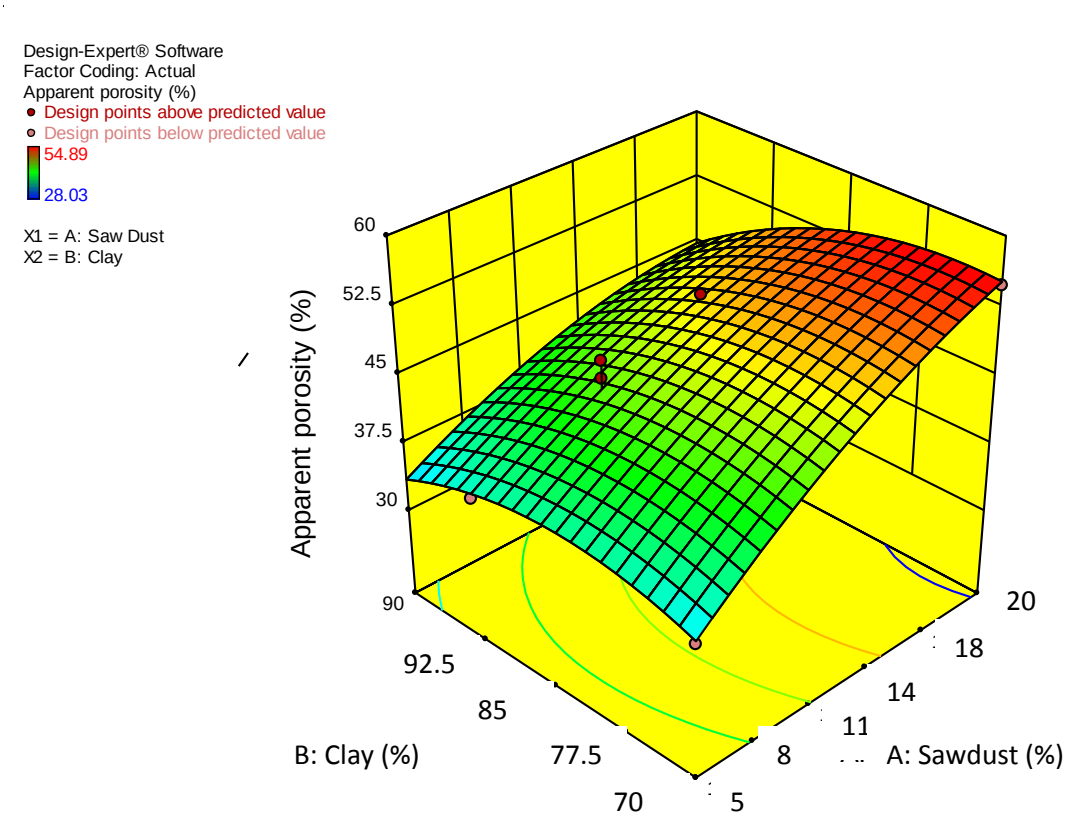

Figure 4.10.5 Three dimension surface plot for the combined effect of the composition of clay and sawdust on the apparent porosity property

Figure 4.10.5 shows the interactive effect of clay and sawdust compositions on apparent porosity. From the Figure, it is seen that the value of apparent porosity

increased with increase in the composition of sawdust additive and decrease in the composition of clay.

At 80% composition of the clay and 20% composition of sawdust additive, 54% value for apparent porosity were obtained. With further increase of clay composition to 92.5% and 7.5% composition of sawdust, apparent porosity decreased to 46%. It was seen that the optimum value of apparent porosity of 33.5% was attained with 95% clay and 5% sawdust additive. The increase in the value of apparent porosity with increase in the sawdust additive attributed larger sizes of pores and also more numbers of pores widely distributed in the brick's structure when more quantities of the additive were used. This increased the porosity of composite brick.

4.10.3 Results for Bulk Density in the Blend of Sawdust

Table 4.10.3A Lack of Fit Tests

Lack of Fit Tests						
	Sum of		**Mean**	**F**	**p-value**	
Source	**Squares**	**df**	**Square**	**Value**	**Prob > F**	
Linear	0.024	6	3.93E-03	2.75	0.1733	
2FI	0.011	5	2.12E-03	1.49	0.3614	
Quadratic	6.32E-04	3	2.11E-04	0.15	0.9262	Suggested
Cubic	0	0				Aliased
Pure Error	5.72E-03	4	1.43E-03			

Table 4.10.3A shows the test for the model's adequacy which was evaluated with the lack of fit test. The test indicates whether a proposed model fit well or not. The test for lack of fit compares the variation around the model with pure variation within replicated observations.

It is seen from the Table that there was a significant (F-value) of 2.75 and 1.49 lack of fit for linear and 2F1 models while the quadratic model showed a non significant F-value of 0.15. The significant results of lack of fit for linear and 2F1 models showed that these models are not adequate for use.

Hence the results obtained in the lack of fit test in Table 4.10.3A showed that the quadratic model can describe the response- bulk density of sawdust blended clay.

Table 4.10.3B Model Summary Statistics

Model Summary Statistics						
	Std.		**Adjusted**	**Predicted**		
Source	**Dev.**	**R-Squared**	**R-Squared**	**R-Squared**	**PRESS**	
Linear	0.054	0.8942	0.873	0.6823	0.088	
2FI	0.043	0.941	0.9214	0.7848	0.06	
Quadratic	0.03	0.9771	0.9607	0.9494	0.014	Suggested
Cubic	0.038	0.9794	0.9381		+	Aliased

Beside the lack of fit test, the correlation observed in the R-squared values was also used to determine the measure of how efficient the variability in the actual response values can be explained by the experimental variables and their interaction. Based on this, it was noted that the values of R-squared, adjusted R-squared and the predicted R-squared shown in Table 4.9.3B for the quadratic model were 0.9771, 0.9607 and 0.9494 respectively. This shows that the best correlation in these values was obtained only in this model when compared to other models.

The measure of how efficient the variability in the actual response values can be explained by the experimental variables and their interaction is given by the R-squared value is to unity, the better the model predicts the response.

Table 4.9.3C ANOVA for Response Surface Quadratic Model

ANOVA for Response Surface Quadratic model						
Analysis of variance table [Partial sum of squares - Type III]						
	Sum of		**Mean**	**F**	**p-value**	
Source	**Squares**	**df**	**Square**	**Value**	**Prob > F**	
Model	0.27	5	0.054	59.67	< 0.0001	significant
A-Saw Dust	0.14	1	0.14	153.76	< 0.0001	
B-Clay	7.73E-03	1	7.73E-03	8.52	0.0224	
AB	0.018	1	0.018	19.77	0.003	
A^2	8.46E-03	1	8.46E-03	9.32	0.0185	
B^2	2.33E-03	1	2.33E-03	2.57	0.1531	
Residual	6.35E-03	7	9.07E-04			
Lack of Fit	6.32E-04	3	2.11E-04	0.15	0.9262	not significant
Pure Error	5.72E-03	4	1.43E-03			
Cor Total	0.28	12				

Table 4.9.3C shows the evaluation of the effect of each parameter with quadratic model. It can be seen that the model F-value of 59.67 implies that the model is significant. There is only a 0.01% chance that an F-value this large could occur due to noise. Values of "Prob>F" less than 0.0500 indicate model terms are significant. Hence, in this case, A, B, AB, A^2 and B^2 are significant model terms. Values greater than 0.1000 indicate the model terms are not significant.

The "lack of fit F-value" of 0.15 implies the lack of fit is not significant relative to pure error. There is a 92.625 chance that a "lack of Fit-value" this large could occur due to noise. Non-significant lack of fit is good which means the model is fit.

Std. Dev.	0.030	R-Squared	0.9771
Mean	1.77	Adj R-Squared	0.9607
C.V. %	1.70	Pred R-Squared	0.9494
PRESS	0.014	Adeq Precision	24.905
-2 Log Likelihood	-62.22	BIC	-46.83
		AICc	-36.22

The "Pred R-Squared" of 0.9494 is in reasonable agreement with the "Adj R-Squared" of 0.9607; i.e. the difference is less than 0.2.

Therefore the equation in terms of coded factors was developed which can be used to make predictions about the response for given levels of each factor. By default, the high levels of factors are coded as +1 and the low levels of the factors are coded as -1.

The equation in terms of coded factor is shown as;

$$\text{Bulk Density} = +1.72 - 0.14*A + 0.081*B + 0.086*AB + 0.020*A^2 + 0.059*B^2. \quad (4.5)$$

(A Stands for sawdust and B stands for clay)

The equation in terms of actual factor is used to make predictions about the response for given levels of each factor. The levels are specified in original units for each factor. It is shown as;

$$\text{Bulk Density} = +16.37510 - 0.84539*X_1 - 0.18049*X_2 + 5.75126E\text{-}003*X_1*X_2 + 8.77899E\text{-}003*X_1^2 + 5.85658E\text{-}004*X_2^2. \quad (4.6)$$

(X_1stands for sawdust and X_2 stands for clay)

The response values obtained by inserting the independent values are the predicted values of the model. These values are compared to the actual and experimental values. The result of the comparison was shown in Figure 4.10.7

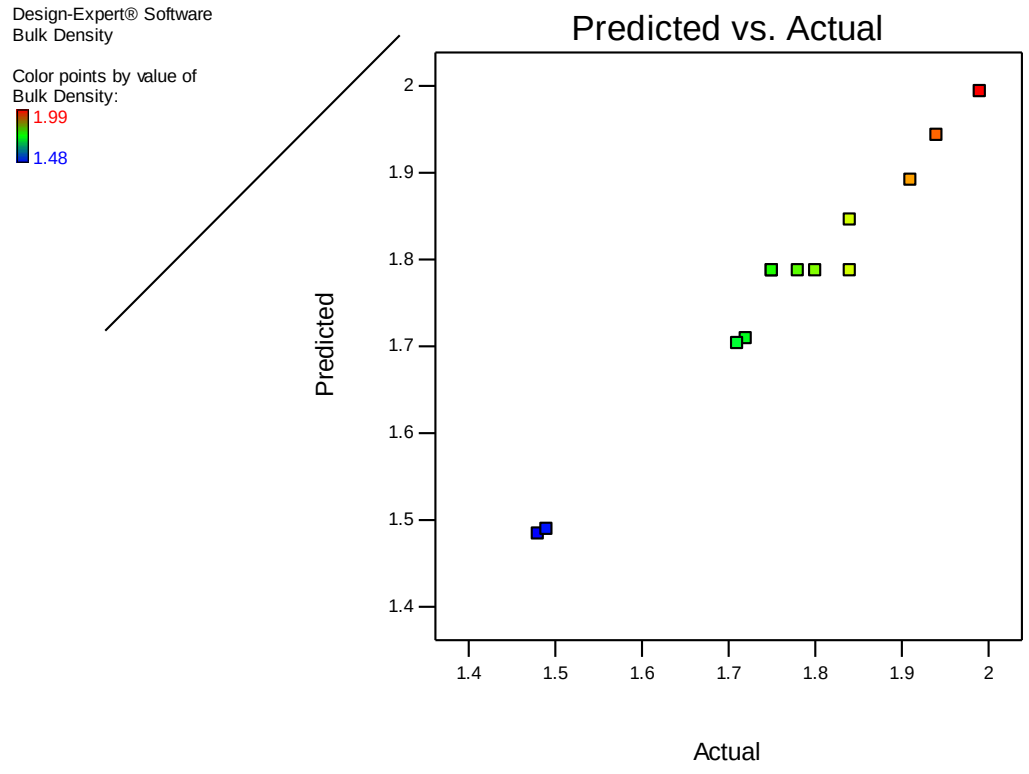

Figure 4.10.7 Linear correlation between predicted Vs actual values for bulk density of blended Nguzu- Amaiyi clay with sawdust additive.

4.10.31 Effects of Model Parameters and their Interactions

The relationship between the experimental variables and the response were studied with the plot of the individual and interactive effects of the two factors- clay and sawdust on the response – bulk density.

The central composite design was used to produce three dimensional (3D) response surface and two dimensional (2D) contour plots. The 3D surfaces and 2D contour plots are graphical representations of the equation for the optimization of the

experimental responses and are the most useful approach in revealing the conditions of the optimum performance of the responses. In the plots, the response functions of the two factors are presented. The results of the interactions between two independent variables and dependent variable are shown in Figures 4.10.8 and 4.10.9.

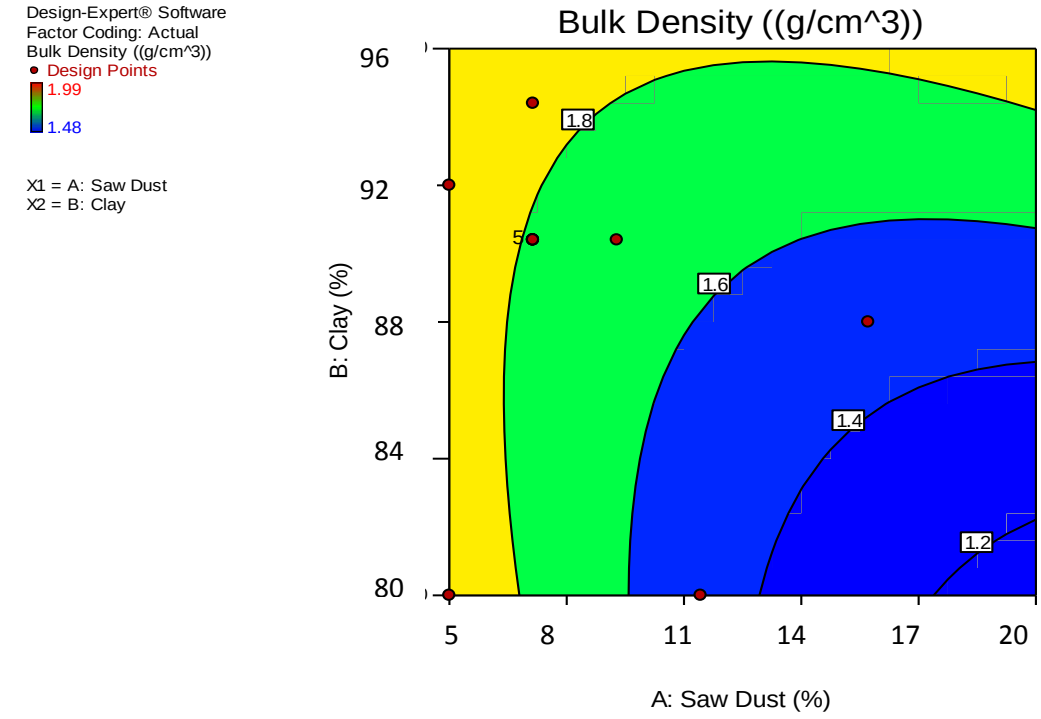

Figure 4.10.8 Two dimension contour plot for the combined effect of the composition of clay and sawdust on the bulk density property

From Figure 4.10.8, it was observed that bulk density value was decreasing with decrease in composition of clay (B) and with increase in the composition of sawdust (A). Maximum value of bulk density value of 1.9g/cm^3 was obtained at

95% composition of clay and 5% of sawdust. The minimum value of bulk density of 1.2g/cm^3 was found when the composition of the clay decreased to82% with the corresponding value of sawdust composition. The decrease in bulk density value with decrease in clay composition and increase in sawdust composition is due to increase in pore sizes as a result of more quantity of sawdust additive being burnt off. These additives that were burnt off during firing leave larger pores in the brick's structure. Consequently, the density is reduced.

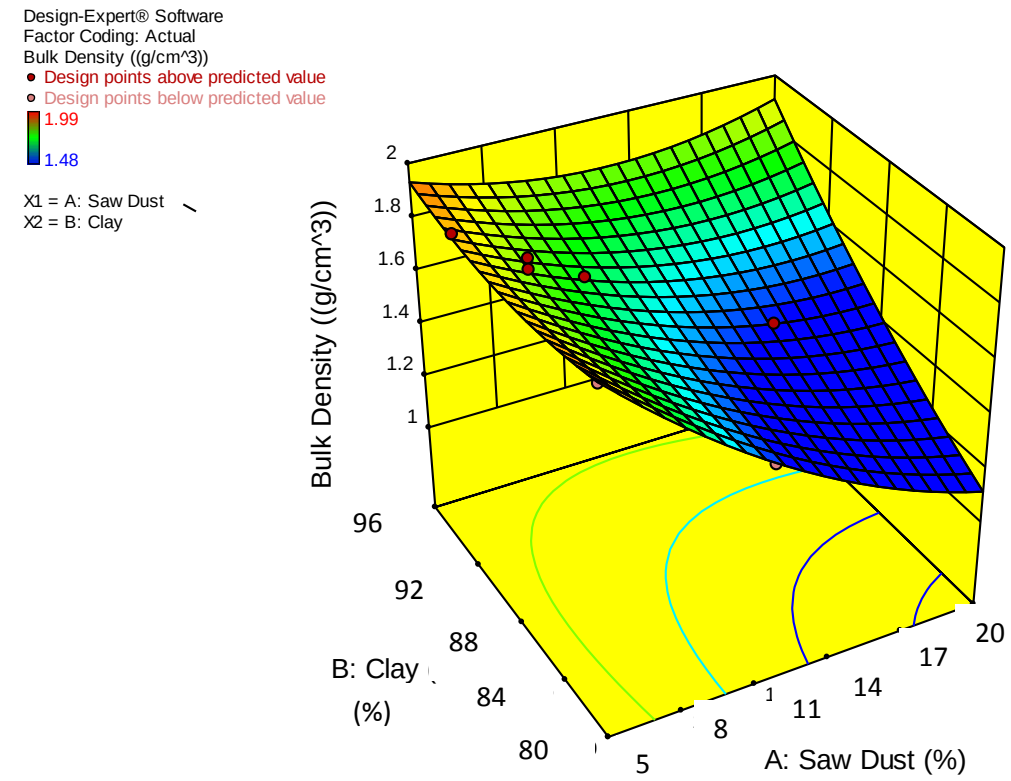

Figure 4.10.9 Three dimension surface plot for the combined effect of the composition of clay and sawdust on the bulk density property

Figure 4.10.9 shows the interactive effect of clay and sawdust compositions on bulk density. It was seen that the value of bulk density was decreasing with decrease in the composition of clay and increase in the composition of sawdust additive. On the reverse, bulk density increased with decrease in the composition of sawdust additive and increase in clay composition. Maximum (optimum) value of bulk density of 1.9g/cm^3 was found in 95% composition of clay with the corresponding value of sawdust composition.

The decrease and increase in the value of bulk density follows such trend because increase in saw dust composition increases porosity and decreases density. In contrast, decrease with sawdust composition with increase in clay composition forms a more homogeneous clay structure which reduces porosity and makes the composite material denser.

Design-Expert® Software
Factor Coding: Actual
Bulk Density ((g/cm^3))

X1 = B: Clay

Actual Factor
A: Saw Dust = 16.5

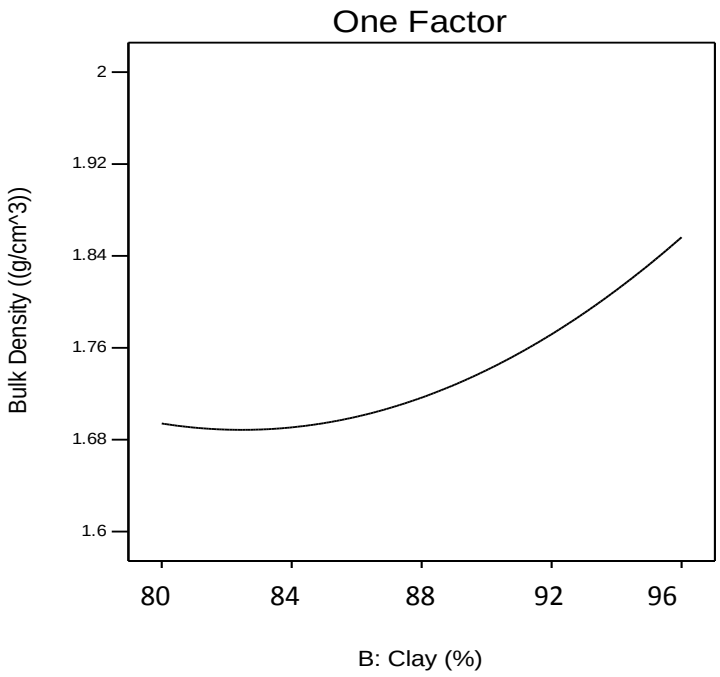

Design-Expert® Software
Factor Coding: Actual
Bulk Density ((g/cm^3))
Design Points

X1 = A: Saw Dust

Actual Factor
B: Clay = 80

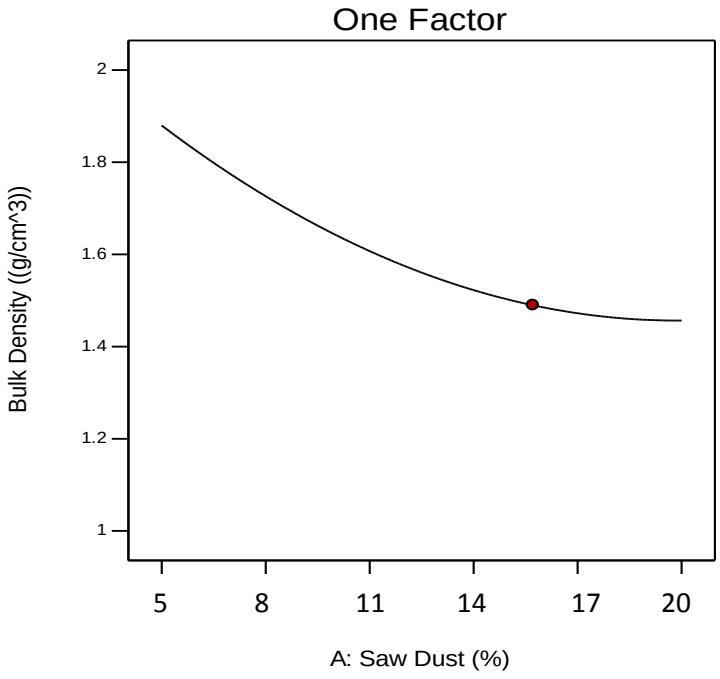

Figure 4.10.10 Single factor plot of the composition of clay and sawdust on the bulk density

The single factor plots show that bulk density increases with increase in clay composition but decreases with increases in sawdust composition.

4.10.4 Results for Modulus of Rupture in the Blend of Sawdust.

Table 4.10.4A Lack of Fit Tests

Lack of Fit Tests						
	Sum of		**Mean**	**F**	**p-value**	
Source	**Squares**	**df**	**Square**	**Value**	**Prob > F**	
Linear	1.19	6	0.2	0.88	0.5772	Suggested
2FI	1.16	5	0.23	1.03	0.5039	
Quadratic	0.049	3	0.016	0.072	0.9718	Suggested
Cubic	0	0				Aliased
Pure Error	0.9	4	0.23			

Table 4.10.4A shows the result for lack of fit test used to test for the model's adequacy. The test indicates whether a proposed model fit well or not. The test for

lack of fit compares the variation around the model with pure variation within replicated observations.

It is seen from the table that there was a significant (F-value) of 0.88 and 1.03 lack of fit for linear and 2F1 models while the quadratic model showed a non significant F-value of 0.072 The " Lack of Fit F-value" of 0.072 implies the lack of Fit is not significant relative to pure error. The results of lack of fit for linear and 2F1 models showed that these models are not adequate for use.

Hence the results obtained in the lack of fit test in table 4.9.4.2 and significance test in Table 4.10.4A showed that the quadratic model can describe the response-modulus of rupture for sawdust blended clay.

Table 4.10.4B Model Summary Statistics

Model Summary Statistics						
	Std.		**Adjusted**	**Predicted**		
Source	**Dev.**	**R-Squared**	**R-Squared**	**R-Squared**	**PRESS**	
Linear	0.46	0.7965	0.7558	0.5419	4.71	Suggested
2FI	0.48	0.7998	0.7331	0.3952	6.23	
Quadratic	0.37	0.9076	0.8416	0.8191	1.86	Suggested
Cubic	0.47	0.9123	0.737		+	Aliased

The correlation observed in the R-squared values was also used to determine the measure of how efficient the variability in the actual response values can be explained by the experimental variables and their interaction. Based on this, it was noted that the values of R-squared, adjusted R-squared and the predicted R-squared shown in Table 4.10.4B for the quadratic model were 0.9076, 0.8416 and 0.8191 respectively. This shows that the best correlation in these values was obtained only in this model when compared to other models.

The measure of how efficient the variability in the actual response values can be explained by the experimental variables and their interaction is given by the R-squared value is to unity, the better the model predicts the response.

Table 4.10.4C ANOVA for Response Surface Quadratic Model

ANOVA for Response Surface Quadratic model						
Analysis of variance table [Partial sum of squares - Type III]						
	Sum of		**Mean**	**F**	**p-value**	
Source	**Squares**	**df**	**Square**	**Value**	**Prob > F**	
Model	9.34	5	1.87	13.75	0.0017	significant
A-Saw Dust	4.56	1	4.56	33.58	0.0007	
B-Clay	8.59	1	8.59	24.33	0.0009	
AB	6.25	1	6.25	12.87	0.0007	

A^2	7.78	1	7.78	15.75	0.0006	
B^2	5.44	1	5.44	10.22	0.0006	
Residual	0.95	7	0.14			
Lack of Fit	0.049	3	0.016	0.072	0.9718	not significant
Pure Error	0.9	4	0.23			
Cor Total	10.29	12				

Table 4.10.4C shows the evaluation of the effect of each parameter with quadratic model. It can be seen that the model F-value of 13.75 implies that the model is significant. There is only a 0.17% chance that an F-value this large could occur due to noise. Values of "Prob>F" less than 0.0500 indicate model terms are significant. Hence, in this case, A, B, AB, A^2 and B^2 are significant model terms. Values greater than 0.1000 indicate the model terms are not significant.

The "lack of fit F-value" of 0.07 implies the lack of fit is not significant relative to pure error. There is a 97.18% chance that a "lack of Fit-value" this large could occur due to noise. Non-significant lack of fit is good which means the model is fit.

The "Pred R-Squared" of 0.8191 is in reasonable agreement with the "Adj R-Squared" of 0.8416; i.e. the difference is less than 0.2.

Therefore the equation in terms of coded factors was developed which can be used to make predictions about the response for given levels of each factor. By default, the high levels of factors are coded as +1 and the low levels of the factors are coded as -1.

The equation in terms of coded factor is shown as;

Modulus of rupture = 29.01 – 0.82*A + 0.71*B + 0.32*AB +

$0.19*A^2 + 0.8*B^2$ (4.7)

(A stands for sawdust while B stands for clay)

The equation in terms of actual factor is used to make predictions about the response for given levels of each factor. The levels are specified in original units for each factor. It is shown as;

Modulus of rupture = +135.14384 – 5.06209*X_1 – 1.56738* X_2 + 0.021645* X_1 * X_2 + 0.084361* X_1^2 + 8.01E-03* X_2^2. (4.8)

(X_1 stands for sawdust while X_2 stands for clay)

The response values obtained by inserting the independent values are the predicted values of the model. These values were compared to the actual and experimental values. The result of the comparison was shown in Figure 4.10.11

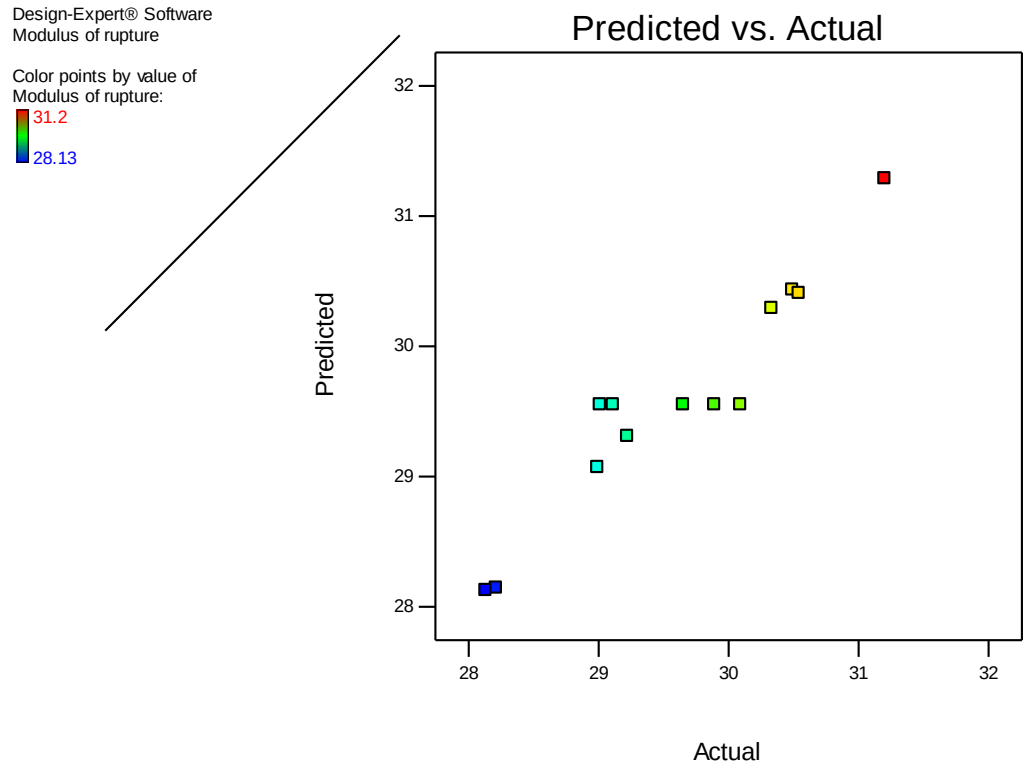

Figure 4.10.11 linear correlation between predicted Vs actual values for modulus of rupture blended Nguzu-Amaiyi clay with sawdust.

4.10.41 Effects of Model Parameters and their Interactions

The relationship between the experimental variables and the response were studied with the plot of the individual and interactive effects of the two factors- clay and sawdust on the response – modulus of rupture.

The central composite design was used to produce three dimensional (3D) response surface and two dimensional (2D) contour plots. The 3D surfaces and 2D contour plots are graphical representations of the equation for the optimization of the

experimental responses and are the most useful approach in revealing the conditions of the optimum performance of the responses.

In the plots, the response functions of the two factors are presented. The results of the interactions between two independent variables and dependent variable are shown in Figures 4.10.12 and 4.10.13.

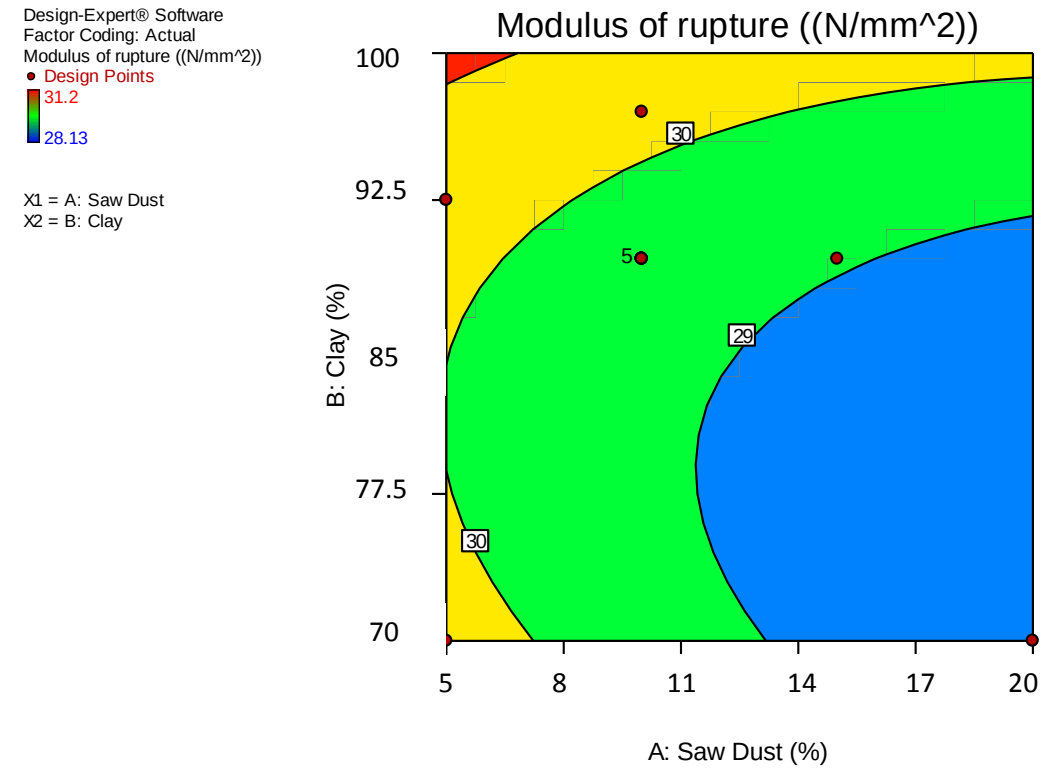

Figure 4.10.11 Two dimension contour plot for the combined effect of the composition of clay and sawdust on the modulus of rupture property

From Figure 4.10.12, It was observed that value of modulus of rupture was decreasing with decrease in composition of clay (B) and with increase in the composition of sawdust (A). Maximum value of modulus of rupture of 31N/mm^2 was obtained between the ranges of 5 -10% composition of sawdust value. Beyond 15% composition of sawdust and its corresponding 85% of clay, modulus of rupture was seen to decrease progressively with increase the composition of the additive.

Hence, it was seen that increase in the quantity of additive has adverse effect of the transverse strength. This is due to the fact that increase in the concentration of additive at the expense of the clay led to the deficiency of the main clay content which is supposed to improve the strength. Also migration of gases through the matrix produced due to burning of the additive created highly porous clay structure which affected the mechanical strength.

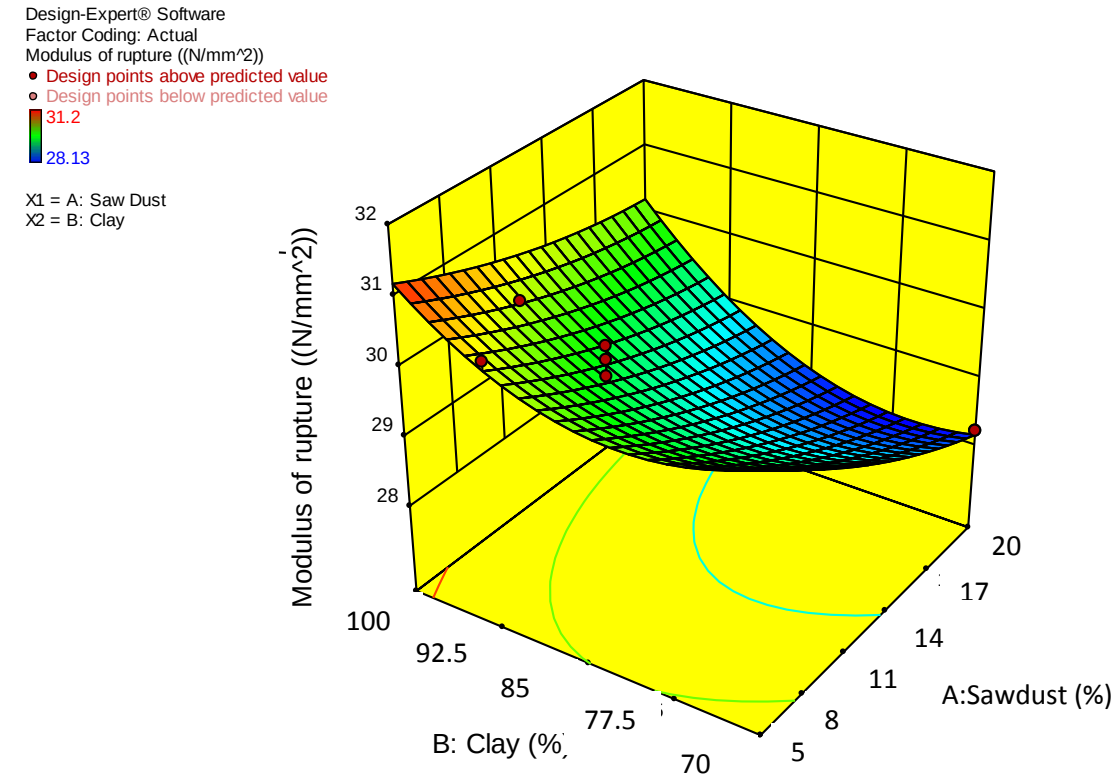

Figure 4.10.12Three dimensional surface plot for the combined effect of the composition of clay and sawdust on the modulus of rupture property.

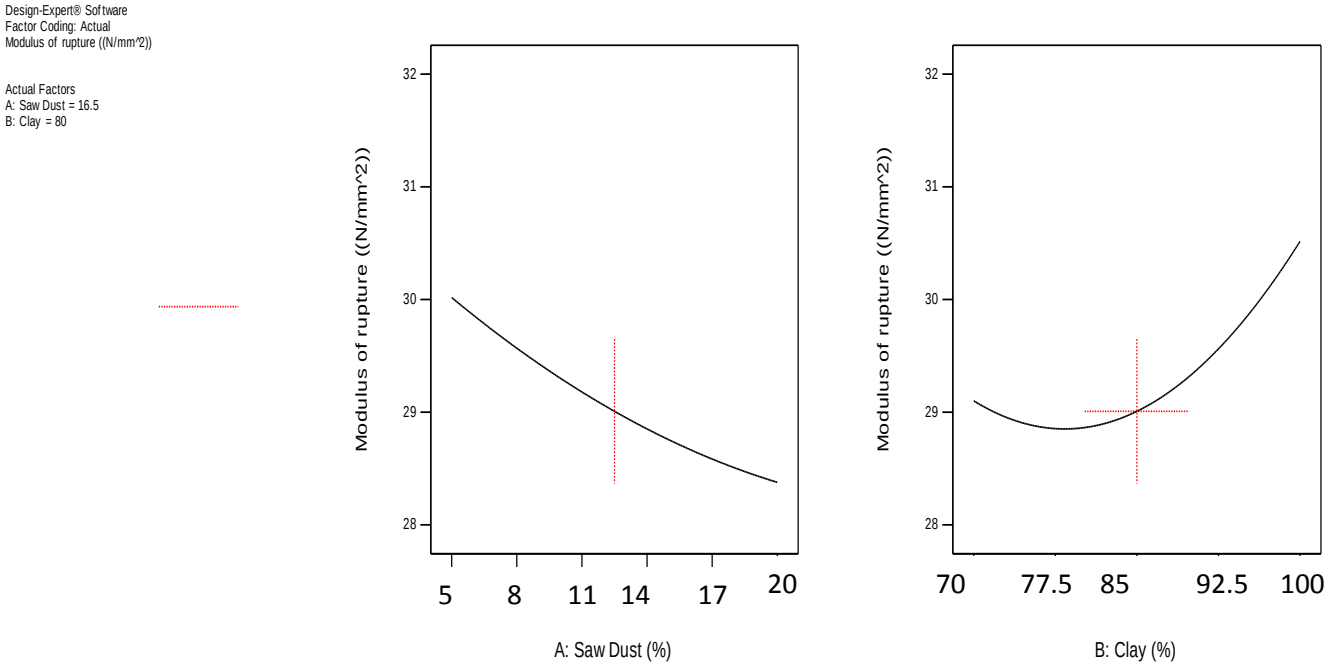

Figure 4.10.13 Single factor plot of the composition of clay and sawdust on the modulus of rupture property

The single plots presented in Figure 4.10.13 shows that modulus of rupture has a linear relationship with the composition of the additive. This shows that the property decreases progressively with increase in the composition of sawdust. In contrast, the composition of clay has non linear relationship with modulus of rupture. The value of modulus of rupture was found to decrease with increase in clay composition initially but beyond 80% composition, the value of modulus of rupture began to increase with subsequent increase in clay composition.

4.11 Results of the Experimental Design for Refractory Properties of Nguzu – Amaiyi Clay Blended with Rice Husk Additive.

The effect of the two independent factors-compositions of rice husk and clay on the responses-refractory properties was studied using response surface methodology with central composite design type. The results of effect of the factors on the responses are shown on Table 4.11. The responses investigated were linear shrinkage, apparent porosity, bulk density and modulus of rupture while the factors were compositions of clay and rice husk additive.

The results shown in Table 4.11show the values of the individual responses in different runs are very distinct to each other. This shows the factors interacted to have significant effect on the dependent variables.

Table 4.11 Design of Experimental Result for Rice Husk Blended Clay

	Factor 1	Factor 2	Response 1	Response 2	Response 3	Response 4
Std	A:Rice Husk	B:Clay	Linear Shrinkage	Apparent porosity	Bulk Density	Modulus of rupture
Unit	%	%	%	%	(g/cm^3)	(N/mm^2)
1	15	95	6.86	32.86	2.12	33.2
2	18	82	10.27	51.7	1.64	30.7
3	6	94	7.12	33.85	2.05	33.3
4	17	83	9.11	46.26	1.86	31.6
5	4	96	5.91	26.4	2.19	34.1
6	20	80	10.46	52.5	1.61	30.6
7	10	90	8.78	44.44	1.85	31.8
8	15	85	7.32	38.49	1.97	33
9	15	85	7.87	38.63	1.94	32.8
10	15	85	8.14	40.68	1.96	32.6
11	15	83	8.3	41.34	1.96	32.3
12	15	83	8.58	42.54	1.92	31.7
13	15	83	8.83	44.37	1.92	31.6

4.11.1 Results of Liner Shrinkage in the Blend of Rice Husk

Table 4.11.1A Results for Lack of Fit Test for Rice Husk Blended Clay

Lack of Fit Tests						
	Sum of		Mean	F	p-value	
Source	Squares	df	Square	Value	Prob > F	
Linear	2.37	6	0.39	2.8	0.169	
2FI	2.26	5	0.45	3.21	0.141	
Quadratic	0.044	3	0.015	0.1	0.9538	Suggested
Cubic	0	0				Aliased
Pure Error	0.56	4	0.14			

The lack of fit test was a done to confirm the model's adequacy. This compares the variation around the model with pure variation within replicated observations. From Table 4.11.1A, it was found that quadratic model showed a non significant F-value of 0.1 while other models indicated significant level for lack of fit which showed that these models are not adequate for use.

Table 4.11.1B Model Summary Statistics

Model Summary Statistics						
	Std.		Adjusted	Predicted		
Source	Dev.	R-Squared	R-Squared	R-Squared	PRESS	
Linear	0.54	0.8546	0.8256	0.5927	8.21	
2FI	0.56	0.8601	0.8135	0.4379	11.33	
Quadratic	0.29	0.9699	0.9484	0.903	1.95	Suggested
Cubic	0.38	0.9721	0.9162		+	Aliased

The correlation observed in the values of the adjusted R-square and predicted R-square values were used to determine the measure of how efficient the variability in the actual response values can be explained by the experimental variables and their interaction. Based on this, it was found that quadratic model showed the best correlation in these values when compared to other models. This is because the difference between the adjusted R-square value and predicted R-square value is less than 0.2. The measure of how efficient the variability in the actual response values can be explained by the experimental variables and their interaction is given

by the R-square value. When it is closer to unity, it shows that the model can predict the response better.

Table 4.11.1C ANOVA for Response Surface Quadratic Model

Response	**1**	**Linear Shrinkage**				
ANOVA for Response Surface Quadratic model						
Analysis of variance table [Partial sum of squares - Type III]						
	Sum of		**Mean**	**F**	**p-value**	
Source	**Squares**	**df**	**Square**	**Value**	**Prob > F**	
Model	19.54	5	3.91	45.09	< 0.0001	significant
A-Rice Husk	10.09	1	10.09	116.44	< 0.0001	
B-Clay	0.96	1	0.96	11.1	0.0126	
AB	0.59	1	0.59	6.76	0.0354	
A^2	1.64	1	1.64	18.92	0.0034	
B^2	0.78	1	0.78	8.99	0.02	
Residual	0.61	7	0.087			
Lack of Fit	0.044	3	0.015	0.1	0.9538	not significant

Pure Error	0.56	4	0.14			
Cor Total	20.15	12				

The Model F-value of 45.09 shown in Table 4.10.1.4 implies the model is significant. There is only a 0.01% chance that an F-value this large could occur due to noise. Values of "Prob > F" less than 0.0500 indicate model terms are significant. In this case A, B, AB, A^2, B^2 are significant model terms. Values greater than 0.1000 indicate the model terms are not significant. The "Lack of Fit F-value" of 0.10 implies the Lack of Fit is not significant relative to the pure error. There is a 95.38% chance that a "Lack of Fit F-value" this large could occur due to noise. Non-significant lack of fit is good because it means the model would fit effectively.

Std. Dev.	0.29	R-Squared	0.9699
Mean	8.27	Adj R-Squared	0.9484
C.V. %	3.56	Pred R-Squared	0.903
PRESS	1.95	Adeq Precision	22.896
-2 Log Likelihood	-2.95	BIC	12.44
		AICc	23.05

Therefore the equation in terms of coded factors was developed which can be used to make predictions about the response for given levels of each factor. By default, the high levels of factors are coded as +1 and the low levels of the factors are coded as -1.

The equation in terms of coded factor is shown as;

$$\text{Linear shrinkage} = 9.1 + 1.22*A - 0.9*B - 0.49*AB - 0.27*A^2 - 1.07*B^2 \quad (4.9)$$

A stands for rice husk additive while B stands for clay.

The equation in terms of actual factor is used to make predictions about the response for given levels of each factor. The levels are specified in original units for each factor. It is shown as;

$$\text{Linear shrinkage} = -142.3141 + 7.47616*X_1 + 2.16613*X_2 - 0.032875*X_1*X_2 - 0.12222*X_1^2 - 0.010713*X_2^2. \quad (4.10)$$

The response values obtained by inserting the independent values are the predicted values of the model. These values were compared to the actual and experimental values. The result of the comparison is shown in Figure 4.11.1

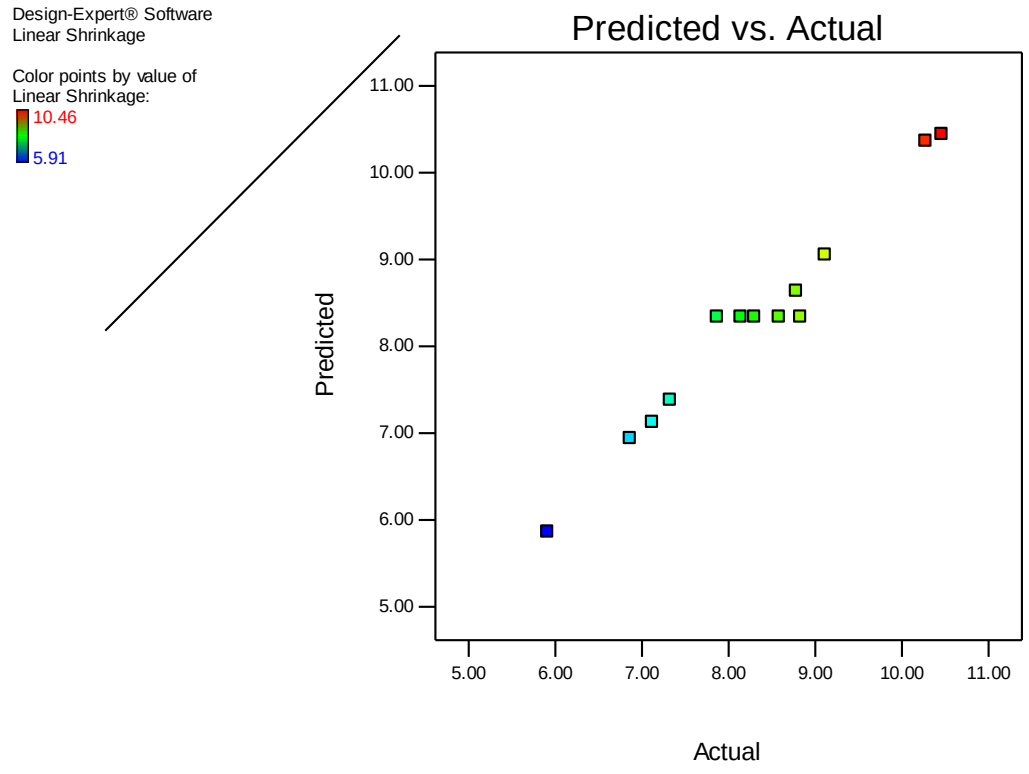

Figure 4.11.1 linear correlation between predicted Vs actual values for linear shrinkage of rice husk blended clay

4.11.11 Effects of Model Parameters and their Interactions

The relationship between the experimental variables and the response were studied with the plot of the individual and interactive effects of the two factors- clay and sawdust on the response- linear shrinkage.

The central composite design was used to produce three dimensional (3D) response surface and two dimensional (2D) contour plots. The 3D surfaces and 2D contour plots are graphical representations of the equation for the optimization of the

experimental responses which is the most useful approach in revealing the conditions of the optimum performance of the responses.

In the plots, the response functions of the two factors are presented. The results of the interactions between two independent variables and the dependent variable are shown in Figures 4.11.2 and 4.11.3.

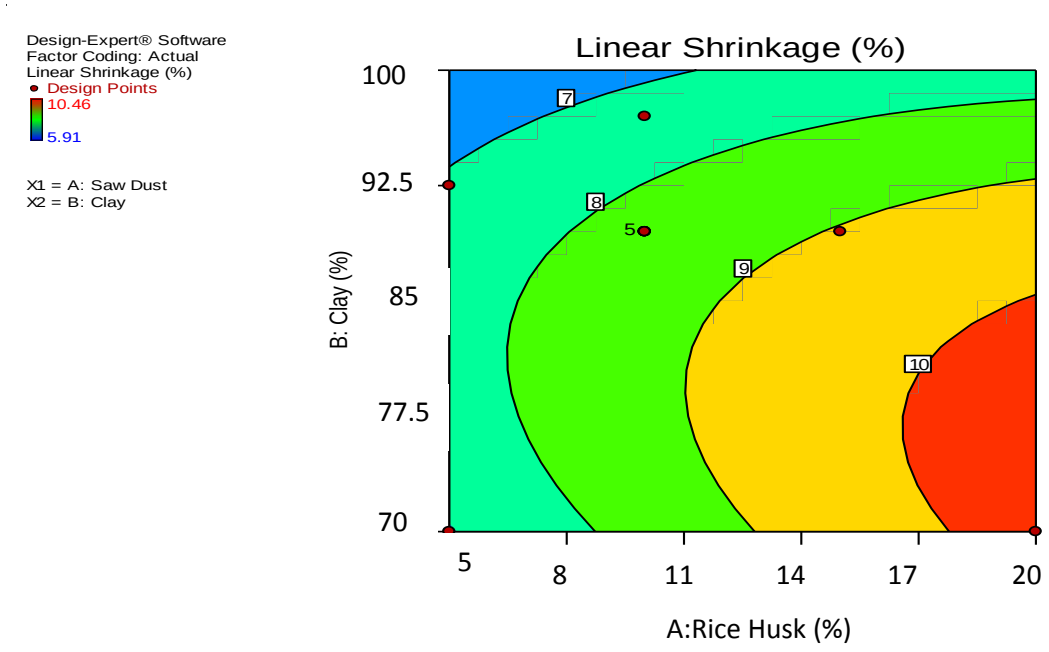

Figure 4.11.2 Two dimension contour plot for the combined effect of the composition of clay and rice husk on linear shrinkage

From figures 4.11.2 and 4.11.3, it is found that in rice husk blend, linear shrinkage increased with increase in rice husk composition and decrease in clay composition. When the composition of clay and rice husk additive were 95 and 5% respectively,

the shrinkage value was 6.1%. This was the lowest and the optimum shrinkage value obtained in this blend. When the value of rice husk increased to 17% and that of clay decreased further to 83%, it found that linear shrinkage increased to 10%. The increase in shrinkage in this trend is due to the re arrangement in the particle and grain of the composite material after firing. This normally produced a more compact structure with higher level of shrinkage.

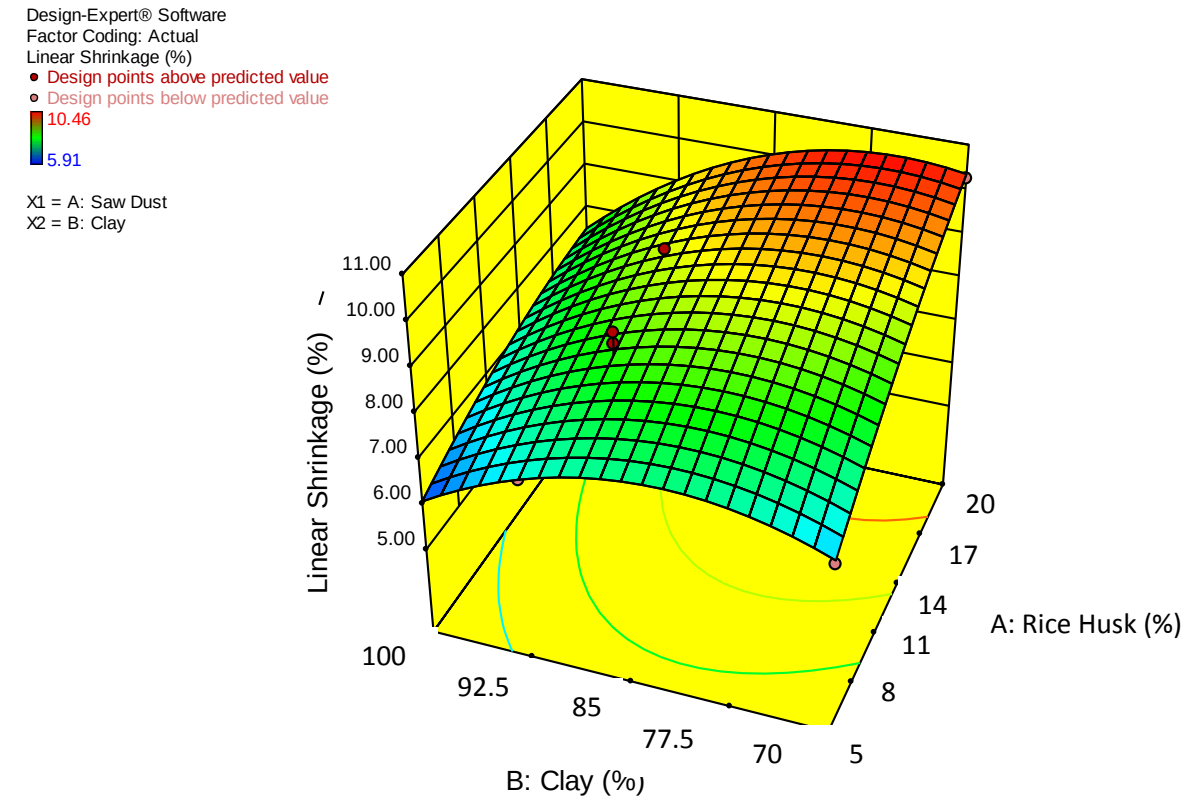

Figure 4.11.3 Three dimension surface plot for the combined effect of the composition of clay and rice husk on linear shrinkage

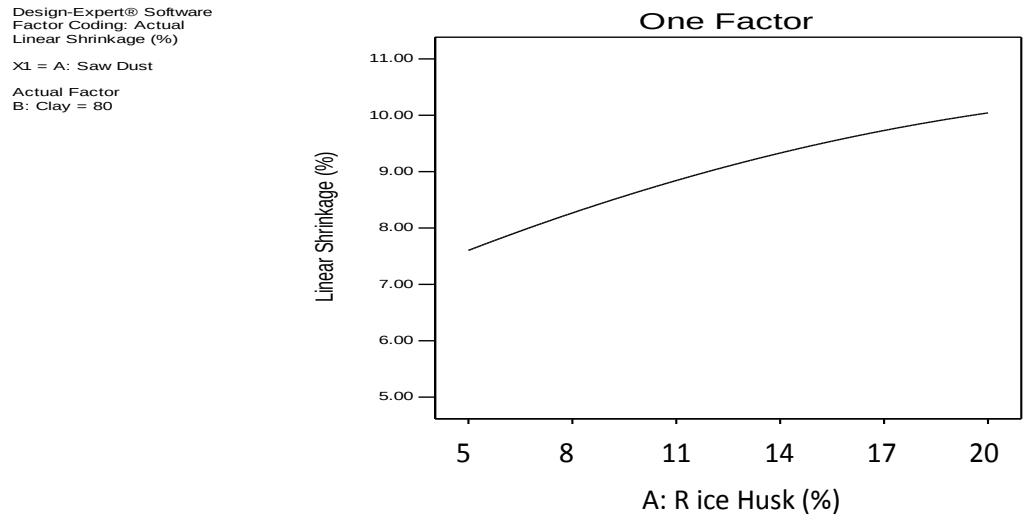

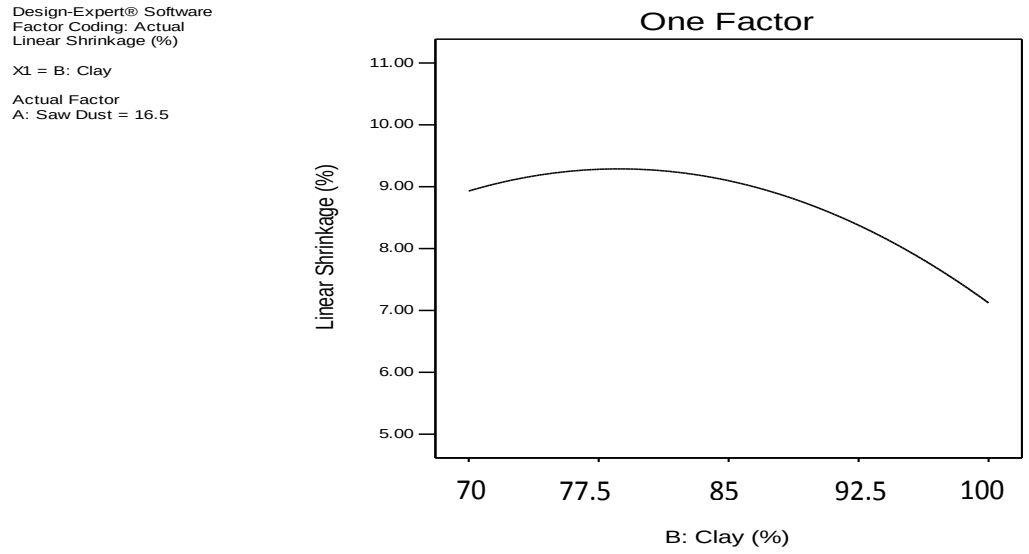

Figure 4.11.4 Single factor plot for the combined effect of the composition of clay and rice husk on linear shrinkage

The single factor plots show that increase in rice husk quantity increases linear shrinkage while the effect of the clay composition showed a non linear relationship with shrinkage. The value of linear shrinkage initially increased with increase in

clay composition till maximum value of 9.2% was attained with 80% composition of clay. Beyond this composition of clay, the shrinkage began to decrease with further increase in clay composition. The observed decrease in firing shrinkage is as a result of high amount of clay oxides like CaO which does not yield increase in shrinkage.

4.11.2 Results for Apparent Porosity in the Blend of Rice Husk

Table 4.11.2A Results for Lack of Fit Test

Lack of Fit Tests						
	Sum of		Mean	F	p-value	
Source	Squares	df	Square	Value	Prob > F	
Linear	85.43	6	14.24	3.12	0.145	
2FI	84.73	5	16.95	3.72	0.1138	
Quadratic	1.19	3	0.4	0.087	0.9636	Suggested
Cubic	0	0				Aliased
Pure Error	18.24	4	4.56			

The lack of fit test was a done to confirm the model's adequacy. This compares the variation around the model with pure variation within replicated observations.

From Table 4.11.2A, it was found that quadratic model showed a non significant F-value of 0.087 while other models indicated significant result of lack of fit which showed that these models are not adequate for use.

Table 4.11.2B Model Summary Statistics

Model Summary Statistics						
	Std.		Adjusted	Predicted		
Source	Dev.	R-Squared	R-Squared	R-Squared	PRESS	
Linear	3.22	0.8386	0.8064	0.4796	334.36	
2FI	3.38	0.8397	0.7863	0.2018	512.82	
Quadratic	1.67	0.9698	0.9482	0.9202	51.25	Suggested
Cubic	2.14	0.9716	0.9148		+	Aliased

The correlation observed in the values of the adjusted R-square and predicted R-square values were used to determine the measure of how efficient the variability in the actual response values can be explained by the experimental variables and their interaction. Based on this, it was found that quadratic model showed the best correlation in these values of 0.9698, 0.9482 and 0.9148 for R-squared, R-squared adjusted and R-squared predicted respectively which other models did not show. The measure of how efficient the variability in the actual response values can be

explained by the experimental variables and their interaction is given by the R-square value. When it closer to unity, it shows that the model can predict the response better.

Table 4.11.2C ANOVA for Response Surface Quadratic Model

Response	**2**	**Apparent porosity**				
ANOVA for Response Surface Quadratic model						
Analysis of variance table [Partial sum of squares - Type III]						
	Sum of		**Mean**	**F**	**p-value**	
Source	**Squares**	**df**	**Square**	**Value**	**Prob > F**	
Model	623.03	5	124.61	44.9	< 0.0001	significant
A-Rice Husk	*397.09*	*1*	*397.09*	*143.09*	*< 0.0001*	
B-Clay	*8.22*	*1*	*67.22*	*19.96*	*0.0089*	
AB	*7.82*	*1*	*76.82*	*24.82*	*0.0071*	
A^2	*80.81*	*1*	*80.81*	*29.12*	*0.001*	
B^2	*6.55*	*1*	*74.55*	*23.36*	*0.0085*	
Residual	19.43	7	2.78			

Lack of Fit	*1.19*	*3*	*0.4*	*0.087*	*0.9636*	*not significant*
Pure Error	*18.24*	*4*	*4.56*			
Cor Total	642.46	12				

The Model F-value of 44.9 shown in Table 4.11.2C implies the model is significant. There is only a 0.01% chance that an F-value this large could occur due to noise. Values of "Prob > F" less than 0.0500 indicate model terms are significant. In this case A, B, AB, A^2, B^2 are significant model terms. Values greater than 0.1000 indicate the model terms are not significant. The "Lack of Fit F-value" of 0.09 implies the Lack of Fit is not significant relative to the pure error. There is a 96.36% chance that a "Lack of Fit F-value" this large could occur due to noise. Non-significant lack of fit is good because it means the model would fit effectively.

The “Pred R-Squared of 0.9202 is in reasonable agreement with the “Adj R-Squared value of 0.9448; i.e. the difference is less than 0.2

Therefore the equation in terms of coded factors was developed which can be used to make predictions about the response for given levels of each factor. By default,

the high levels of factors are coded as +1 and the low levels of the factors are coded as -1.

The equation in terms of coded factor is shown as;

$$\text{Apparent Porosity} = 45.09 + 7.65*A - 2.64*B - 1.80*AB - 1.93*A^2 - 3.10*B^2 \quad (4.11)$$

A stands for rice husk additive while B stands for clay.

The equation in terms of actual factor is used to make predictions about the response for given levels of each factor. The levels are specified in original units for each factor. It is shown as;

$$\text{Apparent Porosity} = -608.67193 + 43.02022*X_1 + 6.68391*X_2 - 0.12008*X_1*X_2 - 0.85803*X_1^2 - 0.031044*X_2^2. \quad (4.12)$$

X_1 stands for rice husk additive while X_2 stands for clay.

The response values obtained by inserting the independent values are the predicted values of the model. These values were compared to the actual and experimental values. The result of the comparison was shown in Figure 4.11.5

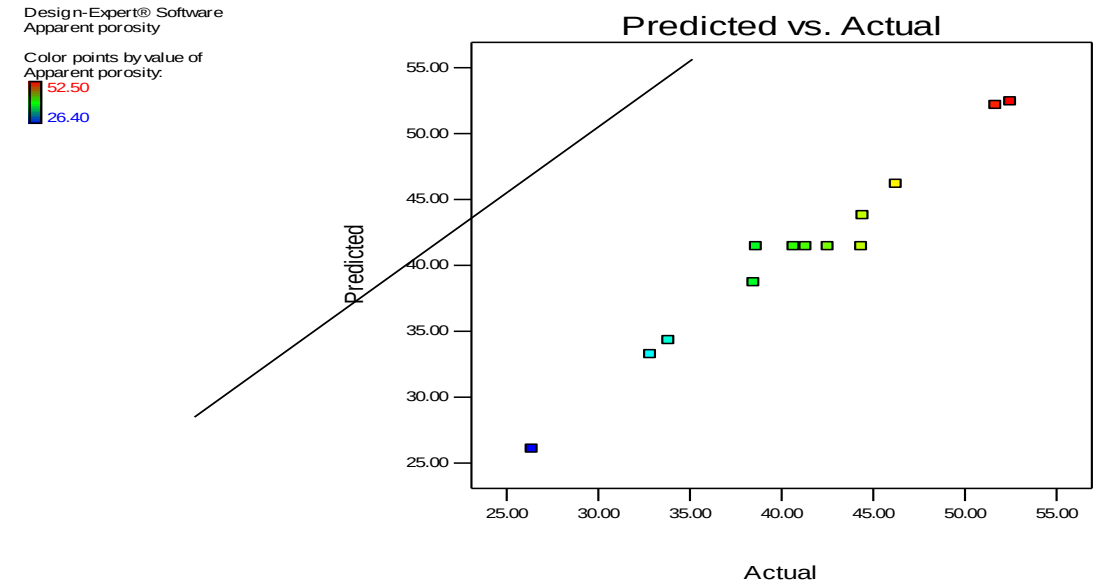

Figure 4.11.6 linear correlation between predicted Vs actual values for apparent porosity of rice husk blended clay

4.11.21 Effects of Model Parameters and their Interactions

The relationship between the experimental variables and the response were studied with the plot of the individual and interactive effects of the two factors- clay and sawdust on the response- apparent porosity.

The central composite design was used to produce three dimensional (3D) response surface and two dimensional (2D) contour plots. The 3D surfaces and 2D contour plots are graphical representations of the equation for the optimization of the experimental responses and are the most useful approach in revealing the conditions of the optimum performance of the responses.

In the plots, the response functions of the two factors are presented. The results of the interactions between two independent variables and dependent variable are shown in Figures 4.11.6 and 4.11.7.

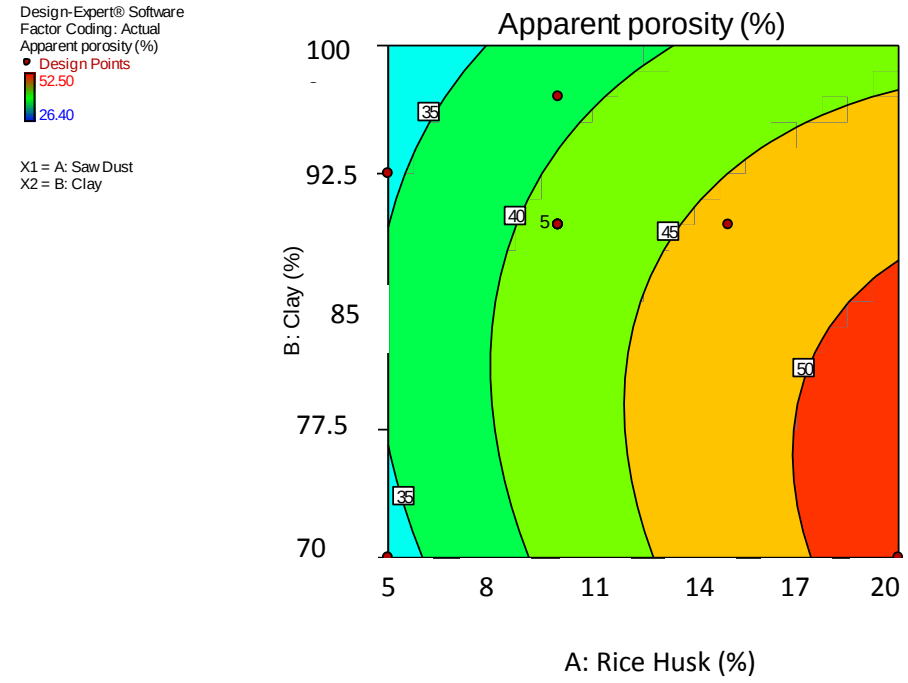

Figure 4.11.6 Two dimension contour plot for the combined effect of the composition of clay and rice husk on apparent porosity

The contour plot in Figure 4.11.6 shows apparent porosity increases with increase in sawdust composition and decrease in clay composition. Optimum value of apparent porosity of 31.5 was obtained at 95 and 5% composition of clay and rice husk respectively. When the composition of rice husk increased to 5.5 and 6.5%,

the value of apparent porosity rose to 35%. Progressive increase in apparent porosity values were observed as the composition of rice husk kept increasing. Figure 4.9.2.3 shows the interactive effect of clay and rice husk compositions on apparent porosity. From the figure, it is seen that the highest value of apparent porosity of 53% was seen at 80 and 20% composition of clay and rice husk respectively while the optimum value of 31.5% was obtained at 95 and 5 composition of clay and rice husk respectively.

The increase in the value of apparent porosity with increase in the sawdust additive attributed larger sizes of pores and also more numbers of pores widely distributed in the brick's structure when more quantities of the additive were used. This increased the porosity of composite brick.

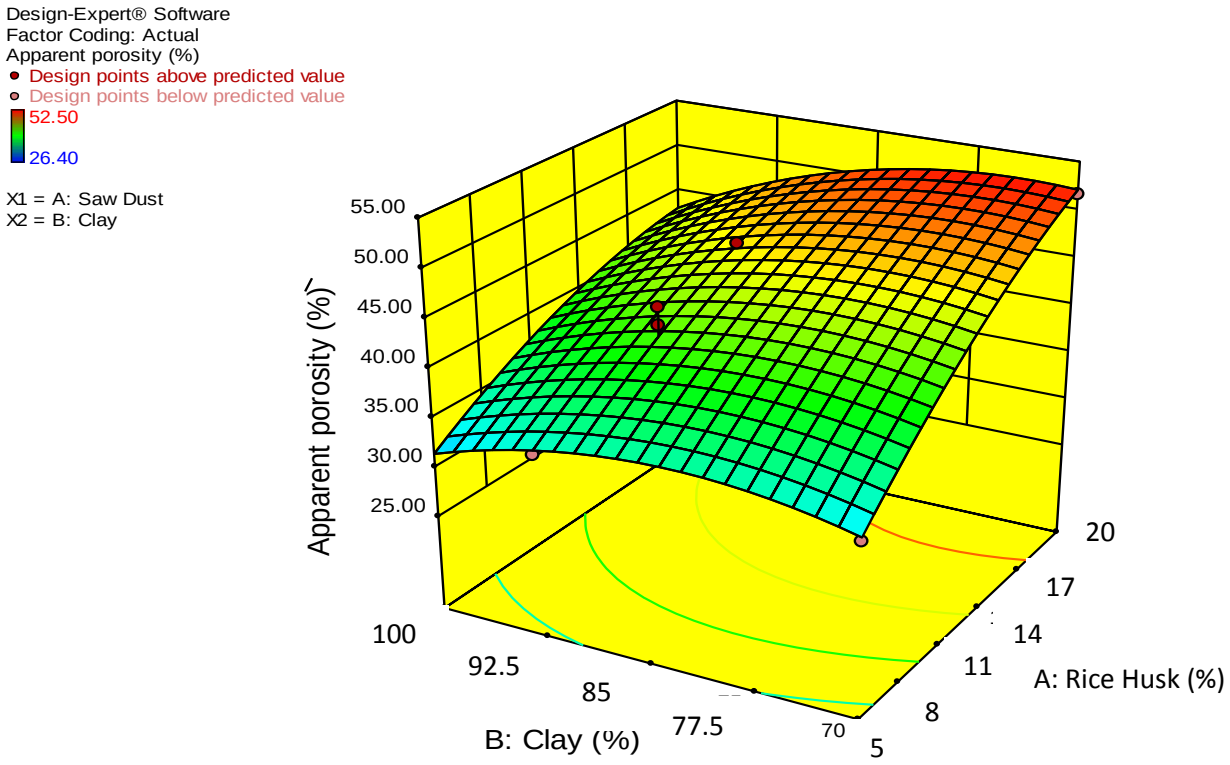

Figure 4.11.7 Three dimension surface plot for the combined effect of the composition of clay and rice husk on apparent porosity

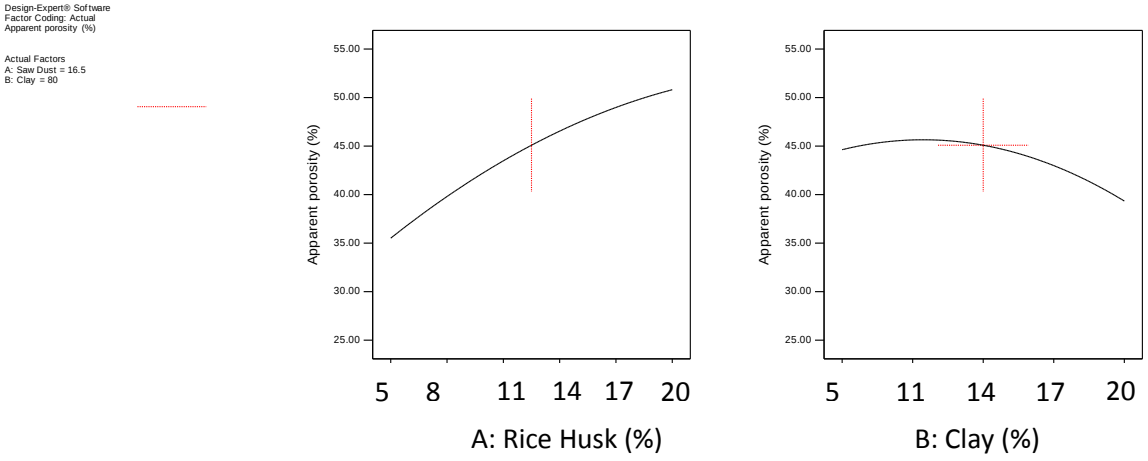

Figure 4.11.8 Single factor plot for the combined effect of the composition of clay and rice husk on apparent porosity

The single factor plots show that increase in rice husk quantity increases apparent porosity while the effect of the clay composition showed a non linear relationship with apparent porosity. The value of apparent porosity was stable with increase in clay composition till 80% composition of clay. Beyond this composition of clay, the porosity began to decrease with further increase in clay composition.

4.11.3 Results for Bulk Density in the Blend of Rice Husk

Table 4.11.3A Results for Lack of Fit Test

Lack of Fit Tests						
	Sum of		Mean	F	p-value	
Source	Squares	df	Square	Value	Prob > F	
Linear	0.022	6	3.60E-03	11.09	0.0179	
2FI	0.012	5	2.41E-03	7.42	0.0375	
Quadratic	3.61E-04	3	1.20E-04	0.37	0.7792	Suggested
Cubic	0	0				Aliased
Pure Error	1.30E-03	4	3.24E-04			

The lack of fit test was a done to confirm the model's adequacy. This compares the variation around the model with pure variation within replicated observations. From Table 4.11.3A, it was found that quadratic model showed a non significant

F-value of 0.37 while other models indicated significant result of lack of fit which showed that these models are not adequate for use.

Table 4.11.3B Model Summary Statistics

Model Summary Statistics						
	Std.		**Adjusted**	**Predicted**		
Source	**Dev.**	**R-Squared**	**R-Squared**	**R-Squared**	**PRESS**	
Linear	0.048	0.9277	0.9132	0.7386	0.083	
2FI	0.038	0.9579	0.9438	0.771	0.072	
Quadratic	0.015	0.9948	0.991	0.954	0.015	Suggested
Cubic	0.018	0.9959	0.9877		+	Aliased

The correlation observed in the values of the adjusted R-square and predicted R-square values were used to determine the measure of how efficient the variability in the actual response values can be explained by the experimental variables and their interaction. Based on this, it was found that quadratic model showed the best correlation in these values of 0.9948, 0.991 and 0.954 for R-squared, R-squared adjusted and R-squared predicted respectively which other models did not show. The measure of how efficient the variability in the actual response values can be explained by the experimental variables and their interaction is given by the R-

square value. When it closer to unity, it shows that the model can predict the response better.

Table 4.11.3C ANOVA for Response Surface Quadratic Model

ANOVA for Response Surface Quadratic model						
Analysis of variance table [Partial sum of squares - Type III]						
	Sum of		**Mean**	**F**	**p-value**	
Source	**Squares**	**df**	**Square**	**Value**	**Prob > F**	
Model	0.31	5	0.063	265.76	< 0.0001	significant
A-Rice Husk	*0.19*	*1*	*0.19*	*789.81*	*< 0.0001*	
B-Clay	*2.85E-03*	*1*	*2.85E-03*	*12.04*	*0.0104*	
AB	*0.013*	*1*	*0.013*	*53.24*	*0.0002*	
A^2	*0.012*	*1*	*0.012*	*48.78*	*0.0002*	
B^2	*4.78E-04*	*1*	*4.78E-04*	*2.02*	*0.1985*	
Residual	1.66E-03	7	2.37E-04			
Lack of Fit	*3.61E-04*	*3*	*1.20E-04*	*0.37*	*0.7792*	*not significant*
Pure Error	*1.30E-03*	*4*	*3.24E-04*			
Cor Total	0.32	12				

The Model F-value of 265 shown in Table 4.11.3C implies the model is significant.

There is only a 0.01% chance that an F-value this large could occur due to noise.

Values of "Prob > F" less than 0.0500 indicate model terms are significant. In this case A, B, AB, A^2, B^2 are significant model terms. Values greater than 0.1000 indicate the model terms are not significant. The "Lack of Fit F-value" of 0.37 implies the Lack of Fit is not significant relative to the pure error. There is a 77.92% chance that a "Lack of Fit F-value" this large could occur due to noise. Non-significant lack of fit is good because it means the model would fit effectively.

The “Pred R-Squared of 0.954 is in reasonable agreement with the “Adj R-Squared value of 0.991; i.e. the difference is less than 0.2 Therefore the equation in terms of coded factors was developed which can be used to make predictions about the response for given levels of each factor. By default, the high levels of factors are coded as +1 and the low levels of the factors are coded as -1.

The equation in terms of coded factor is shown as;

$$\text{Bulk Density} = +1.87 - 0.17*A + 0.049*B + 0.072*AB + 0.023*A^2 + 0.027*B^2. \quad (4.13)$$

A stands for rice husk additive while B stands for clay.

The equation in terms of actual factor is used to make predictions about the response for given levels of each factor. The levels are specified in original units for each factor. It is shown as;

$$\text{Bulk Density} = +14.1584 - 0.83471*X_1 - 0.11703*X_2 + 4.8E\text{-}03*X_1*X_2 + 0.010256*X_1^2 + 2.65E\text{-}04*X_2^2. \quad (4.14)$$

The response values obtained by inserting the independent values are the predicted values of the model. These values are compared to the actual and experimental values. The result of the comparison was shown in Figure 4.11.8

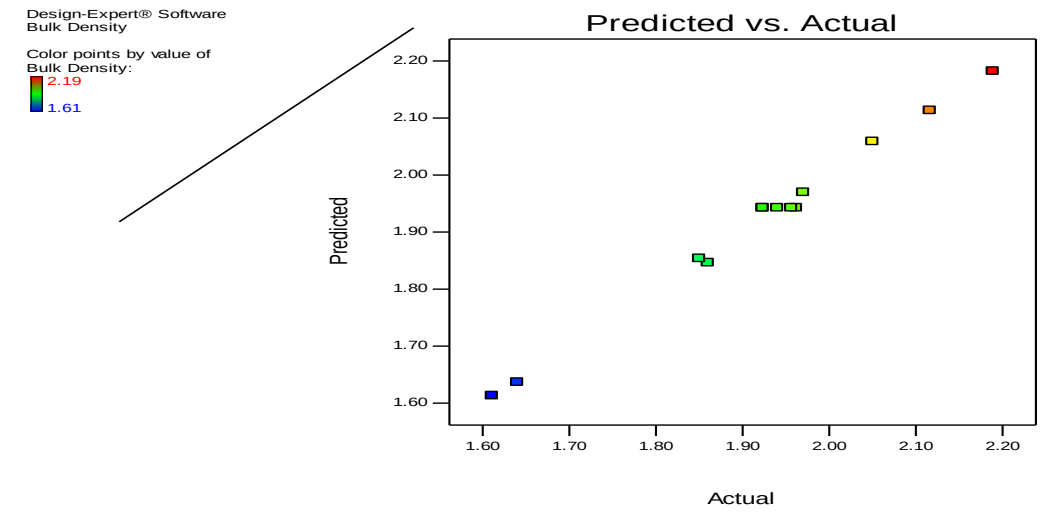

Figure 4.11.8 linear correlation between predicted Vs actual values for bulk density of rice husk blended clay

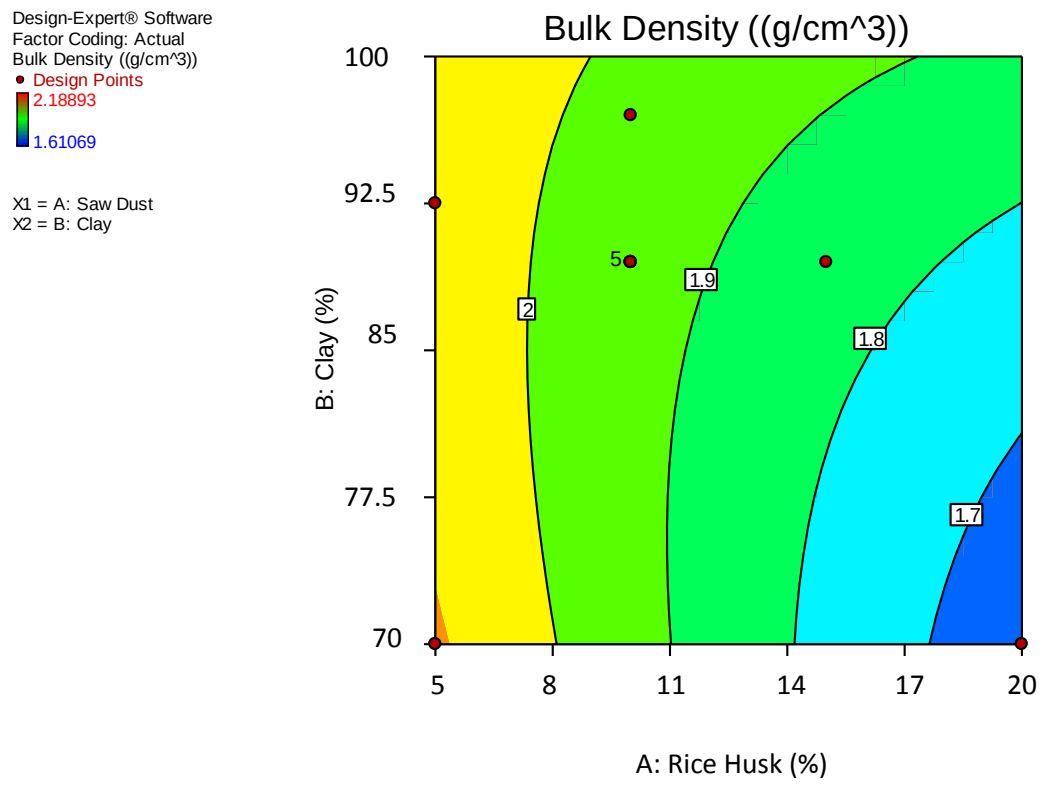

Figure 4.11.9 Two dimension contour plot for the combined effect of the composition of clay and rice husk on bulk density

From Figure 4.11.9, it was observed that bulk density value was decreasing with decrease in composition of clay (B) and with increase in the composition of rice husk (A). Maximum value of bulk density value of 2.0g/cm^3 was obtained at 95% composition of clay and 5% of sawdust. The minimum value of bulk density of 1.7g/cm^3 was found when the composition of the clay decreased to 75% with the corresponding value of sawdust composition. The decrease in bulk density value with decrease in clay composition and increase in sawdust composition is due to

increase in pore sizes as a result of more quantity of rice husk additive being burnt off. These additives that were burnt off during firing leave larger pores in the brick's structure and thereby decreasing the density.

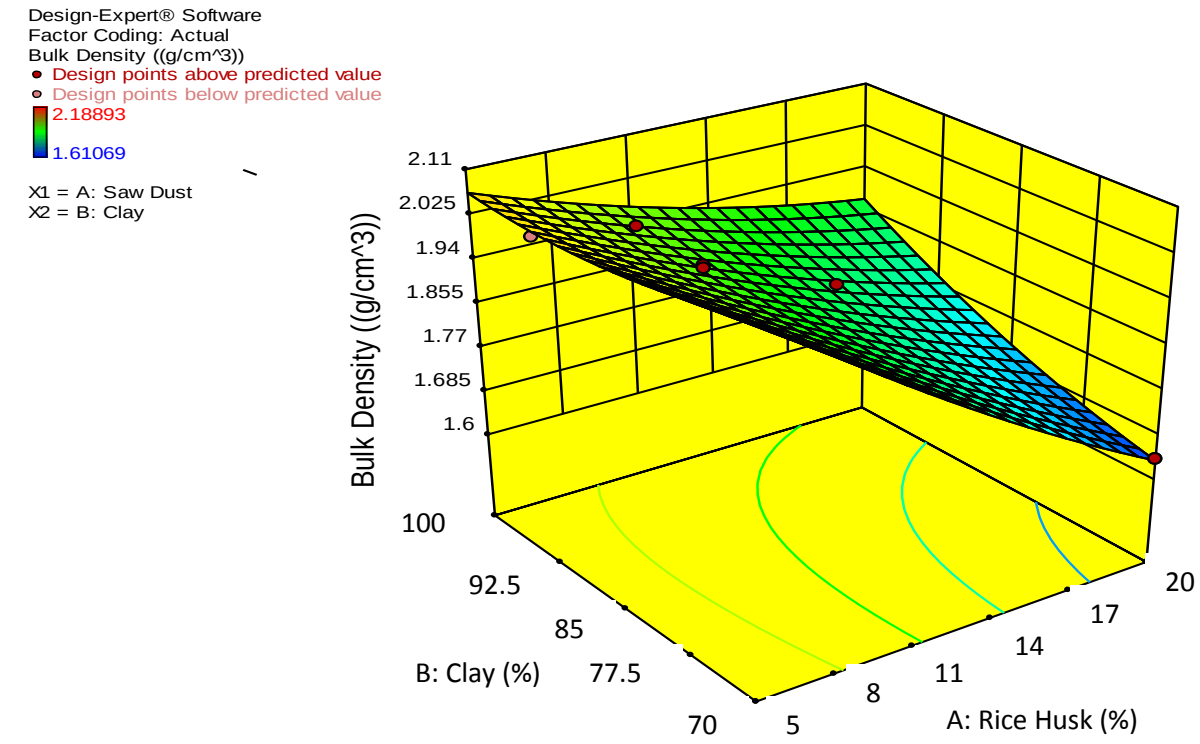

Figure 4.11.10 Three dimension surface plot for the combined effect of the composition of clay and rice husk on bulk density

Figure 4.11.10 shows the interactive effect of clay and rice husk compositions on bulk density. It was seen that the value of bulk density was decreasing with

decrease in the composition of clay and increase in the composition of rice husk additive. On the reverse, bulk density increased with decrease in the composition of rice husk additive and increase in clay composition. Maximum (optimum) value of bulk density of 2.06g/cm^3 was found in 95% composition of clay with the corresponding value of rice husk composition. Further decrease of clay composition to 92.5% and increase of rice husk to 7.5 reduced the bulk density value to 1.94g/cm^3. Progressive decrease in bulk density value was observed with successive decrease in clay composition with increase in rice husk composition.

The decrease and increase in the value of bulk density follows such trend because increase in rice husk composition increases porosity and decreases density. In contrast, decrease with rice husk composition with increase in clay composition forms a more homogeneous clay structure which reduces porosity and makes the composite material denser.

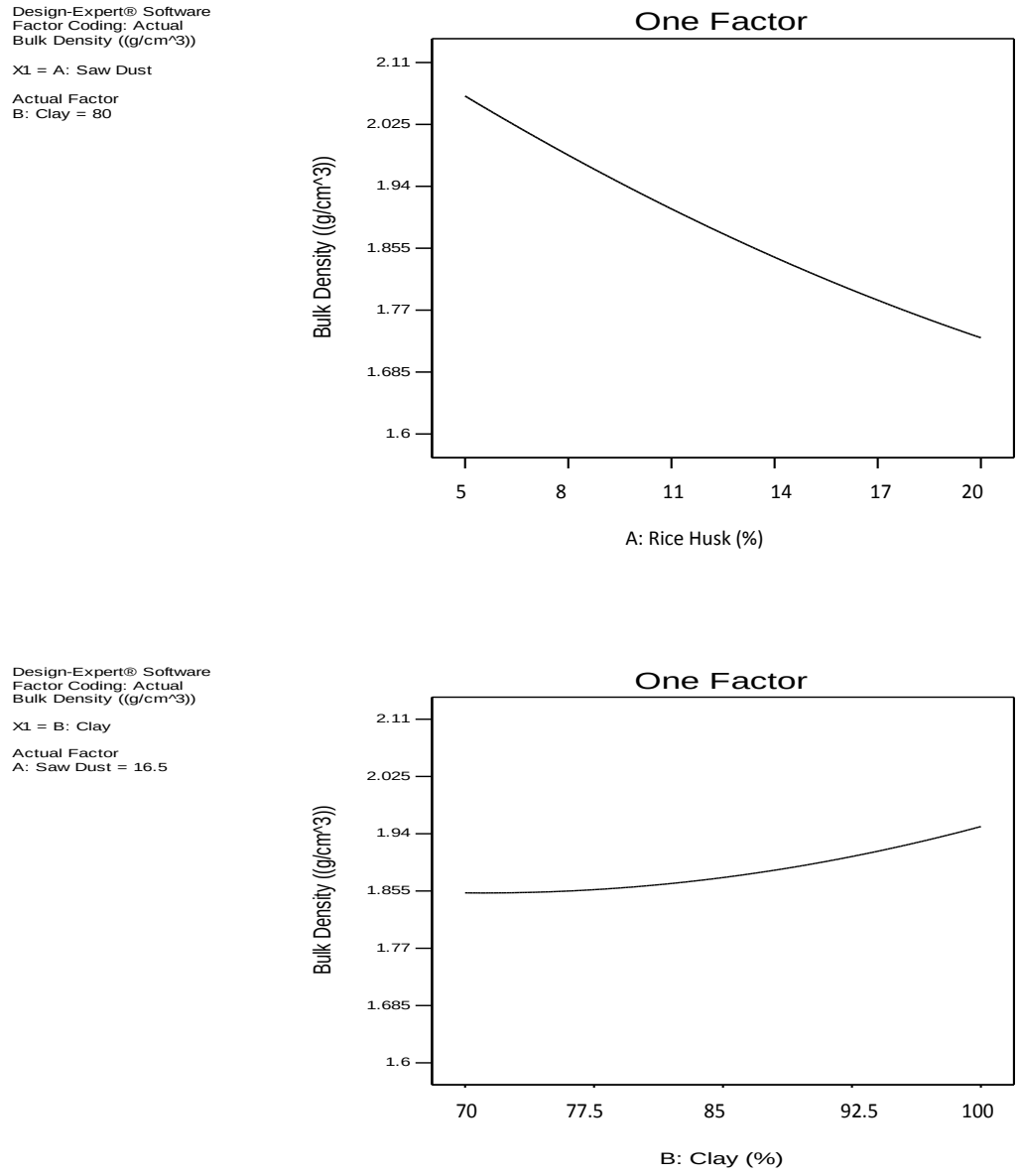

Figure 4.11.11 Single factor plot for the combined effect of the composition of clay and rice husk on bulk density

The single factor plot for the effect of rice husk shows that increase in the composition of the additive yielded decrease in the bulk density while that of the

effect of clay composition shows that increase in clay composition yielded increase in the bulk density.

4.11.4 Results for Modulus of Rupture in the Blend of Rice Husk

Table 4.11.4A Results for Lack of Fit Test

Lack of Fit Tests						
	Sum of		Mean	F	p-value	
Source	Squares	df	Square	Value	Prob > F	
Linear	1.49	6	0.25	0.93	0.5569	
2FI	1.46	5	0.29	1.09	0.4792	
Quadratic	0.04	3	0.013	0.05	0.9834	Suggested
Cubic	0	0				Aliased
Pure Error	1.07	4	0.27			

The lack of fit test was a done to confirm the model's adequacy. This compares the variation around the model with pure variation within replicated observations. From Table 4.10.4, it was found that quadratic model showed a non significant F-value of 0.05 while other models indicated significant result of lack of fit which showed that these models are not adequate for use.

Table 4.10.4B Model Summary Statistics

Model Summary Statistics						
	Std.		**Adjusted**	**Predicted**		
Source	**Dev.**	**R-Squared**	**R-Squared**	**R-Squared**	**PRESS**	
Linear	0.51	0.7967	0.7561	0.5349	5.85	
2FI	0.53	0.7987	0.7315	0.3624	8.02	
Quadratic	0.4	0.9117	0.8487	0.8375	2.04	Suggested
Cubic	0.52	0.9149	0.7447		+	Aliased

The correlation observed in the values of the adjusted R-square and predicted R-square values were used to determine the measure of how efficient the variability in the actual response values can be explained by the experimental variables and their interaction. Based on this, it was found that quadratic model showed the best correlation in these values of 0.9117, 0.8487 and 0.8375 for R-squared, R-squared adjusted and R-squared predicted respectively which other models did not show. The measure of how efficient the variability in the actual response values can be explained by the experimental variables and their interaction is given by the R-square value. When it closer to unity, it shows that the model can predict the response better.

Table 4.11.4C ANOVA for Response Surface Quadratic Model

Response	**4**	**Modulus of rupture**				
ANOVA for Response Surface Quadratic model						
Analysis of variance table [Partial sum of squares - Type III]						
	Sum of		**Mean**	**F**	**p-value**	
Source	**Squares**	**df**	**Square**	**Value**	**Prob > F**	
Model	11.46	5	2.29	14.46	0.0014	significant
A-Rice Husk	5.69	1	5.69	35.87	0.0005	
B-Clay	0.69	1	0.69	4.38	0.0748	
AB	0.26	1	0.26	1.66	0.2383	
A^2	1.04	1	1.04	6.55	0.0376	
B^2	0.52	1	0.52	3.26	0.1139	
Residual	1.11	7	0.16			

The Model F-value of 14.46 shown in Table 4.11.4C implies the model is significant. There is only a 0.14% chance that an F-value this large could occur due to noise. Values of "Prob > F" less than 0.0500 indicate model terms are significant. In this case A, A^2 are significant model terms. Values greater than 0.1000 indicate the model terms are not significant. The "Lack of Fit F-value" of 0.05 implies the Lack of Fit is not significant relative to the pure error. There is a 98.34% chance that a "Lack of Fit F-value" this large could occur due to noise. Non-significant lack of fit is good because it means the model would fit effectively. The “Pred R-Squared of 0.8375 is in reasonable agreement with the “Adj R-Squared value of 0.8487; i.e. the difference is less than 0.2

Therefore the equation in terms of coded factors was developed which can be used to make predictions about the response for given levels of each factor. By default, the high levels of factors are coded as +1 and the low levels of the factors are coded as -1.

The equation in terms of coded factor is shown as;

$$\text{Modulus of rupture} = 31.58 - 0.92*A + 0.77*B + 0.33*AB + 0.22*A^2 + 0.87*B^2 \quad (4.15)$$

A stands for rice husk additive while B stands for clay.

The equation in terms of actual factor is used to make predictions about the response for given levels of each factor. The levels are specified in original units for each factor. It is shown as;

Modulus of rupture = $+146.93292 - 5.58429*X_1 - 1.68304* X_2 + 0.022043* X_1* X_2 + 0.09729* X_1^2 + 8.73\text{-}03* X_2^2$. (4.16)

X_1 Stands for rice husk additive while X_2 stands for clay

The response values obtained by inserting the independent values are the predicted values of the model. These values were compared to the actual and experimental values. The result of the comparison was shown in Figure 4.11.12

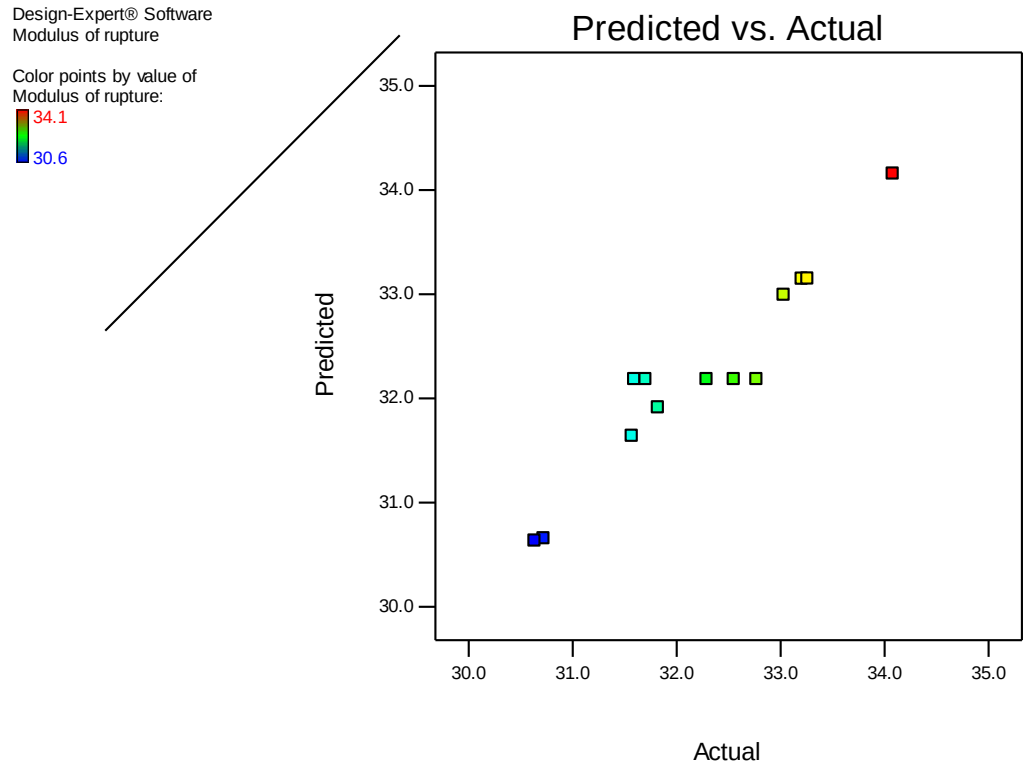

Figure 4.11.12 linear correlation between predicted Vs actual values for modulus of rupture for rice husk blended clay

4.11.21 Effects of Model Parameters and their Interactions

The relationship between the experimental variables and the response were studied with the plot of the individual and interactive effects of the two factors- clay and rice husk on the response- modulus of rupture.

The central composite design was used to produce three dimensional (3D) response surface and two dimensional (2D) contour plots. The 3D surfaces and 2D contour plots are graphical representations of the equation for the optimization of the

experimental responses and are the most useful approach in revealing the conditions of the optimum performance of the responses.

In the plots, the response functions of the two factors are presented. The results of the interactions between two independent variables and dependent variable are shown in Figures 4.11.13 and 4.10.14.

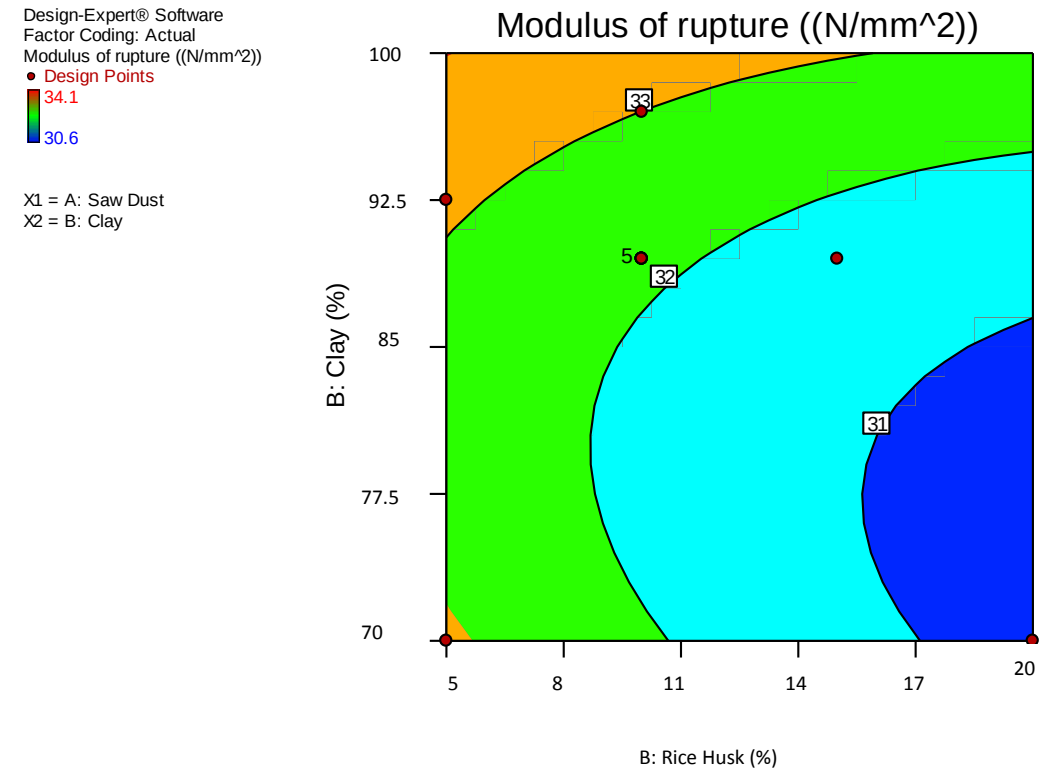

Figure 4.11.13 Two dimension contour plot for the combined effect of the composition of clay and rice husk on modulus of rupture

From Figure 4.11.13, It was observed that value of modulus of rupture was decreasing with decrease in composition of clay (B) and with increase in the

composition of rice husk (A). Maximum value of modulus of rupture of 33N/mm^2 was obtained between the ranges of 5 -10% composition of sawdust value. Beyond 10% composition of rice husk and its corresponding 85% of clay, modulus of rupture was seen to decrease progressively with increase the composition of the additive.

Hence, it was seen that increase in the quantity of additive has adverse effect on the transverse strength. This is due to the fact that increase in the concentration of additive at the expense of the clay led to the deficiency of the main clay content which is supposed to improve the strength. Also migration of gases through the matrix produced due to burning of the additive created highly porous clay structure which affected the mechanical strength.

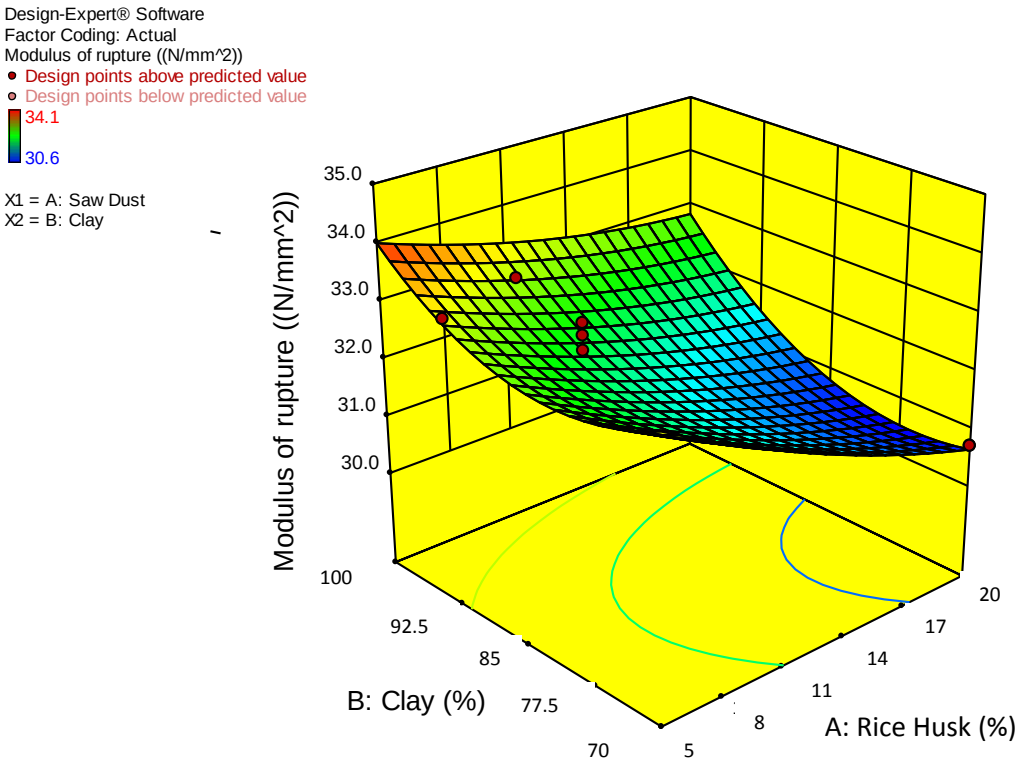

Figure 4.11.14 Three dimension surface plot for the combined effect of the composition of clay and rice husk on modulus of rupture

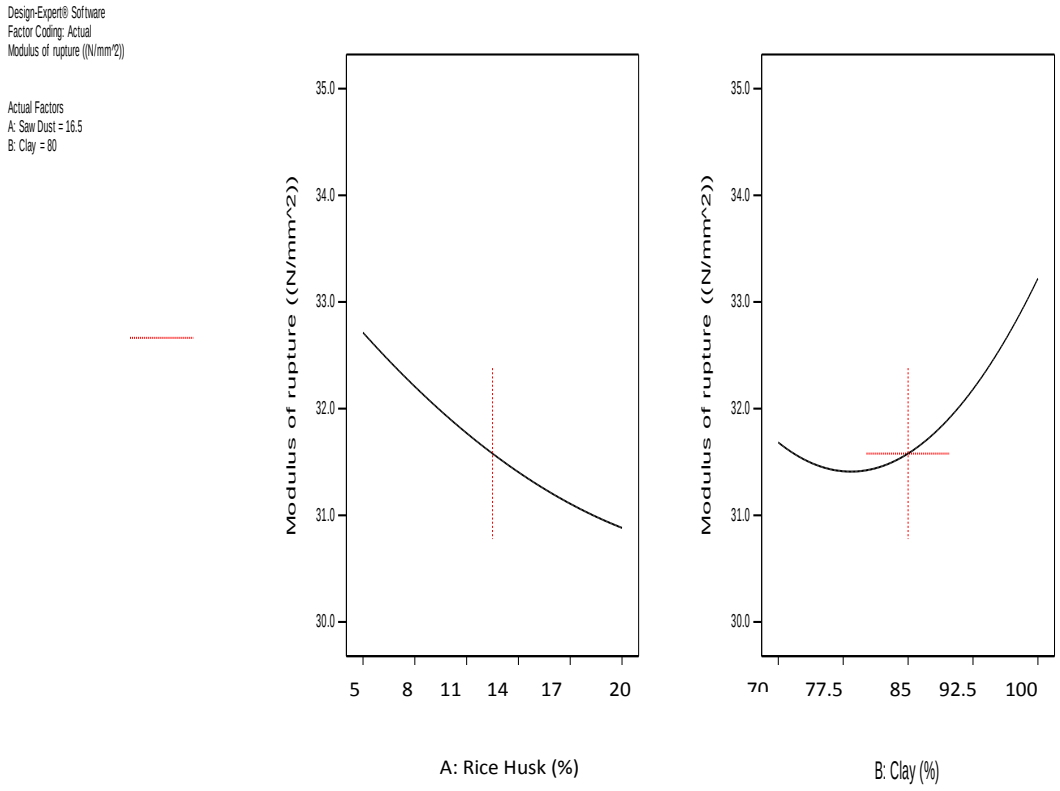

Figure 4.11.15 Single factor plot for the combined effect of the composition of clay and rice husk on modulus of rupture

The single factor plots show that the increase in the composition of rice husk has a linear relationship with modulus of rupture which decreases with increase in the quantity of rice husk. That of the effect of clay has a non linear relationship with modulus of rupture. It decreases with increase in clay up to 77.5 % of clay. Beyond this value of clay composition, it will begin to increase with increase with increase in clay composition.

4.12 Experimental Design for Refractory Properties of Nguzu – Amaiyi Clay Blended with Groundnut Shell Additive.

The effect of the independent factors on the responses was studied using response surface methodology with central composite design type. The predicted results for the responses in the experimental design developed are shown in Table 4.12. The responses investigated were linear shrinkage, apparent porosity, bulk density and modulus of rupture while the factors are compositions of clay and groundnut shell additive. Results shown in Table 4.12 reveal that the independent factors had significant effect on the responses in the various runs which the experiment was conducted.

4.12. Results of the Experimental Design for Groundnut Shell Blended Composite Clay

Table 4.12. Results of the Experimental Design for the Effect of the Factors on the Responses for Groundnut Shell Blended Composite Clay

	Factor 1	Factor 2	Response 1	Response 2	Response 3	Response 4
Std	A:G/nut Shell	B:Clay	Linear Shrinkage	Apparent porosity	Bulk Density	Modulus of rupture
	%	%	%	%	(g/cm^3)	(N/mm^2)
1	6	94	6.12	25.61	2	34.9
2	20	80	8.55	45.46	1.42	32.9
3	5	95	6.35	27.05	1.93	35.4
4	15	85	7.7	36.69	1.71	33.9
5	4	96	5.27	20.93	2.04	36.4
6	20	80	8.7	46.09	1.35	32.8
7	13	87	7.46	35.24	1.72	34
8	10	90	6.53	30.49	1.84	35.3
9	10	90	6.93	30.64	1.84	35.1
10	10	90	7.1	32.26	1.82	34.4
11	10	90	7.24	32.78	1.83	34.5
12	10	90	7.49	33.74	1.81	33.9
13	10	90	7.7	35.18	1.8	33.8

4.12.10 Results for Linear Shrinkage in the Blend of Groundnut Shell

Table 4.12.1A Results for Lack of Fit Test

Lack of Fit Tests						
	Sum of		**Mean**	**F**	**p-value**	
Source	**Squares**	**df**	**Square**	**Value**	**Prob > F**	
Linear	1.58	6	0.26	2.76	0.1727	
2FI	1.56	5	0.31	3.28	0.1366	
Quadratic	0.03	3	0.01	0.11	0.9525	Suggested
Cubic	0	0				Aliased
Pure Error	0.38	4	0.095			

The lack of fit test was a done to confirm the model's adequacy. This compares the variation around the model with pure variation within replicated observations. From Table 4.12.1A, it was found that quadratic model showed a non significant F-value of 0.11. Linear and 2FI models indicated significant result of lack of fit of 2.76 and 3.28 respectively. This showed that these models are not adequate for use.

Table 4.12.1B Model Summary Statistics

Model Summary Statistics						
	Std.		**Adjusted**	**Predicted**		
Source	**Dev.**	**R-Squared**	**R-Squared**	**R-Squared**	**PRESS**	
Linear	0.44	0.82	0.784	0.514	5.29	
2FI	0.46	0.8213	0.7617	0.2603	8.05	
Quadratic	0.24	0.9622	0.9351	0.823	1.93	Suggested
Cubic	0.31	0.9649	0.8948		+	Aliased

The correlation observed in the values of the adjusted R-square and predicted R-square values were used to determine the measure of how efficient the variability in the actual response values can be explained by the experimental variables and their interaction. Based on this, it was found that quadratic model showed the best correlation in these values of 0.9622, 0.9351 and 0.823 for R-squared, R-squared adjusted and R-squared predicted respectively which other models did not show.

Table 4.12.1C ANOVA for Response Surface Quadratic Model

Response	**1**	**Linear Shrinkage**				
ANOVA for Response Surface Quadratic model						
Analysis of variance table [Partial sum of squares - Type III]						
	Sum of		**Mean**	**F**	**p-value**	
Source	**Squares**	**df**	**Square**	**Value**	**Prob > F**	
Model	10.47	5	2.09	35.61	< 0.0001	significant
A-Groundnut Shell	5.61	1	5.61	95.4	< 0.0001	
B-Clay	0.47	1	0.47	7.91	0.026	
AB	0.23	1	0.23	3.92	0.0083	
A^2	1.19	1	1.19	20.3	0.0028	
B^2	0.48	1	0.48	8.12	0.0247	
Residual	0.41	7	0.059			
Lack of Fit	0.03	3	0.01	0.11	0.9525	not significant
Pure Error	0.38	4	0.095			

Cor Total	10.88	12				

The Model F-value of 35.61 shown in table 4.10.3.4 implies the model is significant. There is only a 0.01% chance that an F-value this large could occur due to noise. Values of "Prob > F" less than 0.0500 indicate model terms are significant. In this case A, B, AB, A^2 B^2 are significant model terms. Values greater than 0.1000 indicate the model terms are not significant. The "Lack of Fit F-value" of 0.11 implies the Lack of Fit is not significant relative to the pure error. There is a 95.25% chance that a "Lack of Fit F-value" this large could occur due to noise. Non-significant lack of fit is good because it means the model would fit effectively.

Std. Dev.	0.24	R-Squared	0.9622
Mean	7.17	Adj R-Squared	0.9351
C.V. %	3.38	Pred R-Squared	0.823
PRESS	1.93	Adeq Precision	20.521
-2 Log Likelihood	-7.99	BIC	7.4
		AICc	18.01

The “Pred R-Squared of 0.823 is in reasonable agreement with the “Adj R-Squared value of 0.9251; i.e. the difference is less than 0.2

Therefore the equation in terms of coded factors was developed which can be used to make predictions about the response for given levels of each factor. By default, the high levels of factors are coded as +1 and the low levels of the factors are coded as -1.

The equation in terms of coded factor is shown as;

Linear shrinkage =7.83 + 0.91*A - 0.63*B - 0.31*AB - 0.23*A^2 – 0.84*B^2 (4.12.1)

A stands for groundnut shell additive while B stand for clay.

The equation in terms of actual factor is used to make predictions about the response for given levels of each factor. The levels are specified in original units for each factor. It is shown as;

Linear shrinkage = -106.36599 + 5.69527*X_1 + 1.61821* X_2 - 0.020607* X_1 * X_2-0.10426*X_1^2–8.38E-03*X_2^2. (4.12.2)

X_1 stands for groundnut shell while X_2 stands for clay.

The response values obtained by inserting the independent values are the predicted values of the model. These values were compared to the actual and experimental values. The result of the comparison was shown in Figure 4.11.1

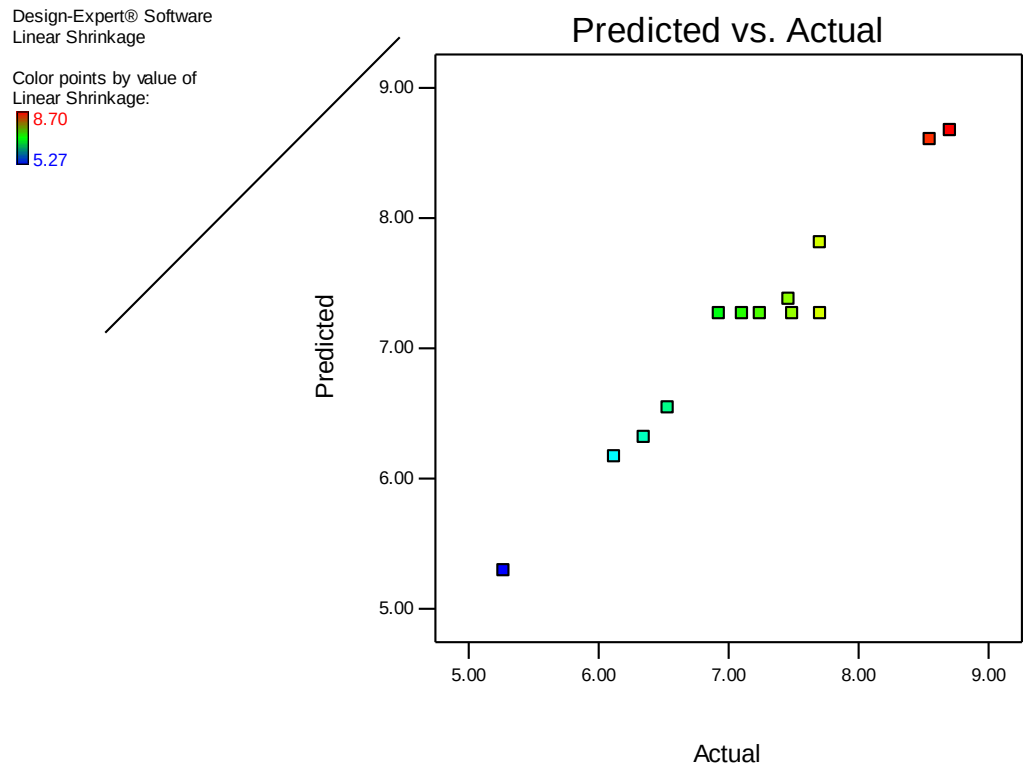

Figure 4.12.1 linear correlation between predicted Vs actual values for linear shrinkage for groundnut shell blended clay

4.12.11 Effects of Model Parameters and their Interactions

The relationship between the experimental variables and the response were studied with the plot of the individual and interactive effects of the two factors- clay and groundnut shell on the response- linear shrinkage.

The central composite design was used to produce three dimensional (3D) response surface and two dimensional (2D) contour plots. The 3D surfaces and 2D contour plots are graphical representations of the equation for the optimization of the

experimental responses and are the most useful approach in revealing the conditions of the optimum performance of the responses.

In the plots, the response functions of the two factors are presented. The results of the interactions between two independent variables and dependent variable are shown in Figures 4.12.2 and 4.12.3.

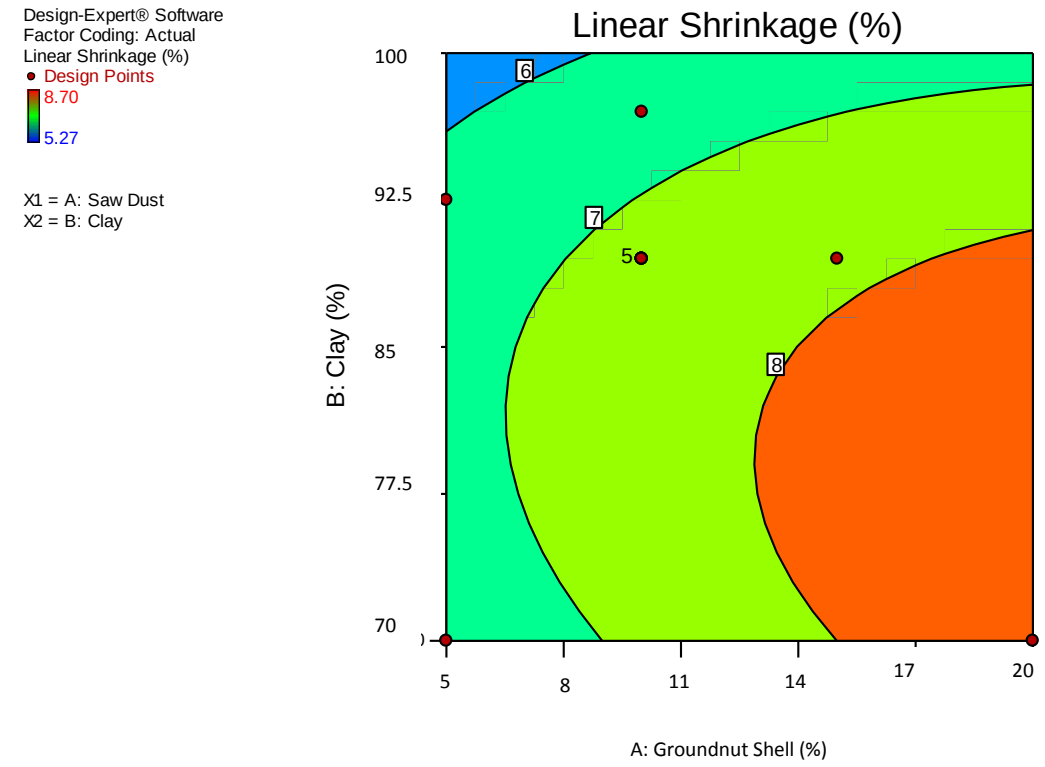

Figure 4.12.2 Two dimension contour plot for the combined effect of the composition of clay and groundnut shell on linear shrinkage

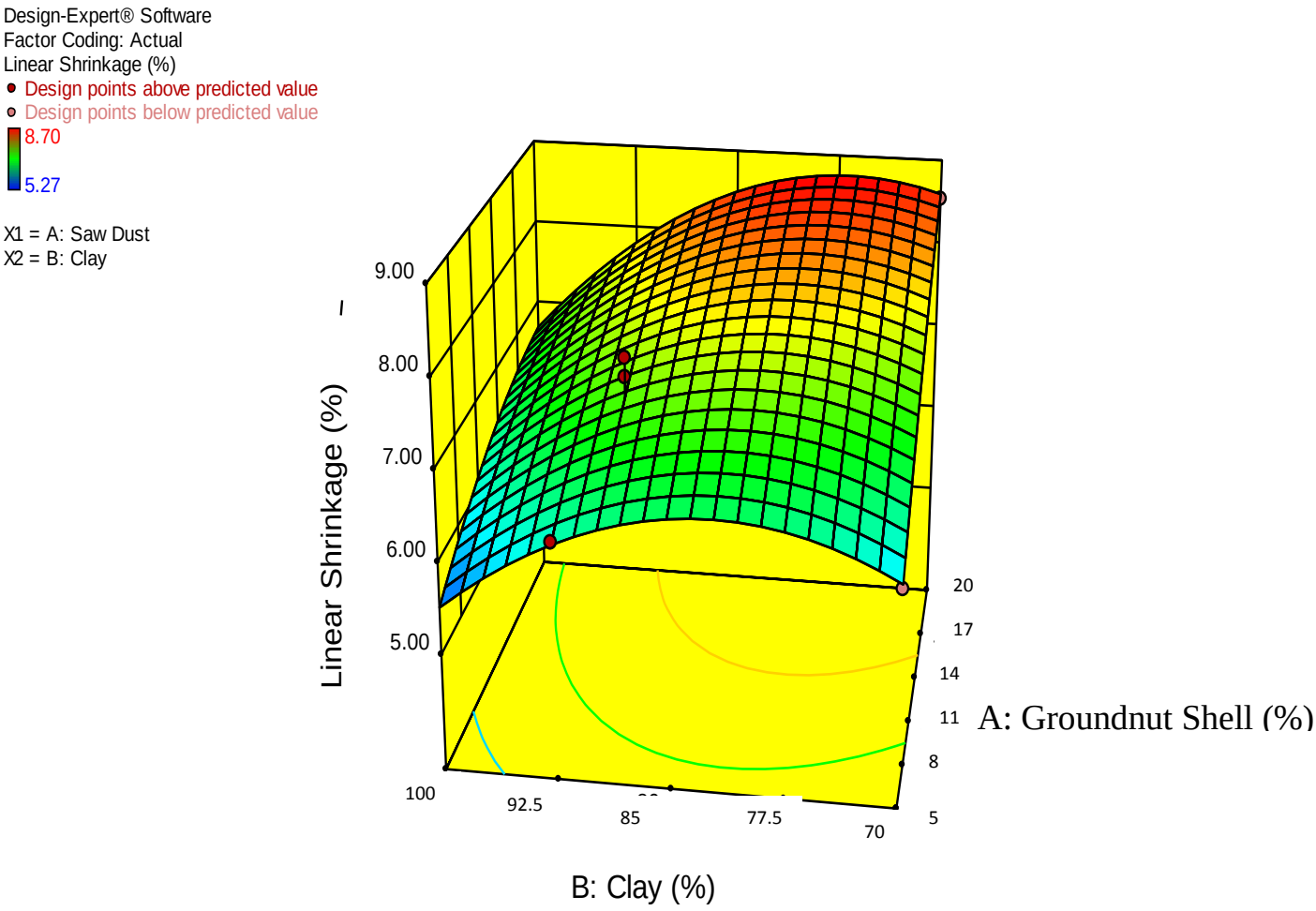

Figure 4.12.3 Three dimension surface plot for the combined effect of the composition of clay and groundnut shell on linear shrinkage

From Figures 4.12.2 and 4.12.3, it was found that in groundnut shell blend, linear shrinkage increased with increase in the composition of the additive and with decrease in clay composition. When the composition of clay and groundnut shell additive were 95 and 5% respectively, the shrinkage value was 5.53%. This was the lowest and the optimum shrinkage value obtained in this blend. When the value

of groundnut shell increased to 14% and that of clay decreased further to 86%, it found that linear shrinkage increased to 8%. The increase in shrinkage in this trend is due to rearrangement in the particle and grain of the composite material after firing. This normally led a more compact structure and higher level of shrinkage.

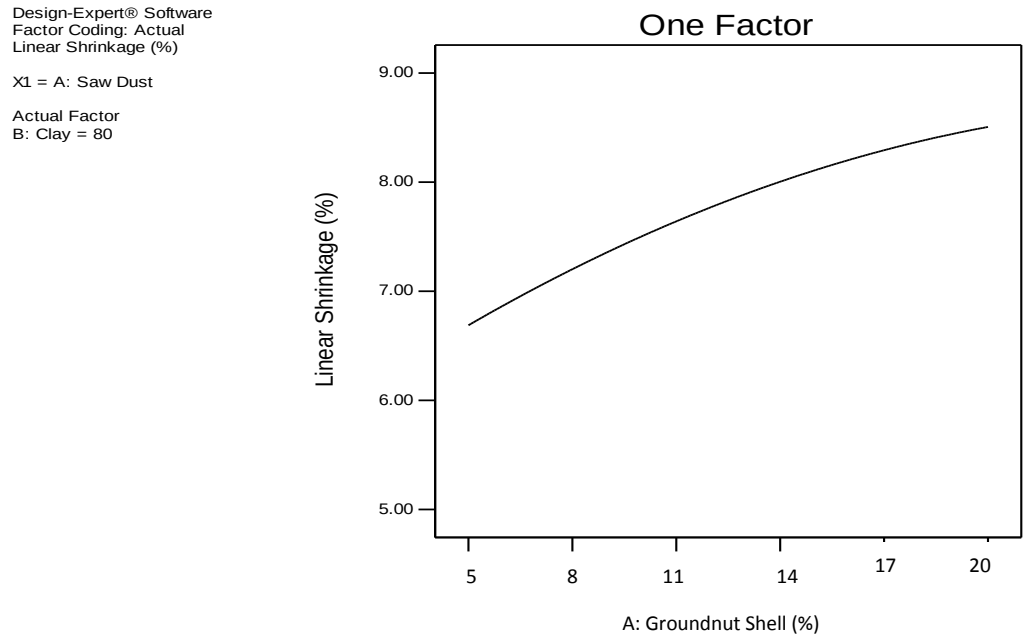

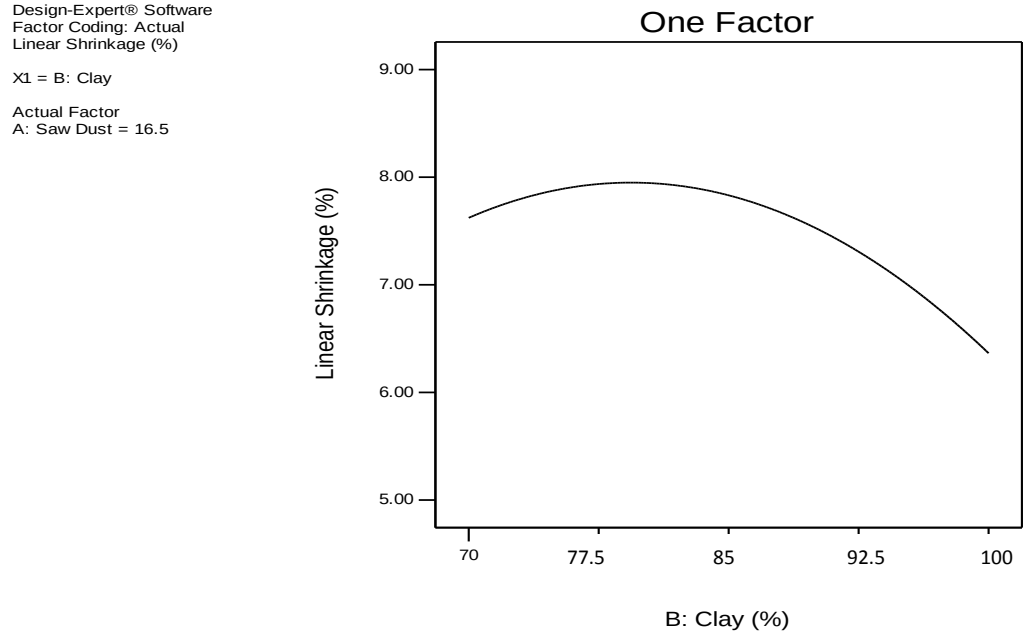

Figure 4.12.4 Single factor plot for the effect of the composition of clay on linear shrinkage

The single factor plot for the effect of the composition of clay on the linear shrinkage of the composite brick shows that the shrinkage value was increasing with increase in clay composition between 70 – 80% compositions of clay. Beyond this range, the trend changed. Increase in composition yielded decrease in linear shrinkage. This is attributed to more quantities of some oxides of clay which reduce shrinkage.

4.12.20 Results for Apparent Porosity in the Blend of Groundnut Shell

Table 4.12.2A Results for Lack of Fit Test

Lack of Fit Tests						
	Sum of		**Mean**	**F**	**p-value**	
Source	**Squares**	**df**	**Square**	**Value**	**Prob > F**	
Linear	45.59	6	7.6	2.65	0.1823	
2FI	36.07	5	7.21	2.52	0.196	
Quadratic	0.7	3	0.23	0.081	0.9669	Suggested
Cubic	0	0				Aliased
Pure Error	11.47	4	2.87			

The lack of fit test was a done to confirm the model's adequacy. This compares the variation around the model with pure variation within replicated observations. From Table 4.12.2A, it was found that quadratic model showed a non significant F-value of 0.081. Linear and 2FI models indicated significant result of lack of fit of 2.65 and 2.52 respectively. This showed that these models are not adequate for use.

Table 4.12.2B Model Summary Statistics

Model Summary Statistics						
	Std.		**Adjusted**	**Predicted**		
Source	**Dev.**	**R-Squared**	**R-Squared**	**R-Squared**	**PRESS**	
Linear	2.39	0.9045	0.8854	0.6884	186.26	
2FI	2.3	0.9205	0.8939	0.6403	214.97	
Quadratic	1.32	0.9796	0.9651	0.9457	32.46	Suggested
Cubic	1.69	0.9808	0.9424		+	Aliased

The correlation observed in the values of the adjusted R-square and predicted R-square values were used to determine the measure of how efficient the variability in the actual response values can be explained by the experimental variables and their interaction. Based on this, it was found that quadratic model showed the best correlation in these values of 0.9796, 0.9651 and 0.9457 for R-squared, R-squared adjusted and R-squared predicted respectively which other models did not show.

Table 4.12.2C ANOVA for Response Surface Quadratic Model

Response	**2**	**Apparent porosity**				
ANOVA for Response Surface Quadratic model						
Analysis of variance table [Partial sum of squares - Type III]						
	Sum of		**Mean**	**F**	**p-value**	
Source	**Squares**	**df**	**Square**	**Value**	**Prob > F**	
Model	585.5	5	117.1	67.38	< 0.0001	significant
A-Groundnut Shell	339.05	1	339.05	195.09	< 0.0001	
B-Clay	10.92	1	10.92	6.29	0.0406	
AB	19.31	1	19.31	11.11	0.0125	
A^2	32.08	1	32.08	18.46	0.0036	
B^2	5.67	1	5.67	3.26	0.1138	
Residual	12.17	7	1.74			
Lack of Fit	0.7	3	0.23	0.081	0.9669	not significant
Pure Error	11.47	4	2.87			
Cor Total	597.66	12				

The Model F-value of 67.38 implies the model is significant. There is only a 0.01% chance that an F-value this large could occur due to noise. Values of "Prob > F" less than 0.0500 indicate model terms are significant. In this case A, B, AB, A^2 are significant model terms. Values greater than 0.1000 indicate the model terms are not significant.

The "Lack of Fit F-value" of 0.08 implies the Lack of Fit is not significant relative to the pure error. There is a 96.69% chance that a "Lack of Fit F-value" this large could occur due to noise. Non-significant lack of fit is good because it means the model would fit effectively.

Std. Dev.	1.32	R-Squared	0.9796
Mean	33.24	Adj R-Squared	0.9651
C.V. %	3.97	Pred R-Squared	0.9457
PRESS	32.46	Adeq Precision	27.987
-2 Log Likelihood	36.03	BIC	51.42
		AICc	62.03

The "Pred R-Squared" of 0.9457 is in reasonable agreement with the "Adj R-Squared" of 0.9651; i.e. the difference is less than 0.2.

Therefore the equation in terms of coded factors was developed which can be used to make predictions about the response for given levels of each factor. By default, the high levels of factors are coded as +1 and the low levels of the factors are coded as -1.

The equation in terms of coded factor is shown as;

$$\text{Apparent Porosity} = 36.26 + 7.07*A - 3.05*B - 2.83*AB - 1.22*A^2 - 2.89*B^2 \quad (4.12.3)$$

A stands for groundnut shell while B stands for clay.

The equation in terms of actual factor is used to make predictions about the response for given levels of each factor. The levels are specified in original units for each factor. It is shown as;

$$\text{Apparent Porosity} = -598.29961 + 37.64869*X_1 + 7.43200*X_2 - 0.18869*X_1*X_2 - 0.54065*X_1^2 - 0.028896*X_2^2. \quad (4.12.4)$$

X_1 stands for groundnut shell while X_2 stands for clay.

The response values obtained by inserting the independent values are the predicted values of the model. These values were compared to the actual and experimental

values. The result of the comparison was shown in Figure 4.11.5

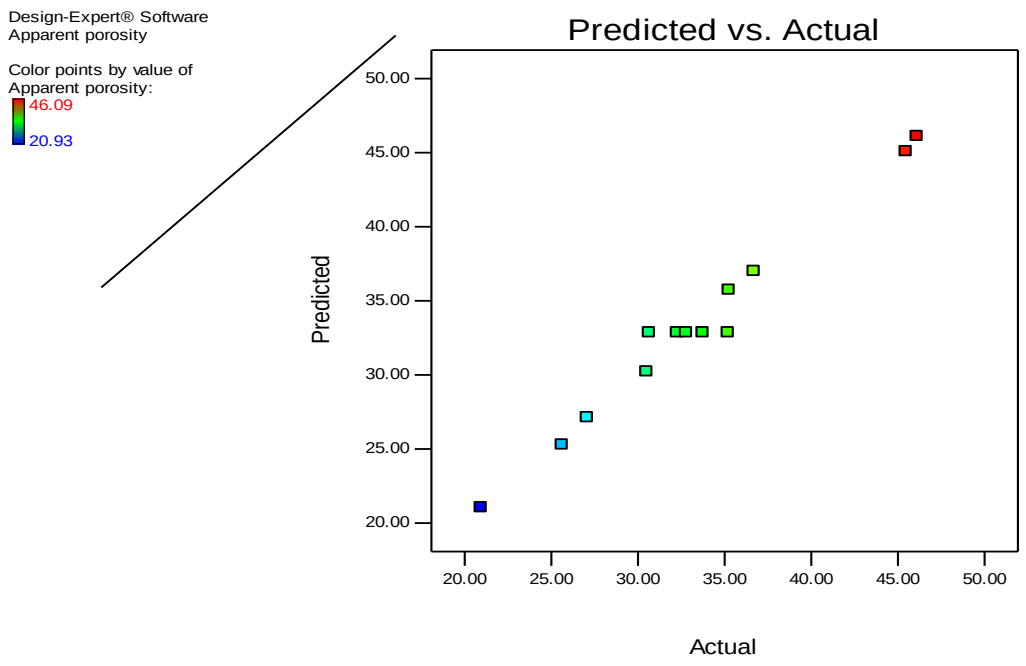

Figure 4.11.5 linear correlation between predicted Vs actual values for apparent porosity for groundnut shell blended clay

4.12.21 Effects of Model Parameters and their Interactions

The relationship between the experimental variables and the response were studied with the plot of the individual and interactive effects of the two factors- clay and groundnut shell on the response- apparent porosity.

The central composite design was used to produce three dimensional (3D) response surface and two dimensional (2D) contour plots. The 3D surfaces and 2D contour plots are graphical representations of the equation for the optimization of the

experimental responses and are the most useful approach in revealing the conditions of the optimum performance of the responses.

In the plots, the response functions of the two factors are presented. The results of the interactions between two independent variables and dependent variable are shown in Figures 4.12.6 and 4.12.7

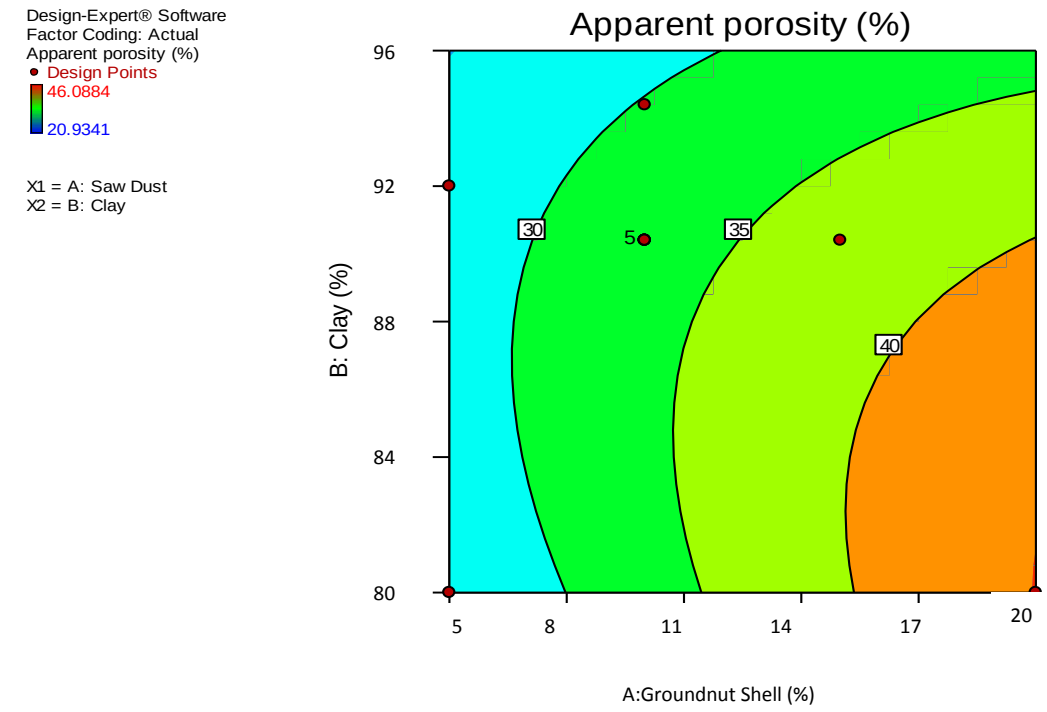

Figure 4.12.6 Two dimension contour plot for the combined effect of the composition of clay and groundnut shell on apparent porosity

It was found from Figure 4.12.7 that apparent porosity increased with increase in groundnut shell additive and with decrease in clay composition. Within the range

shown in the plot, minimum value of porosity of 30% was obtained at 8% composition of groundnut shell additive with 92% composition of clay while the highest value of 40% was obtained at the composition of 15 and 85% for groundnut shell and clay respectively. Optimum apparent porosity of 24.869% was obtained at 95 and 5% composition of clay and groundnut shell additive respectively.

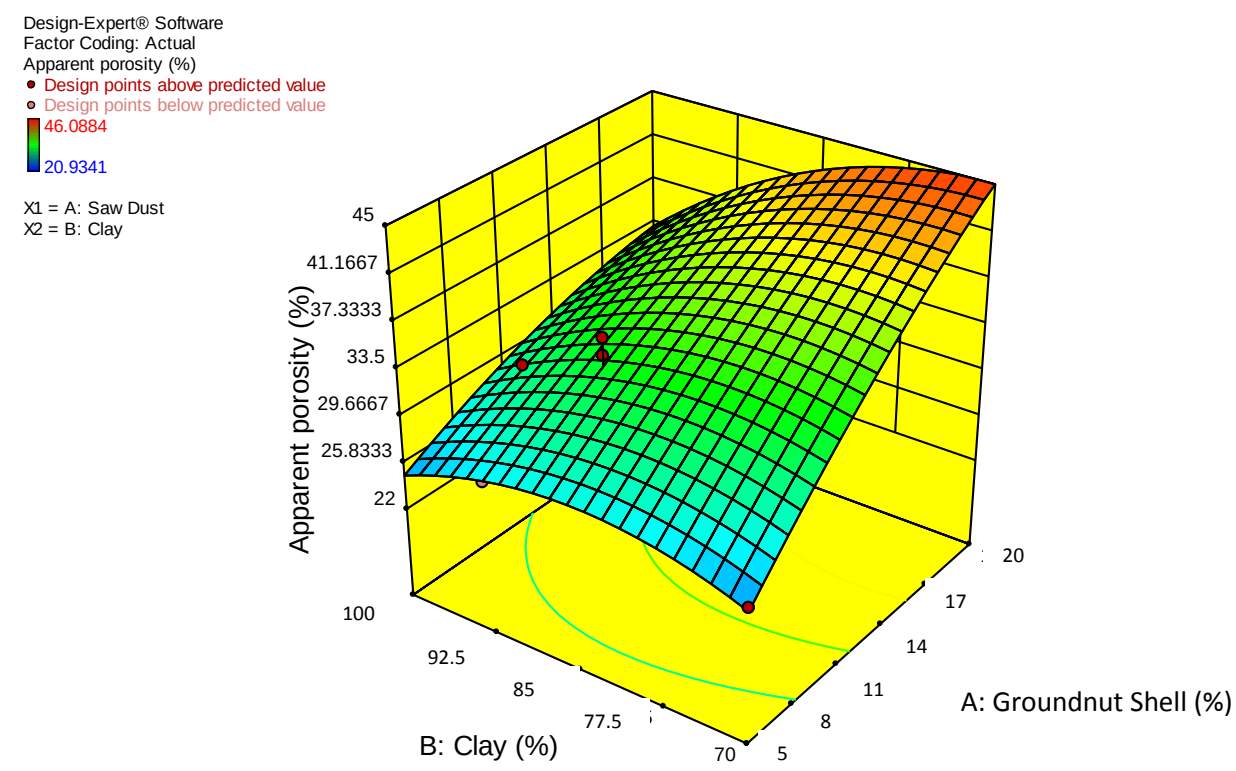

Figure 4.12.7 Three dimension surface plot for the combined effect of the composition of clay and groundnut shell on apparent porosity

From Figure 4.12.7, it can be seen that the interactive effect of clay and groundnut shell show that apparent porosity started increasing from the value of 24.86% with increase in additive composition and decrease in clay composition. However maximum value of porosity was attained at 80% clay. Beyond this composition, porosity was found to decrease.

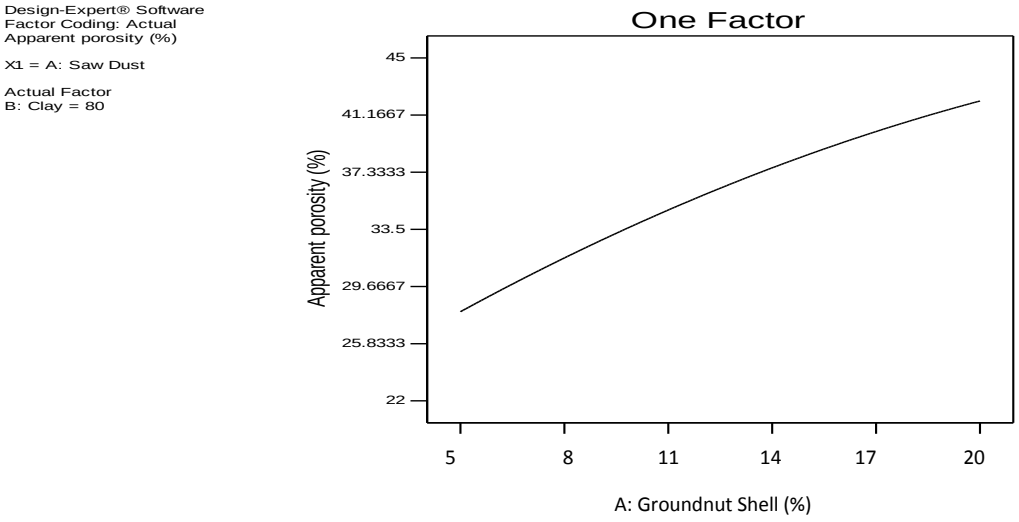

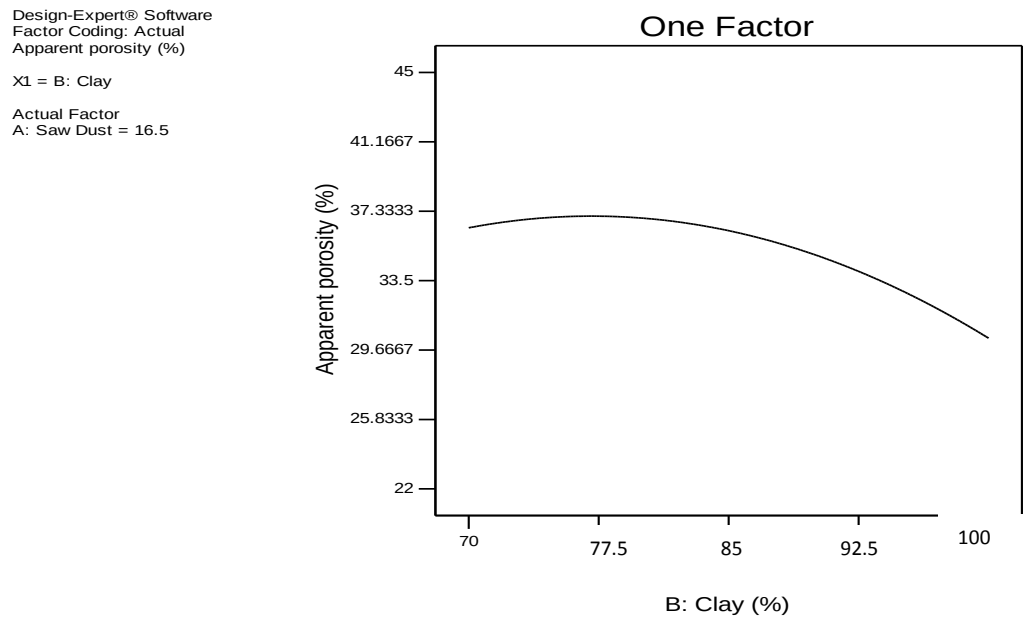

Figure 4.12.8 Single factor plot for the combined effect of the composition of clay and groundnut shell on apparent porosity

The single factor plot for the effect of groundnut shell on apparent porosity shows the composition of the additive maintained a linear relationship with apparent porosity while that of clay indicate a non linear relationship with apparent porosity. Apparent porosity slightly rose in value up to 80% composition of clay and began to fall in value with further increase in clay composition. This show that if the composition of is increased at the expense of that of the additive, the size pores that will be obtained will reduce due to less quantity of burnt material. Hence porosity will gradually begin to reduce as the trend continues.

4.12.30 Results for Bulk Density in the Blend of Groundnut Shell

Table 4.12.3A Results for Lack of Fit Test

Lack of Fit Tests						
	Sum of		**Mean**	**F**	**p-value**	
Source	**Squares**	**df**	**Square**	**Value**	**Prob > F**	
Linear	0.025	6	4.10E-03	14.8	0.0105	
2FI	2.04E-03	5	4.07E-04	1.47	0.3657	
Quadratic	2.48E-04	3	8.28E-05	0.3	0.8259	Suggested
Cubic	0	0				Aliased
Pure Error	1.11E-03	4	2.77E-04			

The lack of fit test was a done to confirm the model's adequacy. This compares the variation around the model with pure variation within replicated observations. From Table 4.12.3A, it was found that quadratic model showed a non significant F-value of 0.3. Linear and 2FI models indicated significant result of lack of fit of 14.8 and 1.47 respectively. This showed that these models are not adequate for use

Table 4.12.3B Model Summary Statistics

Model Summary Statistics						
	Std.		**Adjusted**	**Predicted**		
Source	**Dev.**	**R-Squared**	**R-Squared**	**R-Squared**	**PRESS**	
Linear	0.051	0.9454	0.9345	0.8468	0.072	
2FI	0.019	0.9933	0.9911	0.9727	0.013	
Quadratic	0.014	0.9971	0.9951	0.9782	0.01	Suggested
Cubic	0.017	0.9976	0.9929		+	Aliased

The correlation observed in the values of the adjusted R-square and predicted R-square values were used to determine the measure of how efficient the variability in the actual response values can be explained by the experimental variables and their interaction. Based on this, it was found that quadratic model showed the best correlation in these values of 0.9971, 0.9951 and 0.9782 for R-squared, R-squared adjusted and R-squared predicted respectively which other models did not show

Table 4.12.3C ANOVA for Response Surface Quadratic Model

Response	**3**	**Bulk Density**				
ANOVA for Response Surface Quadratic model						
Analysis of variance table [Partial sum of squares - Type III]						
	Sum of		**Mean**	**F**	**p-value**	
Source	**Squares**	**df**	**Square**	**Value**	**Prob > F**	
Model	0.47	5	0.094	485.11	< 0.0001	significant
A-Groundnut Shell	0.25	1	0.25	1266.46	< 0.0001	
B-Clay	4.32E-03	1	4.32E-03	22.28	0.0022	
AB	0.023	1	0.023	118.68	< 0.0001	
A^2	1.52E-03	1	1.52E-03	7.85	0.0264	
B^2	4.06E-04	1	4.06E-04	2.09	0.1912	
Residual	1.36E-03	7	1.94E-04			
Lack of Fit	2.48E-04	3	8.28E-05	0.3	0.8259	not significant
Pure Error	1.11E-03	4	2.77E-04			
Cor Total	0.47	12				

The Model F-value of 485.11 implies the model is significant. There is only a 0.01% chance that an F-value this large could occur due to noise.

Values of "Prob > F" less than 0.0500 indicate model terms are significant. In this case A, B, AB, A^2 are significant model terms. Values greater than 0.1000 indicate the model terms are not significant. If there are many insignificant model terms (not counting those required to support hierarchy), model reduction may improve your model. The "Lack of Fit F-value" of 0.30 implies the Lack of Fit is not significant relative to the pure error. There is a 82.59% chance that a "Lack of Fit F-value" this large could occur due to noise. Non-significant lack of fit is good because it means the model would fit efficiently.

Std. Dev.	0.014	R-Squared	0.9971
Mean	1.78	Adj R-Squared	0.9951
C.V. %	0.78	Pred R-Squared	0.9782
PRESS	0.010	Adeq Precision	72.510
-2 Log Likelihood	-82.28	BIC	-66.89
		AICc	-56.28

The "Pred R-Squared" of 0.9782 is in reasonable agreement with the "Adj R-Squared" of 0.9951; i.e. the difference is less than 0.2.

Therefore the equation in terms of coded factors was developed which can be used to make predictions about the response for given levels of each factor. By default, the high levels of factors are coded as +1 and the low levels of the factors are coded as -1.

The equation in terms of coded factor is shown as;

$$\text{Bulk Density} = +1.75 - 0.19*A + 0.061*B + 0.098*AB + 8.379E\text{-}003*A^2 + 0.024*B^2 \quad (4.12.5)$$

The equation in terms of actual factor is used to make predictions about the response for given levels of each factor. The levels are specified in original units for each factor. It is shown as;

$$\text{Bulk Density} = 14.52908 - 0.77073*X_1 - 0.14051*X_2 + 6.51E\text{-}03*X_1*X_2 + 3.72E\text{-}03*X_1^2 + 2.44E\text{-}04*X_2^2. \quad (4.12.6)$$

X_1 stands for groundnut shell while X_2 stands for clay.

The response values obtained by inserting the independent values are the predicted values of the model. These values were compared to the actual and experimental values. The result of the comparison was shown in Figure 4.12.9

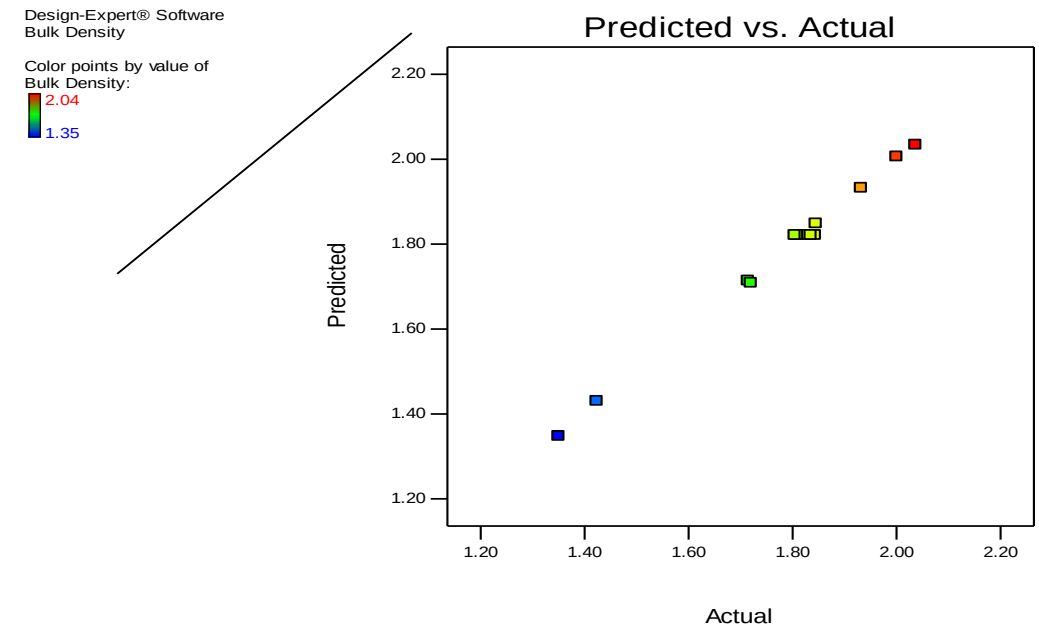

Figure 4.12.9 linear correlation between predicted Vs actual values for bulk density for groundnut shell blended clay

4.12.31 Effects of Model Parameters and their Interactions

The relationship between the experimental variables and the response were studied with the plot of the individual and interactive effects of the two factors- clay and groundnut shell on the response- bulk density.

The central composite design was used to produce three dimensional (3D) response surface and two dimensional (2D) contour plots. The 3D surfaces and 2D contour plots are graphical representations of the equation for the optimization of the

experimental responses and are the most useful approach in revealing the conditions of the optimum performance of the responses.

In the plots, the response functions of the two factors are presented. The results of the interactions between two independent variables and dependent variable are shown in Figures 4.12.10 and 4.12.11.

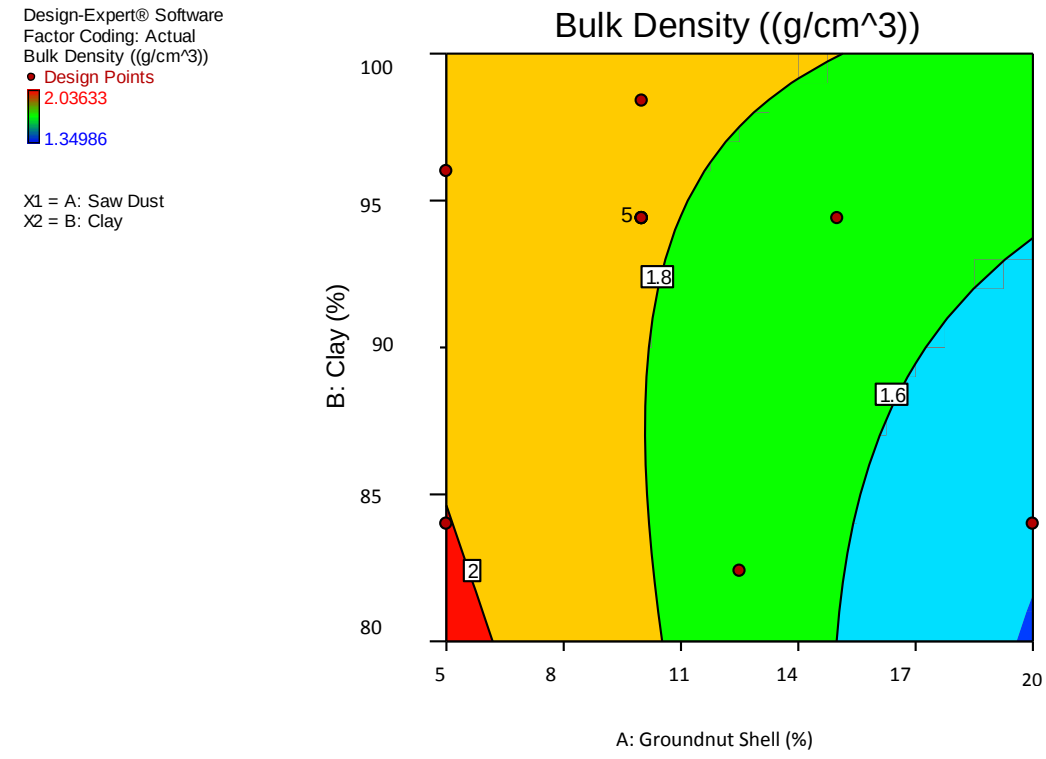

Figure 4.12.10 Two dimension contour plot for the combined effect of the composition of clay and groundnut shell on bulk density

The contour and plots show that decrease in bulk density is obtained with decrease in composition of clay and increase in the composition of the additive. The maximum value of bulk density of 2.00g/cm^3 was obtained with 95% of clay and 5% of groundnut shell additive. It was observed that the bulk density decreased further to1.6g/cm^3 when the composition of clay and the additive got to 85 and 15% respectively.

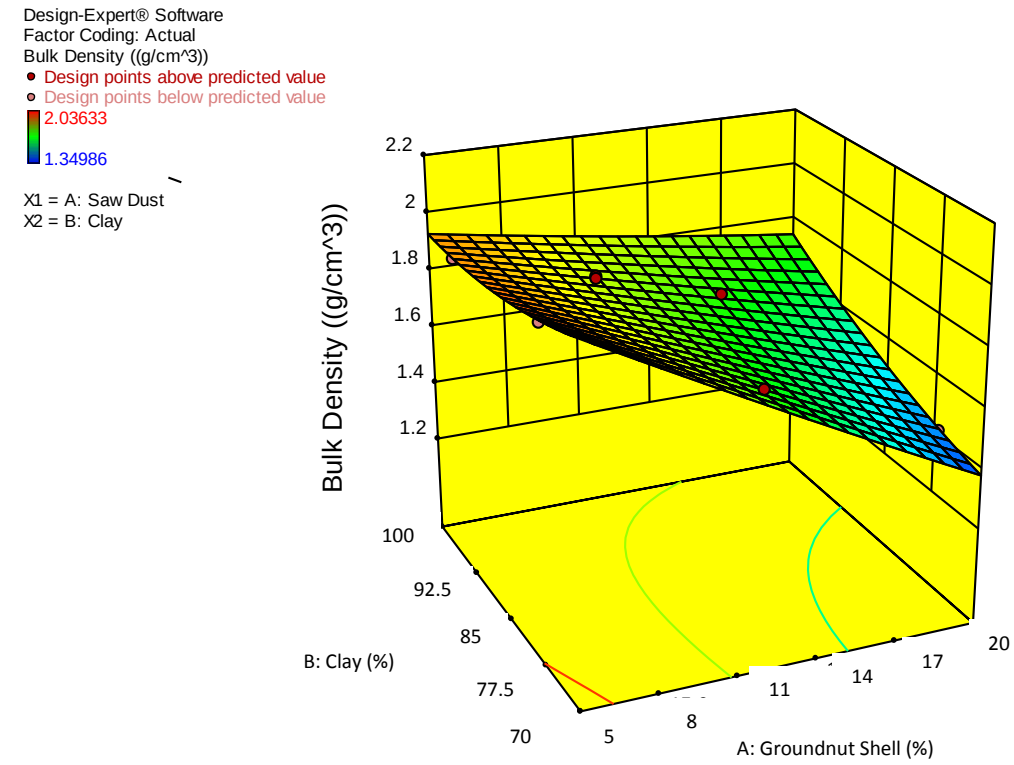

Figure 4.12.11 Three dimension surface plot for the combined effect of the composition of clay and groundnut shell on bulk density

Figure 4.12.11 shows the interactive effect of clay and groundnut shell compositions on bulk density. It was seen that both factors affected bulk density. The value of bulk density was decreasing with decrease in the composition of clay and increase in the composition of rice husk additive. Optimum bulk density value of 1.9g/cm^3 was obtained at 95 and 5% composition of clay and groundnut shell respectively. Progressive decrease in bulk density value was observed with successive decrease in clay composition with increase in groundnut shell composition.

The decrease and increase in the value of bulk density follows such trend because increase in rice husk composition increases porosity and decreases density. In contrast, decrease with groundnut shell composition with increase in clay composition forms a more homogeneous clay structure which reduces porosity and makes the composite material denser.

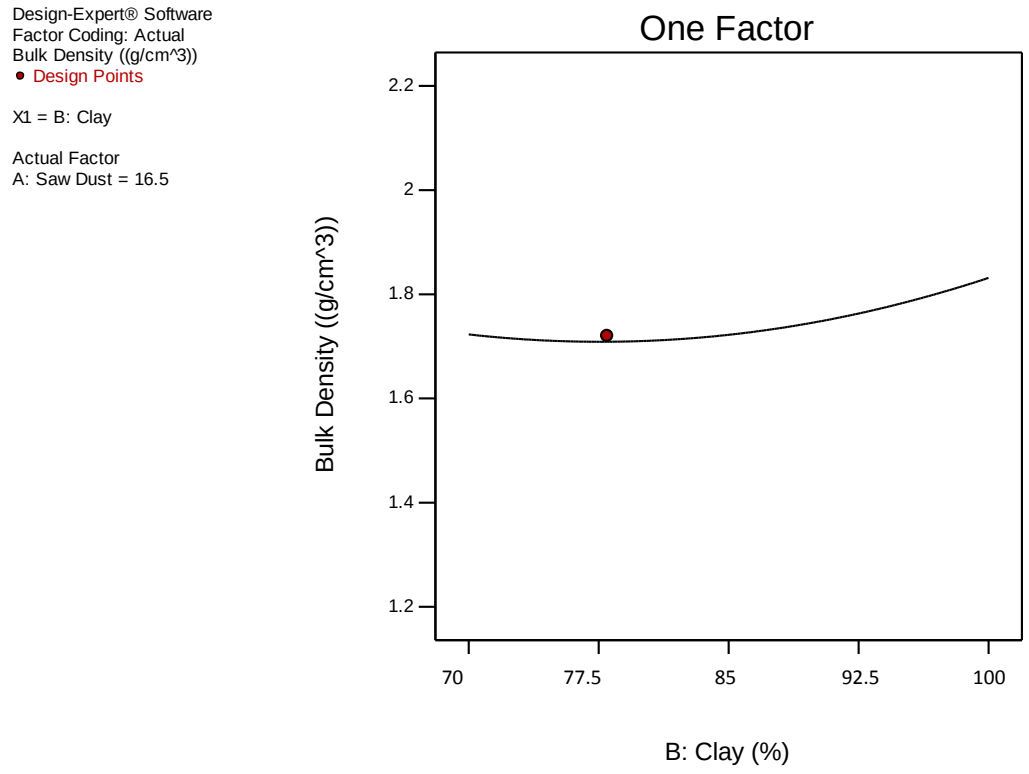

Figure 4.12.12 Single effect plot for the combined effect of the composition of clay and groundnut shell on bulk density

4.12.4 Results for Modulus Rupture in the Blend of Groundnut Shell

Table 4.12.4A Results for Lack of Fit Test

Lack of Fit Tests						
	Sum of		**Mean**	**F**	**p-value**	
Source	**Squares**	**df**	**Square**	**Value**	**Prob > F**	
Linear	1.35	6	0.22	0.87	0.5833	
2FI	1.32	5	0.26	1.02	0.5059	
Quadratic	3.94E-03	3	1.31E-03	5.07E-03	0.9994	Suggested
Cubic	0	0				Aliased
Pure Error	1.04	4	0.26			

The lack of fit test was a done to confirm the model's adequacy. This compares the variation around the model with pure variation within replicated observations. From Table 4.12.4A, it was found that quadratic model showed a non significant F-value of 5.07E-03. Linear and 2FI models indicated significant result of lack of fit of 0.87 and 1.02 respectively. This showed that these models are not adequate for use

Table 4.12.4B Model Summary Statistics

Model Summary Statistics						
	Std.		**Adjusted**	**Predicted**		
Source	**Dev.**	**R-Squared**	**R-Squared**	**R-Squared**	**PRESS**	
Linear	0.49	0.81	0.772	0.6335	4.6	
2FI	0.51	0.8121	0.7494	0.4625	6.74	
Quadratic	0.39	0.9172	0.858	0.876	1.56	Suggested
Cubic	0.51	0.9175	0.7524		+	Aliased

The correlation observed in the values of the adjusted R-square and predicted R-square values were used to determine the measure of how efficient the variability in the actual response values can be explained by the experimental variables and their interaction. Based on this, it was found that quadratic model showed the best correlation in these values of 0.9172, 0.858 and 0.876 for R-squared, R-squared adjusted and R-squared predicted respectively which other models did not shows

Table 4.12.4C ANOVA for Response Surface Quadratic Model

Response	4	Modulus of rupture				
ANOVA for Response Surface Quadratic model						
Analysis of variance table [Partial sum of squares - Type III]						
	Sum of		**Mean**	**F**	**p-value**	
Source	**Squares**	**df**	**Square**	**Value**	**Prob > F**	
Model	11.51	5	2.3	15.5	0.0011	significant
A-Groundnut Shell	4.84	1	4.84	32.57	0.0007	
B-Clay	1.06	1	1.06	7.15	0.0002	
AB	0.053	1	0.053	0.36	0.0003	
A^2	0.81	1	0.81	5.43	0.0426	
B^2	0.65	1	0.65	4.35	0.0255	
Residual	1.04	7	0.15			
Lack of Fit	3.94E-03	3	1.31E-03	5.07E-03	0.9994	not significant
Pure Error	1.04	4	0.26			
Cor Total	12.55	12				

The Model F-value of 15.50 implies the model is significant. There is only a 0.11% chance that an F-value this large could occur due to noise. Values of "Prob > F" less than 0.0500 indicate model terms are significant. In this case A, B are significant model terms. Values greater than 0.1000 indicate the model terms are not significant.

The "Lack of Fit F-value" of 0.01 implies the Lack of Fit is not significant relative to the pure error. There is a 99.94% chance that a "Lack of Fit F-value" this large could occur due to noise. Non-significant lack of fit is good because it means the model would fit efficiently.

Std. Dev.	0.39	R-Squared	0.9172
Mean	34.41	Adj R-Squared	0.858
C.V. %	1.12	Pred R-Squared	0.876
PRESS	1.56	Adeq Precision	13.887
-2 Log Likelihood	4.05	BIC	19.44
		AICc	30.05

The "Pred R-Squared" of 0.8760 is in reasonable agreement with the "Adj R-Squared" of 0.8580; i.e. the difference is less than 0.2.

Therefore the equation in terms of coded factors was developed which can be used to make predictions about the response for given levels of each factor. By default, the high levels of factors are coded as +1 and the low levels of the factors are coded as -1.

The equation in terms of coded factor is shown as;

Modulus of rupture = $33.7 - 0.84*A + 0.95*B + 0.15*AB + 0.19*A^2$

$+ 0.97*B^2$ (4.12.7)

The equation in terms of actual factor is used to make predictions about the response for given levels of each factor. The levels are specified in original units for each factor. It is shown as;

Modulus of rupture = $+134.12931 - 4.18007*X_1 - 1.62747* X_2 + 9.86587E\text{-}003* X_1 * X_2 + 0.085697* X_1^2 + 9.74822E\text{-}003* X_2^2$.

X_1 stands for groundnut shell while X_2 stands for clay.

The response values obtained by inserting the independent values are the predicted values of the model. These values were compared to the actual and experimental values. The result of the comparison was shown in Figure 4.12.13

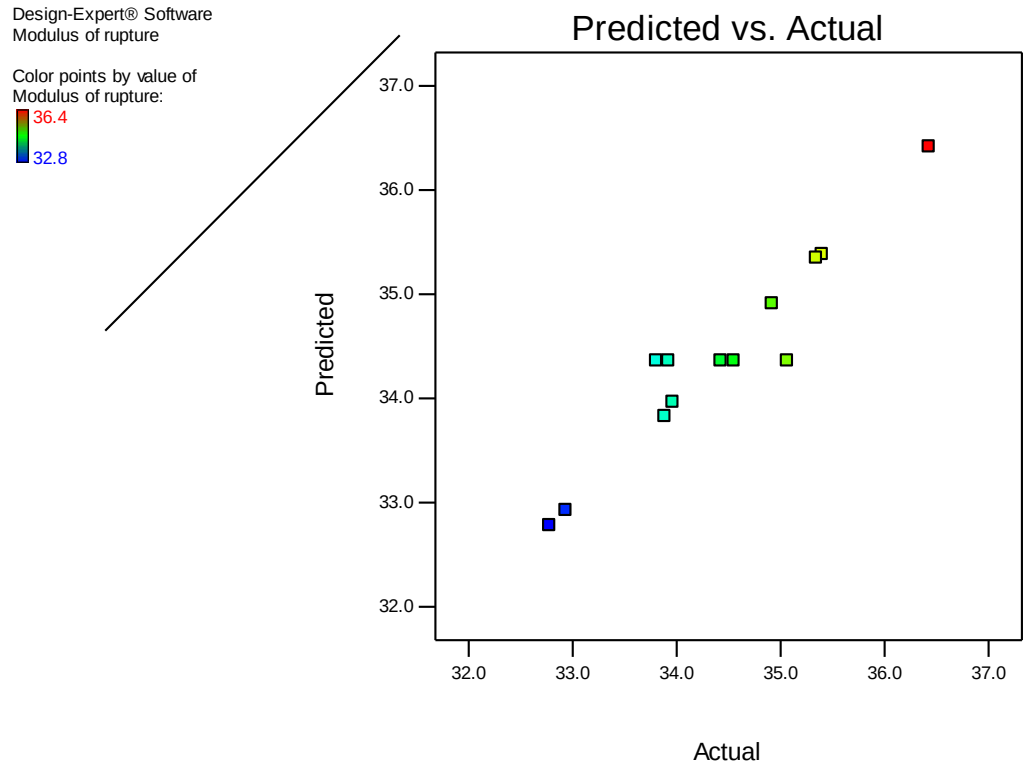

Figure 4.12.13 linear correlation between predicted Vs actual values for modulus of rupture for groundnut shell blended clay

4.12.41 Effects of Model Parameters and their Interactions

The relationship between the experimental variables and the response were studied with the plot of the individual and interactive effects of the two factors- clay and groundnut shell on the response-modulus of rupture.

The central composite design was used to produce three dimensional (3D) response surface and two dimensional (2D) contour plots. The 3D surfaces and 2D contour

plots are graphical representations of the equation for the optimization of the experimental responses and are the most useful approach in revealing the conditions of the optimum performance of the responses.

In the plots, the response functions of the two factors are presented. The results of the interactions between two independent variables and dependent variable are shown in Figures 4.12.14 and 4.12.15

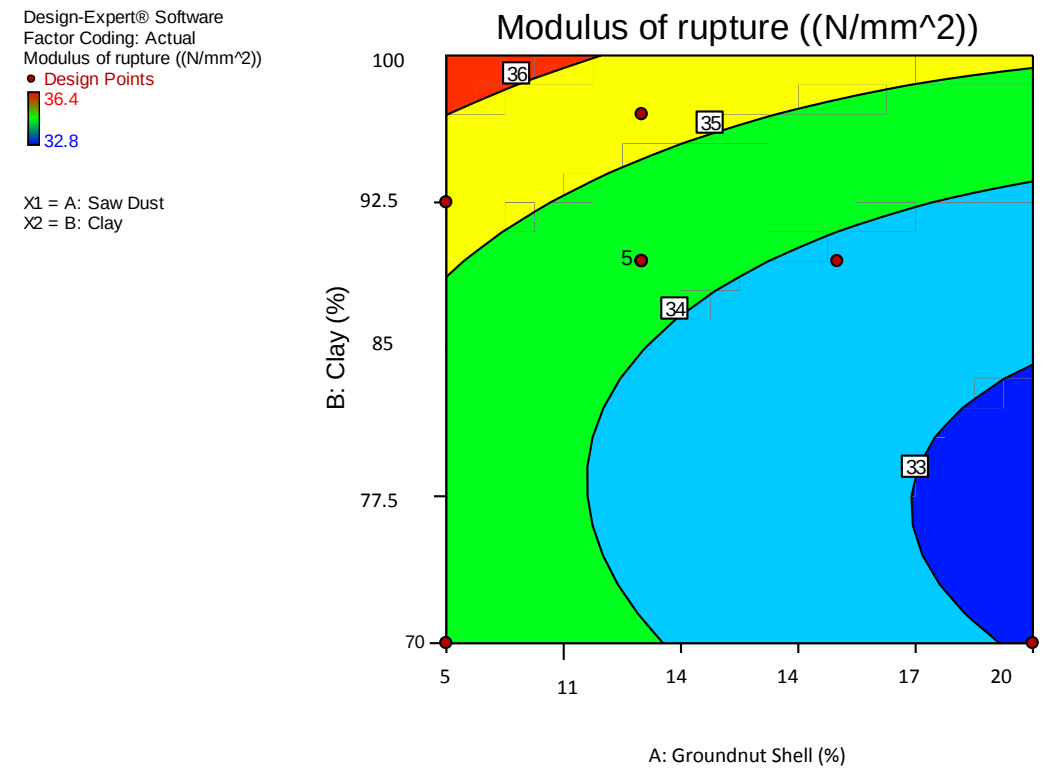

Figure 4.12.14 Two dimension contour plot for the combined effect of the composition of clay and groundnut shell on modulus of rupture

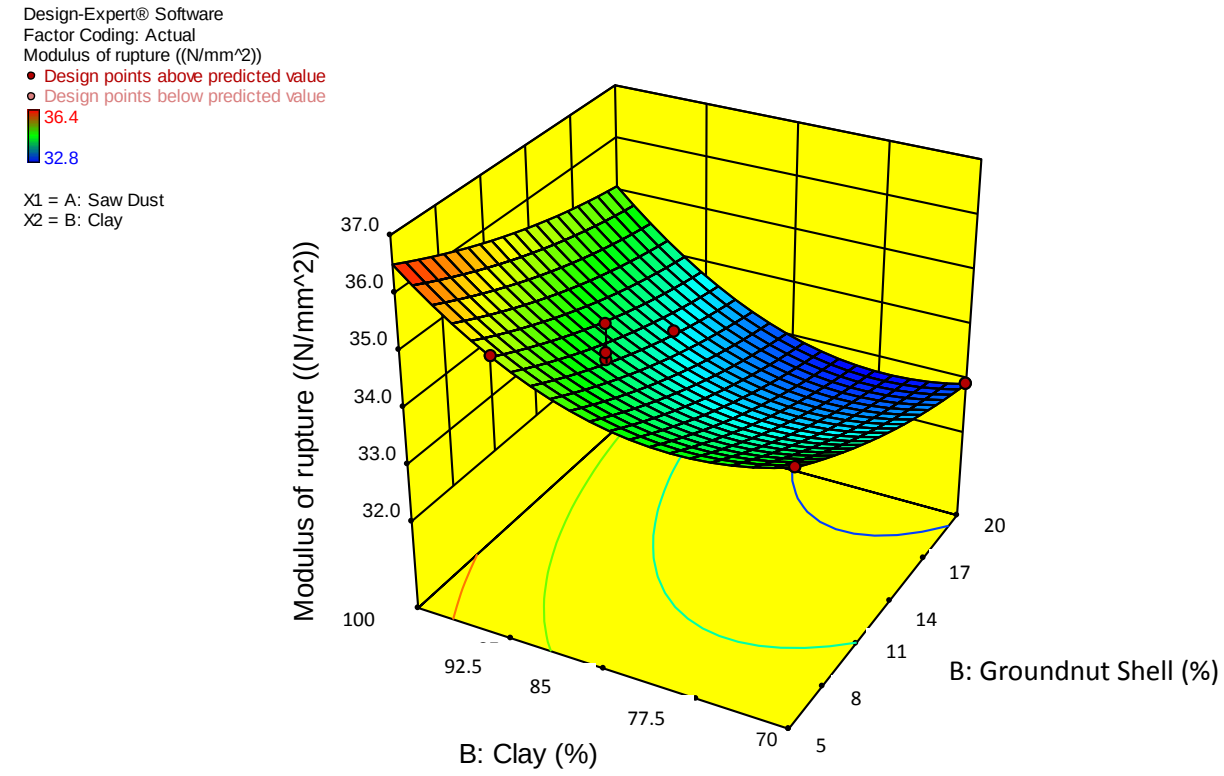

Figure 4.12.15 Three dimension surface plot for the combined effect of the composition of clay and groundnut shell on modulus of rupture

From Figure 4.12.15, it was observed that value of modulus of rupture was a function of both clay and the additive's composition. It was decreasing with decrease in composition of clay (B) and with increase in the composition of groundnut shell (A). Maximum value of modulus of rupture of 36N/mm^2 was obtained between the ranges of 5 -10% composition of groundnut shell value. Between 14 - 15% composition of groundnut shell and its corresponding 86 - 85% of clay, modulus of rupture was seen to decrease to value ranging from 34 –

35N/mm^2.Minimum value of this property of 33N/mm^2 was obtained at 17% composition of clay.

Hence, it was seen that increase in the quantity of additive has adverse effect on the transverse strength. This is due to the fact that increase in the concentration of additive at the expense of the clay led to the deficiency of the main clay content which is supposed to improve the strength. Also migration of gases through the matrix produced due to burning of the additive created highly porous clay structure which affected the mechanical strength.

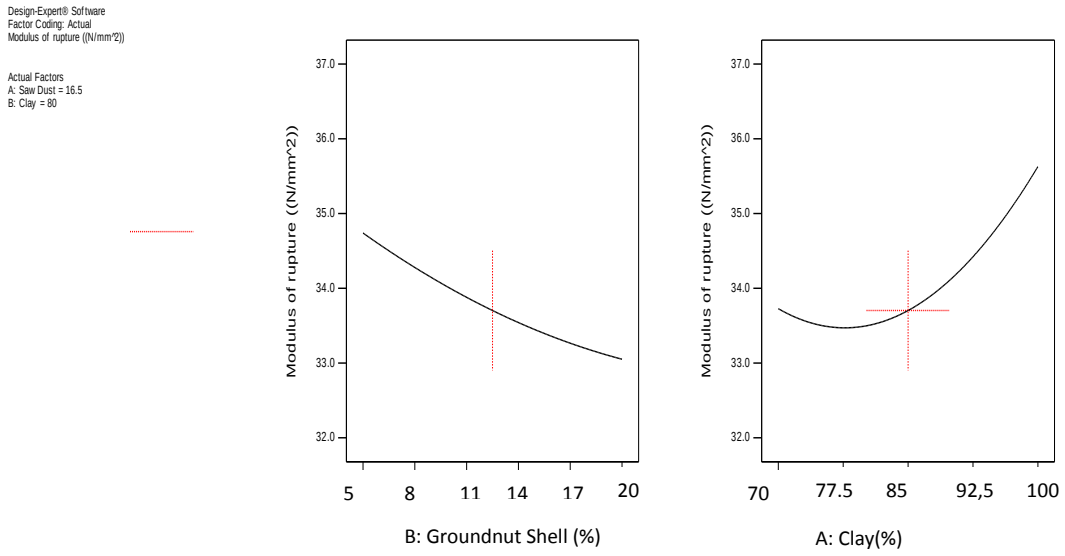

Figure 4.12.16 Single effect plot for the combined effect of the composition of clay and groundnut shell on modulus of rupture

4.13 Results for the Process Optimization

The optimization process was conducted using the design optimization function. By using the numerical optimization technique which is a feature of central composite design in the design expert software, optimum conditions that yielded the best responses was obtained. A validation experiment was then performed using the optimal result of the numerical optimization executed by design expert.

Table 4.13.1 Constraints and the Set Objectives for Sawdust Blended Clay

Name	**Goal**	**Low limit**	**Upper limit**	**Importance**
A:Sawdust	Is in range	5	20	3
B:Clay	Is in range	80	95	3
Linear Shrinkage	minimize	6	7	3
Apparent Porosity	minimize	28	54	3
Bulk Density	minimize	1.7	1.8	3

Modulus of Rupture	maximize	31	32	3

Table 4.13.2 Constraints and the Set Objectives for Rice Husk Blended Clay

Name	**Goal**	**Low limit**	**Upper limit**	**Importance**
A:Rice Husk	Is in range	5	20	3
B:Clay	Is in range	80	95	3
Linear Shrinkage	minimize	5.90783	10.4591	3
Apparent Porosity	minimize	26.3987	52.4966	3
Bulk Density	minimize	1.61069	2.18893	3
Modulus of Rupture	maximize	30.6339	34.08	3

Table 4.13.3 Constraints and the set objectives for Groundnut Shell Blended clay

Name	Goal	Low limit	Upper limit	Importance
A:Groundnut Shell	Is in range	5	20	3
B:Clay	Is in range	80	95	3
Linear Shrinkage	minimize	5.26919	8.70352	3
Apparent Porosity	minimize	20.9341	46.0884	3
Bulk Density	minimize	1.34986	2.03633	3
Modulus of Rupture	maximize	32.776	36.4256	3

Based on these, the software predicted optimum responses for sawdust, rice husk and groundnut shell blends respectively. They are shown in Tables 4.13.4 A, B and C.

Table 4.13.4A .Values of Responses at Optimum Condition for Sawdust Blend

Number	Sawdust	Clay	L/shrinkage	A/porosity	B/density	M/rupture
1	5	95	6.241	33.539	1.933	31.201

Table 4.13.4B. Values of Responses at Optimum Condition for Rice Husk Blend

Number	Rice Husk	Clay	L/shrinkage	A/porosity	B/density	M/rupture
1	5	95	6.12	31.563	2.067	34.024

Table 4.13.4C. Values of Responses at Optimum Condition for Groundnut shell Blend

Number	Groundnut Shell	Clay	L/shrinkage	A/porosity	B/density	M/rupture
1	5	95	5.53	24.869	1.932	36.517

4.13.1 The Prediction of the Optimum Condition for the Response Functions

The model's adequacy for predicting the optimum response function was confirmed by carrying new experiment using the optimum levels as shown in Figure 4.13.5. The result from the Table shows that there is good agreement between the predictive and experimental results at the optimum levels. This gave high validity of the model.

Table 4.13.5 Validation of Optimum Results

	Different Blends of Composite Clay					
Responses	Sawdust blend		Rice husk blend		G/nut Shell blend	
	P	E	P	E	P	E
Linear shrinkage (%)	6.241	7.53	6.12	6.5	5.53	6.52
Apparent porosity (%)	33.539	30.23	31.563	31.58	24.869	21.95
Bulk density g/cm^3	1.933	1.95	2.067	2.26	1.932	2.05
Modulus of rupture N/mm^2	31.201	31.2	34.024	33.2	36.517	39.6

P stands for predictive value while E stands for experimental value.

Table 4.13.5 shows the comparison of the responses for both the experimental and predicted values at the optimum condition. It is seen that the values for each response are very close. This shows that the predicted values are acceptable.

Hence, the model is considered valid and adequate for use in evaluating the effect of the independent variable on the response function.

CHAPTER FIVE

CONCLUSIONS AND RECOMMENDATIONS

5.1 Conclusions.

This research investigation characterized the two clays together with the three agro waste additives and understudied the influence of each, combination of two and three of the additives at different formulations when fired at 1200^0C.

In view of this, it was found that both clays have both low alumina content as well as low alumina – silica ratio required for good refractory material and hence need to be improved. The values of alkali and alkaline earth materials were not more than the required standard. Hence there is no need for leaching and beneficiation of the clay to reduce the quantity further.

Furthermore, the groundnut additive was found to have high alumina content while saw dust and rice husk had good quantity of phosphorus oxide which are responsible for enhancement of refractoriness, strength and other related properties respectively.

The introduction of all the additives increased shrinkage but the presence of aluminum phosphate bond restored the clay's stability with stronger cohesive and binding force which was responsible for enhancement of thermal shock resistance and modulus of rupture of the material. The

increased shrinkage with higher apparent porosity that was associated with increase in additive composition improved insulating property (thermal conductivity). It was generally found that maximum enhancement of the properties by the additives were obtainable with combination of the three additives at 5% and 10% formulation.

Based on these findings, the following conclusions were drawn:

-A combination of agro waste comprising of groundnut shell, saw dust and rice husk can be utilized or exploited as potential raw material additive for production of insulating brick. This is because the major oxides that are responsible for the improvement of the properties are found in these agro waste materials.

-The properties of refractory material are affected by both mineralogical and chemical composition, manufacturing process, composition and constituent of the additive and this is why a non-linear relationship was established between the properties and composition of the additives

-The properties of the refractory materials are interrelated. Enhancement of one has direct consequence on the other.

-Introduction of the agro additives improved thermal shock resistance of the material by increasing pore sizes which impeded the propagation of thermal induced crack.

It is also concluded that combination of response surface methodology and central composite design is a powerful tool in carrying out the optimization of refractory of properties of composite brick.

5.2 Recommendations.

- Agro additives like groundnut shell, rice husk and saw dust should be used to improve refractory properties of clay material considered to be deficient in properties.
- 5 and 10% formulations of such additives should be preferred for high performance and durable refractory products for industrial use.
- The characterized clay materials should be exploited as raw material for refractory production for melting of non ferrous metal.
- Further work should carried out with synthetic and animal wastes and the effect of varied temperature should be investigaged.

5.3 Contributions to Knowledge

- This work has characterized the two clay deposits for the first time. Hence, it has given both the clays and agro waste materials an industrial exposure for exploration.
- The significant discovery has been made on how to select the percentage composition of the additive that yields the best performance needed for a specific application.

- The effect of groundnut shell, saw dust, rice husk and combination of the two and three of the additives on the clays has been established, thereby opening them up for foundry applications as secondary raw material in production of insulating bricks.
- The study has provided an alternative solution to waste management and conversion to useful industrial material.

REFERENCES

SAgbo, A. O., Idenyi, N. E. and Mbah, C. M. (2015). Characterization of Nkalagu Obukpa clay deposits for industrial uses. *International Journal of Multidisciplinary Research and Development*. pp. 689-692.

Ajay, K., Kalyani, M., Davendra and Parkash, O. (2012). Properties and Industrial application of rice husk. *International Journal of Emerging Technology and Advanced Engineering.* pp 86-90.

Aliyu, S., Garba, B., Danshehu, B. G., Argungu, G. M. and Isah, A. D. (2014). The *International Journal of Engineering and Science (IJES)* pp. 62-67.

Altayework Tadessa Belayeh, (2013). Effect of firing temperature on some physical properties of burnt clay brick produced around Addis Ababa. Thesis submitted to the Department of Civil Engineering for MSC in construction Technology and Management. pp. 23 – 23.

Aremu, D. A., Aremu, J. A. and Ibrahim, U. H. (2013), Analysis of Mubi clay deposits as a furnace lining. *International Journal of Science and Technology Resarch*, pp. 182-186.

Banhid, V. and Gomze, L. (2008). Improvement of insulation properties of conventional brick products. Material Science Forum. Pp 1- 6

Brindley, G. W., Bailey, S.W., Johns, W.D., Martin, R.T., and Ross, M (1951). The nomenclature of clay minerals. AM Mineralogist. pp 36, 370-371.

Callister, W. D. (2003). Material science and engineering: An introduction, 6th edition. New York: John Wiley, pp. 384-410, 425-443.

Chen, G., Chen, J., Srinivasakannan, C., Peng, J., (2011). Application of response surface methodology for optimization of the synthesis of synthetic rutile from titania slag. Appl Surf. Sci. 3068-3073.

Chester, J. H. (1973). Refractories, production and properties of iron and steel Institute, London. pp 4-13, 295-315.

Chima, O. M. (2015). Refractoires, fuel and furnace: Term paper submitted to Metallurgical and Material Engineering Department, NAU.

Chung, D. D. L. (2003)Acid aluminum phosphate for the binding and coating of materials. Journal of materials science.. pp 2785-2791.

Danupon, T. (2008). Effects of rice husk ash on characteristics of light weight clay brick. Technology and innovation for sustainable development conference (TISD2008) pp. 35-39.

Decker Jens in Siljan O. S. (2003), Advantages of liquid phosphate bonded refractories. Proceedings of Xth International Conference on Preparation of Ceramic Materials. Herl'any 18-20 June 2013. Intern Symposium 53/03 VDEH.

Demir, I, (2008). Effect of organic residues addition on the technological properties of clay bricks. Waste Mange. Pp 622-627

Edwin, E. M. (2015). Characterization and preparation of lightweight silica based ceramics for building application. PhD thesis submitted to the Department of Engineering Sciences and Mathematics, Division of Material Science. Lulea University of Technology.

Enass Mohy Hadi Al Amer and Mahasin F. Hadi Al – kadhemg (2015). Improving the physical properties of Iraqi Bauxite Refractory Brick. Journal of A – Naharin University. pp. 67 – 73.

Fatai, O. A. and Saliu, O. S. (2012), Production of refractory lining for diesel fried rotary furnace, from locally sourced kaolin and potter's clay. *Journal of Minerals and Material Characterization and Engineering*. pp. 75-79.

Folarami Joshua. (2009), The effect of saw dust additive on the properties of clay. *AUJ.T.*, pp 53-56.

Gilchrist, J. P. (1977). Fule, furnace and refractories. Pergamum Press.

Grimshaw, R.W.4th Edition. The chemistry and physics of clay and Allied Ceramic Materials. (New York, Willey Inter Science, 1971) 16 – 89.

Gutierrez De, R.M. and Delvasto, (1995). Use of Rice Husk in Ceramic Bricks. Ceramurgia. Pp 1-11

Hassan, S.B, (1985), Effects of certain additives on some refractory properties of Kankara clay. B. Eng project, Dept of Material and Metallurgical Engineering, ABU Zaria, Kaduna State. Nigeria.

Hassan, M. A., Yami, A. M., Raji, A. and Ngala, M. J. (2014), Effects of sawdust and rice husk additives on properties of local refractory clay. *The International Journal of Engineering and Science (IJES)*, pp. 40-44.

Hurlbert, C. S. and Klein, C. (1977). Manual of Mineralogy, 19th Edition. New York: John Wiley and Sons, pp. 1, 49.

http://www.ebonyionline.com

Idenyi and Nwajagu (2003). Non-metallic materials technology, Enugu: Olicon Publications, pp. 1-47.

Izwan, J., Syamsuhaili, S. and Ramadhansy, P. J. (2011), Chemical and physical properties of fired-clay brick at different types of rice husk ash. *International Conference of Environment Science and Engineering (IPCBEE)*, pp. 171-174.

John, F. A. and Olayinka, O. A. (2014), The effect of saw dust in the insulating effect of Ikere clay as refractory lining. *AUJ.T*. pp. 143-147.

Lingling, X, Wei, G, Tao, W. and Nanru, Y, (2005). Study on the fired bricks with replacing clay by fly ash in high volume ratio. Construction Buid. Mater. Pp 243 -247.

Manukaji, J. U. (2013)A, The effect of sawdust addition on the insulating characteristics of clays from the Federal Capital Territory of Abuja.

International Journal of Engineering Research and Applications, pp. 006-009.

Manukaji, J. U. (2013)B, The effects of groundnut shell addition on the insulating properties of clay samples from Kogi state Nigeria. *American Journal of Engineering Research (AJER)*, pp. 12-15.

Manukaji, J. U. (2013)C, The insulating effects of rice husk addition on the mechanical properties of clay samples from Kaduna State Nigeria. *IOSR Journal of Engineering (IOSRREN)*, pp. 01-04.

Mariva, A. G. and Fatima, M. M. (2009). Factors affecting the performance of fire clay refractory bricks. Gornictwo.i Geoinzynieria. Rok 33. Zeszyt 4 pp 49-60.

Mark, U. (2007), Investigation of some refractory properties on kaolinite clays from four different locations in Abia state Nigeria. M. Eng. Thesis. Materials and Metallurgical Engineering Dept. FUTO.

McKelvery, V. E. (1986). Mineral Resources definitions, uses, classification and future availability in Bever, M. B. (ed). *Encyclopedia of Materials Science and Engineering*, pp. 3073-3081.

Michele D. and Francesca, M. (2004), Thermal conductivity of clay bricks. *Journal of Materials in Civil Engineering*, pp. 8-14.

Musa, U., Aliyu, M. A., Mohammed, I. A. and Sadiq, M. M. (2012). A comparative study on the refractory properties of selected clays in North Central Nigeria. *Academic Research International*, pp. 393-398.

Naveen, T., Satyendra, S., Parihar, A. S. and Tripathi, D. N. (2013). Measurements and analysis of thermal conductivity of insulating material. *International Journal of Application or Innovation in Engineering and Management (IJAIEM)*, pp. 550-556.

Ndaliman, M. B. (2007). Refractory properties of termite hills under varied proportions of additives.

Nigeria Metallurgical Development Centre, Jos (1999). Research and Development efforts at Nigerian metallurgical development centre, Jos. Toward arresting the declining fortunes of the Nigerian metallurgical industry. *Proceeding of the Nigerian metallurgical society, the 16th Annual Conference*, pp. 8-29.

Nuhu, A.A and Abdullahi, T. A. (2008), Estimation of the effect of kaoline clay addition on the mechanical properties of foundry moulding sand bonded with grade 3 and 4 Nigerian gum Arabic (Acacia species). Middle East journal of science research, pp 126 – 133.

Nnuka, E. E. and Apeh, M. O. (1991), Characterization of Ukpo clay deposit. *Proceedings of the 1991 Annual Conference of the NMS*, pp. 71-76.

Nnuka, E. E. and Okuonye (1991). Industrial potentials of Ukpor clay. *Proceedings of the 1991 Annual Conference of the NMS*, pp. 34 -39.

Nnuka, E. E., Ogo, D. U. I. and Elechukwu, J. (1992). Sustainable refractory sourcing of our industries. *Proceedings Annual conference of NMS*, pp. 18 - 20.

Nnuka, E. E. and Adekwu, J. O. (1997). Refractory characteristics of Kwi clay deposit in Plateau State NSE Technical Transaction.

Nnuka, E. E. and Agbo, U. J. E. (2000). Evaluation of the refractory characteristics of Otukpo clay deposit. NSE technical transaction, pp. 32- 40.

Nnuka, E. E. and Enejor, C. (2001). Characterization of Nahuta clay for industrial and commercial applications. *Nigerian Journal of Engineering Management*, pp. 9 -13.

Obidiegwu, E.O, Esezobor, D.E, Agunsoye, J.O, and Lawal, G.I. (2015), Enhancement of Insulating Refractory Properties of Selected Nigeria Fire Clays Using Coconut Shell. *Journal of Minerals and Materials Characterization and Engineering*, pp. 458-468.

Odo, J. U., Nwoye, C. I., Ameh,. E. M. and Nnachi, P. S. (2013), Production of fireclay insulating bricks from a blend of clays and rice husks. Conference proceeding of the 2013 Nigerian Material Science Society.

Omowumi, O. J. (2001). Characterization of some Nigerian clay as refractory material for furnace lining. Nigerian Journal of Engineering Measurement, pp 1-4.

Opoku, E. V. (2015). Substitution of rice husk ash for quartz in ceramic wall tiles formulation. PhD thesis submitted to the Department of Industrial Design. Ahmadu Bello University Zaria, Nigeria.

Rahman, M.A. (1988). Effect of Rice Husk Ash on the Properties of Bricks made from Fired Lateritic Soil Clay Mix. Material and Structures. Pp 222-227.

Rajput, R. K. (2002). Heat and mass transfer. Second edition. New Delhi: S. Chand and Co. Ltd, pp. 1-21.

Saidsyamsuhach, Izwan J, Jaya R.P (2001). Chemical and physical properties of fire clay bricks at different type of rice husk ash.International conference on environmental science and Engineering, Pp.171-174

Schacht, A. S. (2004). Refractories handbook. New York. Basel. Marcel Dekker, Inc.pp 10-350

Salas de Delvasto, S de Gutierrez R. M. and Lange, D. (2009). Comparison of two processes of treating rice husk ash for use in high performance concrete, cement and concrete composite, pp. 158-160.

Safer Ahmad, Yaseen Igbal and Raz Muhammad (2017). Effects of coal and wheat husk additives on the physical, thermal and mechanical properties of clay brick. Boletin de la Societad Espannola de Ceramica. Pp 131-138

Singer F and Singer S. (1996), Industrial ceramics. Chapman and hell, London PP 1075 1084.

Taran, M and Agbaie, E,(2015). Designing and Optimization of separation process of iron impurities from kaolin by oxalic acid in bench-scale stirred-tank reactor. Appl. Clay Science. 107, 109-116

The engineering toolbox thermal conductivity of some common materials ad gases. *Resource tools and basic information for engineering and design of technical application*.

Velde, B. (1992). Introduction to clay mineral-chemistry, origins, uses and environmental significance. London: Chapman and Hall. pp 1-3, 12, 1-80, 164-178.

WWW.ima-na.org. Industrial Mineral Association-North America (IMA-NA) Washington DC 20036

Yami, M. A. (2007), Characterization of some Nigerian clays as refractory material for furnace lining. *Continental Journal of Engineering Science*, pp. 30-35.

APPENDIX 1. XRF Result for Chemical Composition of Nguzu Clay

Sample results

Sample ident
NGUZU CLAY

Application	<Standardless>
Sequence	1 of 1
Measurement time	18-Dec-2015 09:48:09
Position	4

Compound	Al2O3	SiO2	SO3	K2O	CaO	TiO2	V2O5	Cr2O3	MnO	Fe2O3	CuO	ZnO
Conc	21.8	54.4	2.0	1.77	0.490	1.87	0.10	0.033	0.005	14.62	0.022	0.010
Unit	%	%	%	%	%	%	%	%	%	%	%	%

Compound	Ga2O3	MoO3	Ag2O	Eu2O3	Re2O7	IrO2	Bi2O3
Conc	0.001	0.57	0.845	0.17	0.08	0.12	1
Unit	%	%	%	%	%	%	%

APPENDIX 2. XRF Result for Chemical Composition of Amaiyi Clay

18-Dec-2015 10:14:32 Page

Sample results

Sample ident
AMIYIADDA CLAY

Application	<Standardless>
Sequence	1 of 1
Measurement time	18-Dec-2015 09:53:18
Position	5

Compound	Al2O3	SiO2	SO3	K2O	CaO	TiO2	V2O5	Cr2O3	Fe2O3	CuO	ZnO	Ga2O3
Conc	22.9	48.9	5.15	1.74	2.79	1.63	0.098	0.037	10.51	0.019	0.020	0.018
Unit	%	%	%	%	%	%	%	%	%	%	%	%

Compound	MoO3	Ag2O	Eu2O3	Au	HgO
Conc	3.9	1.98	0.14	0.072	0.12
Unit	%	%	%	%	%

DIRECTOR
DATE 18/12/15
KADUNA

APPENDIX 3. XRF Result for Chemical Composition of Sawdust

18-Dec-2015 10:14:18 Page

Sample results

Sample ident
MALINA SAW DUST

Application	<Standardless>
Sequence	1 of 1
Measurement time	18-Dec-2015 09:32:44
Position	1

Compound	SiO2	P2O5	SO3	K2O	CaO	TiO2	MnO	Fe2O3	CuO	ZnO	Re2O7
Conc	17.2	4.7	3.0	19.2	47.4	1.0	0.65	5.73	0.44	0.2	0.4
Unit	%	%	%	%	%	%	%	%	%	%	%

DIRECTOR
DATE 18/12/15
KADUNA

APPENDIX 4. XRF Result of Chemical Composition of Groundnut Shell

18-Dec-2015 10:14:26 Page

Sample results

Sample ident
GROUNDNUT SHELL

Application	<Standardless>
Sequence	1 of 1
Measurement time	18-Dec-2015 09:42:59
Position	3

Compound	Al2O3	SiO2	P2O5	SO3	K2O	CaO	TiO2	V2O5	MnO	Fe2O3	NiO	CuO
Conc	7.6	16	8.0	5.1	10.6	30.4	1.5	0.0	0.94	13.0	0.2	1.2
Unit	%	%	%	%	%	%	%	%	%	%	%	%

Compound	ZnO	BaO	CeO2	Eu2O3	Yb2O3
Conc	0.3	1.5	0.6	2.2	0.9
Unit	%	%	%	%	%

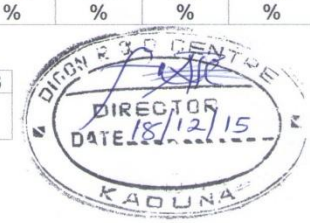

APPENDIX 5. XRF Result for Chemical Composition of Rice Husk

18-Dec-2015 10:14:20 Page

Sample results

Sample ident
RICE HUSK

Application	<Standardless>
Sequence	1 of 1
Measurement time	18-Dec-2015 09:37:48
Position	2

Compound	SiO2	P2O5	SO3	K2O	CaO	TiO2	V2O5	MnO	Fe2O3	NiO	CuO	ZnO
Conc	60.8	21.3	2.76	7.77	3.07	0.35	0.00	0.771	2.41	0.024	0.059	0.24
Unit	%	%	%	%	%	%	%	%	%	%	%	%

Compound	BaO	Eu2O3	Re2O7
Conc	0.13	0.09	0.19
Unit	%	%	%

DIRECTOR
DATE 18/12/15
KADUNA

APPENDIX 6. X-ray Diffraction Pattern for Gmalina Sawdust

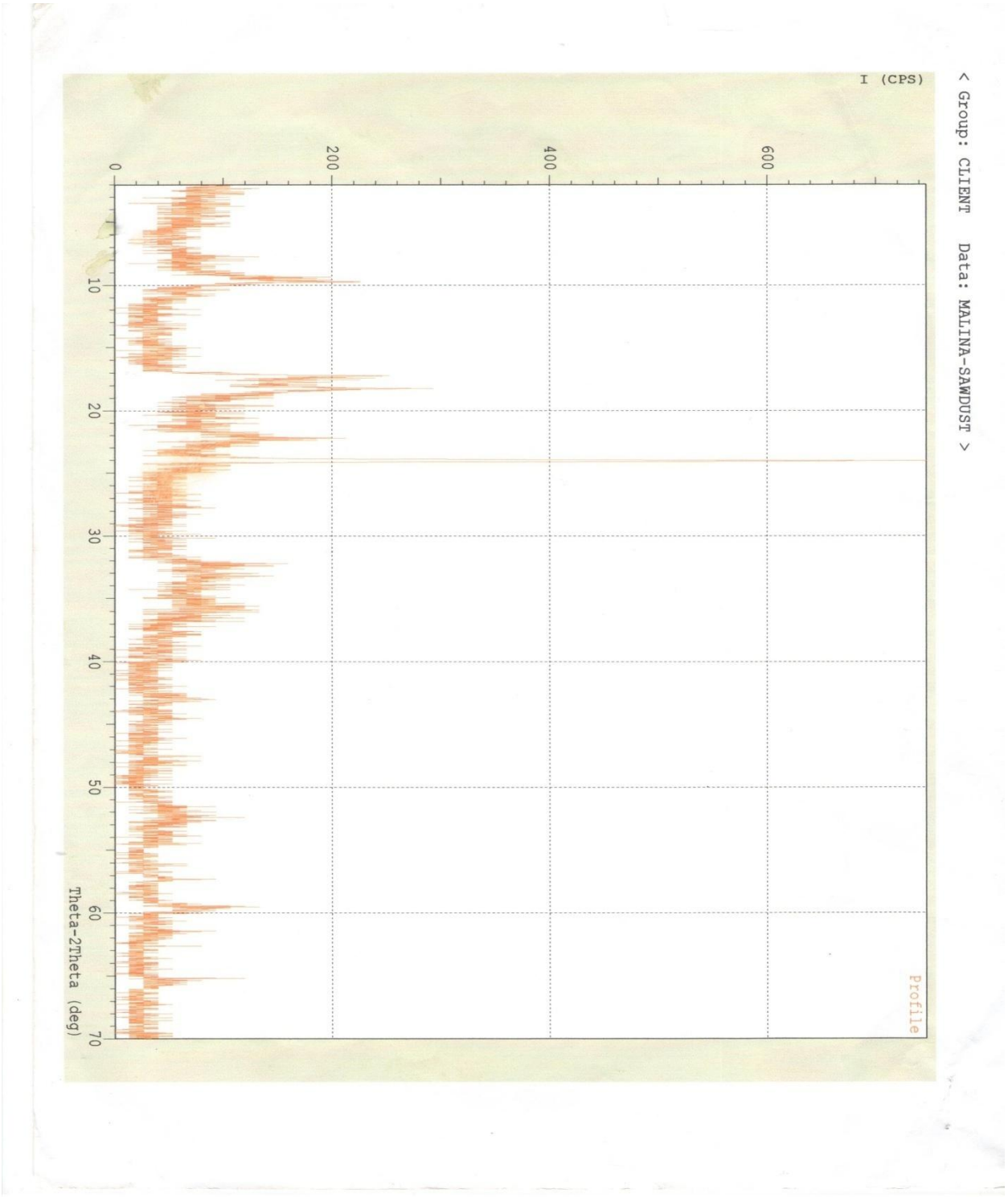

APPENDIX 7. XRD Result for Mineralogical Composition for Gmalina Sawdust

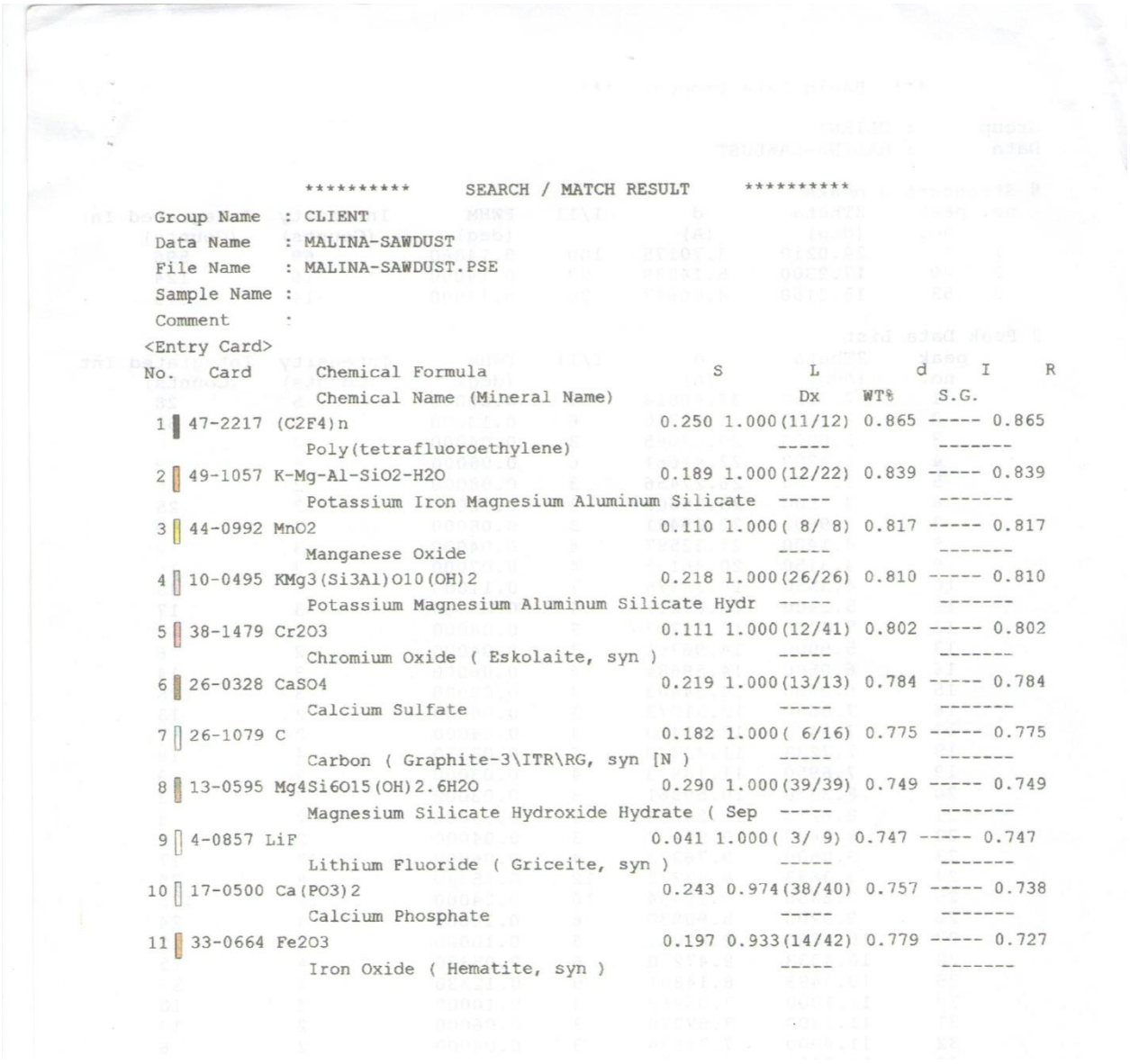

********** SEARCH / MATCH RESULT **********

Group Name : CLIENT
Data Name : MALINA-SAWDUST
File Name : MALINA-SAWDUST.PSE
Sample Name :
Comment :

<Entry Card>

No.	Card	Chemical Formula / Chemical Name (Mineral Name)	S	L	Dx	d	WT%	I	S.G.	R
1	47-2217	(C2F4)n	0.250	1.000	(11/12)	0.865	-----		0.865	
		Poly(tetrafluoroethylene)			-----		-------			
2	49-1057	K-Mg-Al-SiO2-H2O	0.189	1.000	(12/22)	0.839	-----		0.839	
		Potassium Iron Magnesium Aluminum Silicate			-----		-------			
3	44-0992	MnO2	0.110	1.000	(8/ 8)	0.817	-----		0.817	
		Manganese Oxide			-----		-------			
4	10-0495	KMg3(Si3Al)O10(OH)2	0.218	1.000	(26/26)	0.810	-----		0.810	
		Potassium Magnesium Aluminum Silicate Hydr			-----		-------			
5	38-1479	Cr2O3	0.111	1.000	(12/41)	0.802	-----		0.802	
		Chromium Oxide (Eskolaite, syn)			-----		-------			
6	26-0328	CaSO4	0.219	1.000	(13/13)	0.784	-----		0.784	
		Calcium Sulfate			-----		-------			
7	26-1079	C	0.182	1.000	(6/16)	0.775	-----		0.775	
		Carbon (Graphite-3\ITR\RG, syn [N)			-----		-------			
8	13-0595	Mg4Si6O15(OH)2.6H2O	0.290	1.000	(39/39)	0.749	-----		0.749	
		Magnesium Silicate Hydroxide Hydrate (Sep			-----		-------			
9	4-0857	LiF	0.041	1.000	(3/ 9)	0.747	-----		0.747	
		Lithium Fluoride (Griceite, syn)			-----		-------			
10	17-0500	Ca(PO3)2	0.243	0.974	(38/40)	0.757	-----		0.738	
		Calcium Phosphate			-----		-------			
11	33-0664	Fe2O3	0.197	0.933	(14/42)	0.779	-----		0.727	
		Iron Oxide (Hematite, syn)			-----		-------			

APPENDIX 8. XRD Experimental Parameters for Gmalina Sawdust

*** Basic Data Process ***

Group : CLIENT
Data : MALINA-SAWDUST

Strongest 3 peaks

no.	peak no.	2Theta (deg)	d (A)	I/I1	FWHM (deg)	Intensity (Counts)	Integrated Int (Counts)
1	73	24.0210	3.70175	100	0.14860	69	596
2	49	17.2300	5.14239	23	0.14000	16	124
3	53	18.2150	4.86647	20	0.17000	14	119

Peak Data List

peak no.	2Theta (deg)	d (A)	I/I1	FWHM (deg)	Intensity (Counts)	Integrated Int (Counts)
1	2.3250	37.96814	7	0.09000	5	28
2	2.7650	31.92710	6	0.13000	4	38
3	3.0000	29.42665	3	0.04000	2	8
4	3.2200	27.41661	6	0.08000	4	19
5	3.3600	26.27456	3	0.08000	2	15
6	3.7800	23.35606	3	0.12000	2	25
7	3.9600	22.29481	3	0.08000	2	9
8	4.1400	21.32587	4	0.04000	3	10
9	4.3150	20.46135	4	0.07000	3	16
10	4.5550	19.38378	7	0.11000	5	40
11	5.2900	16.69211	4	0.06000	3	17
12	5.4200	16.29203	3	0.08000	2	13
13	5.9000	14.96761	3	0.04000	2	6
14	6.0500	14.59684	4	0.06000	3	14
15	6.2000	14.24403	4	0.08000	3	28
16	7.0600	12.51073	3	0.08000	2	13
17	7.3400	12.03410	3	0.04000	2	7
18	7.7233	11.43769	6	0.03330	4	19
19	7.8950	11.18933	4	0.03000	3	9
20	8.3350	10.59961	3	0.03000	2	3
21	8.6250	10.24386	3	0.03000	2	8
22	8.8600	9.97267	3	0.04000	2	6
23	9.0500	9.76372	4	0.06000	3	17
24	9.3633	9.43772	12	0.15330	8	75
25	9.6850	9.12494	16	0.24000	11	130
26	9.9200	8.90930	6	0.12000	4	24
27	10.0200	8.82061	3	0.10000	2	12
28	10.4333	8.47210	6	0.05330	4	25
29	10.8483	8.14891	9	0.12330	6	59
30	11.1000	7.96469	3	0.10000	2	10
31	11.2300	7.87278	3	0.06000	2	10
32	11.4000	7.75576	3	0.04000	2	6
33	11.7250	7.54150	3	0.05000	2	5
34	11.8933	7.43516	4	0.02670	3	8
35	12.3633	7.15354	4	0.04670	3	13
36	12.7000	6.96463	3	0.08000	2	10
37	12.9100	6.85181	3	0.14000	2	15
38	13.1400	6.73239	3	0.04000	2	6
39	13.4600	6.57304	7	0.06000	5	32
40	13.7600	6.43040	6	0.08000	4	45
41	14.3400	6.17160	3	0.04000	2	6
42	15.0650	5.87618	4	0.05000	3	12
43	15.2600	5.80153	3	0.10000	2	18
44	15.8550	5.58512	3	0.03000	2	3
45	16.3650	5.41220	4	0.03000	3	10
46	16.5200	5.36177	3	0.04000	2	6
47	16.7000	5.30438	3	0.04000	2	5
48	16.9683	5.22111	4	0.03670	3	8
49	17.2300	5.14239	23	0.14000	16	124
50	17.3800	5.09834	16	0.14000	11	91

APPENDIX 9. X-ray Diffraction Pattern for Rice Husk

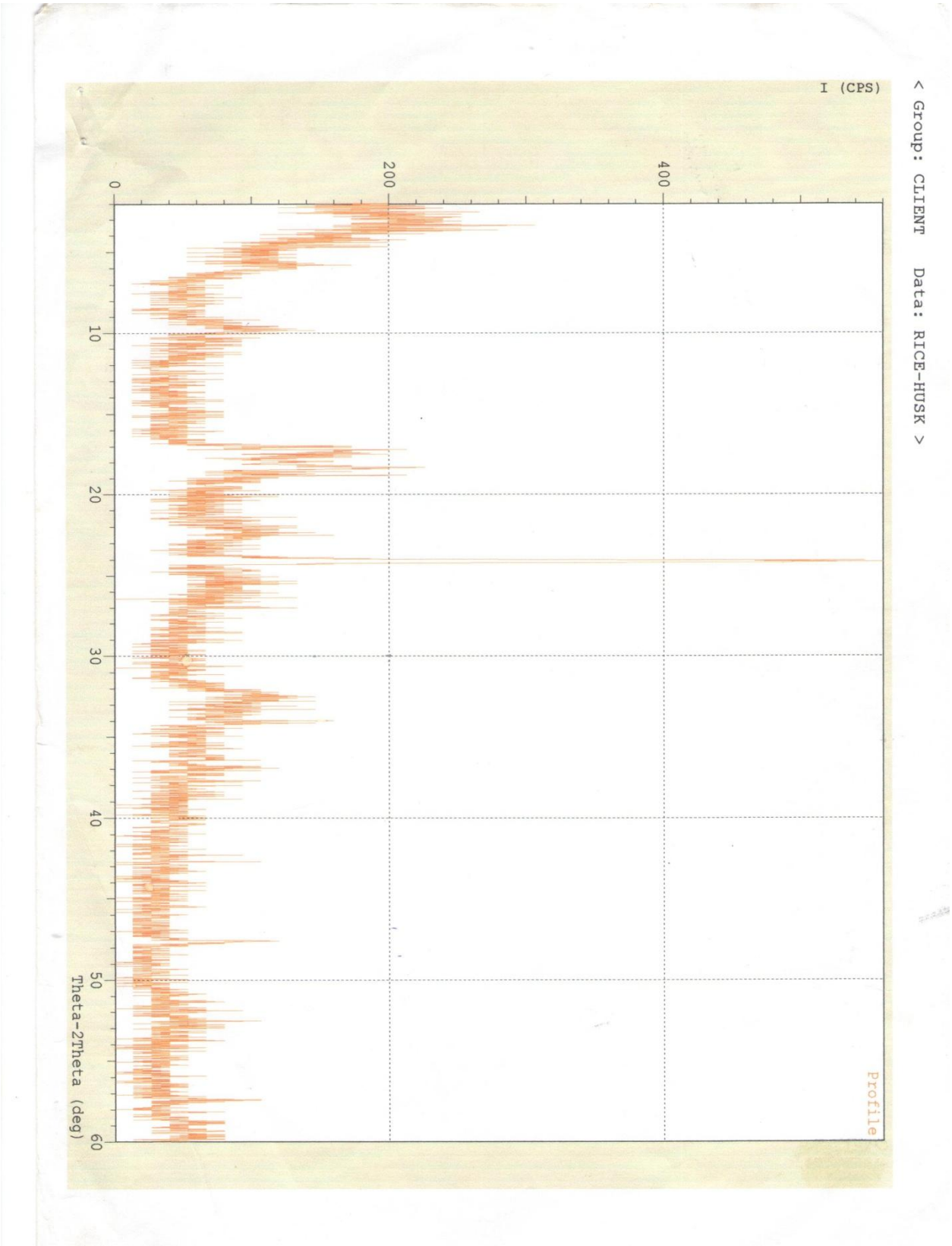

APPENDIX 1O. XRD Result for Mineralogical Composition of Rice Husk

********** SEARCH / MATCH RESULT **********

Group Name : CLIENT
Data Name : RICE-HUSK
File Name : RICE-HUSK.PSE
Sample Name :
Comment :

<Entry Card>

No.	Card	Chemical Formula / Chemical Name (Mineral Name)	S	L	d	I	R
				Dx	WT%	S.G.	
1	37-0031	ZrO2	0.053	1.000(4/ 7)	0.914	0.818	0.748
		Zirconium Oxide		-----		-------	
2	30-0279	CaSO4	0.104	0.900(9/10)	0.720	0.588	0.381
		Calcium Sulfate		-----		-------	
3	21-0963	Mg3Si2O5(OH)4	0.175	0.875(21/27)	0.755	0.550	0.363
		Magnesium Silicate Hydroxide (Antigorite-		-----		-------	
4	39-1352	Zn3(PO4)2.4H2O	0.224	0.810(34/42)	0.777	0.488	0.307
		Zinc Phosphate Hydrate (Parahopeite)		-----		-------	
5	10-0357	(Na,K)(Si3Al)O8	0.269	0.882(15/17)	0.747	0.446	0.294
		Potassium Sodium Aluminum Silicate (Sanid		-----		-------	
6	21-1276	TiO2	0.108	0.714(5/38)	0.813	0.496	0.288
		Titanium Oxide (Rutile, syn)		-----		-------	
7	23-0125	Ca6Si6O17(OH)2	0.260	0.893(25/39)	0.780	0.411	0.286
		Calcium Silicate Hydrate (Xonotlite, syn		-----		-------	
8	26-0911	(K,H3O)Al2Si3AlO10(OH)2	0.214	0.941(16/18)	0.693	0.417	0.272
		Potassium Aluminum Silicate Hydroxide (Il		-----		-------	
9	27-1402	Si	0.151	1.000(3/11)	0.606	0.431	0.261
		Silicon (Silicon, syn)		-----		-------	
10	21-1272	TiO2	0.174	0.857(6/39)	0.794	0.373	0.254
		Titanium Oxide (Anatase, syn)		-----		-------	
11	44-0142	MnO2	0.185	0.950(19/42)	0.775	0.334	0.246
		Manganese Oxide (Ramsdellite, syn)		-----		-------	
12	38-1479	Cr2O3	0.104	0.900(9/41)	0.788	0.343	0.243
		Chromium Oxide (Eskolaite, syn)		-----		-------	
13	44-0517	CaSO3	0.275	0.868(33/42)	0.732	0.354	0.225
		Calcium Sulfite		-----		-------	
14	26-1079	C	0.165	0.800(4/16)	0.647	0.402	0.208
		Carbon (Graphite-3\ITR\RG, syn [N)		-----		-------	

APPENDIX 11. XRD Experimental Parameter for Rice Husk

*** Basic Data Process ***

Group : CLIENT
Data : RICE-HUSK

Strongest 3 peaks

no.	peak no.	2Theta (deg)	d (A)	I/I1	FWHM (deg)	Intensity (Counts)	Integrated Int (Counts)
1	45	24.0802	3.69278	100	0.19460	50	522
2	33	18.3133	4.84057	20	0.18670	10	70
3	29	17.2400	5.13943	20	0.12000	10	132

Peak Data List

peak no.	2Theta (deg)	d (A)	I/I1	FWHM (deg)	Intensity (Counts)	Integrated Int (Counts)
1	2.7150	32.51497	8	0.09000	4	21
2	2.8800	30.65249	8	0.20000	4	40
3	3.1150	28.34053	10	0.15000	5	40
4	3.3833	26.09367	14	0.11330	7	63
5	3.7400	23.60576	10	0.04000	5	19
6	4.6450	19.00841	4	0.03000	2	3
7	5.4350	16.24710	4	0.03000	2	3
8	5.8000	15.22544	6	0.04000	3	19
9	6.0000	14.71837	6	0.10000	3	37
10	7.2100	12.25078	4	0.30000	2	42
11	7.7300	11.42780	4	0.10000	2	20
12	8.3000	10.64423	6	0.04000	3	13
13	8.5800	10.29748	6	0.04000	3	16
14	8.8600	9.97267	4	0.08000	2	25
15	9.1700	9.63622	6	0.06000	3	15
16	9.3400	9.46121	4	0.08000	2	12
17	9.6200	9.18645	12	0.12000	6	36
18	9.8000	9.01812	10	0.24000	5	71
19	10.4800	8.43445	6	0.04000	3	15
20	10.8800	8.12524	4	0.04000	2	10
21	11.1800	7.90788	6	0.04000	3	15
22	11.3600	7.78298	6	0.04000	3	17
23	12.0450	7.34185	4	0.13000	2	17
24	12.3600	7.15544	4	0.08000	2	17
25	13.2100	6.69687	4	0.10000	2	12
26	14.5900	6.06640	4	0.06000	2	12
27	14.8300	5.96876	6	0.06000	3	12
28	17.0050	5.20992	14	0.09000	7	45
29	17.2400	5.13943	20	0.12000	10	132
30	17.6200	5.02944	10	0.04000	5	37
31	17.9350	4.94181	8	0.09000	4	23
32	18.2000	4.87044	10	0.12000	5	32
33	18.3133	4.84057	20	0.18670	10	70
34	18.7700	4.72381	10	0.08000	5	36
35	19.5000	4.54858	4	0.12000	2	17
36	21.0200	4.22297	4	0.04000	2	8
37	21.3800	4.15267	4	0.04000	2	5
38	21.5850	4.11369	6	0.07000	3	16
39	21.7950	4.07453	4	0.03000	2	3
40	21.9950	4.03793	6	0.07000	3	13
41	22.1250	4.01450	6	0.05000	3	9
42	22.3250	3.97898	8	0.13000	4	30
43	22.5700	3.93634	4	0.14000	2	25
44	23.8000	3.73562	10	0.08000	5	35
45	24.0802	3.69278	100	0.19460	50	522
46	24.6400	3.61014	10	0.08000	5	29
47	24.9850	3.56106	4	0.07000	2	8
48	25.1500	3.53807	4	0.22000	2	40
49	25.4800	3.49299	6	0.04000	3	11
50	25.7500	3.45698	4	0.10000	2	19

APPENDIX 12. X-ray Diffraction Pattern for Nguzu Clay

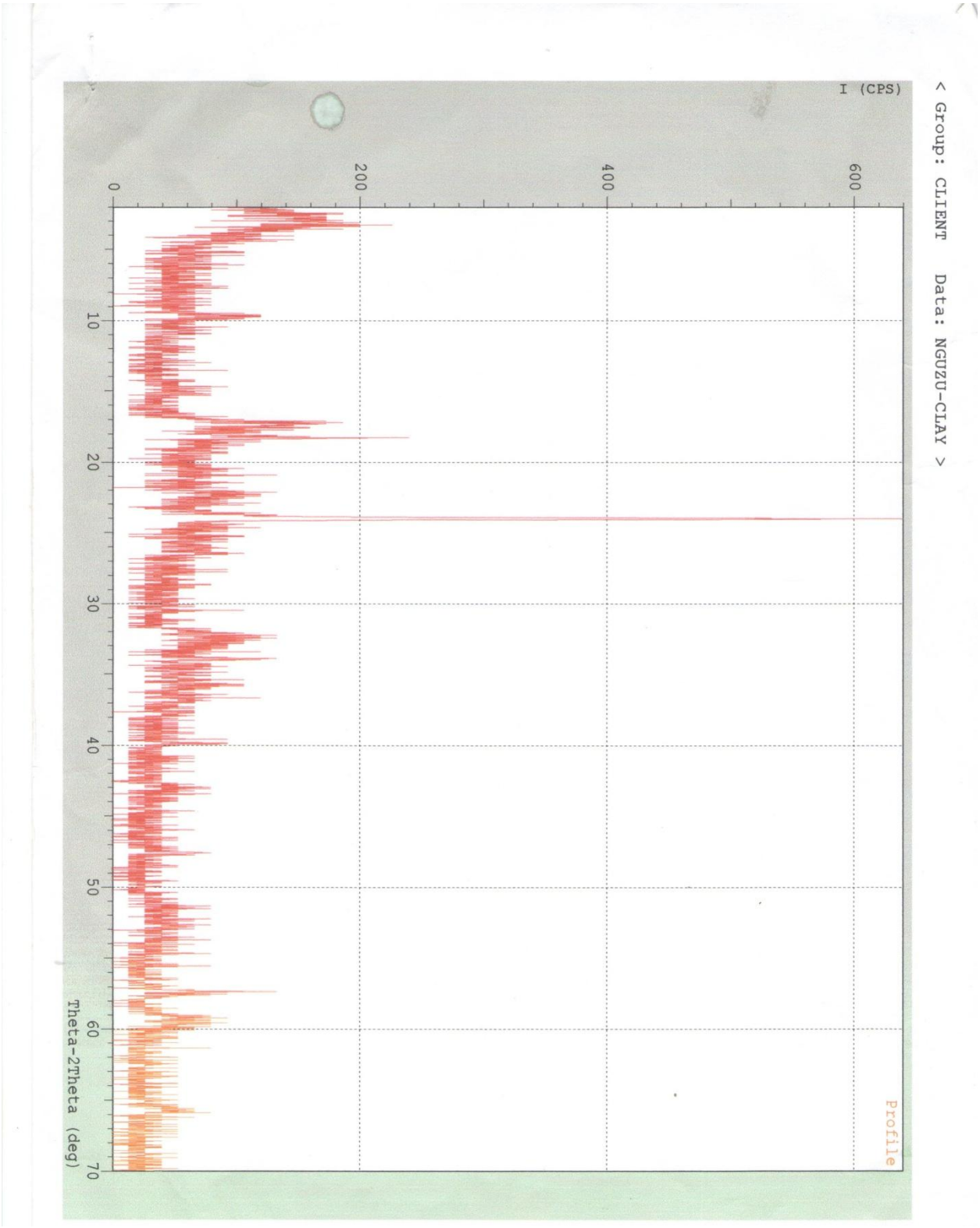

APPENDIX 13. XRD Result for Mineralogical Composton of Nguzu Clay

********** SEARCH / MATCH RESULT **********

Group Name : CLIENT
Data Name : NGUZU-CLAY
File Name : NGUZU-CLAY.PSE
Sample Name :
Comment :

<Entry Card>

No.	Card	Chemical Formula / Chemical Name (Mineral Name)	S	L	d	I	R
				Dx	WT%	S.G.	
1	45-0946	MgO	0.098	1.000	(3/10)	0.784	0.558 0.438
		Magnesium Oxide (Periclase, syn)	-----			-------	
2	13-0135	Ca0.2(Al,Mg)2Si4O10(OH)2.4H2O	0.150	1.000	(15/17)	0.738	0.575 0.424
		Calcium Magnesium Aluminum Silicate Hydrox	-----			-------	
3	31-0794	(Mg,Al)9(Si,Al)8O20(OH)10.4H2O	0.200	1.000	(17/17)	0.786	0.496 0.390
		Magnesium Aluminum Silicate Hydroxide Hydr	-----			-------	
4	16-0613	Mgx(Mg,Fe)3(Si,Al)4O10(OH)2.4H2O	0.234	0.938	(30/32)	0.768	0.488 0.351
		Magnesium Iron Aluminum Silicate Hydroxide	-----			-------	
5	13-0595	Mg4Si6O15(OH)2.6H2O	0.317	0.974	(38/39)	0.753	0.466 0.342
		Magnesium Silicate Hydroxide Hydrate (Sep	-----			-------	
6	21-0963	Mg3Si2O5(OH)4	0.150	0.917	(22/27)	0.813	0.446 0.333
		Magnesium Silicate Hydroxide (Antigorite-	-----			-------	
7	10-0357	(Na,K)(Si3Al)O8	0.262	1.000	(17/17)	0.746	0.393 0.293
		Potassium Sodium Aluminum Silicate (Sanid	-----			-------	
8	29-1016	KMg2Al3(Si10Al2)O30	0.222	0.879	(29/33)	0.772	0.431 0.293
		Potassium Magnesium Aluminum Silicate (Os	-----			-------	
9	49-1057	K-Mg-Al-SiO2-H2O	0.213	1.000	(12/22)	0.708	0.408 0.289
		Potassium Iron Magnesium Aluminum Silicate	-----			-------	
10	6-0263	KAl2(Si3Al)O10(OH,F)2	0.273	0.881	(37/42)	0.792	0.409 0.286
		Potassium Aluminum Silicate Hydroxide (Mu	-----			-------	
11	19-1061	(Na,Ca)2(Fe,Mn)3Fe2(Si,Al)8O22(OH,F	0.371	0.833	(30/38)	0.675	0.485 0.272
		Sodium Iron Silicate Hydroxide (Riebeckit	-----			-------	
12	25-0645	Mg3[Si2-xO5](OH)4-4x	0.252	1.000	(16/18)	0.776	0.344 0.267
		Magnesium Silicate Hydroxide (Chrysotile	-----			-------	
13	26-0911	(K,H3O)Al2Si3AlO10(OH)2	0.245	0.889	(16/18)	0.733	0.385 0.251
		Potassium Aluminum Silicate Hydroxide (Il	-----			-------	

APPENDIX 14. XRD Experimental Parameters for Nguzu Clay

*** Basic Data Process ***

Group : CLIENT
Data : NGUZU-CLAY

Strongest 3 peaks

no.	peak no.	2Theta (deg)	d (A)	I/I1	FWHM (deg)	Intensity (Counts)	Integrated Int (Counts)
1	58	24.0291	3.70052	100	0.13110	59	431
2	40	18.2820	4.84878	27	0.08400	16	69
3	85	33.9200	2.64069	19	0.07200	11	55

Peak Data List

peak no.	2Theta (deg)	d (A)	I/I1	FWHM (deg)	Intensity (Counts)	Integrated Int (Counts)
1	2.4200	36.47787	8	0.04000	5	22
2	2.5400	34.75477	10	0.04000	6	25
3	2.7600	31.98493	8	0.04000	5	18
4	2.9383	30.04443	8	0.05670	5	20
5	3.1466	28.05599	14	0.09330	8	74
6	3.7550	23.51150	5	0.03000	3	7
7	3.9933	22.10897	5	0.02670	3	5
8	4.3300	20.39051	8	0.14000	5	55
9	4.4600	19.79645	5	0.00000	3	0
10	5.2200	16.91579	5	0.08000	3	14
11	5.4800	16.11378	5	0.02000	3	5
12	5.6200	15.71268	3	0.04000	2	4
13	5.7600	15.33109	5	0.02000	3	4
14	5.8800	15.01847	5	0.02000	3	6
15	6.0766	14.53301	8	0.03330	5	14
16	6.3466	13.91533	7	0.06670	4	24
17	6.5750	13.43245	5	0.03000	3	10
18	7.1166	12.41135	7	0.03330	4	13
19	7.7050	11.46482	3	0.03000	2	6
20	8.1866	10.79142	5	0.02670	3	6
21	8.4400	10.46798	3	0.04000	2	7
22	8.8950	9.93351	3	0.03000	2	3
23	10.7000	8.26152	7	0.08000	4	22
24	10.8800	8.12524	7	0.02660	4	6
25	11.8000	7.49373	5	0.04000	3	16
26	12.0400	7.34489	3	0.02000	2	4
27	12.2800	7.20188	5	0.04000	3	11
28	12.7350	6.94557	3	0.05000	2	20
29	13.3700	6.61709	3	0.06000	2	21
30	13.8700	6.37965	3	0.06000	2	13
31	14.1400	6.25844	3	0.04000	2	9
32	14.3600	6.16305	3	0.04000	2	7
33	14.8625	5.95578	8	0.04500	5	16
34	14.9900	5.90541	5	0.06000	3	21
35	15.3300	5.77519	3	0.08000	2	22
36	15.7200	5.63278	3	0.04000	2	5
37	15.8400	5.59038	3	0.04000	2	9
38	16.4100	5.39746	5	0.06000	3	25
39	18.1400	4.88642	10	0.10660	6	47
40	18.2820	4.84878	27	0.08400	16	69
41	18.4600	4.80243	3	0.02000	2	3
42	18.6150	4.76279	5	0.03000	3	6
43	18.7200	4.73631	3	0.04000	2	6
44	18.9800	4.67201	3	0.02000	2	2
45	19.2866	4.59843	10	0.05330	6	27
46	20.2500	4.38178	3	0.06000	2	7
47	20.4700	4.33518	3	0.10000	2	17
48	20.8833	4.25030	7	0.03330	4	14
49	21.1500	4.19731	3	0.10000	2	14
50	21.4550	4.13832	7	0.07000	4	27

APPENDIX 15. X-Ray Diffraction Pattern for Amaiyi Edda Clay

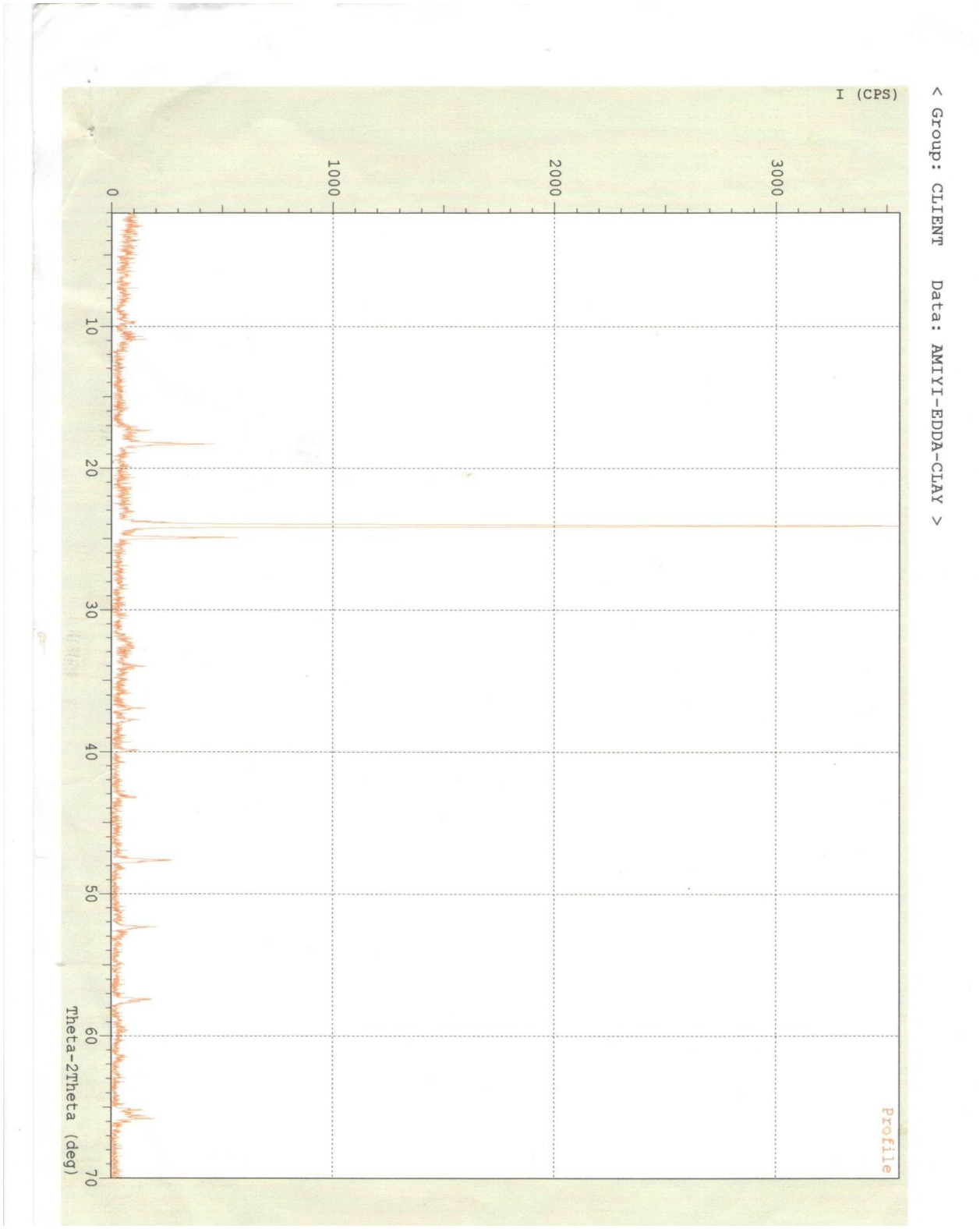

APPENDIX 16. XRD Result for the Mineralogical Composition of Amaiyi Clay

********** SEARCH / MATCH RESULT **********

Group Name : CLIENT
Data Name : AMIYI-EDDA-CLAY
File Name : AMIYI-EDDA-CLAY.PSE
Sample Name :
Comment :

<Entry Card>

No.	Card	Chemical Formula / Chemical Name (Mineral Name)	S	L / Dx	d / WT%	I / S.G.	R
1	10-0492	KMg3(Si3Al)O10(OH)2	0.600	0.192(5/26)	0.852	-----	0.164
		Potassium Magnesium Aluminum Silicate Hydr	-----	-----		-------	
2	49-1057	K-Mg-Al-SiO2-H2O	0.216	0.250(3/22)	0.575	-----	0.144
		Potassium Iron Magnesium Aluminum Silicate	-----	-----		-------	
3	29-1488	Al2Si2O5(OH)4	0.167	0.158(3/21)	0.882	-----	0.139
		Aluminum Silicate Hydroxide (Kaolinite-1\	-----	-----		-------	
4	23-0125	Ca6Si6O17(OH)2	0.467	0.219(7/39)	0.589	-----	0.129
		Calcium Silicate Hydrate (Xonotlite, syn	-----	-----		-------	
5	25-0645	Mg3[Si2-xO5](OH)4-4x	0.652	0.250(4/18)	0.501	-----	0.125
		Magnesium Silicate Hydroxide (Chrysotile	-----	-----		-------	
6	46-1045	SiO2	0.533	0.222(4/42)	0.536	-----	0.119
		Silicon Oxide (Quartz, syn)		-----		-------	
7	37-1496	CaSO4	0.688	0.172(5/42)	0.672	-----	0.116
		Calcium Sulfate (Anhydrite, syn)		-----		-------	
8	29-1016	KMg2Al3(Si10Al2)O30	0.588	0.152(5/33)	0.740	-----	0.112
		Potassium Magnesium Aluminum Silicate (Os	-----	-----		-------	
9	43-0662	Mg3Si2O5(OH)4	0.506	0.250(3/13)	0.407	-----	0.102
		Magnesium Silicate Hydroxide (Clinochryso	-----	-----		-------	

APPENDIX 17. XRD Experimental Parameters for Amaiyi Clay

*** Basic Data Process ***

Group : CLIENT
Data : AMIYI-EDDA-CLAY

Strongest 3 peaks

no.	peak no.	2Theta (deg)	d (A)	I/I1	FWHM (deg)	Intensity (Counts)	Integrated Int (Counts)
1	2	24.1320	3.68497	100	0.13040	387	2850
2	3	24.9594	3.56466	12	0.12520	46	303
3	1	18.3338	4.83520	9	0.13250	33	296

Peak Data List

peak no.	2Theta (deg)	d (A)	I/I1	FWHM (deg)	Intensity (Counts)	Integrated Int (Counts)
1	18.3338	4.83520	9	0.13250	33	296
2	24.1320	3.68497	100	0.13040	387	2850
3	24.9594	3.56466	12	0.12520	46	303
4	36.9512	2.43073	3	0.09000	12	73
5	39.9172	2.25669	3	0.11330	12	80
6	47.6139	1.90831	8	0.13900	30	266
7	52.3702	1.74563	5	0.13400	19	142
8	57.3952	1.60417	5	0.13200	21	171
9	65.1647	1.43043	3	0.16400	12	105
10	65.5983	1.42202	3	0.13830	12	107
11	65.8025	1.41810	3	0.12000	12	72

APPENDIX 18. X-ray Pattern for Ground nut Shell

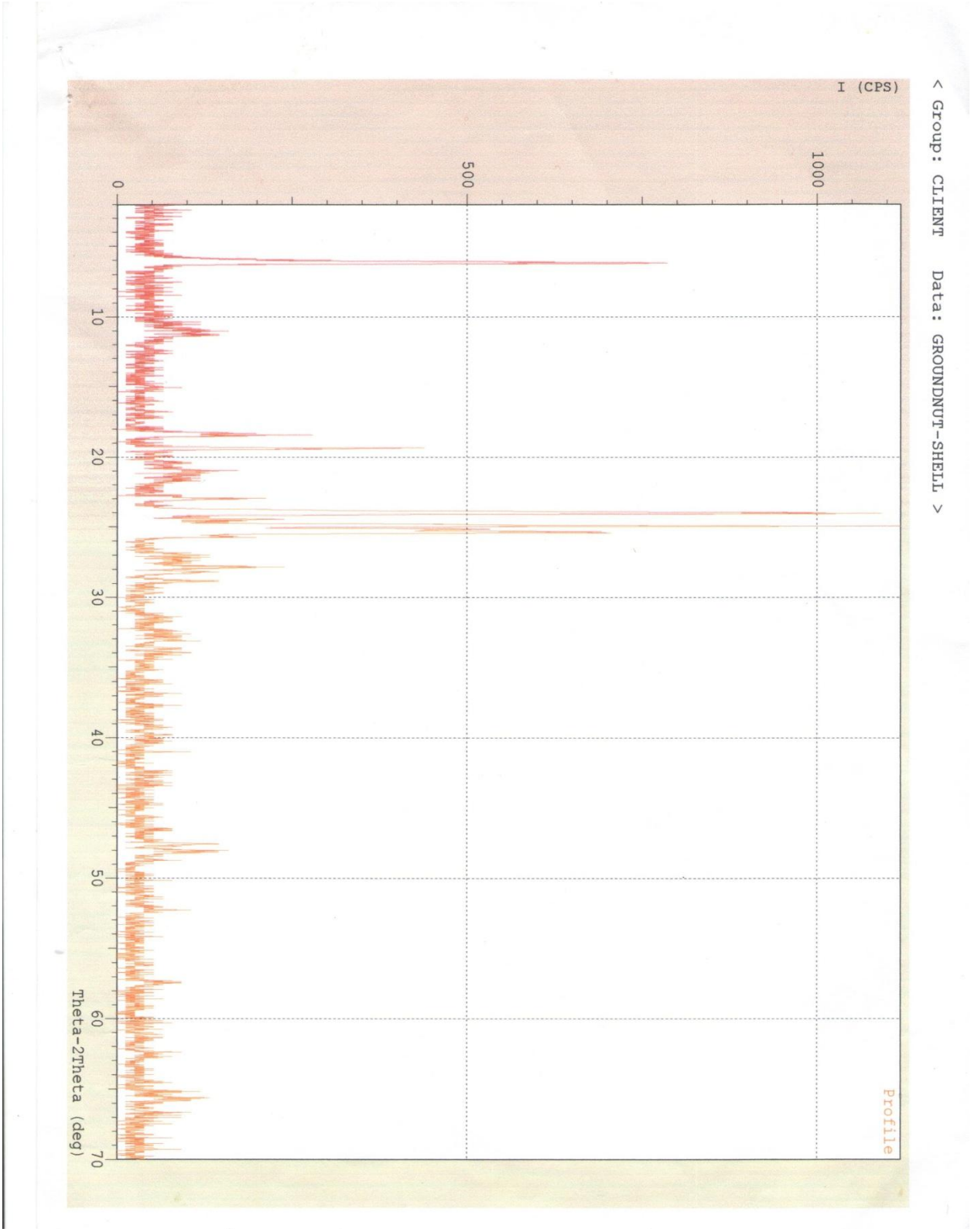

APPENDIX 19. XRD Results for Mineralogical Composition of Groundnut Shell

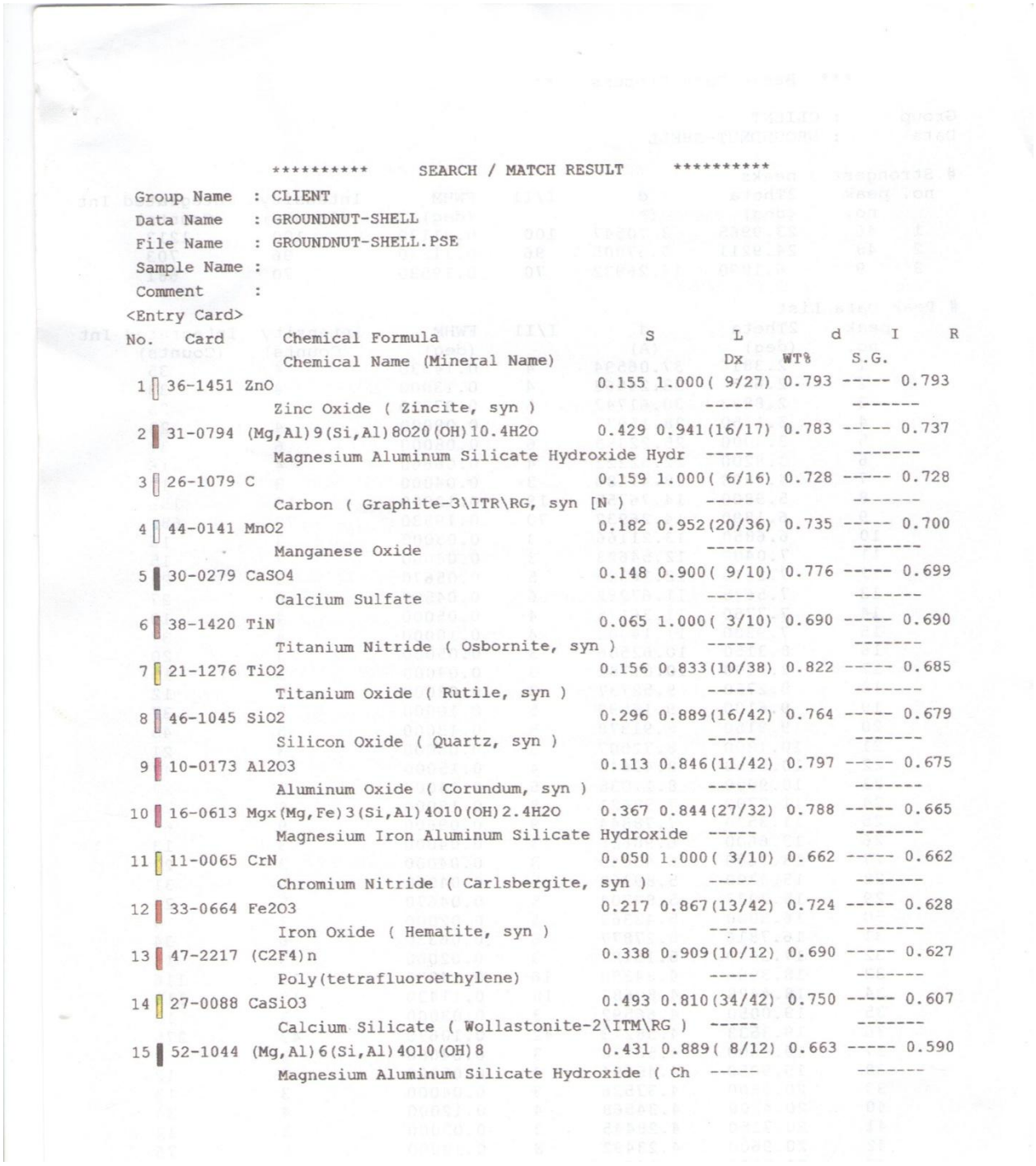

********** SEARCH / MATCH RESULT **********

Group Name : CLIENT
Data Name : GROUNDNUT-SHELL
File Name : GROUNDNUT-SHELL.PSE
Sample Name :
Comment :

<Entry Card>

No.	Card	Chemical Formula / Chemical Name (Mineral Name)	S	L	d	I	R
				Dx	WT%	S.G.	
1	36-1451	ZnO	0.155	1.000 (9/27)	0.793	-----	0.793
		Zinc Oxide (Zincite, syn)		-----		-------	
2	31-0794	(Mg,Al)9(Si,Al)8O20(OH)10.4H2O	0.429	0.941 (16/17)	0.783	-----	0.737
		Magnesium Aluminum Silicate Hydroxide Hydr		-----		-------	
3	26-1079	C	0.159	1.000 (6/16)	0.728	-----	0.728
		Carbon (Graphite-3\ITR\RG, syn [N)		-----		-------	
4	44-0141	MnO2	0.182	0.952 (20/36)	0.735	-----	0.700
		Manganese Oxide		-----		-------	
5	30-0279	CaSO4	0.148	0.900 (9/10)	0.776	-----	0.699
		Calcium Sulfate		-----		-------	
6	38-1420	TiN	0.065	1.000 (3/10)	0.690	-----	0.690
		Titanium Nitride (Osbornite, syn)		-----		-------	
7	21-1276	TiO2	0.156	0.833 (10/38)	0.822	-----	0.685
		Titanium Oxide (Rutile, syn)		-----		-------	
8	46-1045	SiO2	0.296	0.889 (16/42)	0.764	-----	0.679
		Silicon Oxide (Quartz, syn)		-----		-------	
9	10-0173	Al2O3	0.113	0.846 (11/42)	0.797	-----	0.675
		Aluminum Oxide (Corundum, syn)		-----		-------	
10	16-0613	Mgx(Mg,Fe)3(Si,Al)4O10(OH)2.4H2O	0.367	0.844 (27/32)	0.788	-----	0.665
		Magnesium Iron Aluminum Silicate Hydroxide		-----		-------	
11	11-0065	CrN	0.050	1.000 (3/10)	0.662	-----	0.662
		Chromium Nitride (Carlsbergite, syn)		-----		-------	
12	33-0664	Fe2O3	0.217	0.867 (13/42)	0.724	-----	0.628
		Iron Oxide (Hematite, syn)		-----		-------	
13	47-2217	(C2F4)n	0.338	0.909 (10/12)	0.690	-----	0.627
		Poly(tetrafluoroethylene)		-----		-------	
14	27-0088	CaSiO3	0.493	0.810 (34/42)	0.750	-----	0.607
		Calcium Silicate (Wollastonite-2\ITM\RG)		-----		-------	
15	52-1044	(Mg,Al)6(Si,Al)4O10(OH)8	0.431	0.889 (8/12)	0.663	-----	0.590
		Magnesium Aluminum Silicate Hydroxide (Ch		-----		-------	

APPENDIX 2O. XRD Experimental Parameters for Groundnut Shell

*** Basic Data Process ***

Group : CLIENT
Data : GROUNDNUT-SHELL

Strongest 3 peaks

no.	peak no.	2Theta (deg)	d (A)	I/I1	FWHM (deg)	Intensity (Counts)	Integrated Int (Counts)
1	46	23.9965	3.70547	100	0.21170	100	1213
2	48	24.9211	3.57005	96	0.11220	96	703
3	9	6.1890	14.26932	70	0.19530	70	681

Peak Data List

peak no.	2Theta (deg)	d (A)	I/I1	FWHM (deg)	Intensity (Counts)	Integrated Int (Counts)
1	2.3816	37.06594	4	0.14330	4	35
2	2.6550	33.24963	4	0.13000	4	33
3	2.8833	30.61742	5	0.07330	5	25
4	3.1350	28.15977	4	0.09000	4	23
5	3.5000	25.22389	6	0.08000	6	37
6	3.9200	22.52222	4	0.06660	4	16
7	4.7800	18.47186	3	0.04000	3	12
8	5.9800	14.76755	19	0.12000	19	151
9	6.1890	14.26932	70	0.19530	70	681
10	6.6850	13.21166	3	0.03000	3	16
11	7.0400	12.54623	3	0.04000	3	15
12	7.2616	12.16385	5	0.05670	5	22
13	7.5675	11.67282	6	0.04500	6	27
14	7.7750	11.36175	4	0.05000	4	18
15	7.9300	11.14002	4	0.10000	4	37
16	8.3150	10.62506	3	0.05000	3	20
17	8.8200	10.01781	3	0.04000	3	15
18	9.2750	9.52737	3	0.03000	3	12
19	9.6100	9.19599	5	0.10000	5	37
20	9.9150	8.91378	5	0.13000	5	45
21	10.1300	8.72507	3	0.08000	3	21
22	10.5150	8.40645	4	0.15000	4	47
23	10.9000	8.11038	5	0.14000	5	37
24	11.0700	7.98621	8	0.18000	8	78
25	11.3520	7.78844	9	0.09600	9	60
26	12.6600	6.98655	3	0.04000	3	13
27	13.7600	6.43040	3	0.04000	3	22
28	15.0200	5.89368	5	0.04000	5	31
29	15.2033	5.82304	5	0.04670	5	24
30	16.3000	5.43363	3	0.02000	3	4
31	16.7816	5.27877	6	0.06330	6	34
32	17.2000	5.15129	3	0.02000	3	16
33	18.3006	4.84390	16	0.14530	16	116
34	18.4428	4.80687	18	0.11430	18	119
35	19.0050	4.66592	3	0.03000	3	10
36	19.3533	4.58273	42	0.10670	42	275
37	19.6800	4.50738	3	0.04000	3	9
38	19.9050	4.45694	4	0.05000	4	12
39	20.2800	4.37536	3	0.04000	3	13
40	20.4200	4.34568	4	0.12000	4	34
41	20.7150	4.28445	3	0.05000	3	12
42	20.9600	4.23492	8	0.12000	8	76
43	21.3100	4.16615	5	0.10000	5	34
44	21.5500	4.12029	5	0.06000	5	39
45	22.9723	3.86831	17	0.08740	17	130
46	23.9965	3.70547	100	0.21170	100	1213
47	24.4640	3.63571	18	0.07200	18	99
48	24.9211	3.57005	96	0.11220	96	703
49	25.1800	3.53393	52	0.10580	52	301
50	25.3629	3.50885	65	0.18760	65	631